THE POTENTIAL ROLE OF SUPERANTIGENS IN THE PATHOGENESIS OF BOVINE THEILERIOSIS

by

E. Fiona Houston

Institute for Animal Health,
Compton,
Newbury,
Berkshire,
RG20 7NN.

Department of Veterinary Parasitology,
Faculty of Veterinary Medicine,
University of Glasgow.

A thesis submitted for the degree of Doctor of Philosophy.

September 1997.

DECLARATION

I declare that the work presented in this thesis is my own original work, except where mentioned in the acknowledgements, and it does not include work forming part of a thesis presented successfully for a degree in this or another University.

Fiona Houston.

ACKNOWLEDGEMENTS

I would like to thank Professor F. J. Bourne and Professor W. I. Morrison for making the facilities of the Institute available to me for carrying out this work. I am also grateful to the BBSRC for providing the Veterinary Fellowship that funded the project.

I am indebted to my supervisor, Ivan Morrison, for his guidance, intellectual insights, and support throughout the laboratory work and the preparation of this thesis. Thanks are also due to Dr C. J. Howard and Dr. R. A. Collins for many useful discussions, practical help, and encouragement during my time with the Cellular Immunology group. Many other members of the group, including Kate Gelder, Keith Parsons, Katherine Griffiths and Lai Shan Kwong, assisted me with learning new techniques. I am particularly grateful to Paul Sopp for his expert assistance with cell sorting, and for technical advice on flow cytometry. I would also like to acknowledge the contributions of Wallace Bulimo and Jane Scott to the *in situ* hybridization studies.

These experiments would not have been possible without generous provision of tick stabilate and sporozoite suspensions by Professor C. G. D. Brown of the Centre for Tropical Veterinary Medicine, University of Edinburgh, whose contribution is gratefully acknowledged.

I am also grateful to Dr. D. J. McKeever of the International Livestock Research Institute, Nairobi, for his assistance with the cannulation studies, and for allowing me to use the facilities of his laboratory during my visit to Kenya.

Many other people at Compton have been of great assistance. I would particularly like to acknowledge; Sue Hacker and Helen Matthews for their assistance in preparing histological sections, and for performing acid phosphatase staining; Dave Aldis and the compound staff for their care of the experimental animals; and Jim White-Cooper and Bernard Clark for photographic services.

Finally, I would like to thank my family and friends for their support and encouragement throughout this period of study.

CONTENTS

Chapter Four. Analysis of *In Vitro* Responses to *Theileria parva*.

Chapter Five. Cloning, Sequencing and Classification of Bovine *TCRBV* Genes.

LIST OF FIGURES

LIST OF TABLES

ABBREVIATIONS

ABI	Applied Biosystems, Inc.
APS	Ammmonium persulphate
AMV-RT	Avian myeloblastoma virus reverse transcriptase
ATP	Adenosine triphosphate
BCIP	5-bromo-4-chloro-3-indoyl phosphate
bo	Bovine
BoLA	Bovine lymphocyte antigen
bp	Nucleotide base pairs
BSA	Bovine serum albumin
BW	Binding and washing buffer
°C	degrees Celsius
CD	Cluster of differentiation
cDNA	Complementary deoxyribonucleic acid
CDR	Complementarity determining region
C_H	Constant region of immunoglobulin heavy chain
C_L	Constant region of immunoglobulin light chain
CMV	Cytomegalovirus
CO_2	Carbon dioxide
ConA	Concanavalin A
COOH	Carboxyl terminus of protein
cpm	Counts per minute
CTL	Cytotoxic T lymphocyte
CTLp	Cytotoxic T lymphocyte precursor
Cys	Cysteine
dATP	2'-deoxyadenosine triphosphate
dCTP	2'-deoxycytidine triphosphate
DDW	Double distilled water
ddATP	2',3'-dideoxyadenosine triphosphate
ddCTP	2',3'-dideoxycytidine triphosphate
ddGTP	2',3'-dideoxyguanosine triphosphate
ddTTP	2',3'-dideoxythymidine triphosphate
DEPC	Diethyl pyrocarbonate
dGTP	2'-deoxyguanosine triphosphate
DIG	Digoxigenin
dITP	2'-deoxyinosine triphosphate
DNA	Deoxyribonucleic acid
dNTPs	Deoxyribonucleotides
DTT	Dithiothreitol
dTTP	2'-deoxyribothymidine triphosphate
EBV	Epstein-Barr virus
ECF	East Coast fever
EDTA	Ethylenediaminetetraacetic acid
ELL	Efferent lymph lymphocytes
Fab	Antigen-binding fragment (of antibody)
FACS	Fluoresence-activated cell sorting
FBS	Foetal bovine serum
FF	FacsFlow

FITC	Fluorescein isothiocyanate
FSC	Forward scatter
g	Force of gravity
GCG	Genetics Computer Group
Gln	Glutamine
Gy	Grays
h	hours
HCl	Hydrochloric acid
HEPES	N-[2-hydroxyethyl]piperazine-N'-[2-ethanesulfonic acid]
HLA	Human lymphocyte antigen
HIV	Human immunodeficiency virus
hu	human
HVR	Hypervariable region
IAH	Institute for Animal Health
ICAM	Intercellular adhesion molecule
IFN	Interferon
Ig	Immunoglobulin
IL	Interleukin
ILRI	International Livestock Research Institute
ISH	*In situ* hybridization
K	Potassium
KCl	Potassium chloride
kDa	KiloDaltons
kb	Kilo base pairs (nucleotides)
LB	Luria-Bertani
Leu	Leucine
LFA	Lymphocyte function-associated antigen
LNC	Lymph node cells
M	Molar
mAb	Monoclonal antibody
MBq	Mega-Becquerels
$MgCl_2$	Magnesium chloride
$MgSO_4$	Magnesium sulphate
MHC	Major histocompatibility complex
min	Minute
ml	Millilitre
µl	Microlitre
MLR	Mixed leucocyte reaction
Mls	Minor lymphocyte stimulating locus
mM	Millimolar
µM	Micromolar
MMTV	Mouse mammary tumour virus
MNC	Mononuclear cells
MOPS	3-[N-morpholino]propanesulphonic acid
mRNA	Messenger ribonucleic acid
Mtv	Endogenous mammary tumour virus locus
NaCl	Sodium chloride
NaH_2PO_4	Monosodium phosphate
Na_2HPO_4	Disodium phosphate

NBT	Nitroblue tetrazolium
NH_2	Amino terminus of protein
$(NH_4)_2SO_4$	Ammonium sulphate
NK	Natural killer
PBMC	Peripheral blood mononuclear cells
PBS	Phosphate buffered saline
PCR	Polymerase chain reaction
PE	Phycoerythrin
PEG	Polyethylene glycol
PIM	Polymorphic immunodominant antigen
pmol	picomole
PMA	Phorbol 12-myristate 13-acetate
PWM	Pokeweed mitogen
RAG	Recombination activating gene
RE	Restriction endonuclease
RFLP	Restriction fragment length polymorphism
RNA	Ribonucleic acid
RNase	Ribonuclease
RPMI	Roswell Park Memorial Institute (medium)
RSS	Recombination signal sequence
RT	Reverse transcriptase
RT-PCR	Reverse transcriptase polymerase chain reaction
s	Second
SAG	Superantigen
SDS	Sodium dodecyl sulphate
SE	Staphylococcal enterotoxin
SI	Schizont index
SSC (1)	Side scatter
SSC (2)	Sodium saline citrate buffer
TBE	Tris-borate-EDTA buffer
TCR	T cell receptor
TCGF	T cell growth factors
T_d	Dissociation temperature (oligonucleotides)
TdT	Terminal deoxynucleotidyl transferase
TE	Tris-HCl,EDTA buffer
TEMED	N,N,N',N'-tetramethylethyldiamine
Th cells	T helper cells
T_m	Melting temperature (oligonucleotides)
TNF	Tumour necrosis factor
Tris	2-amino-2-(hydroxymethyl)-1,3-propanediol
Trp	Tryptophan
TSST	Toxic shock syndrome toxin
Tyr	Tyrosine
U	Unit
UTP	Uridine triphosphate
UV	Ultra-violet
V_L	Variable region of immunoglobulin light chain
V_H	Variable region of immunoglobulin heavy chain
v/v	Volume to volume

w/v	Weight to volume
WC	Workshop cluster
X-gal	5-bromo-4-chloro-3-indolyl-β-D-galactoside

ABSTRACT

Theileria parva is an intracellular protozoan parasite that produces an acute and often fatal lymphoproliferative disease (East Coast fever) in susceptible cattle. Studies of experimentally infected cattle have demonstrated a massive increase in the cellularity of the lymph node draining the site of inoculation in the early stages of the infection, when the proportion of parasitized cells in the node was very low. The increased cellularity was associated with a marked increase in the number of lymphoblasts within the node. This suggested that an immune response to the parasite does occur in the regional lymph nodes of naïve animals, but is ineffective in controlling the infection.

The objective of this study was to characterize the primary immune response in the drainage lymph nodes of cattle infected with *T. parva* and , in particular, to determine whether or not a superantigen was responsible for inducing lymphocyte activation. Flow cytometric analysis of the phenotype of lymph node cells from infected animals revealed that an unusual $CD2^-CD8^+$ subset of α/β T cells formed a major component of the responding population. The appearance of this subset coincided with the initial detection of parasites in the node; the numbers peaked 1-2 days later, and then declined rapidly as the proportion of parasitized cells increased. These cells were refractory to stimulation *in vitro*, and cells with this phenotype did not participate in the *in vitro* proliferative response of peripheral blood mononuclear cells from naïve animals to autologous parasitized cells. Another interesting feature of the lymph node response in *T. parva*-infected animals was a large influx of macrophages between days 7 and 9 post-infection. The possibility that a superantigen might be triggering the lymph node response of infected animals was investigated by comparing the *TCRBV* gene usage of responding cells with the *TCRBV* repertoire expressed by normal lymph node T cells. Purified populations of activated T cells and $CD2^-CD8^+$ T cells expressed a diverse repertoire of *TCRBV* genes, which suggests that a superantigen is not involved in the response. In this study a total of 29 new *TCRBV* gene segments were sequenced, permitting the first detailed classification of bovine *TCRBV* subfamilies, and revealing that diversification of the *TCRBV* repertoire in cattle has involved gene duplication events distinct from those of humans and mice.

CHAPTER ONE

GENERAL INTRODUCTION.

1.1. *Theileria parva.*

Theileria parva is an intracellular protozoan parasite that infects cattle and causes an acute lymphoproliferative disease known as East Coast fever (ECF). The parasite is transmitted by the three-host tick *Rhipicephalus appendiculatus*, and the incidence of the disease closely follows the distribution of the tick vector throughout East and Central Africa. *T. parva* also infects the African buffalo (*Syncerus caffer*), but establishes clinically inapparent persistent infections in this species. The buffalo acts as a reservoir of parasites maintaining infection in the tick population. The number of ticks varies according to local climatic conditions and season, so that in some areas there is a relatively constant challenge, while in others disease occurs only when rainfall and temperature permits.

The classification of *T. parva* places it in the phylum Apicomplexa and the order Piroplasmida. Three subtypes of *T. parva* have been described; *T. p. parva*, *T. p. bovis* and *T. p. lawrencei*, which are distinguished on the basis of their clinical and epidemiological characteristics (Uilenberg, 1981). *T. p. parva* is transmitted between cattle and causes classic ECF; *T. p. lawrencei* is transmitted from buffalo to cattle, causing corridor disease; and *T. p. bovis* is much less virulent than the other two subtypes and is responsible for seasonal outbreaks of disease in Southern Africa. Although *T. p. parva* and *T. p. lawrencei* may produce clinical reactions of equal severity in cattle, the latter subtype gives rise to lower levels of schizonts and death occurs before high levels of piroplasms are produced. However, passage of buffalo-derived parasites through cattle gives rise to *T. p. parva*-like parasites. Although this could reflect parasite adaptation to the bovine host, analyses of parasitized cell lines derived from infected buffalo indicate that they often contain a mixed population of parasites, thus there may be selection for strains that produce piroplasms before the death of the host (Conrad *et al.*, 1987b). The three subtypes are morphologically and serologically indistinguishable, and monoclonal antibodies and DNA probes that have been used to detect heterogeneity

among different parasite isolates fail to show a clear distinction between the buffalo- and cattle-derived parasites (Conrad *et al.*, 1989a). Thus, there is no clear biological or genetic basis for the classification of *T. parva* into distinct subspecies.

Originally parasite strains were distinguished by the geographical location where they were originally isolated, and by cross-protection experiments in cattle. With the development of *in vitro* assays for detection of genotypic and phenotypic variation, a more precise terminology based on that used for defining trypanosome populations was adopted for use with *Theileria* (Irvin *et al.*, 1983). The definitions relevant to the present discussion are:

1. **Isolate:** viable organisms isolated on a single occasion from a field sample in experimental hosts, culture systems or stabilate.
2. **Stock:** all the populations derived from an isolate without any implication of homogeneity or characterization. Populations comprising a single stock include infected cell lines and tick stabilates and subsequent parasite preparations derived from them.
3. **Stabilate:** a sample of organisms preserved alive (usually in replicate) on a single occasion.
4. **Parasite clone:** *Theileria* species line derived from a single parasite.
5. **Strain:** A population of homogeneous organisms possessing a set of defined characters. Unambiguous characterization of a strain can be assured only if the population of organisms was initiated from a parasite clone.

1.1.1. Parasite life cycle and disease pathogenesis.

The life cycle of *T. parva* has been described in detail by Mehlhorn and Schein (1984) and reviewed by Morrison *et al.* (1986). Transmission of *T. parva* by *R. appendiculatus* occurs trans-stadially i.e. infection acquired during larval and nymphal stages is transmitted, after moulting, in the succeeding developmental stage. Ticks become infected by ingestion of erythrocytes containing piroplasms from infected buffalo or cattle. Infected erythrocytes are lysed in the tick gut, and the parasite differentiates into male and female gametes which fuse to produce a zygote. Zygotes invade cells of the

intestinal wall (Schein *et al.*, 1977), and undergo transformation into motile kinetes. Kinetes are released into the haemolymph during and after tick moulting and migrate to the salivary glands where they invade E cells of the type III acini (Fawcett *et al.*, 1982a,b). Sporogony proceeds when the tick begins to feed on another host; a large multinucleate labyrinthine structure is formed which gives rise to large numbers of mature sporozoites. Infective sporozoites are released into the saliva 3-5 days after feeding commences and injected into the host.

Following inoculation into the bovine host, the parasite is not readily detected for several days, thus events occurring during this early period have not been studied in detail. However, *in vitro* studies have shown that sporozoites can enter bovine lymphocytes within minutes by a process of receptor-mediated endocytosis. The surrounding host cell membrane is rapidly broken down, and sporozoites are released into the cytoplasm where they become closely associated with host cell microtubules. Disintegration of the host cell membrane is associated with release of the contents of parasite rhoptries and microspheres (Fawcett *et al.*, 1982c; Shaw *et al.*, 1991). Prior incubation of lymphocytes with tick salivary gland extract or human recombinant interleukin-2 (IL-2) has been shown to increase their susceptibility to infection (Shaw *et al.*, 1993). Within three days the parasite nucleus divides to form a multinucleate schizont located in the Golgi region of the cell (Stagg *et al.*, 1981). At this stage, the infected lymphocyte undergoes blast transformation and starts to divide. Microscopic examination of parasitized cell lines has shown that the schizonts divide at the same time as the host cells (Hulliger *et al.*, 1964; Irvin *et al.*, 1982). The parasite is closely associated with the mitotic spindle during cell division, resulting in infection of both daughter cells and clonal expansion of the infected cell population (Hulliger *et al.*, 1964).

Following inoculation of susceptible cattle with sporozoites, schizont-infected lymphocytes are first detected in the lymph node draining the site of inoculation after 4-14 days, depending on the initial infective dose. During this period infected lymphocytes become disseminated to lymphoid tissues throughout the body, where they are detectable a few days after their initial appearance in the drainage lymph node (Emery, 1981a; Morrison *et al.*, 1981). Over the next 5-7 days, the proportion of parasitized cells in lymphoid tissues increases rapidly as a result of massive uncontrolled proliferation of

schizont-infected lymphoblasts, in a manner analogous to tumour cells (Jarrett *et al.*, 1969; Radley *et al.*, 1974; Morrison *et al.*, 1981). Levels of parasitosis of 30% or more may be found in the lymphoid tissues at this stage (DeMartini and Moulton, 1973a; Morrison *et al.*, 1981). As infection progresses, the number of nuclei per schizont increases (Jarrett *et al.*, 1969), and a proportion of the parasites differentiate to produce merozoites which are released following rupture of the host cell and invade erythrocytes to form piroplasms, thus completing the parasite life cycle.

In susceptible cattle naturally exposed to infection with *T. parva*, mortality can reach 95% (Brocklesby *et al.*, 1961), with death occurring within 2-4 weeks depending on the initial parasite dose. The lymphoproliferative phase of the infection is associated with the onset of the disease, characterized initially by enlargement of superficial lymph nodes and sustained pyrexia. Parasitized lymphoblasts are detected in efferent and thoracic duct lymph and in blood during the second week of infection (DeMartini and Moulton, 1973b; Morrison *et al.*, 1981; Emery, 1981a). During the later stages of the disease, infected cells invade the thymus and bone marrow and infiltrate a variety of nonlymphoid tissues, notably the lamina propria of the intestine and the interstitial lung tissue (Irvin and Morrison, 1987). The presence of numerous parasitized cells in the lung is associated with pulmonary oedema which causes severe respiratory distress, a common feature of the terminal stages of the disease. In the later stages of the infection, widespread lymphocytolysis occurs, affecting both parasitized and non-parasitized lymphocytes. The mechanisms of lymphocytolysis are unclear, but the result is a profound depletion of lymphocytes in organised lymphoid tissues and in the recirculating pool (DeMartini and Moulton, 1973a,b; Morrison *et al.*, 1981, Emery *et al.*, 1981a). There is also a severe leucopenia in the terminal stages of disease, but this follows a gradual decline in blood leucocyte counts after the onset of lymphoproliferation, and probably reflects bone marrow suppression by the parasite as well as leucocyte destruction (Wilde, 1966; Shatry *et al.*, 1981; Morrison *et al.*, 1981). Infiltration and destruction of primary lymphoid tissue in the thymus and bone marrow may also contribute to leucopenia by impairment of lymphopoiesis. Although up to 50% of erythrocytes may be infected with piroplasms, proliferation of piroplasms is minimal, and thus anaemia is normally mild in ECF, in contrast to infections with some other *Theileria* species e.g. *T. annulata*, where anaemia is a prominent feature of the disease (Wilde, 1966; Shatry *et al.*, 1981). Animals that

recover from ECF are carriers of the infection, but this carrier state is most likely due to residual infection of lymphoid cells.

1.1.2. Target cells for infection.

Sporozoites attach to and invade a subpopulation of bovine mononuclear cells; development of the schizont is accompanied by a rapid change in the morphology of the host cell, which becomes characteristically lymphoblastoid in appearance, with a large nucleus containing a prominent nucleolus, extensive cytoplasm and a prominent Golgi complex (Stagg *et al.*, 1981; Fawcett *et al.*, 1982c). The first clue as to the identity of the target cells came from experiments in which infected cell lines and parasitized cells from infected cattle were shown to be negative for surface or intracellular immunoglobulin, suggesting that the parasite preferentially infected T lymphocytes (Duffus *et al.*, 1978; Emery, 1981a).

More detailed analysis of the phenotype of infected cells was permitted by the development of techniques for infecting lymphocytes with sporozoites *in vitro* (Brown *et al.*, 1973), and the characterization of monoclonal antibodies specific for differentiation antigens on bovine lymphocytes (summarized by Howard *et al.*, 1991). Various subpopulations of bovine lymphocytes were purified by flow cytometry and incubated with sporozoites at limiting dilutions *in vitro*. These studies demonstrated that α/β T cells (both $CD4^+$ and $CD8^+$), γ/δ T cells and B cells can all be infected with similar frequencies, and establish cell lines with distinct cell surface phenotypes. Cell lines were not established from monocytes or granulocytes (Lalor *et al.*, 1986; Baldwin *et al.*, 1988; Spooner *et al.*, 1989).

Studies using electron microscopy to examine the processes of parasite invasion of host cells *in vitro* have shown that sporozoites enter lymphocytes by an energy-dependent process of receptor-mediated endocytosis (Fawcett *et al.*, 1982c; Shaw *et al.*, 1991). This technique has also been applied to investigate the range of host cells that are susceptible to infection with sporozoites of *T. parva* (Shaw *et al.*, 1993). In this study, sporozoites were observed to bind to and invade afferent lymph veiled cells (dendritic

cells) and, to a lesser extent, monocytes and macrophages, as well as lymphocytes. However, transformed cell lines could not be derived from veiled cells or monocytes/macrophages. Sporozoite binding and internalization by granulocytes and fibroblasts was very rare. These observations suggest that sporozoites bind to specific receptors expressed on a limited range of host cells, but that only lymphocytes possess the cellular components necessary for transformation, and are therefore the only cell type that is permissive for parasite multiplication and differentiation following invasion. The molecular nature of the parasite-host cell interaction that determines the cell tropism of the sporozoite is not known. Monoclonal antibodies reactive with common determinants on bovine class I MHC molecules and with β_2-microglobulin have been shown to inhibit sporozoite binding and entry into lymphocytes (Shaw *et al.*, 1991). In addition, using bovine deletion mutant cell lines from which expression of one or both MHC class I haplotypes has been lost, it was demonstrated that sporozoite binding and entry correlated with the level of class I surface expression (Shaw *et al.*, 1995). However, the specificity of sporozoites for a restricted range of cells must involve additional parasite host-cell interactions, since MHC class I molecules are expressed on the surface of virtually all nucleated cells.

Despite the fact that *T. parva* infections can be established in all the major subpopulations of bovine lymphocytes at similar frequencies *in vitro*, most bulk cell lines and clones derived from *in vitro* infection of PBMC or from infected animals have been shown to possess cell surface markers indicative of T cell origin (Baldwin *et al.*, 1988; Emery *et al.*, 1988; Spooner *et al.*, 1989). In addition, the vast majority of parasitized lymphoblasts isolated from the efferent lymph of cattle undergoing lethal infections with *T. parva* were found to express the T lymphocyte markers CD2, CD4 or CD8 (Emery *et al.*, 1988). However, examination of the phenotype of recently established cultures of infected PBMC revealed that large numbers of parasitized B cells were present after 7 days, but by day 14, the percentage of B cells in the cultures had declined markedly (Morrison *et al.*, 1996). Similarly, Baldwin *et al.* (1988) observed that although bulk cell lines derived from the drainage lymph node of an infected animal were clearly of T cell origin, clones of *T. parva*-transformed cells established from the same organ were negative for T cell markers, and therefore most likely derived from infected B cells.

These observations suggest that, in most cases, infected T cells overgrow infected B cells in culture, either through a difference in the replication rate of the two cell types, or by suppression of B cell growth by parasitized T cells.

The pathogenicity of the different infected cell types *in vivo* has been examined by sorting PBMC into $CD2^+$, $CD4^+$, $CD8^+$ and B cell (surface Ig^+) subpopulations, and incubating the cells *in vitro* with sporozoites before inoculation of susceptible cattle with the purified populations. While the T cell subpopulations produced severe clinical reactions with high levels of parasitosis, infected B cells gave rise to mild self-limiting infections with low numbers of parasites, even when a ten-fold higher dose of cells was administered (Morrison *et al.*, 1996). The explanation for the reduced pathogenicity of parasitized B cells is unknown, but may reflect either the inability of this cell type to sustain high levels of parasite replication, or increased susceptiblity of infected B cells to host immune responses.

1.1.3. Characteristics of infected lymphocytes.

Lymphocytes undergo extensive phenotypic changes following infection with *T. parva*. Phenotypic analysis of cell lines derived from different lymphocyte populations *in vitro* showed that, while α/β T cells retain expression of differentiation antigens such as CD2, CD4 and CD8, most B cells downregulate expression of surface immunoglobulin following continued subculture and do not express T cell differentiation antigens (Lalor *et al.*, 1986; Baldwin *et al.*, 1988). Infected γ/δ T cell lines continue to express high levels of the lineage-specific marker WC1 and usually acquire expression of CD2 and/or CD8, but not CD4. Some parasitized cell lines and clones derived from PBMC express both CD4 and CD8, although CD8 is expressed only on a proportion of the $CD4^+$ cells and at variable levels (Baldwin *et al.*, 1988; Emery *et al.*, 1988; Spooner *et al.*, 1988). In cattle infected with *T. parva*, $CD4^+CD8^+$ T lymphoblasts are also found in large numbers in efferent lymph during the second week of infection, and a high proportion of these cells are parasitized (Emery *et al.*, 1988). This phenotype is considered to arise as a result of *de novo* expression of CD8 on parasitized $CD4^+$ T cells, since $CD4^+$ T cells infected *in vitro* frequently acquire expression of CD8, while infected $CD8^+$ T cells

remain negative for CD4 (Baldwin *et al.*, 1988; Emery *et al.*, 1988). Studies with monoclonal antibodies that react with different determinants on the α and β chains of bovine CD8 suggest that, on $CD4^+CD8^+$ *Theileria*-infected cell lines, the CD8 molecule is expressed as a homodimer of the α chain (MacHugh *et al.*, 1991). Induction of CD8 expression on infected $CD4^+$ cells probably reflects the activated state of parasitized cells, since it has previously been demonstrated that CD8 is expressed on a proportion of human and rat $CD4^+$ T cells activated by mitogens or alloantigens (Blue *et al.*, 1985; Bevan and Chisholm, 1986), and that human $CD4^+$ T cell clones stimulated in the presence of IL-4 upregulate expression of CD8 (Paliard *et al.*, 1988).

Following transformation, parasitized lymphocytes acquire additional differentiation antigens typical of activated lymphocytes (Naessens *et al.*, 1985; Lalor *et al.*, 1986). MHC class II antigens are constitutively expressed on infected cell lines derived from T cells, as well as on B cell lines; however, the proportion of positive cells and the levels of expression may be variable, particularly in newly established cultures (Lalor *et al.*, 1986; Spooner *et al.*, 1988). Expression of MHC class II molecules has previously been demonstrated on rat T cells activated by mitogens or alloantigens, but expression is transient (Bevan and Chisholm, 1986). Induction of MHC class II expression was also observed on bovine T cells cultured with mitogen (DeMartini *et al.*, 1993). Interestingly, when MHC class II expression was monitored in PBMC and lymph node cells of cattle undergoing lethal infections with *T. parva*, MHC class II-negative parasitized cells progressively outnumbered those expressing MHC class II (DeMartini *et al.*, 1993).This suggests that, *in vivo*, MHC class II-positive parasitized cells are selectively destroyed or sequestered, or that differentiation of parasitized cells *in vivo* results in downregulation of expression of MHC class II molecules. Lymphocytes infected *in vitro* and *in vivo* retain expression of MHC class I molecules, and their pattern of reactivity with serological class I typing reagents remains similar to that of cells of the donor animal (Spooner and Brown, 1980).

Other activation markers which are expressed on almost all activated and proliferating leucocytes are the transferrin receptor (Trowbridge and Omary, 1981) and the high-affinity IL-2 receptor (IL-2R) (Lipkowitz *et al.*, 1984). Recently, a monoclonal antibody

has been characterized that detects expression of the bovine transferrin receptor on bone marrow erythroid cells and proliferating lymphocytes (Naessens *et al.*, 1996). Expression of the molecule was also demonstrated on all *T. parva*-transformed cell lines that were tested, including both B cell- and T cell-derived lines. Expression of the α chain (CD25; formerly designated Tac antigen) of the bovine IL-2R has also been demonstrated at the messenger RNA (mRNA) and protein level in all *T. parva*-infected cell lines of either T cell or B cell origin (Coquerelle *et al.*, 1989; Dobbelaere *et al.*, 1990). The α chain is an essential component of the high affinity IL-2 receptor expressed on activated lymphocytes (Kondo *et al.*, 1986). In parasitized cell lines expression of biologically functional IL-2R was shown to be constitutive, in contrast to the transient expression normally detected on activated T cells (Coquerelle *et al.*, 1989; Dobbelaere *et al.*, 1990).

The phenotypic changes described above indicate that lymphocytes infected with *T. parva* become constitutively activated, and acquire many characteristics of leukaemia cell lines. They proliferate continuously in culture independently of exogenous growth factors or feeder cells, can be cloned by limiting dilution or in soft agar (Nelson and Hirumi, 1981), and cause invasive tumours when injected into irradiated athymic mice (Irvin *et al.*, 1975). However, the lymphoblastoid transformation caused by *T. parva* is completely reversible; treatment of cultures with theilericidal drugs based on derivatives of naphthoquinone results in elimination of schizonts from infected cells and reversion of the cells to the morphology of resting lymphocytes, leading to growth arrest (Pinder *et al.*, 1981; Dobbelaere *et al.*, 1988).

The mechanisms by which the parasite induces and maintains the transformed state of host lymphocytes are not known. The observation that parasitized cells constitutively express high-affinity IL-2R and respond to T cell growth factors (TCGF) or human recombinant IL-2 (hurIL-2) with increased proliferation led to the proposal that continued growth of parasitized cells might be maintained by a IL-2/IL-2R autocrine loop (Brown and Logan, 1986; Dobbelaere *et al.*, 1988). In support of this hypothesis, low levels of TCGF activity have been detected in the supernatants of some parasitized cell lines (Brown and Logan, 1986; Dobbelaere *et al.*, 1991). Constitutive expression of mRNA for IL-2 was also demonstrated in all *T. parva*-infected cell lines that were

examined, including two B cell lines (Heussler *et al.*, 1992); however, the levels of expression were low compared with the amount of IL-2 mRNA found in concanavalin A (ConA) stimulated lymphocytes, and in a number of lines transcripts could only be detected following amplification in the polymerase chain reaction (PCR). In addition, while anti-IL-2 antibodies caused significant inhibition of the growth of some cell lines, other cell lines were unaffected or only marginally inhibited, and proliferation was never completely eliminated (Dobbelaere *et al.*, 1991; Heussler *et al.*, 1992). Thus although IL-2 may play an important role in stimulating growth of parasitized cells, it is clearly not the sole mechanism responsible for maintaining proliferation of infected cells *in vitro*.

Other cytokines produced by *T. parva*-infected cells may also have growth factor activity that contributes to proliferation. There is evidence that bovine T cell lines transformed by *T. parva* secrete IFNγ (Entrican *et al.*, 1991; Ahmed *et al.*, 1993), and transcripts for other cytokines including TNFα, IL-6 and IL-10 have been detected in a range of cell lines examined by multiplex PCR (McKeever *et al.*, 1997). The effects of some of these cytokines on the establishment of infection in bovine lymphocytes and on the proliferation of schizont-infected cell lines have been examined in two studies, with somewhat contradictory results. Thus, while DeMartini and Baldwin (1991) reported that addition of bovine recombinant IFNγ (borIFNγ) and borIL-2 to the culture medium marginally enhanced the establishment of parasitized cell lines, Preston *et al.* (1992) concluded that borIFNγ, borTNFα, huIFNα, hurIL-2 and hurIL-6 significantly inhibited the development of the parasite in freshly infected cells. It is not easy to explain this discrepancy in view of the different methods employed by the investigators to assess the development of infected cell lines. For example, the effects noted by DeMartini and Baldwin were most apparent when infected cells were plated at limiting dilutions of 1000 to 4000 cells/well, while in the study of Preston *et al.* cell inputs of 5×10^5 cells/well were used in all experiments, making direct comparison of the results difficult. Although IL-2 (and to a lesser extent, borTNFα) enhanced the proliferation of established *T. parva*-infected cell lines and clones, IFNγ neither inhibited nor stimulated the proliferation of parasitized cells. This is in contrast to infections with other intracellular protozoa, such as *Leishmania* (Liew *et al.*, 1990), *Plasmodium* (Schofield *et al.*, 1987)

and *Toxoplasma* (Suzuki *et al.*, 1988), where IFNγ has been shown to inhibit intracellular multiplication of the organisms within macrophages or hepatocytes.

In addition to cytokines, cell-cell contact has also been demonstrated to play an important role in maintaining proliferation of parasitized cells. Dobbelaere *et al.* (1991) found that proliferation of highly diluted *T. parva*-infected cells could be restored in a dose-dependent manner by the addition of autologous glutaraldehyde-fixed stimulator cells, or membrane preparations from infected cells. Uninfected allogeneic lymphoblasts and alveolar macrophages were as effective as autologous infected cells in stimulating proliferation, and the response was not inhibited by the addition of anti-MHC class I or class II monoclonal antibodies to the culture. These findings suggest that interactions of costimulatory molecules on the surfaces of parasitized cells help to maintain continuous proliferation. Normally, signals provided by costimulatory molecules (for example, CD28 bound by B7) are necessary for the expression of proliferative responses and cytokine production in T cells activated by engagement of the T cell receptor (TCR) with its ligand. However *Theileria*-infected cells may be able to respond to costimulatory signals alone, in the absence of an antigen-specific stimulus through the TCR.

The TCR signal transduction pathway involves a complex series of biochemical reactions, culminating in activation of transcription factors, such as NF-κB. NF-κB is a transcriptional activator, which is involved in the regulation of IL-2 and IL-2R expression, and can be found in the activated form in the nuclei of *T. parva*-infected cells (Ivanov *et al.*, 1989). The similarities between *T. parva*-infected cells and activated T cells suggest that the parasite may induce a state of constitutive activation in bovine lymphocytes by interaction or interference with the antigen receptor signalling cascade. In support of this hypothesis, two protein tyrosine kinases involved in TCR signal transduction, $p56^{lck}$ and $p59^{fyn}$, were also shown to be activated in infected cells (Eichhorn and Dobbelaere, 1994). However, the nature of the interaction between parasite molecules and constituents of the signalling pathway is unknown at present.

1.1.4. Immunity to *Theileria parva.*

1.1.4.1. Methods of immunization.

Control of East Coast fever currently relies on the regular application of acaricides to susceptible cattle to prevent tick infestation. However, cattle that recover spontaneously from infection demonstrate solid long-lasting immunity to the disease, and considerable efforts have been directed towards developing a method of vaccination suitable for application in the field. Successful immunization of cattle against ECF has been achieved by "infection and treatment" strategies or inoculation of live macroschizont-infected cells. The former technique is based on the finding that administration of tetracyclines during the prepatent period of the infection resulted in self-limiting infections and subsequent immunity. Practical application of this immunization strategy became possible following the development of methods to extract and cryopreserve sporozoite suspensions (stabilates) from infected ticks (Cunningham *et al.*, 1973). Titration of this material resulted in a graded series of responses in cattle, permitting induction of reproducible experimental infections with predictable kinetics (Cunningham *et al.*, 1974; Radley *et al.*, 1974; Dolan *et al.*, 1984a). Simultaneous inoculation of an infective tick stabilate and treatment with a long-acting formulation of oxytetracycline is effective in inducing immunity to challenge with the homologous parasite stock (Radley, 1981). An alternative method of immunization involves treatment of infected animals at the onset of clinical signs with a theilericidal drug such as parvaquone (Dolan *et al.*, 1984b). These vaccination strategies have a number of drawbacks that may limit their practical application. First, the use of live parasites requires facilities for transport and storage of cryopreserved stabilate in liquid nitrogen. Second, immunization with one parasite stock may not provide protection against challenge with heterologous stocks, due to strain variation among different isolates of *T. parva* (Radley *et al.*, 1975). However, this problem can be overcome by combining different stocks for immunization. Third, a prolonged carrier state has been demonstrated in immunized cattle, so that these animals can maintain infection in the tick population, and may transmit vaccine strains of the parasite to susceptible individuals (Kariuki *et al.*, 1995). Nevertheless, this immunization strategy has been successfully implemented in the field, using locally isolated stocks of *T. parva.*

A vaccine based on live macroschizont-infected cells, attenuated by prolonged culture *in vitro*, has been successfully applied in the field to protect against infection with *T. annulata* (Pipano, 1981). Inoculation of susceptible cattle with varying numbers of autologous *T. parva*-infected cells demonstrated that only 10^2 cells were required to induce immunity, while doses of 10^6 or more cells produced lethal infections (Büscher *et al.*, 1984; Dolan *et al.*, 1984c). However, 10^8 or more infected allogeneic cells were required to obtain reproducible immunity to *T. parva* (Pirie *et al.*, 1970; Büscher *et al.*, 1984), which renders this approach uneconomic as a strategy for field immunization. With allogeneic cells, induction of immunity is dependent on establishment of an active infection in the cells of the recipient animal (Emery *et al.*, 1981a). Transfer of *T. parva* between cells is a rare event, but occurs more readily with *T. annulata*, with the result that 10^5 or less allogeneic infected cells are sufficient to induce immunity against the latter species.

1.1.4.2. The role of humoral immune mechanisms.

Following immunization or recovery from ECF, cattle produce antibodies to schizont and piroplasm antigens, initially detectable at the time of elimination of infection (Wagner *et al.*, 1975). This response does not appear to contribute to immunity against the disease. Cattle immunized with semi-purified schizont antigens or killed schizont-infected cells are fully susceptible to challenge with *T. parva*, despite developing titres of anti-schizont antibody comparable to those in immune cattle (Wagner *et al.*, 1974; Emery *et al.*, 1981a). In addition, transfer of serum or concentrated gammaglobulin from immune to naive animals produced no protective effect against experimental challenge (Muhammed *et al.*, 1975).

After immunization of cattle with *T. parva* by infection and treatment, a weak anti-sporozoite antibody response is observed which, on subsequent challenge, fails to prevent the infection becoming established in host lymphocytes. Thus, responses to sporozoites were initially not considered to play an important role in protective immunity. However, immunized cattle subjected to repeated challenge with infected ticks develop high titres of antibodies that neutralize the infectivity of sporozoites *in vitro* (Musoke *et al.*, 1982). Sera and monoclonal antibodies raised against *T. parva*

sporozoites neutralize the infectivity of several parasite stocks that do not cross-protect *in vivo* (Musoke *et al.*, 1984; Dobbelaere *et al.*, 1984). Neutralizing antibodies have been shown to react with a 67 kDa sporozoite-specific surface antigen (p67), which has been investigated as a possible candidate antigen for inclusion in a subunit vaccine, because of its potential for stimulating cross-protective immunity to all strains of *T. parva*. The gene encoding p67 has been cloned and was shown to be identical in sequence in five different cattle-derived parasite stocks; the protein encoded by a buffalo-derived parasite was also very similar in sequence but contained a short insert (Nene *et al.*, 1992,1996). Recombinant p67 has been expressed in *E. coli* as a fusion protein with part of a non-structural protein (NS1) of influenza virus A. Repeated inoculations of cattle with the purified fusion protein emulsified in saponin resulted in high levels of antibody and induced protective immunity in a proportion of the immunized cattle (Musoke *et al.*, 1992). However, the effectiveness of this immunization procedure in inducing protection against a high-dose challenge or field challenge has not yet been evaluated.

1.1.4.3. The role of cell-mediated immune mechanisms.

The failure to demonstrate a role for antibody responses in protection against *T. parva* suggested that immunity was mediated by cellular immune responses. Following homologous challenge of immunized cattle, small numbers of parasitized cells are often transiently detectable in the drainage lymph node, indicating that immunity does not prevent infection but operates at the level of the schizont-infected cell (Eugui and Emery, 1981). Cattle immunized by infection and treatment are protected against challenge with parasitized cells, and immunization with autologous or allogeneic infected cell lines renders animals resistant to challenge with sporozoites (Pirie *et al.*, 1970; Emery *et al.*, 1982; Büscher *et al.*, 1984). Further confirmation of the importance of cell-mediated immune mechanisms came from experiments in which adoptive transfer of thoracic duct lymphocytes from immune to naive chimaeric twin calves was shown to confer protection against challenge with *T. parva* (Emery, 1981b).

A role for cytotoxic cells in the immune response to *T. parva* was first proposed by Pearson *et al.* (1979), who demonstrated that cytotoxic cells could be induced in PBMC of immune animals following co-culture with autologous *Theileria*-infected cell lines. In

cattle undergoing lethal infections with *T. parva*, cytotoxic cells capable of killing allogeneic, but not autologous, infected cell lines and a mouse tumour cell line were detected in the peripheral blood during the later stages of the infection (Emery *et al.*, 1981b). In contrast, in cattle recovering from primary infections, or in immunized animals undergoing challenge infection, cytotoxic cells are transiently detected in the peripheral blood at about the same time as schizonts disappear from the drainage lymph node (Emery *et al.*, 1981b; Eugui and Emery, 1981; Morrison *et al.*, 1987). These cytotoxic cells kill autologous parasitized cells but not uninfected lymphoblasts or allogeneic cell lines infected with the same parasite. The effector cells are confined to the $CD8^+$ fraction of PBMC and lymphatic lymphocytes, are specific for parasitized cells and are class I MHC-restricted (Goddeeris *et al.*, 1986a; Morrison *et al.*, 1987; McKeever *et al.*, 1994). Parasite-specific cytotoxic T cell (CTL) clones can be generated and maintained *in vitro* following repeated stimulation of PBMC from immune animals with autologous parasitized cells (Goddeeris *et al.*, 1986b). Application of limiting dilution analysis has permitted estimation of the frequency of *T. parva*-specific CTL precursors (CTLp) in the peripheral blood of immune cattle. In animals immunized 6-8 weeks earlier, frequencies of CTLp ranging from 1:5300 to 1:3600 were found, and a similar range of frequencies was demonstrated up to 6 months after immunization (Taracha *et al.*, 1992).

Direct evidence for the role of cytotoxic $CD8^+$ T cells in mediating immune responses to *T. parva* has come from experiments involving adoptive transfer of lymphocytes enriched for $CD8^+$ cells from immune to naive monozygotic twins (McKeever *et al.*, 1994). The immune twins were challenged, and 9-12 days later, lymphocytes were collected from the efferent duct of the lymph node draining the site of challenge. The cells were enriched for $CD8^+$ T cells by complement-mediated lysis of the other lymphocyte populations, and transferred to the naive twins 6-9 days after infection with a lethal dose of *T. parva.* In two sets of twins, the animals receiving the $CD8^+$ enriched population controlled the infection. In another set of twins, $CD8^+$ T cells were also depleted and a contaminating population of lymphocytes expressing CD2 and CD6 was transferred. The recipient in this case underwent a severe infection comparable to that in the challenge control. These results indicate that $CD8^+$ cells are required to mediate protective responses.

When PBMC from immune animals were restimulated at weekly intervals with autologous parasitized cells, a large proportion of the proliferating cells were shown to be $CD4^+CD8^-$ lymphocytes (Goddeeris *et al.*, 1986a; Baldwin *et al.*, 1987). Clones derived from these cells exhibit a parasite-specific proliferative response, restricted by MHC class II molecules, when stimulated with autologous parastized cells or extracts of parasitized cells presented by conventional accessory cells (Baldwin *et al.*, 1987; Brown *et al.*, 1989). The clones have characteristics of helper T cells in that the antigen-specific proliferative responses occurs in the absence of exogenous growth factors, and the responding cells produce T cell growth factor activity. Although cytolytic activity was demonstrated in some clones (Baldwin *et al.*, 1992), the functional significance of these cells in protective immune responses is unknown.

1.1.4.4. Parasite strain specificity of cytotoxic T cell responses.

Heterogeneity of *T. parva* parasites has been demonstrated in a number of *in vitro* assays. A panel of monoclonal antibodies to schizont antigens detected polymorphisms among different stocks of the parasite (Minami *et al.*, 1983). Most of these antibodies react with a single antigen expressed by schizonts and sporozoites, referred to as the polymorphic immunodominant molecule (PIM). In addition to the expression of polymorphic epitopes, the PIM associated with different parasite strains exhibits variation in molecular weight (Toye *et al.*, 1991). Genomic diversity in different parasite stocks has also been demonstrated by using parasite-specific probes based on repetitive genomic sequences to detect restriction fragment length polymorphisms (RFLP) in Southern blots of parasite DNA (Conrad *et al.*, 1987a; Allsopp and Allsopp, 1988). In addition, the use of these techniques has revealed that various stocks of cattle- and buffalo- derived parasites contain a mixture of parasite populations (Conrad *et al.*, 1987b,1989a,b; Allsopp and Allsopp, 1988; Toye *et al.*, 1991).

Studies of the strain specificity of CTL responses to *T. parva* have focussed on two selected stocks of the parasite, Muguga and Marikebuni. In cross-protection experiments, cattle immunized with the Marikebuni stock were consistently immune to challenge with the Muguga stock, while a proportion of cattle immunized with Muguga were susceptible when challenged with Marikebuni (Irvin *et al.*, 1983). Initial studies of

CTL reponses in cattle immunized with the Muguga stock showed that in some instances the response was parasite strain-specific i.e. CTL specifically lysed Muguga-infected target cells but not cells infected with Marikebuni. In other animals, cross-reactive CTL were induced that could kill cells infected with either stock of the parasite (Goddeeris *et al.*, 1986a; Morrison *et al.*, 1987). However, study of the relationship between cross-protection and the strain specificity of CTL responses was complicated by the discovery that the Marikebuni stock contains a heterogeneous mixture of parasite strains (Conrad *et al.*, 1989b; Toye *et al.*, 1991). To overcome this problem, a cloned parasite population has been isolated from the Marikebuni stock (Marikebuni 3219) which shows a uniform profile with parasite-specific monoclonal antibodies and probes (Taracha *et al.*, 1995a). Two groups of cattle were immunized either with the Muguga stock or with Marikebuni 3219, and the specificity of the CTL responses was analysed in a limiting dilution assay. In both groups, the CTL responses were specific for the immunizing strain in a proportion of animals, whereas the CTL in the remaining animals recognized both parasites. There was a close correlation between the specificity of the responses and susceptibility to challenge with the heterologous parasite. Animals with cross-reactive CTL were immune, whereas those showing strain-specific CTL responses developed severe clinical reactions but recovered from the infection. These experiments provide further evidence for the importance of CTL responses in mediating immunity to *T. parva*.

Early studies on the MHC restriction of CTL responses to *T. parva* in cattle heterozygous at the bovine lymphocyte antigen (BoLA)-A locus demonstrated a bias in the response to one or other BoLA specificity (Morrison *et al.*, 1987). These observations have subsequently been confirmed in more detailed investigations of the relationship between strain specificity of CTL responses and MHC phenotype (Goddeeris *et al.*, 1990; Taracha *et al.*, 1995b). The CTL responses in most cattle were shown to be restricted entirely by the products of one MHC haplotype, and there was a hierarchy in dominance among the haplotypes examined, with a consistent bias to some haplotypes in preference to others. One of the dominant haplotypes carries the genes encoding the serological specificities A10 and KN104. The majority of Muguga-immunized animals carrying this haplotype exhibit strain-specific CTL responses restricted entirely by the KN104 class I molecule. However, when animals carrying the A10, KN104 haplotype were immunized with Marikebuni 3219, they produced CTL responses that were either

A10-restricted and specific for Marikebuni or KN104-restricted and cross-reactive (Taracha *et al.*, 1995b). These differences were also observed in sets of identical twins where one of each pair had been immunized with Muguga and the other with Marikebuni. This is in agreement with previous studies which demonstrated that CTL clones with different MHC restriction specificities generated from a single animal recognized distinct parasite strains (Goddeeris *et al.*, 1990). Taken together, these findings provide evidence that the parasite strain used for immunization can influence the MHC restriction and/or the parasite specificity of the CTL response.

1.1.4.5. Immune responses to primary infections.

The very high mortality rate following infection of susceptible cattle with *T. parva* demonstrates the failure of the immune system to mount an effective response to the parasite. Rapid replication of the parasitized cells is thought to outpace the development of cellular immune responses. However, at the time when schizonts are first detected at very low levels in the lymph node draining the site of inoculation, there is a massive increase in the cellularity of the node (Morrison *et al.*, 1981). At about the same time, uninfected T lymphoblasts form a significant proportion (up to 25%) of cells in the efferent lymph draining the node, while less than 2% of the cells are parasitized (Emery, 1988). Subsequently, there is a rapid increase in the numbers of parasitized cells in the lymph node and efferent lymph, such that during the second week of infection over 95% of blasts in the efferent lymph were found to contain schizonts (Emery, 1981a). These observations suggest that the initial increased cellularity of the drainage lymph node is due, at least in part, to a T cell response to parasitized cells occurring within the node. However, there is no evidence that the early T cell response has any inhibitory effect on the course of the infection. Parasite-specific cytotoxic cells are not detected at any stage during lethal infections with *T. parva* (Emery *et al.*, 1981b) and CTLp cannot be detected in the peripheral blood of naive cattle by limiting dilution analysis (Taracha *et al.*, 1992). Nevertheless, parasitized cells stimulate potent proliferative responses in PBMC from naive as well as immune animals (Pearson *et al.*, 1982; Goddeeris and Morrison, 1987). However, when PBMC from naive cattle were repeatedly stimulated *in vitro*, low levels of cytotoxicity were found in only a proportion of lines, and the responses were not MHC-restricted (Goddeeris *et al.*, 1986a). The responding cells

recognise cell surface determinants on infected cells, because glutaraldehyde-fixed stimulator cells can also stimulate a proliferative response, and supernatants from cultures of infected cells do not stimulate proliferation (Goddeeris and Morrison, 1987). The early T cell lymphoblast response in the drainage lymph node may reflect a similar process of non-specific T cell activation occurring *in vivo*.

1.1.4.6. Potential role of primary immune responses in pathogenesis of the infection.

Some of the observations made on the characteristics of parasitized cells during *in vitro* studies may be of relevance when considering the pathogenesis of the infection *in vivo*. Infected lymphocytes of all phenotypes constitutively express high-affinity IL-2 receptors (Dobbelaere *et al.*, 1990). Although parasitized cell lines can be maintained *in vitro* without exogenous growth factors, they fail to proliferate at cell densities of less than 2 x 10^2 cells/ml. However, addition of exogenous IL-2 significantly enhances the growth of infected cells seeded at suboptimal densities (Dobbelaere *et al.*, 1988). Thus IL-2, and possibly other cytokines, have the potential to stimulate the growth of parasitized cells *in vivo*. Stimulation of PBMC from both naive and immune cattle *in vitro* with autologous parasitized cells induces proliferative responses of similar magnitude and kinetics (Goddeeris and Morrison, 1987). Similarly, cells isolated from the lymphoid organs of infected cattle stimulate proliferative responses in autologous PBMC, even when the percentage of schizont-infected cells is very low (Emery and Morrison, 1980). If parasitized cells are able to induce comparable responses *in vivo*, cytokines produced by the responding cells could enhance the proliferation of parasitized cells and thus contribute to the pathogenesis of the disease.

Parasitized cells have the characteristics of constitutively activated lymphoblasts, and thus they may also be able to influence the development of immune responses by the host. The infected cells express MHC class II molecules and probably costimulatory molecules, and may therefore be able to present parasite antigens and induce activation of uninfected lymphocytes. Infected cell lines have been found to express mRNA for a variety of cytokines, and secretion of IL-2 and IFNγ has been detected using bioassays

(Brown and Logan, 1986; Entrican *et al.*, 1991; McKeever *et al.*, 1997). It has been clearly shown that cytokines present in the local microenvironment during priming of naive $CD4^+$ T cells have an important influence on their subsequent differentiation into Th1- or Th2-type effectors. Th1-type $CD4^+$ cells produce IL-2, IFNγ and TNFβ and induce cell-mediated immune responses (e.g. delayed-type hypersensitivity reactions, macrophage activation) that are effective against intracellular pathogens. Th2-type responses are induced by extracellular pathogens and allergens, and are characterized by the production of IL-4, IL-5 and IL-10, which promote differentiation of B cells to antibody producing cells and recruitment and activation of mast cells and eosinophils (Mosmann and Coffman, 1989). Inappropriate induction of Th2-type responses in BALB/c mice infected with *Leishmania major* is associated with progressive disseminated infections due to failure to control parasite replication (Heinzel *et al.*, 1991). The induction of Th2-type responses is dependent on the presence of IL-4 during priming of naive $CD4^+$ precursors, while differentiation into Th1-type effectors is promoted by IL-12 (Hsieh *et al.*, 1992; Seder *et al.*, 1993; Mattner *et al.*,1996). These cytokines also inhibit differentiation of the reciprocal Th subset. Thus the relative amounts of different cytokines present during priming of T cell responses may have a significant effect on the outcome of infection.

Parasitized cells may also produce cytokines or other soluble factors that have an immunosuppressive effect on host immune responses. Supernatants from infected T cell lines grown at high cell densities have a marked inhibitory effect on allogeneic mixed leucocyte reactions (MLR), but supernatants from parasitized B cell lines have no suppressive activity (Goddeeris and Morrison, 1987). It is possible that parasitized T cells may also produce such suppressive factors *in vivo*, resulting in inhibition of parasite-specific immune responses. However, these observations *in vitro* suggest that immune suppression might only be significant when high levels of parasitosis are reached.

The finding that *T. parva*-infected cells can induce potent *in vitro* proliferative responses in PBMC from naive cattle suggests that the parasite may possess a mechanism for non-specific lymphocyte activation. As discussed above, triggering of a similar response *in vivo* could benefit the parasite by producing cytokines that promote proliferation of

schizont-infected lymphocytes while failing to generate parasite-specific effector cells capable of eliminating the infection. The large number of T lymphoblasts detected in the drainage lymph node at the time when parasites are first detected is evidence that such a response may be occurring. One possible mechanism by which the parasite could trigger non-specific activation of large numbers of T cells is by expression of a superantigen. Unlike conventional antigens, superantigens interact only with the Vβ element of the TCR, and activate all T cells expressing a restricted subset of Vβ regions. In order to determine whether a superantigen is responsible for T cell activation during *T. parva* infections, an important aim of this project was to examine the TCR Vβ repertoire expressed by T cells participating in the response to the parasite *in vivo.* Thus, to provide the background to this investigation, the remainder of the introduction will focus on the T cell receptor and the properties of superantigens.

1.2. The T Cell Receptor.

An essential feature of the immune system of vertebrates is the ability to mount highly specific responses against a vast array of foreign antigens, and to discriminate between these and self-antigens derived from the host cell proteins. The cells responsible for the specificity of the response are B and T lymphocytes, and the basis for their specificity lies in the expression of polymorphic antigen receptors on the cell surface. For B cells these receptors are immunoglobulin molecules, which recognise conformational determinants on protein and non-protein molecules. The T cell antigen receptor (TCR) recognizes peptide fragments of foreign antigens in association with MHC molecules on the surface of antigen presenting cells. Peptides are generated by enzymatic degradation of proteins by cytosolic proteosomes or lysosomal enzymes. Fragments of cytosolic proteins are translocated into the endoplasmic reticulum, where they form stable complexes with MHC class I heavy chains and β_2-microglobulin that are exported and expressed on the cell surface (this is termed the *endogenous* pathway of antigen processing). Before being expressed at the cell surface, newly synthesized MHC class II molecules are targeted to a specialized compartment of the endosomal-lysosomal system, where they bind fragments of proteins that have been internalized by phagocytosis or endocytosis and degraded by lysosomal proteases (the *exogenous* pathway of antigen processing). In both MHC class I and MHC class II molecules, the peptides are bound in a groove formed by two α-helices in the membrane-distal domains of the molecule. The T cell receptor recognizes determinants on both the antigenic peptide and the associated MHC molecule. The affinity of the interaction between the TCR and peptide/MHC complex is low, but is stabilized in part by coreceptors expressed on T cells that interact with non-polymorphic determinants on the MHC molecules. CD4 molecules are expressed by helper T cells and bind to MHC class II molecules, while CD8 molecules are expressed on cytotoxic T cells and bind to MHC class I molecules. Further stabilization of the ternary complex of TCR, MHC molecule and peptide is provided by the interactions of a number of cell surface molecules on T cells with their specific ligands on antigen presenting cells, for example, CD28/B7, CD2/LFA-3, LFA-1/ICAM-1. In addition to their role in cell-cell adhesion, these molecules are also involved in the transduction of signals essential for T cell activation; for this reason, they are commonly referred to as costimulatory molecules.

1.2.1. Structure and diversity of the T cell receptor.

The T cell antigen receptor was initially characterized using clonotypic monoclonal antibodies that could either block or stimulate the activation of T cell clones and immunoprecipitate polymorphic disulphide-linked heterodimeric molecules (Kappler *et al.*, 1983). Subsequently, isolation and sequencing of complementary DNA clones encoding these polypeptides revealed that they contained sequences homologous to those of immunoglobulins, encoding a variable and a constant domain (Hedrick *et al.*, 1984; Sim *et al.*, 1984). The heterodimers were composed of α and β chains in the majority of T cells in the mouse; however a second type of TCR, composed of γ and δ chains was also identified (Brenner *et al.*, 1986). Transfer of the genes encoding the α and β chains of the TCR was shown to transfer both antigen and MHC specificity between T cells (Dembic *et al.*, 1986). Both α/β and γ/δ heterodimers are expressed at the cell surface in association with a complex of non-polymorphic polypeptides, collectively termed CD3. The CD3 complex contains at least five proteins, termed γ, δ, ε, ζ, and η, which are involved in signal transduction from the antigen receptor to the interior of the cell. These invariant chains are also necessary for the assembly and transport of the TCR complex to the cell surface.

1.2.1.1. Genomic organization of the TCR genes.

Sequence analysis of cDNA clones encoding the four TCR polypeptides (α, β, γ, δ) showed that the molecules contained sequences homologous to the variable (*V*), diversity (*D*), junctional (*J*) and constant (*C*) gene segments of immunoglobulins. The genomic organization of the TCR genes is also very similar to that of the immunoglobulin loci; i.e. tandem arrays of *V*, *D*, *J* and *C* gene segments are arranged over a considerable length of chromosomal DNA. For example, the human TCR β chain locus covers almost 700kb of DNA and encodes eight trypsinogen genes in addition to the TCR gene segments (Rowen *et al.*, 1996). Specific *V*, *D* (β and δ chains only) and *J* segments are joined by a process of somatic recombination to form a complete V region-coding exon immediately 5' to a *C* gene segment. As for immunoglobulin gene rearrangements, recombination is controlled by conserved recombination signal

sequences (RSS) that flank the *V*, *D* and *J* gene segments (Toyonaga *et al.*, 1985; Yoshikai *et al.*, 1985). The RSS consist of conserved heptamer and nonamer sequences separated by non-conserved spacer regions of either 12 or 23 nucleotides. An RSS with a 12 base pair (bp) spacer may recombine only with one containing a 23 bp spacer and *vice versa*; thus the arrangements of RSSs flanking the various gene segments determines which gene combinations are possible. The mechanisms for rearrangement of gene segments involve both looping-out and deletion and inversion, depending on the orientation of the sequences being joined. The products of two homologous recombination activating genes, RAG-1 and RAG-2, are essential for the rearrangement of antigen receptor genes in B and T cells, although their exact function is unknown (Schatz *et al.*, 1989; Shinkai *et al.*, 1992).

The TCR α, β, γ, and δ chains are encoded by *TCRA*, *TCRB*, *TCRG* and *TCRD* genetic loci respectively. The *TCRA* locus is unique among antigen receptor loci in that it contains the entire *TCRD* locus within the region encompassing the *AV* and *AJ* gene segments. There is considerable variation between the different TCR loci in both the numbers of gene segments and the overall organization of genes. Figure 1.1 gives a schematic representation of the *TCRA* and *TCRB* loci in humans. In mice and humans, the *TCRB* locus contains two very similar (and functionally equivalent) *TCRBC* gene segments, each of which is associated with a single *TCRBD* gene segment and a cluster of *TCRBJ* gene segments located 5' to the *BC* gene. In the mouse, the two *TCRBJ* clusters (*BJ1* and *BJ2*) each contain six functional gene segments and one pseudogene. The human locus contains six *BJ1* gene segments and seven *BJ2* gene segments, all of which are functional. Most of the *TCRBV* gene segments are located 5' to the *BD-BJ-BC* gene clusters. The DNA sequence for the entire human *TCRB* locus on chromosome 7 has recently been published (Rowen *et al.*, 1996). A cluster of six non-functional *TCRBV* genes (designated orphon genes) has also been identified on chromosome 9 (Robinson *et al.*, 1993). Sixty-five *TCRBV* gene segments were identified, of which 46 appeared to be functional. These gene segments are grouped into 30 subfamilies, whose members share at least 75% nucleotide sequence identity. The criterion of 75% similiarity for subfamily members derives from studies in which the numbers of *TCRAV* and *TCRBV* genes were estimated from the number of bands hybridizing to V region-specific probes in Southern

blots of genomic DNA (Barth *et al.*, 1985; Kimura *et al.*, 1987), nucleotide sequence homologies of about 75% or greater being required for cross-hybridization. Members of 24 human *TCRBV* subfamilies are expressed, and some also contain pseudogenes; the other subfamilies contain only pseudogenes. Most of the subfamilies contain multiple members, with the largest subfamilies being *BV5* (7 members), *BV6* (9 members), *BV8* (5 members), and *BV13* (8 members). In contrast, most of the 25 murine *TCRBV* subfamilies contain a single member, the exceptions being *BV5* and *BV8*, which each have three members (Arden *et al.*, 1995b). Five subfamilies contain pseudogenes (Louie *et al.*, 1989), so that the number of functional *TCRBV* gene segments in the mouse is estimated at twenty-two. A summary of the numbers of different *TCRB* gene segments in mice and humans is given in Table 1.1.

Comparison of the sequences of different *TCRBV* subfamilies within a species reveals that, on average, they display less than 40% identity at the amino acid level. However, when the deduced protein sequences of human and mouse *TCRBV* gene segments were compared, 14 murine subfamilies were shown to display >60% similarity to their human homologues (Clark *et al.*, 1995). Genome mapping of *TCRBV* gene segments has revealed that the relative order of the homologous *TCRBV* subfamilies is highly conserved in mice and humans (Lai *et al.*, 1988). In humans, multi-membered *TCRBV* subfamilies have arisen as a result of internal duplications and subsequent divergence within the *TCRB* locus (Rowen *et al.*, 1996). In some cases, the duplications have increased the size of individual *BV* subfamily gene clusters, e.g. *BV8* (Sui *et al.*, 1986), while in others, tandem duplication of *BV* gene segments from different subfamilies has resulted in interspersion of clusters of *BV* genes unrelated by homology, for example, members of the *BV5*, *BV6* and *BV13* subfamilies (Li *et al.*, 1991).

The organization of the *TCRA* locus is also very similar in humans and mice. Both species have a single *TCRAC* gene segment separated from the upstream *AV* region by an extended cluster of *TCRAJ* gene segments, containing 61 functional elements in humans, and 50 in mice. The *TCRDV* gene segments are interspersed among the *TCRAV* segments, and a limited number of *V* gene segments are used in both α and δ chains. Human *AV* gene segments are grouped into 32 subfamilies, the majority of which contain

a single member (Arden *et al.*, 1995a). In contrast, 88 *AV* gene segments have been identified in mice, which fall into 20 subfamilies, most of which have multiple members (Arden *et al.*, 1995b). A summary of the *TCRA* genes of mice and humans is presented in Table 1.1. As described for the human *TCRB* locus, members of the different murine and human *TCRAV* subfamilies are interspersed on the chromosome.

Table 1.1. Summary of the numbers of *TCRA* and *TCRB* gene segments in humans and mice.

Gene segments	Human		Mouse	
	TCRA	*TCRB*	*TCRA*	*TCRB*
TCRC	1	2	1	2
TCRJ	61	13	50	12
TCRD	-	2	-	2
TCRV	40[a]	65[b]	88[a]	29[a]
Multi-membered *TCRV* subfamilies (number of members)[a]	*AV1* (5) *AV2* (3) *AV4* (2) *AV7* (2) *AV14* (2)	*BV5* (7) *BV6* (9) *BV7* (3) *BV8* (5) *BV9* (2) *BV12* (3) *BV13* (8) *BV21* (3)	*AV1* (8) *AV2* (9) *AV3* (8) *AV4* (11) *AV5* (3) *AV7* (2) *AV8* (15) *AV9* (2) *AV10* (8) *AV11* (7) *AV13* (2) *AV14* (2) *AV16* (2) *AV17* (3) *AV18* (2)	*BV5* (3) *BV8* (3)

Notes: a) These figures are derived from the classification of Arden *et al.* (1995a,b) and include non-functional *TCRV* gene segments (pseudogenes)
b) This figure is derived from the sequence of the entire human *TCRB* locus published by Rowen *et al.* (1996).

A.

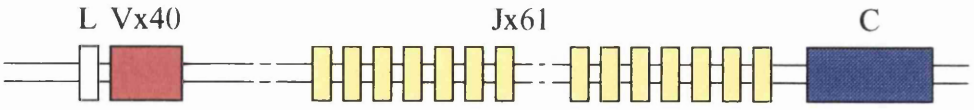

B.

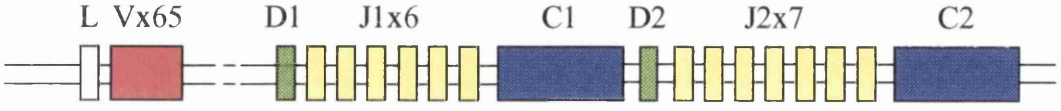

Figure 1.1. The organization of the human *TCRA* (A) and *TCRB* (B) gene loci. L = leader sequence, V, D, J and C stand for variable, diversity, joining, and constant gene segments respectively. See text for full explanation.

Although the genomic organization of bovine TCR genes has not been investigated, cDNA clones encoding the bovine TCR α, β, γ, and δ chains have been isolated and sequenced (Ishiguro *et al.*, 1990; Tanaka *et al.*, 1990; Takeuchi *et al.*, 1992). Clones containing *TCRA* and *TCRB* sequences were isolated from a cDNA library prepared from bovine peripheral blood lymphocytes. Seven full-length *TCRAV* sequences were grouped into five subfamilies, and eighteen different *TCRAJ* segments were identified (Ishiguro *et al.*, 1990). Thirteen distinct *TCRBV* gene segments representing nine different subfamilies were identified in clones containing functional *TCRB* transcripts, and twelve different *TCRBJ* gene segments were also found (Tanaka *et al.*, 1990). Probing of Southern blots of genomic DNA with *AC*- and *BC*-specific probes confirmed that, in common with most other species, cattle possess one *TCRAC* gene segment and two *TCRBC* segments. Southern blots of genomic DNA from four bovine breeds were also hybridized with eight *BV*-specific probes and two different *BC*-specific probes. This analysis failed to detect any restriction fragment length polymorphisms (RFLP) with the enzymes *Pst* I and *Eco* RI and, furthermore, the *BV*-specific probes hybridized with a limited number of bands, suggesting that bovine *TCRBV* subfamilies have relatively few members (Tanaka *et al.*, 1990). However, four RFLP alleles were subsequently detected in bovine genomic DNA digested with *Taq* I, using an uncharacterized *BV*-specific probe (Lundén *et al.*, 1991).

Comparison of the bovine *TCRBV* sequences with those of homologous human *TCRBV* subfamilies revealed sequence similarities of at least 63% at the protein level, while the amino acid similarity between *BV* genes from the different bovine subfamilies ranged from 18% to 53% (Tanaka *et al.*, 1990). This is in agreement with the results obtained from comparison of mouse and human *TCRBV* sequences (see above). In fact, when the analysis was extended to subfamilies within the *TCR A/D* and *G* families, sequences in almost every murine subfamily were found to have closer homology to a human *V* gene segment than to a member of another mouse subfamily (Clark *et al.*, 1995). Although extensive sequence comparisons have not been possible in other species, the limited data available suggests that this general principle holds true in, for example, rabbits and horses (Isono *et al.*, 1994; Schrenzel *et al.*, 1994; Schrenzel and Ferrick, 1995). The degree of conservation varies between different subfamilies; for example, some members of the

TCRBV6 subfamily have been extensively conserved between different mammalian groups (Buitkamp *et al.*, 1993). These observations suggest that a set of ancestral *V* gene segments has been retained during the evolution of species, but that different diversification strategies involving gene duplication and/or deletion have modified the repertoire as the species diverged.

1.2.1.2. Nomenclature for TCR gene segments.

Historically, the V gene segments and subfamilies have been named according to their order of discovery. According to this arbitrary numerical nomenclature, members of the same subfamily share the first digit and differ in the second, for example, Vβ8.1, Vβ8.2 and Vβ8.3 are all members of the Vβ8 subfamily. A standardized system of nomenclature for TCR gene segments suitable for application in all species has recently been devised by the WHO-IUIS Nomenclature Sub-Committee on TCR Designation (Williams *et al.*, 1993). The names for the genetic loci (*A*, *B*, *G*, *D*) and gene segments (*V*, *D*, *J*, *C*) are self-explanatory and have been used so far in this discussion. *S* refers to gene segments and is used to enumerate and distinguish subfamily members. Based on these principles, a revised nomenclature has been proposed, following detailed analysis of all the available human and mouse TCR variable gene sequences (Arden *et al.*, 1995a,b). However, the traditional numbering of *V* gene segments in the order of their discovery was preserved, except where there was conflict with the names of other segments. Thus, murine homologues of human *V* gene segments do not have the same subfamily designation. In other species a convention of numbering *TCRV* gene segments according to the human *TCRV* subfamilies to which they showed closest sequence homology has generally been adopted (Tanaka *et al.*, 1990; Isono *et al.*, 1994; Schrenzel *et al.*, 1994).

Following the publication of the complete genomic sequence of the human *TCRB* locus by Rowen *et al.* (1996), these workers proposed that *V* subfamilies should be assigned consecutive numbers, starting at the 5' end of the locus. Individual subfamily members would then be numbered sequentially after the subfamily designation. However, this system has not been adopted as yet and, if it is to be applied to all *TCRV* gene segments, will require complete mapping or sequencing of all the TCR loci.

1.2.1.3. Generation of diversity in T cell receptors.

The basis for the diverse repertoire of B cell and T cell receptor specificities lies in the organization of the *IG* (encoding immunoglobulins) and *TCR* genetic loci. Most of the antigen receptor diversity is generated during the rearrangement of *V*, (*D*) and *J* gene segments to form the exon encoding the V region. Although most of the genetic mechanisms for the generation of diversity are common to both B and T cells, their relative contribution varies, with the result that variability is concentrated in different parts of the binding sites of immunoglobulins and TCR.

Combinatorial diversity in both immunoglobulins and TCRs is generated by the random association of different *V*, *D* and *J* elements during gene rearrangements. The number of potential combinations is a function of the numbers of different gene segments encoded in the germline. The repertoire of *V* gene segments used by the TCR is small in comparison to that of immunoglobulins; for example, approximately 20 *BV* and 100 *AV* gene segments are employed by the murine α/β TCR, compared to the 250-1000 *VH* or *VK* gene segments available to immunoglobulins. Thus, assuming that there is random association of TCR α and β chains, the estimated number of Vα x Vβ combinations is only 2000, while the immunoglobulins can generate up to 250000 different V region combinations (Davis and Bjorkman, 1988). However, the diversity at the V-J junction of TCRs greatly exceeds that of immunoglobulins. Junctional diversity is generated by a number of mechanisms. A relatively large number of *J* gene segments (in mice, 50 *AJ* and 12 *BJ*) are used by TCRs compared to the 4 *J* elements found in mouse *IGH* and *IGK* loci. The boundaries of the gene segments to be joined are cleaved by exonucleases, which also remove a variable number of nucleotides from the ends of the *V* (3'), *D* (5' and 3') and *J* (5') elements (Rowen *et al.*, 1996). Non-germline (N) nucleotides are then added to the junctions between gene segments by the enzyme terminal deoxynucleotidyl transferase (TdT). N region diversification is found in all four TCR polypeptides, but is confined to the heavy chains of immunoglobulins. In addition, the *D* gene segments of TCR β and δ chains can be translated in all three reading frames, a rare event in immunoglobulin heavy chains (Abergal and Claverie, 1991). When these mechanisms are taken into account, an estimated 10^{15} different junctional combinations can be predicted

for murine α/β T cells, compared to only 10^{11} combinations for immunoglobulins (Davis and Bjorkman, 1988).

Further diversification of immunoglobulins occurs by a process of somatic hypermutation during B cell differentiation into antibody-producing cells following stimulation by specific antigen. Although one report provided preliminary evidence for somatic hypermutation of TCR Vα regions in germinal centres (Zheng *et al.*, 1994), these findings have not subsequently been confirmed, and it is unlikely that this mechanism contributes to TCR diversity.

1.2.1.4. The structure of the α/β T cell receptor.

The similarities between the deduced primary sequences of the TCR α and β polypeptide chains and those of immunoglobulins suggested that the molecules would also have a similar three-dimensional structure. Both molecules are part of the immunoglobulin superfamily which includes many proteins involved in cell recognition in the immune system, e.g. MHC class I and class II molecules, β_2-microglobulin, CD2, CD4 and CD8. The extracellular portion of members of this superfamily is composed of a variable number of discrete domains, each of which has a characteristic tertiary structure known as the immunoglobulin fold. The basic features of the immunoglobulin fold have been elucidated by X-ray analysis of crystallized antibodies. Each domain is approximately 110 amino acids long, and comprises two β-sheets consisting of 3-4 anti-parallel β strands. The β-sheets are stabilized by interactions between hydrophobic amino acids and by an intrachain disulphide bond. Pairs of domains on separate chains can fold together in turn to create a functional quaternary structure as, for example, in V_L-V_H and C_L-C_H pairing to form functional immunoglobulins.

Calculations of variability, defined as the number of different amino acids occurring at a given position divided by the frequency of the most common amino acid at that position (the Wu-Kabat coefficient of variability), have demonstrated that immunoglobulin V regions have three distinct hypervariable regions (HVRs) separated by relatively conserved framework regions. The first two HVRs are located within the *V* gene

segment, while the third occurs at the *V-J* or *V-D-J* junction. In X-ray crystallographic studies of the structure of antibodies, it was demonstrated that the HVRs in V_H and V_L domains are brought together by pairing of heavy and light chains to form a cluster of loops at the tip of the Fab arm of the molecule, which corresponds to the antigen-binding site. Since the HVRs are responsible for antigen binding, they are also commonly referred to as complementarity-determining regions (CDRs). When the combining site of an immunoglobulin molecule is viewed from above, the first and second CDRs on V_L are separate from their counterparts on V_H, and the space between them is occupied by the two CDR3 regions.

Although the overall sequence homology between immunoglobulin and TCR polypeptides is relatively low, residues that are responsible for the conserved structure of the domain framework are identical or very similar in both sets of molecules (Patten *et al.*, 1984). From an analysis of immunoglobulins of known structure, Chothia *et al.* (1988) identified 40 sites crucial for the conserved structure of the variable domains. The sites responsible for the conserved framework are buried between the domain β-sheets, or on the loops between the strands. In addition, the residues that determine the way in which the V_L and V_H domains pack together, and residues in V_H that form contacts with conserved residues in the C_H1 domain, were identified. When the sequences of Vα and Vβ regions were examined, they were found to contain the same or very similar residues at sites homologous to the 40 conserved residues in immunoglobulin V domains. Based on these results, it was predicted that the α/β TCR would have a framework structure very close to that found in immunoglobulins, and that the Vα and Vβ domains would pack together with a geometry close to that of V_L and V_H domains. To facilitate comparison of the protein sequences of immunoglobulins and TCRs, a common numbering system for the amino acid residues was proposed by Kabat *et al.* (1991), based on the alignment of functionally conserved residues, and has been widely used in studies of TCR structure.

Computation of the Wu-Kabat coefficient of variability for amino acid positions in Vα or Vβ regions demonstrates a much broader distribution of variability throughout the V region, rather than the three distinct hypervariable regions found in immunoglobulins.

Nevertheless, three hypervariable regions can be distinguished that are similar in size and position to the antibody CDRs, with the greatest variability being concentrated in the third HVR (Concannon *et al.*, 1986; Jores *et al.*, 1990). Thus, in the predicted structure of the α/β TCR, these hypervariable loops are arranged in a manner similar to that found in the antigen-binding site of immunoglobulins (see Figure 1.1.). A fourth hypervariable region (HVR4), which is located between CDR2 and CDR3, has been identified in the TCR β-chain; in the predicted three-dimensional structure of the molecule this region formed a loop that lay in close proximity to CDR1β and CDR2β (Jores *et al.*, 1990), as shown in Figure 1.1.

Recently, the crystal structure of the complete extracellular fragment of a glycosylated α/β TCR has been resolved by X-ray diffraction studies (Garcia *et al.*, 1996). The TCR was derived from a murine cytotoxic T cell clone with specificity for a self-peptide bound to MHC class I H-2K^{b} molecules. The results of this analysis showed that the the TCR α and β chains fold into a quaternary structure that resembles the antigen binding region (Fab) of antibodies, and confirmed the predictions of the earlier models of TCR structure. The structure determined by Garcia *et al.* is illustrated in Figure 1.2, with the CDRs and the HVR4 region of the β-chain highlighted in colour.

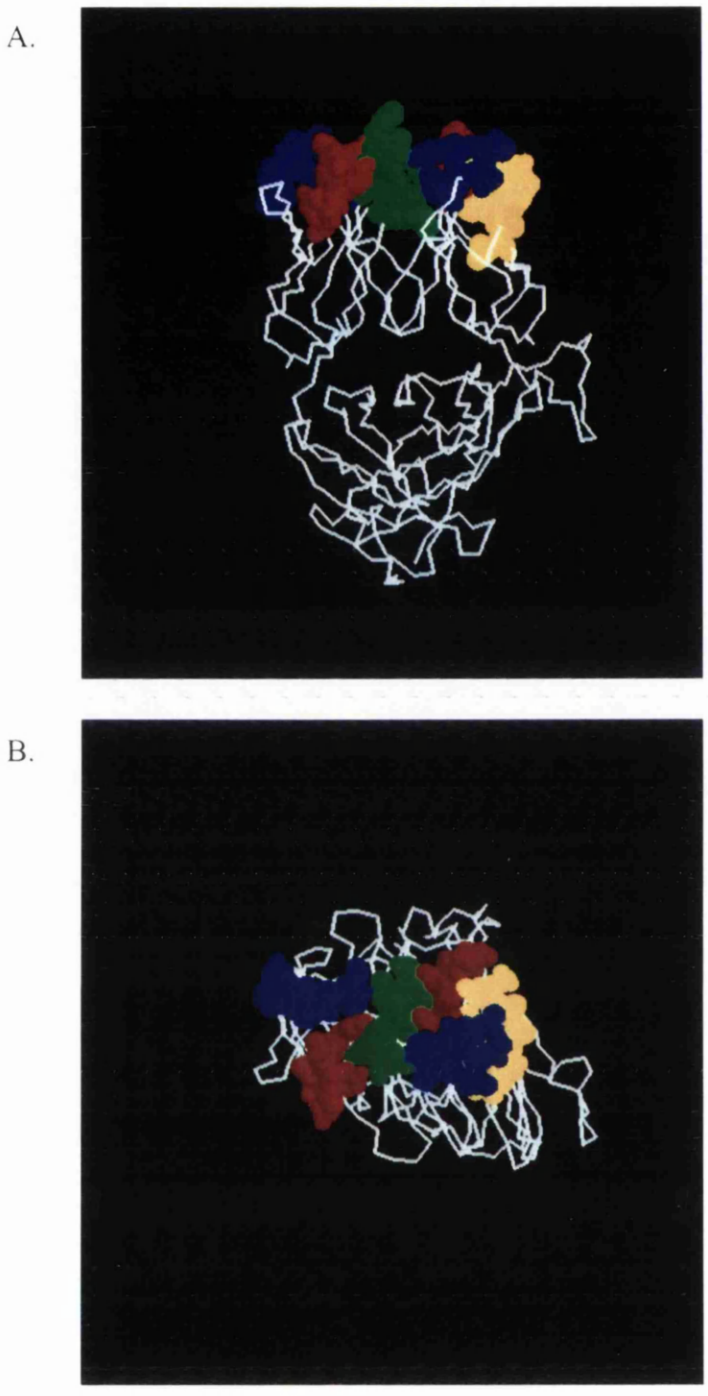

Figure 1.2. Three-dimensional structure of the α/β TCR plotted from the co-ordinates deposited in the Brookhaven Database by Garcia *et al.* (1996). A. Side view of the TCR with the α-chain on the left and the β-chain on the right. B. The TCR rotated 90° towards the viewer, looking directly down on the antigen/MHC binding site. The CDR1 loops are shown in red, the CDR2s in blue and the CDR3s in green. The HVR4 loop on the β-chain, which has been implicated in superantigen binding, is shown in yellow.

The TCR Vα and Vβ regions can be further classified into various subgroups, which have certain framework residues in common. These variations in certain residues are predicted to produce small and local differences in the framework structure of different subgroups (Chothia *et al.*, 1988). TCR Vβ sequences were first divided into two subgroups by Schiffer *et al.* (1986), based on the presence of paired residues that can form a salt bridge. Salt bridges have been detected in all immunoglobulin molecules examined by X-ray crystallography, suggesting that they may be an important feature of the protein structure. The majority of sequences in subgroup I are capable of forming a salt bridge between an aspartate residue (Asp) at postion 86 and an arginine (Arg), lysine (Lys) or histidine (His) at position 64. The residues that form salt bridges in immunoglobulins are found at similar locations. In contrast, subgroup II sequences have glycine (Gly) at position 63 and glutamine (Gln) at position 86 and are therefore incapable of forming a salt bridge. In addition, all subgroup I sequences have a phenylalanine (Phe) at position 65 and serine (Ser) at position 87, while subgroup II sequences have a tyrosine (Tyr) at position 65, and most have a threonine (Thr) at position 87.

As greater numbers of sequences became available, the subgroup classification was extended by Chothia *et al.* (1988), who proposed six Vα and five Vβ subgroups. In this system, subgroups consist of sequences whose protein sequences are >50% identical if they are from the same species, or >40% identical if they are from different species. The Vβ subgroups I-III correspond to Schiffer's subgroup I, in that they contain an invariant Phe at position 65 and other conserved residues capable of forming a salt bridge. Subgroup IV sequences have an invariant Tyr at position 65 (as in Schiffer's subgroup II). Subgroup V contains only two sequences, one murine and one human, which both contain a leucine (Leu) at position 65. Subsequently, the discovery of human and murine sequences that do not fit into this classification has led to the proposal of further subgroups (Robinson, 1991). So far, the subgroup classification has not been extended to species other than humans, mice and rabbits.

1.2.1.5. Interaction of the α/β TCR with peptide/MHC.

X-ray crystal structures of MHC class I and class II molecules have shown that peptide fragments of antigens are located in a specific binding groove, formed by the outer domains of the molecules and comprising a β-pleated sheet bounded on either side by α-helices (Bjorkman *et al.*, 1987). From these structures it has also become apparent that many of the polymorphic residues of MHC molecules are focused on interactions with peptides. Based on the predicted similarities in structure between the α/β TCR and immunoglobulins, a model for TCR interaction with peptide/MHC was put forward (Davis and Bjorkman, 1988; Chothia *et al.*, 1988). This model proposed that the CDR1 and CDR2 loops on Vα and Vβ contact relatively conserved residues on the α-helices of the MHC molecule, while the highly diverse CDR3 loops are principally responsible for peptide contact. Support for this hypothesis has come from studies in which mutation of residues in the CDRs of TCR α and β chains has been shown to affect T cell recognition, with certain substitutions resulting in complete abolition of the T cell response (Nalefski *et al.* 1992; Bellio *et al.*, 1994). However, attempts to transfer peptide or MHC specificity by exchanging the CDR loops of one TCR β-chain for those of another have been unsuccessful (Patten *et al.*, 1993).

In an attempt to identify Vα and Vβ elements or junctional sequences involved in recognition of antigen/MHC, numerous studies have related the primary structure of TCR α and β chains from T cell clones to their fine specificity for a defined peptide/MHC combination. In some cases, the majority of clones specific for a particular peptide/MHC complex express the same *TCRAV* and *BV* gene segments and have conserved junctional sequences (CDR3) in the α- and/or β-chain (Hedrick *et al.*, 1988; Urban *et al.*, 1988; Casanova *et al.*, 1992). For example, most murine T cell clones specific for the carboxyl-terminal fragment of pigeon cytochrome c (pcc) presented by the MHC class II molecule I-E^k express Vα11.1 and Vβ3, and show striking conservation of the β-chain junctional sequence encoding CDR3, although the response is clearly polyclonal (Hedrick *et al.*, 1988). In particular, an asparagine residue, partly encoded by N-region nucleotides, is found at position 100 in almost every clone. Mutation of this residue resulted either in abolition of the response or in altered antigen

fine specificity, confirming its importance in antigen recognition (Engel and Hedrick, 1988). Similar patterns of conservation of the V elements and junctional sequences have also been found in human CTL clones specific for influenza A virus matrix protein or nucleoprotein peptides presented by the MHC class I molecules HLA-A0201 and HLA-B27, respectively (Moss *et al.*, 1991; Bowness *et al.*, 1993; Lehner *et al.*, 1995). However, there are many other examples of both MHC class I and class II restricted responses, in which the responding T cells exhibit diverse TCR gene usage, or Vβ conservation alone (Taylor *et al.*, 1990; Casanova *et al.*,1991; Boitel *et al.*, 1992). These results suggest that contacts between the TCR and MHC/peptide complex can be made in a number of different ways. In fact, in studies using MHC molecules mutated at residues predicted to interact with the TCR, it has been shown that very limited changes in either a CDR3 loop of the TCR or in a contact residue of the antigenic peptide can have a profound effect on relatively distant TCR/MHC interactions (Ehrich *et al.*, 1993). Thus the same TCR can contact an MHC molecule in different ways depending on the interaction with peptide residues.

The X-ray structure of a crystallized ternary complex of a TCR, MHC class I molecule and peptide has recently been determined (Garcia *et al.*, 1996). The Vα and Vβ CDR3s, as predicted, were located over the central part of the peptide and appeared to play a prominent role in peptide interaction. CDRs 1 and 2 contacted the α-helices of the MHC molecule; however, the CDRα1 and CDRβ1 loops also contacted residues at the amino and carboxyl terminals of the peptides respectively. Thus, although previous models were derived for TCR/MHC class II systems, the predictions they make are largely in agreement with the results of structural analysis.

1.2.2. Factors influencing the T cell receptor repertoire.

As discussed already, T cells have the potential to express a vast array of different antigen receptors, generated by the recombination of large numbers of different *V*, (*D*) and *J* gene segments and mechanisms for introducing junctional diversity. However, the TCR repertoire expressed by mature T cells in the periphery is more limited than that which would be predicted by completely random association of gene segments. The

major influences on the TCR repertoire are genetic polymorphisms within the *TCR* loci, and the processes of positive and negative selection during thymocyte maturation.

In the mouse, germline deletions within the *TCRB* locus, involving up to half the *TCRBV* gene segments, have been found both in inbred laboratory strains and in wild mice (Behlke *et al.*, 1986; Pullen *et al.*, 1990a). In one laboratory strain (NZW) a deletion containing *TCRBC1*, *TCRBD2* and the *BJ2* cluster has also been identified (Kotzin *et al.*, 1985). At least two such deletions have also been found in the *TCRB* locus in humans (Seboun *et al.*, 1989), one of which involves two functional *TCRBV* gene segments (Zhao *et al.*, 1994). Although mice with massive deletions within the *TCRB* locus appear healthy and phenotypically normal, their ability to respond to certain antigens is impaired, indicating that there are limits to the redundancy of the TCR repertoire (Nanda *et al.*, 1991; Kumar and Sercarz, 1994).

The extent of the expressed TCR repertoire is also influenced by allelic polymorphisms within the coding regions of *TCRV* genes. Restriction fragment length polymorphism (RFLP) analyses have suggested the existence of a small number of alleles for most *TCRV* genes in mice and humans (Klotz *et al.*, 1989; Charmley *et al.*, 1990; Posnett, 1990). However, direct sequence analysis of *V* gene segments isolated from genomic DNA demonstrated that, in most cases, polymorphisms within the coding regions of different alleles were confined to a limited number of nucleotide substitutions (usually less than five), some of which were silent (Robinson, 1989; Smith *et al.*, 1990; Li *et al.*, 1990; Cornélis *et al.*, 1993; Reyburn *et al.*, 1993). Some of the coding substitutions may influence interactions with peptide/MHC; a single amino acid substitution in the predicted CDR1 of murine Vβ3 was shown to alter dramatically the TCR α/β repertoire used in an antigen-specific, MHC-restricted immune response (Gahm *et al.*, 1991). However, allelic polymorphism may also limit the expressed TCR repertoire through the introduction of point mutations which produce stop codons (Wade *et al.*, 1988; Charmley *et al.*, 1993) or substitution of functionally important residues (Luyrink *et al.*, 1993). Surprisingly, the resultant null alleles were maintained at relatively high frequencies in the human populations studied (Charmley *et al.*, 1993; Barron and Robinson, 1994). Polymorphisms located in the non-coding regions of *V* genes may also

influence the level of expression of certain gene segments; for example, an allele of the human *BV3* gene that differs only by a single nucleotide substitution in the 23bp spacer of the RSS is expressed at very low levels, presumably due to an alteration in the recombination process (Posnett *et al.*, 1994). Mapping of polymorphic loci in different individuals has demonstrated that multiple distinct *TCRB* haplotypes result from frequent recombination between these loci (Cornélis *et al.*, 1993; Day *et al.*, 1994).

The peripheral α/β TCR repertoire is also profoundly influenced by the processes of positive and negative selection to which thymocytes are exposed during thymic maturation. The thymus is colonized by stem cells migrating from the bone marrow, which are negative for T cell markers. These cells undergo expansion and differentiation over a period of about three weeks to produce mature immunocompetent T cells, expressing functional α/β TCRs and T cell differentiation antigens, including either CD4 or CD8 (Shortman, 1992). Only a small proportion of thymocytes (<5%) differentiate fully to produce mature T cells that are exported to the periphery; the majority die within the thymus as a result of selection processes or the failure to express a functional TCR. The *TCRB* locus is rearranged first, and expression of a productively rearranged β-chain inhibits further recombination at this locus, a phenomenon known as allelic exclusion (Uematsu *et al.*, 1988). Expression of a functional β-chain as part of the pre-TCR also promotes survival and expansion of the immature $CD4^-CD8^-$ thymocytes, permitting differentiation to the next developmental stage, the double positive ($CD4^+CD8^+$) thymocyte (Mombaerts *et al.*, 1992; Groettrup and von Boehmer, 1993). This involves rearrangement of the *TCRA* genes, and α/β TCRs are initially expressed at low levels by double positive (DP) thymocytes. DP thymocytes expressing functional TCRs are then selected based on the interaction of their TCRs with self-MHC molecules expressed by thymic stromal cells; cells bearing TCRs that do not recognize self-MHC molecules undergo apoptosis. Low affinity interactions between the TCR and self-MHC/ peptide promote survival of immature thymocytes and differentiation into mature thymocytes that express either CD4 or CD8 (positive selection) (von Boehmer, 1994). DP thymocytes expressing TCRs with high affinity for self MHC/peptide combinations, i.e. potentially self-reactive cells, are eliminated by a deletional mechanism (negative selection) (Nossal, 1994). The TCR repertoire of those cells that survive thymic selection

and are exported to the periphery is therefore determined both by the MHC phenotype of the individual and by the products of "background" polymorphic genes that generate some of the self peptides complexed to MHC molecules in the thymus (Vukusic *et al.*, 1995).

The influence of MHC genes on the peripheral TCR repertoire has been demonstrated in MHC disparate strains of mice (Bill *et al.*, 1988), and in studies of large human families, HLA-identical sibs had more similar patterns of *V* segment frequencies than mismatched or haploidentical sibs (Akolkar *et al.*, 1993). In addition, significant biases in the expression of certain *V* gene segments towards either the $CD4^+$ or the $CD8^+$ subset of T cells have been observed, which may reflect a differential effect of MHC class II and class I molecules on positive selection of thymocytes (Singer *et al.*, 1990; Akolkar *et al.*, 1993). Although evidence has been presented for the involvement of polymorphic non-MHC genes in thymic selection, few have actually been characterized (Fry *et al.*, 1989). An exception are the *Mtv* loci in mice (formerly designated *Mls*), which correspond to endogenous retroviruses (mouse mammary tumour viruses) integrated into the genome. These loci encode superantigens which mediate intrathymic deletion of the majority of T cells expressing specific Vβ elements, and can therefore significantly alter the peripheral TCR repertoire (Vacchio and Hodes, 1989). There is no evidence for similar superantigen-mediated Vβ deletions in humans (Baccala *et al.*, 1991).

Despite considerable inter-individual variation, the peripheral TCR repertoire has a similar overall pattern of *BV* and *BJ* gene usage even in individuals of differing MHC phenotype, in that some gene segments are frequently expressed while others are rarely utilised (Okada and Weissman, 1989; Rosenberg *et al.*, 1992; Malhotra *et al.*, 1992). This variation is independent of thymic selection, as examination of the TCR repertoire of unselected thymocytes reveals similar biases in the use of certain gene segments (Okada and Weissman, 1989; Baccala *et al.*, 1991; Jores and Meo, 1993). The cause of differential expression of *BV* genes is unknown, but presumably reflects their relative ability to undergo recombination. However, there is no obvious correlation between the order of murine *BV* gene segments on the genome and their relative levels of expression

(Okada and Weissman, 1989), and human *BV* subfamily members expressed at different levels have conserved promoter and RSS sequences (Rowen *et al.*, 1996).

Environmental factors, such as exposure to infectious agents, superantigens or mitogens, may also play a role in shaping the TCR repertoire. In normal human subjects, the *TCRBV* repertoire of circulating $CD8^+$ T cells is frequently altered as a result of the oligoclonal expansion of $CD8^+$ subsets (Hingorani *et al.*, 1993). These expanded subsets have a 'memory' phenotype and presumably arise initially in response to infection, but in some cases have been shown to persist for months or even years.

1.3. Superantigens.

The term 'superantigen' was coined to describe molecules capable of stimulating a strong proliferative response in unprimed T cells, comparable to that induced by mitogens. It was used initially to describe certain soluble bacterial toxins, such as the staphylococcal enterotoxins, which stimulate potent T cell proliferative responses *in vitro* (Choi *et al.*, 1989). These proteins were found to be capable of stimulating T cells that express a specific set of *TCRBV* gene segments, regardless of the other variable components of the TCR (Kappler *et al.*, 1989). At about the same time, different groups of investigators observed that, in mice expressing the proteins encoded by the *Mls-1*^{a} genes, T cell subsets bearing specific Vβ elements were deleted from the pool of immature thymocytes (Kappler *et al.*, 1988; MacDonald *et al.*, 1988). Furthermore, a high frequency of T cells or T cell hybridomas expressing these Vβ elements proliferated *in vitro* in response to stimulation with splenocytes from *Mls-1*^{a} mice. Thus it appeared that the bacterial superantigens and the product of the *Mls-1*^{a} gene might interact with the TCR in a similar manner. The *Mls* loci were originally described by Festenstein (1973), who found that vigorous mixed leukocyte reactions (MLR) could be initiated between MHC-identical strains of mice. The polymorphic genetic loci controlling the response mapped outside the MHC, and their products were named minor lymphocyte stimulating (*Mls*) antigens. Genetic studies showed that the *Mls* antigens were encoded by a number of unlinked biallelic loci, and that only one allele from each *Mls* locus is

stimulatory in an MLR. However, the nature and function of the *Mls* antigens remained obscure until comparatively recently.

The nature of the antigens encoded by the *Mls* loci became clearer following the discovery of a genetic linkage between expression of the *Mls* antigens and the presence of endogenous mouse mammary tumour viruses (MMTV) integrated into the host genome (Dyson *et al.*, 1991; Frankel *et al.*, 1991). Infection of neonatal mice with exogenous MMTVs transmitted in milk was also shown to result in Vβ-specific deletion of subsets of T cells (Ignatowicz *et al.*, 1992). Subsequently, it was demonstrated that mice transgenic for the MMTV(GR) genome or the open reading frame (*orf*) within the 3' long terminal repeat (LTR) of the virus, deleted $V\beta14^+$ T cells from their peripheral repertoire (Acha-Orbea *et al.*, 1991). In addition, transfection of the *orf* sequence into a B cell line conferred the ability to stimulate $V\beta14^+$ T cells and hybridomas *in vitro* (Choi *et al.*, 1991). These findings provided definitive proof that an MMTV gene encoded a protein with *Mls*-like properties. Accordingly, the *Mls* loci are now more commonly referred to as *Mtv* loci.

1.3.1. Properties of superantigens.

As outlined above, superantigens interacting with T lymphocytes through the Vβ domain of the TCR are able either to activate a high proportion of unprimed mature T cells, or delete immature thymocytes. Since there is a relatively small number of *TCRBV* genes, the estimated frequency of precursors responding to *Mls* antigens in limiting dilution analyses is in the range 1:30 to 1:10 (MacPhail *et al.*, 1985). In contrast, T cell recognition of a conventional foreign peptide/MHC complex, involves all the variable components of the TCR (Vα, Jα, Vβ, Dβ, Jβ, and non-templated junctional residues) and, accordingly, the estimated frequencies of precursors in unprimed populations are of the order of $1:10^6$ to $1:10^4$.

Although MHC class II molecules are required for the presentation of superantigens to T cells, presentation differs from that of conventional antigens in several ways. There does not appear to be a requirement for antigen processing, since fixed antigen-presenting

cells are capable of presenting staphlyococcal enterotoxins (SE) to T cells (Yagi *et al.*, 1988). In addition, the T cell response is not restricted to antigen-presenting cells bearing autologous MHC molecules; superantigens can be also be recognized in the context of multiple MHC class II alleles and isotypes, including xenogeneic class II molecules (Fleischer *et al.*, 1989; Mollick *et al.*, 1989). Conventional MHC class II-restricted T cell responses are confined to the $CD4^+$ subset; however, superantigens bound to class II molecules can activate both $CD4^+$ and $CD8^+$ T cells.

1.3.1.1. Structure of superantigens.

The staphylococcal enterotoxins and toxic shock syndrome toxin-1 (TSST-1) are the most intensively studied of the bacterial superantigens. The X-ray crystallographic structures for SEB and TSST-1 have been determined (Swaminathan *et al.*, 1992; Prasad *et al.*, 1993). They are globular basic proteins, with a similar general structure consisting of two closely packed domains. Mutagenesis studies of SEB have identified two MHC-binding sites widely separated on one face of the molecule, and TCR contact residues in the groove formed by the domain interface (Kappler *et al.*, 1992).

In contrast, much less is known about the protein structure of the superantigens of MMTV, partly due to low levels of expression. *In vitro* translation experiments have demonstrated that the *orf* gene in the 3' LTR (also referred to as the *sag* gene) has the potential to produce a Type II transmembrane glycoprotein with a short amino (NH_2) terminal cytoplasmic tail and a large extracellular carboxyl (COOH) terminus (Korman *et al.*, 1992; Choi *et al.*, 1992). Comparison of the sequences of the MMTV and *Mtv* superantigens reveals approximately 85% overall amino acid homology, with most of the differences concentrated in a stretch of highly polymorphic amino acids at the COOH-terminus. The *sag* genes can be grouped into seven families of homologous sequences that correlate with the TCR Vβ specificities of the gene products (SAGs) (Acha-Orbea and MacDonald, 1995). When chimeric SAGs were tested for activity, it was found that only the polymorphic COOH-terminus was required to confer Vβ specificity (Yazdanbakhsh *et al.*, 1993). A monoclonal antibody (mAb) raised against a COOH-terminal SAG peptide can detect low levels of expression on the surface of activated B

cells, and block T cell responses. Immunoprecipitation studies with the same mAb revealed a 45 kDa glycosylated protein as the predominant intracellular form of the molecule; however, an 18 kDa fragment was expressed at the cell surface (Winslow *et al.*, 1992). Proteolytic processing of the 45 kDa precursor is required for superantigen activity, and the 18 kDa product has been shown to bind to MHC class II molecules (Winslow *et al.*, 1994; Park *et al.*, 1995).

1.3.1.2. Interactions of superantigens with MHC molecules and T cell receptors.

The discovery that bacterial exotoxins did not require processing for presentation by MHC class II molecules (Yagi *et al.*, 1990), and could be shown to bind directly to MHC class II molecules, independently of allotype or isotype (Scholl *et al.*, 1989; Mollick *et al.*, 1989), suggested that they bound to relatively non-polymorphic residues on the MHC molecule and not in the peptide binding groove. This was confirmed by Dellabona *et al.*, (1990) who showed that mutation of the residues in one of the α-helices forming the antigen-binding groove of a class II MHC molecule could abolish presentation of conventional peptide antigens but had negligible effects on superantigen presentation. However, individual MHC class II molecules vary in their effectiveness at presenting bacterial superantigens to T cells, reflecting preferential binding to certain class II isotypes. In general, the bacterial toxins bind HLA-DR molecules better than HLA-DQ and have little affinity for HLA-DP proteins (Scholl *et al.*, 1989; Herrmann *et al.*, 1989).

It appears that the superantigenic toxins have slightly different, but overlapping, binding sites on the MHC class II molecule. SEA has two separate MHC binding sites, one of which binds with high affinity and involves a histidine residue at position 81 on the DRβ chain, while the other mediates a low-affinity interaction with the DRα chain, permitting cross-linking of MHC class II molecules by the toxin (Hudson *et al.*, 1995). The structure of SEB bound to HLA-DR1 has been determined by X-ray crystallography (Jardetzky *et al.*, 1994). The MHC-binding face of this interacts with residues of the α1 domain of DR1 outside the peptide-binding site, as predicted by mutagenesis studies. Using chimeric α- and β-chains of DR and DP, it has been shown that the α1 domain of

DR is also essential for high affinity binding of TSST-1 (Karp *et al.*, 1990). Recently it has been found that the peptides bound by MHC class II molecules have an influence on the binding of SEA and TSST-1, and that a restricted subset of peptides are able to promote the presentation of these SAGs (Wen *et al.*, 1996).

The association of *Mtv* superantigens with MHC class II molecules is less well defined; however, indirect evidence suggests that class II molecules are also essential for presentation of MMTV SAgs. For many *Mtv* SAGs, expression of the mouse MHC class II I-E molecules (the murine homologue of DR) is crucial for induction of clonal deletion, whereas others can also be presented with varying efficiency by different I-A alleles (the murine homologue of DQ) (Kappler *et al.*, 1988; MacDonald *et al.*, 1989). Similarly, the SAGs encoded by exogenous MMTVs are most efficiently presented by I-E molecules (Held *et al.*, 1994b). In addition, an 18 kDa fragment of the *Mtv-7* SAG generated by proteolytic processing of a precursor protein has been shown to bind to MHC class II molecules (Winslow *et al.*, 1994). As for bacterial SAgs, the product of *Mtv-7* can also be presented to mouse T cells by human MHC class II DR molecules (Subramanyam *et al.*, 1993). However, HLA-DR molecules that had been mutated at the residues responsible for binding SEA, SEB and TSST-1 were still able to present *Mtv* SAGs, indicating the two types of superantigens have different binding sites on class II molecules (Thibodeau *et al.*, 1994).

The first insight into the elements of the TCR that interact with *Mtv* superantigens came from analyses of wild mice that expressed alleles of Vβ8.2 which differed by a few amino acids. One allele conferred *Mls-1*^{a} (*Mtv-7*) reactivity to T cells, while the others did not (Pullen *et al.*, 1990a). Analysis of the amino acid differences, and subsequent mutagenesis experiments, identified three residues that were responsible for interaction with the SAG (Pullen *et al.*, 1990b). One of these residues was located in the putative CDR1 while the others were found in the fourth hypervariable region (HVR4) and in the predicted three-dimensional structure of the TCR the residues were clustered in close proximity to one another on the lateral solvent-exposed face of the Vβ domain. Similarly, T cells bearing the human Vβ13.2 element respond to the toxin SEC2, whereas those expressing Vβ13.1 do not. Introduction of ten amino acid residues at positions 67-77 of

Vβ13.2 into Vβ13.1 conferred reactivity to SEC2 on the mosaic molecule. This is the same region of the Vβ domain that was implicated in the binding of Mls-1^a (Choi *et al.*, 1990a). In addition, mutation of residues in the Vβ CDR1 has been shown to affect recognition of staphylococcal toxins (Bellio *et al.*, 1994), and in mutagenesis studies involving the transfer of CDR loops from Vβ3 onto a Vβ1 framework, transfer of CDR1 and CDR2 could confer reactivity to SEB and SEA (Patten *et al.*, 1993). The crystal structures of a TCR β-chain complexed with SEC2 and SEC3 have been determined, and confirmed that these SAGs contacted residues in CDR1, CDR2, HVR4, as well as neighbouring framework residues (Fields *et al.*, 1996).

In the X-ray crystal structure of SEB bound to HLA-DR1, the TCR binding site of the toxin is positioned above and to the side of the MHC peptide-binding groove. The alignment of these residues with the HVR4 of a TCR Vβ domain leads to a model of the MHC/SAG/TCR complex in which the CDRs of the TCR are oriented over the peptide-binding site, and the Vα domain is above the class II β1 domain. This model is consistent with a role for both TCR α-chain and MHC polymorphism in modulating superantigen stimulation through direct TCR-MHC interactions (Jardetzky *et al.*, 1994). In fact, it has been shown that for certain SAG-TCR interactions the Vα or Dβ-Jβ regions and the MHC haplotype of the presenting cell may influence superantigen recognition (Woodland *et al.*, 1993; Waanders *et al.*, 1993; Borrero *et al.*, 1995). It was proposed that when a superantigen has relatively weak affinity for the MHC or Vβ, the TCR-MHC contacts may play an important role in stabilising the trimolecular complex. However, if the affinity of the SAG for both MHC and TCR is strong, the TCR-MHC interaction is irrelevant, and T cells expressing the relevant Vβ element will be activated irrespective of the paired Vα domain or presenting MHC class II molecule (Woodland and Blackman, 1993). A schematic representation of the interaction of a superantigen with an MHC class II molecule and a TCR is shown in Figure 1.3.

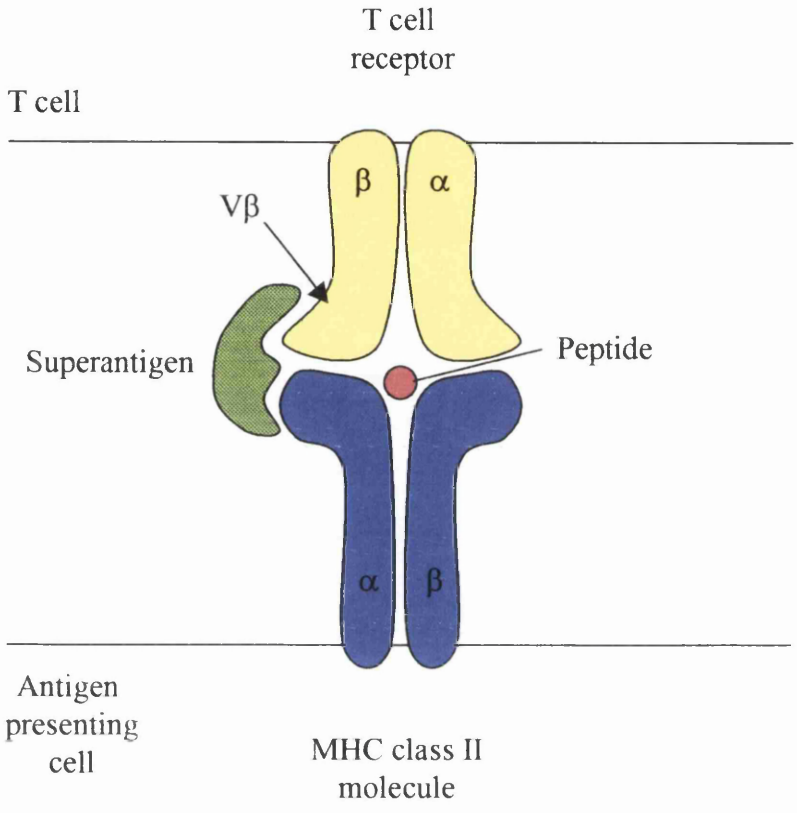

Figure 1.3. Schematic diagram illustrating the interaction of an exogenous superantigen, e.g. staphylococal enterotoxin B, with an MHC class II molecule and a T cell receptor (TCR). Conventional peptide antigens are bound in a groove formed by the membrane-distal domains of the α and β chains of the MHC molecule, and interact with determinants of both the Vα and Vβ domains of the TCR. In contrast, the superantigen binds to the α chain of the MHC class II molecule outside the peptide-binding groove, and interacts with the lateral surface of the TCR Vβ domain.

1.3.1.3. Superantigen-mediated T cell activation and tolerance.

The responses of T cells to superantigens and conventional peptide antigens appear very similar, with either stimulus capable of triggering proliferation, cytokine production and effector functions such as cytotoxicity (Fischer *et al.*, 1990; Bette *et al.*, 1993; Herrmann *et al.*, 1990). However, there is evidence that T cell activation by superantigens is mediated by pathways that are distinct from those used in responses to conventional antigens (reviewed by Webb and Gascoigne, 1994). Superantigen stimulation of T cell clones with *Mtv* antigens or SEB failed to trigger phosphatidylinositol hydrolysis or a rise in the intracellular free calcium ion concentration, changes that accompany T cell activation by conventional antigens, despite inducing comparable proliferative responses and IL-2 production (Liu *et al.*, 1991; Oyaizu *et al.*, 1992). The differences in T cell activation induced by conventional peptide antigens and superantigens, and by different superantigens, may reflect the different modes of interaction of these molecules with the TCR ligand, leading to activation of functionally distinct signalling pathways, and/or a differential contribution from accessory molecules.

In addition to specific engagement of the TCR by a peptide/MHC complex, normal T cell responses are dependent on costimulatory signals mediated by accessory molecules on T cells and antigen presenting cells for full expression of the activated phenotype. The CD4 and CD8 coreceptors are also believed to play a role in TCR signal transduction through an associated cytoplasmic tyrosine kinase ($p59^{lck}$). In contrast, the requirements for co-stimulation and engagement of coreceptors during T cell activation by superantigens appear to be less strict. Anti-CD4 MAbs can inhibit proliferation and IL-2 production of $CD4^+$ T cell clones in response to a specific peptide, but have no inhibitory effect on the response of the same clones to stimulation with SEB (Oyaizu *et al.*, 1992). $CD8^+$ T cells bearing the appropriate TCR Vβ region respond to superantigens presented by MHC class II molecules, in contrast to conventional peptide antigens which must be presented on MHC class I molecules for recognition by $CD8^+$ T cells. SAG-stimulated $CD8^+$ T cells lyse class II^+ target cells in the presence of the SAG, and lysis is not inhibited by anti-CD8 mAbs (Herrmann *et al.*, 1990). These findings suggest that binding of the CD4 and CD8 coreceptors to MHC class II and class I molecules is not required for T cell

recognition of superantigens. This may be explained by the much higher affinity binding of the TCR to SAG/MHC class II complexes than to MHC /peptide combinations (Seth *et al.*, 1994), or by a higher density of SAG/MHC complexes on antigen presenting cells.

Costimulatory signals for T cell activation can be delivered by the interaction of a number of cell surface molecules with their ligands on antigen-presenting cells. These receptor-ligand pairs include CD2/LFA-3, LFA-1/ICAM-1 or ICAM-2 and CD28/B7. The differential effect of these costimulatory molecules on T cells is not well understood; however, the interaction of CD28 and B7 molecules provides one of the most potent costimulatory pathways for activation of resting T cells. The requirement for costimulation in T cell responses to superantigens is controversial. In the absence of antigen-presenting cells, a soluble mAb to CD28 was able to synergize with SEB to produce a proliferative $CD4^+$ T cell response *in vitro* (Goldbach-Mansky *et al.*, 1992). However, proliferative responses of T cells to SEA and SEB presented by IFNγ-treated keratinocytes (which express MHC class II molecules, ICAM-1 and B7) were inhibited by mAbs against LFA-1 or ICAM-1, but not by mAbs against the B7 ligands of CD28 (Nickoloff *et al.*, 1993). These *in vitro* findings have been confirmed in studies using mice with targeted disruption of the genes encoding certain adhesion molecules. Mice deficient in ICAM-1 are unable to mount a proliferative response of SAG-reactive splenic T cells following injection of SEB (Gonzalo *et al.*, 1995). In contrast, in adult mice deficient in CD28 expression, Vβ-specific expansion of SAG-reactive T cells still occurs following infection with MMTV, although the response is reduced in comparison to that of wild-type mice (Palmer *et al.*, 1996). These studies suggest that the requisite costimulatory signals for conventional antigens and superantigen are different. The CD28/B7 costimulatory pathway is not essential for T cell activation by SAGs, but appears to increase the sensitivity of T cells to SAG stimulation (Muraille *et al.*, 1995).

In adult mice injected with SEB or cells expressing Mtv SAGs, there is a marked T cell proliferative response followed by clonal deletion or anergy (antigen-specific non-responsiveness) of SAG-reactive cells (Webb *et al.*, 1990; MacDonald *et al.*, 1991). Although both $CD4^+$ and $CD8^+$ T cells bearing the appropriate Vβ element are expanded in the initial proliferative response to SEB, clonal deletion and anergy induction seem to

affect mainly $CD4^+$ T cells (Kawabe and Ochi, 1990,1991; Herrmann *et al.*, 1992). SAG-reactive T cells appear to be eliminated by apoptotic cell death, and there is evidence that proliferation is required for clonal deletion *in vivo* (Kawabe and Ochi, 1991; Renno *et al.*, 1995). This agrees with a study of T cell responses to *Mtv* SAGs, in which the degree of clonal deletion correlated with the extent of the initial T cell proliferative response, and was influenced by various factors including the MHC haplotype of the host, the Vβ element examined and the particular *Mtv* SAG studied (Webb *et al.*, 1994). However, repeated administration of very low doses of SEA to mice resulted in almost complete elimination of $V\beta3^+$ T cells without detectable prior expansion of this population, suggesting that a massive proliferative response is not an essential prerequisite for SAG-mediated T cell deletion (McCormack *et al.*, 1993).

SAG-reactive T cells that escape clonal deletion *in vivo* appear to be rendered anergic; that is, when restimulated *in vitro* with the SAG used for priming, they fail to proliferate and have a defect in IL-2 production (Rammensee *et al.*, 1989; Kawabe and Ochi, 1990; MacDonald *et al.*, 1991). However, it seems that the state of apparent anergy observed *in vitro* is not reflected in unresponsiveness of SAG-primed T cells *in vivo*. Upon challenge of SE-primed mice with the homologous toxin, SAG-reactive $CD8^+$ cells display cytolytic activity and produce normal levels of IFNγ (Kawabe and Ochi, 1990; Sundstedt *et al.*, 1994). In addition, although SAG-reactive $CD4^+$ T cells are not clonally expanded following restimulation, they also appear to retain effector functions such as cytokine production and help for B cell differentiation (Bandeira *et al.*, 1991; Gaus *et al.*, 1994; Heeg *et al.*, 1995). Thus the state of anergy is reversible, perhaps reflecting different activation signals that operate during *in vivo* but not *in vitro* stimulation.

1.3.2. The role of superantigens in the pathogenesis of disease.

Although the properties of superantigens and their interactions with cells of the immune system have been the subject of detailed investigation and are now quite well understood, less is known about their role in the host-pathogen interactions occurring during infectious diseases. In addition to the MMTV SAGs and staphylococcal exotoxins, superantigen activity has been associated with a range of pathogenic organisms including

streptococci (Marrack and Kappler, 1990; Tomai *et al.*, 1990), *Mycoplasma arthriditis* (Cole and Atkin, 1991), *Mycobacterium tuberculosis* (Ohmen *et al.*, 1994), rabies virus (Lafon *et al.*, 1992) and Epstein-Barr virus (EBV) (Sutkowski *et al.*, 1996). The discovery that a large proportion of patients infected with the human immunodeficiency virus (HIV) show selective anergy of $V\beta8^+$ T cells has fuelled speculation that a superantigen may play a role in the pathogenesis of the acquired immunodeficiency syndrome (AIDS), although this is still a controversial theory (Dadaglio *et al.*, 1994; Westby *et al.*, 1996).

The infection of mice with exogenous MMTVs provides the most completely understood example of the important role that superantigens can play in the life cycle of an infectious organism (reviewed by Acha-Orbea and MacDonald, 1995). Exogenous MMTVs are transmitted from mother to pups in milk and enter the Peyer's patches through the gut epithelium. Infection is lifelong, and the major target cells for virus replication are epithelial cells of the mammary gland. Transmission of infection from the gut to the mammary gland is dependent on an intact immune system. Transgenic mice expressing high levels of a MMTV SAG showed specific deletion of $V\beta14^+$ T cells and failed to transmit the homologous virus when infected by the natural route, suggesting that SAG-reactive T cells are required for the virus to complete its life cycle (Golovkina *et al.*, 1992). The inoculation of an exogenous MMTV into the footpad of mice produces initial marked expansion of SAG-reactive $CD4^+$ T cells in the drainage lymph nodes, followed by deletion of these cells (Held *et al.*, 1992), and this model has been used to dissect the role of superantigens in the life cycle of the virus. It appears that the initial targets for infection are B cells, which present the virus-encoded SAG to $CD4^+$ T cells following integration of the MMTV genome. The expansion of SAG-reactive $CD4^+$ T cells is paralleled by an increase in the numbers of IgG-secreting B cells, as a result of T cell-dependent activation and differentiation of infected cells (Held *et al.*, 1993a, 1994a). When SAG-reactive T cells are absent as a result of deletion by endogenous SAGs or expression of a transgenic TCR β chain that does not react with the viral SAG, MMTV transmission does not occur (Held *et al.*, 1993b). Thus, it appears that expression of the viral superantigen is necessary for clonal expansion of the infected B cell population, permitting efficient transmission of virus to the mammary gland. In neonatal mice

infected by the oral route, expansion of SAG-reactive $CD4^+$ T cells can be detected in the intestinal Peyer's patches within 5 days of infection, suggesting that the experimental model also reflects events occurring during natural infection (Karapetian *et al.*, 1994).

The role of superantigens in bacterial infections is less clear. The staphylococcal enterotoxins are associated with food poisoning in humans, producing acute, self-limiting attacks of vomiting and diarrhoea. The relevance of superantigenic T cell activation in the production of these symptoms has not been addressed. There is evidence that other bacterial exotoxins may be associated with the shock-like symptoms observed during certain staphylococci and streptococcal infections. Toxic shock syndrome is one such disease, characterized by fever and shock, and associated with infection by strains of *Staphylococcus aureus* that produce TSST-1. The majority of human T cells stimulated *in vitro* with TSST-1 specifically express Vβ2, and in a group of patients with toxic shock syndrome, most individuals were found to have marked expansions of $V\beta2^+$ T cells ($CD4^+$ and $CD8^+$) in the peripheral blood (Choi *et al.*, 1989,1990b). However, there was no evidence for deletion or anergy of the $V\beta2^+$ population following infection. In a murine model of toxic shock syndrome, T cells were shown to be essential for the development of lethal shock following injection of TSST-1. The pathogenesis of lethal shock appears to be mediated principally by TNF produced by T cells and activated macrophages (Miethke *et al.*, 1992; Bette *et al.*, 1993). However, under natural conditions the induction of shock by toxin-producing bacteria is a relatively rare event, and it is not clear how superantigen production benefits the bacteria.

It has been suggested that bacterial superantigens may contribute to the development of various autoimmune disorders by activation of potentially autoreactive T cells which are normally tolerant to self-antigens (reviewed by Renno and Acha-Orbea, 1996). For example, comparison of the *TCRBV* repertoire expressed by T cells infiltrating the joints of patients with rheumatoid arthritis with that of peripheral blood revealed oligoclonal expansion of T cells bearing a restricted subset of *BV* genes, including *BV3*, *BV14* and *BV17* (Paliard *et al.*, 1991; Howell *et al.*, 1991). There is high sequence similiarity among these *BV* genes, especially in the HVR4 region. This led to the proposal that, following T cell activation by a microbial superantigen, a few cross-reactive cells specific

for self-antigens may home to the joints and initiate an inflammatory response. This theory is supported by experiments with a number of different rodent models but, as yet, there is no definitive proof that SAGs are involved in human autoimmune diseases (Renno and Acha-Orbea, 1996).

A number of protozoan parasites, including *Plasmodium falciparum* and *Trypanosoma cruzi* have been shown to stimulate strong *in vitro* proliferative responses in T cells from non-immune individuals, leading to speculation that these organisms may also produce superantigens (Good *et al.*, 1987; Piuvezam *et al.*, 1993). The response of human PBMC from unexposed donors to stimulation with a *P. falciparum* schizont lysate or whole parasitized erythrocytes has been studied in some detail. The responding cells are predominantly 'memory' (i.e. $CD45RO^+$) $CD4^+$ α/β T cells and $V\gamma9/V\delta2$ T cells (Jones *et al.*, 1990; Goodier *et al.*, 1992; Currier *et al.*, 1992). However, the response is dependent on antigen-processing, and $CD4^+$ T cell clones generated from the responding population exhibit MHC-restricted responses to malaria parasites. The clones are also cross-reactive with a variety of different environmental organisms, and express a diverse array of TCR $V\beta$ elements (Currier *et al.*, 1995; Fell *et al.*, 1996). Similarly, the proliferative response of human T cells to *T. cruzi* is also dependent on antigen-processing, and the responding cells display heterogeneous *TCRBV* usage (Piuvezam *et al.*, 1993). These findings are inconsistent with superantigen-mediated T cell stimulation of the responses.

Recent studies by Denkers *et al.* (1994,1996) have provided evidence that there is a superantigen associated with *Toxoplasma gondii*. Non-immune mouse splenocytes stimulated *in vitro* with intact tachyzoites or soluble tachyzoite antigen show strong proliferative responses and produce IFNγ. The response was blocked by anti-MHC class II MAbs, but was not MHC-restricted, and cellular processing of the soluble antigen was not required for presentation. Among the proliferating cells, there was a preferential expansion of $CD8^+V\beta5^+$ T cells. In addition, selective expansion of both $CD4^+$ and $CD8^+$ $V\beta5^+$ T cells was observed during the acute phase of *T. gondii* infection of mice, and $V\beta5^+$ T cells from chronically infected or vaccinated animals were unresponsive to *in vitro* stimulation with a plate-bound Vβ-specific MAb. The induction of IFNγ production

by a parasite SAG might be expected to benefit the host, since IFNγ is crucial in controlling parasite infection. However, overproduction of IFNγ could also contribute to disease pathogenesis by stimulating high systemic levels of proinflammatory cytokines such as TNFα and IL-1. Early induction of IFNγ may be beneficial in reducing parasite numbers to levels that are not harmful to the host, while non-responsiveness of SAG-reactive T cells in the later stages of infection could prevent immune-mediated pathology, resulting in an optimal balance for survival of both pathogen and host.

Thus, although superantigen activity has been associated with a wide variety of pathogens, in many cases the potential advantage of this activity for survival of the organism is unclear. However, it is possible to speculate that the Vβ-specific activation of T cells with a wide variety of mostly irrelevant antigen specificities provides an important mechanism for evading protective immune responses. In addition, clonal deletion or tolerance induction of SAG-reactive cells may also limit the capacity of the immune system to mount an effective response.

1.4. Aims of the project.

Theileria parva preferentially infects bovine lymphocytes and induces a state of constitutive activation in the parasitized cells. Immune responses to the parasite in cattle are directed against the schizont-infected lymphocytes, and $CD8^+$ cytotoxic T cells have been demonstrated to play an important role in protective immunity. In susceptible cattle, however, MHC-restricted parasite-specific cytotoxic T cell responses are not detected, and it has been assumed that parasite replication outpaces the capacity of the immune system to respond to the infection. However, the presence of large numbers of lymphoblasts in the lymph nodes draining the site of inoculation, at a time when parasite numbers are very low, suggests that the host does mount a primary immune response which is ineffective in controlling the infection. The massive increase in the cellularity of the lymph node is evidence that the parasite is capable of stimulating a potent response. In line with this observation, parasitized cells induce strong *in vitro* proliferative responses in autologous PBMC from naïve cattle. The large numbers of responding cells

in the absence of detectable effector function suggests that the parasite may induce non-specific activation of lymphocytes. The ability to stimulate a strong immune response *in vivo* may paradoxically be of benefit to the parasite. The cytokines produced by the uninfected lymphoblasts could potentiate the growth of parasitized cells, which express functional IL-2 receptors. The action of a parasite-derived superantigen is one possible mechanism for non-specific activation of a high proportion of T lymphocytes in an unexposed individual.

The aim of the current study was to examine the nature of the primary immune response to infection with *T. parva* and, in particular, to determine whether a superantigen may be responsible for inducing lymphocyte activation in the drainage lymph node *in vivo*, and stimulating the strong proliferative responses generated by parasitized cells *in vitro*. The initial objective was to perform a detailed analysis of the phenotype of the responding cells in the drainage lymph nodes of cattle during the early stages of infection with *T. parva*. The cellular changes in the drainage lymph node were examined histologically, using immunocytochemistry. The expression of cytokines in the lymph nodes of infected cattle was also investigated. Phenotypic analysis of the responding cells in cultures of PBMC from naïve animals with autologous parasitized cells was carried out to determine whether this system could be used to model events in the lymph node.

The potential involvement of a superantigen in stimulating the T cell response in the drainage lymph nodes of animals infected with *T. parva* was assessed by analysis of *TCRBV* expression of uninfected lymphoblasts purified from lymph node suspensions. T cells responding to superantigens express a restricted subset of *TCRBV* genes, regardless of the MHC phenotype of the host. Since the extent of the bovine *TCRBV* repertoire has not been established, it was necessary initially to establish the background *TCRBV* repertoire in a normal lymph node as a basis for comparison, using the anchored PCR to permit inclusion of bovine *TCRBV* gene segments that had not been previously identified.

CHAPTER TWO

MATERIALS AND METHODS

2.1. Experimental Infections.

Calves used for experimental infections with *Theileria parva* were assumed to be naive, as the parasite does not occur in the UK. In each experiment, pairs of calves were infected by subcutaneous inoculation with a lethal dose of infective tick stabilate, half the dose being given on either side of the neck. The stabilate was generously provided by Professor C. G. D. Brown, Centre for Tropical Veterinary Medicine, University of Edinburgh, and was prepared from ticks infected with the Muguga stock of *T. parva,* according to the method described by Cunningham *et al.* (1973). The course of the infection was monitored daily by taking the rectal temperature, by assessment of lymph node size, and by staining smears obtained by needle biopsy of the prescapular lymph nodes for the presence of schizonts from day 5 of infection. Calves were either treated by intramuscular injection of buparvaquone (Butalex®; Coopers) at a dose of 20mg/kg on day 11 of infection, or were euthanased at different times after infection for collection of the prescapular lymph nodes.

2.1.1. Staining of lymph node biopsies for detection of schizonts.

Small numbers of lymph node cells were obtained by needle biopsy of the prescapular lymph node, and used to make smears on clean microscope slides. The smears were air-dried, then fixed in acetone for 10s, and washed with cold phosphate buffered saline (PBS – A.1). A few drops of a monoclonal antibody (MAb5) specific for the polymorphic immunodominant antigen (PIM) expressed by *T. parva* schizonts (ascitic fluid diluted 1:400 in culture medium) were added to the smears, and the slides were incubated in a humidified box for 30min at room temperature. They were then washed twice in cold PBS, and a few drops of fluorescein isothiocyanate (FITC)-conjugated goat anti-mouse IgG monoclonal antibody (Southern Biotechnology Associates Inc., Birmingham, Alabama, USA), diluted 1:40 in PBS, were added before incubating for a further 30min at room temperature in a humidified box. The slides were again washed twice in cold PBS, then a coverslip was placed over the smear for examination under

ultra-violet light on the microscope. A number of fields were examined under x40 power, the percentage of parasitized cells calculated from the number of schizonts counted per 2000 lymphoid cells. The schizont index is defined as the number of schizonts, both intracellular and extracellular, per 100 cell nuclei.

2.2. Techniques in cellular immunology.

2.2.1. Isolation of leucocytes.

2.2.1.1. Isolation of peripheral blood mononuclear cells (PBMC).

Blood was collected from calves by jugular venupuncture, using sodium heparin (Leo, Bucks., UK) at 10U/ml as anti-coagulant. The blood was diluted with an equal volume of sterile PBS in a 50ml Blue Max polypropylene tube (Falcon, Oxford, UK) and carefully underlaid with Histopaque (density 1.083; Sigma Chemicals Co. Ltd., Poole, Dorset, UK), then centrifuged at 1200xg for 30min. Separated leucocytes were harvested at the interface, washed three times in sterile PBS, counted and resuspended at the appropriate cell concentration in sterile culture medium (A.3) or PBS.

In experiments carried out at the International Livestock Research Institute (ILRI), Nairobi, Kenya, the procedure for isolating PBMC was slightly different. Blood was collected by jugular venupuncture into an equal volume of sterile Alsever's solution (A.2), which contains sodium citrate as anti-coagulant. This mixture was carefully underlaid with Ficoll-Paque (Pharmacia Biotech, St. Albans, Herts., UK), then centrifuged as above. The harvested leucocytes were washed three times in sterile Alsever's solution.

2.2.1.2. Collection of lymph node cells by needle biopsy.

Lymph node cells were collected into culture medium containing 10U/ml sodium heparin (Leo) at selected time points during the infection, by aspiration with a 21G needle and syringe. The cell suspension was made up to 5ml with sterile PBS and carefully underlaid with 4ml Histopaque in a 15ml Blue Max Jr. polypropylene tube (Falcon). Mononuclear cells were separated by centrifugation at 1200xg for 30min, harvested from the interface, and washed twice with sterile PBS by centrifugation at 200xg for 5min (4°C). The cells

were then resuspended at 5 x 10^6 cells/ml in PBS containing 0.1% w/v sodium azide (PBS/azide) and distributed at 5 x 10^5 cells/well in a 96-well U well microtitre plate (Sterilin, Stone, Staffs., UK) for staining with monoclonal antibodies. Alternatively, cells to be sorted were resuspended in sterile culture medium containing 1mM EDTA.

2.2.1.3. Isolation of leucocytes from lymph nodes.

Prescapular lymph nodes were removed from the calves immediately following euthanasia. Using sterile instuments, samples of the lymph nodes were teased apart in sterile Petri dishes (Sterilin) containing sterile PBS, and small pieces were gently disrupted by passing through a fine-meshed steel sieve. The resulting cell suspension was transferred to a 50ml Blue Max tube and left for a few minutes to allow large particles to settle. The supernatant was transferred to a fresh Blue Max tube and centrifuged at 200xg for 5min to pellet the cells. The cells were resuspended in PBS, counted and diluted to 10^7 cells/ml. Gradients were set up by carefully underlaying 10ml of cell suspension with 4ml Histopaque, and centrifuging at 1200xg for 30min. The cells harvested from the interface were pooled, washed twice with PBS and counted.

2.2.2. Flow cytometry and cell sorting.

2.2.2.1. Phenotypic analysis of leucocytes by immunofluorescent staining.

Monoclonal antibodies (mAbs) used in the phenotypic analysis of lymphocytes and cell lines are listed in Table 2.1. Antibodies derived from culture supernatants were used at a dilution of 1:10 for single staining and 1:5 for two-colour staining, while those derived from ascitic fluid were diluted 1:1000 for single staining or 1:500 for two-colour staining. The fluorochrome-labelled secondary antibodies mentioned below were supplied by Southern Biotechnology Associates, Inc., Birmingham, Alabama, and diluted 1:400 or 1:200 before use.

Cells distributed at 2-5 x 10^5 cells/well in a 96-well U well plate were resuspended in 25µl of primary antibody (for single staining) or 25µl each of two primary antibodies of different Ig isotypes (for two-colour staining). The cells were incubated either at room temperature for 10min or at 4°C for 30min, and then washed 3 times in 100µl PBS/azide

by spinning the plates at 200xg for 2min and discarding the supernatant. They were then resuspended in 25µl of the appropriate isotype-specific secondary antibodies, conjugated either to fluorescein isothiocyanate (FITC) or phycoerythrin (PE). Incubation conditions were as above, and the cells were again washed three times in PBS/azide, then resuspended in 100µl PBS/azide and diluted in 0.5ml sheath fluid (A.5) before examination on a FACScan analyser (Becton Dickinson, Mountain View, CA, U.S.A.). Negative controls were incubated with irrelevant antibodies of the same isotype as the test antibodies, and either the FITC- or PE-conjugated secondary antibodies. For two-colour staining the compensation was set using two controls, each stained with a test mAb and either the FITC- or PE-conjugated secondary antibodies.

2.2.2.2. Three-colour immunofluorescent staining.

5 x 10^5 cells from each animal were stained first with IL-A43 (anti-CD2; $IgG2_a$) and GB21A (anti-γδTCR; $IgG2_b$) mAbs by incubation with 25µl of each antibody (diluted as above) for 30min at 4°C. The cells were washed twice with PBS/azide and incubated with 25µl each of PE-conjugated goat anti-mouse $IgG2_a$ and FITC-conjugated goat anti-mouse $IgG2_b$ for 10min at room temperature. After one wash in PBS/azide, the cells were incubated for 10min at room temperature with 25µl PBS/azide containing 10% v/v normal mouse serum to block non-specific binding of the third mAb by the secondary monoclonals. The cells were washed again, then incubated with biotinylated CC63 (anti-CD8; diluted 1:2000) for 10min at room temperature, washed twice and incubated with Streptavidin-Cy-Chrome complex (Pharmingen, San Diego, CA, USA; diluted 1:25 in PBS/azide) as before. Two final washes were performed and the cells were resuspended in PBS/azide before analysis on the FACScan as above. Negative controls consisted of cells stained with irrelevant $IgG2_a$ and $IgG2_b$ mAbs and the appropriate FITC- and PE-conjugated isotype-specific secondary antibodies, and cells incubated with an irrelevant biotinylated mAb and Streptavidin-Cy-Chrome. The compensation circuits were set using three controls incubated with the test mAbs and FITC- or PE-conjugated secondary mAbs or Streptavidin-Cy-Chrome.

Table 2.1. Monoclonal antibodies used in phenotypic analysis and purification of bovine leucocytes.

Monoclonal antibody	Isotype	Specificity	Cell distribution
IL-A43[a]	$G2_a$	CD2	T cells
CC42[a]	G1	CD2	As above
CH128A[a]	G1	CD2	As above
IL-A45[a]	$G2_b$	CD2	As above
MM1A[b]	G1	CD3	T cells
CC30[c]	G1	CD4	Class II restricted T cells
CC8[c]	$G2_a$	CD4	As above
IL-A12[c]	$G2_a$	CD4	As above
CC63[d]	$G2_a$	CD8α chain	Class I restricted T cells
CACT80C[d]	G1	CD8α chain	As above
IL-A105	$G2_a$	CD8	As above
IL-A51[d]	G1	CD8α chain	As above
CC58[e]	G1	CD8β chain	As above
GB21A[f]	$G2_b$	γδ TCR	All γδ T cells
CC15[g]	$G2_a$	WC1	Peripheral γδ T cells
IL-A29[g]	G1	WC1	As above
IL-A58[h]	$G2_a$	Ig light chain	B cells
IL-A30[i]	G1	IgM	As above
CC21[k]	G1	CD21	As above
CC-G33[l]	G1	CD14	Monocytes/macrophages
CC94[m]	G1	CD11b	As above
IL-A24[n]	G1	MyD-1	Monocytes/macrophages/DC
CC149[n]	$G2_b$	MyD-1	As above
IL-A21	$G2_a$	MHC class II	As above
IL-A111[o]	G1	CD25	Activated lymphocytes
CACT108A[o]	$G2_a$	CD25	As above
NCL-Ki67-MM1[p]	G1	Ki67	Proliferating cells
MAb5[q]	-	PIM	*T. parva*-infected lymphocytes
AV29	$G2_b$	Chicken CD4	-
TRT3[r]	$G2_a$	G surface glycoprotein of turkey rhinotracheitis virus	-
TRT1[r]	G1	As above	-

Notes: References defining the specificity of mAbs: Davis and Splitter, (1991)[a], Davis *et al.* (1993)[b], Bensaid and Hadam, (1991)[c], MacHugh and Sopp, (1991)[d], MacHugh *et al.* (1991)[e], Davis *et al.* (1996)[f], Morrison and Davis, (1991)[g], Williams *et al.* (1990)[h], Naessens *et al.* (1988)[i], Sopp (1996)[k], Sopp *et al.* (1996)[l], Hall *et al.* (1993)[m], Brooke and Howard, (1996)[n], MacHugh *et al.* (1993)[o], Gerdes *et al.* (1984)[p], Toye *et al.* (1991)[q], Cook *et al.* (1993)[r].

2.2.2.3. Staining procedures for purification of lymphocyte subpopulations.

Lymph node cells obtained from infected animals on days 9 or 10 of infection were sorted by flow cytometry to obtain a purified population of $CD2^-CD8^+$ cells. The primary and secondary mAbs were diluted to the appropriate working dilution in sterile culture medium as described above, and passed through a 0.2μm syringe filter (Acrodisc, Gelman Sciences, Ann Arbor, MI, U.S.A.). 10^8-10^9 lymph node cells were incubated with primary mAbs against CD2 (CC42; IgG1) and CD8 (CC63; $IgG2_a$), in a volume of 25μl diluted antibody/10^6 cells, for 10min at room temperature, then washed three times in 10ml sterile culture medium by centrifugation at 200xg for 5min. Then the cells were resuspended in 10ml each of isotype-specific secondary antibodies (FITC-conjugated goat anti-mouse IgG1 and PE-conjugated goat anti-mouse $IgG2_a$), diluted to 1:200, and incubated as above. The washing steps were repeated three times as above, and the labelled cells were resuspended in 1.5ml sterile culture medium for sorting on a FACStar Plus fluorescence-activated cell sorter (Becton Dickinson).

In some experiments the cells were enriched for $CD8^+$ cells prior to sorting on the FACStar by staining with magnetic beads and separation on MACS VS^+ Separation Columns (Miltenyi Biotec, 51429 Bergisch Gladbach, Germany). In these experiments the primary monoclonals used were IL-A43 (CD2; $IgG2_a$) and CACT80C (CD8; IgG1). The staining procedure was essentially the same as described above, except that the washing steps were performed using FACSFlow (FF) medium (Becton Dickinson - composition not disclosed) containing 0.5% w/v bovine serum albumin (BSA; Sigma) and filtered through a 0.2μm syringe filter. Following the final wash, the cells were incubated with MACS beads coupled to an anti-FITC monoclonal antibody (Miltenyi Biotec) for 10min at room temperature (in a volume of 10μl beads/10^7cells), before washing three times as above and resuspension in 2ml FACSFlow medium. The cell suspension was applied to the magnetic separation column and allowed to flow through, $CD8^+$ cells being retained on the column. The column was washed twice with 2ml FACSFlow containing 0.5% BSA (FF/BSA), then removed from the magnet and the cells eluted in 1.5ml FF/BSA. An equal volume of sterile culture medium was added before sorting on the FACStar.

2.2.2.4. Sorting T cell subpopulations using magnetic beads.

Lymphocytes were isolated from the prescapular lymph nodes of infected and control calves as described in Section 2.2.1.3. The mAbs used for sorting were CC8, to isolate $CD4^+$ T lymphocytes, and CC63, to isolate $CD8^+$ T lymphocytes. Both antibodies were available as culture supernatants of hybridomas and were used diluted 1:10 in sterile culture medium. 10^8 cells were resuspended in 2.5ml of each diluted antibody and incubated for 10min at room temperature. The cells were then washed three times in 10ml FF/BSA, by centrifugation at 200xg for 5min. They were resuspended with 100µl MACS beads coupled to an anti-mouse IgG mAb (Miltenyi Biotec) and incubated at room temperature for 10min. A further three washes in FF/BSA were performed as above and the cells resuspended in 1.5ml FF/BSA. Positive cells were separated on a MiniMACS magnetic column (Miltenyi Biotec). The column was pre-wet with 0.5ml FF/BSA before adding the cell suspension, allowing it to flow through under gravity. The column was washed three times with 0.5ml FF/BSA, before removing it from the magnet and eluting the retained cells in 1ml FF/BSA. 25µl of the eluted cell suspension was mixed with 25µl FITC-conjugated goat anti-mouse IgG (Southern Biotechnology Associates) diluted 1:200 in PBS, and incubated for 10min at room temperature before washing and analysing on the FACScan to assess the purity of the sorted population.

2.2.3. Generation of parasitized cell lines.

2.2.3.1. Preparation of sporozoite suspensions.

Suspensions of infective sporozoites were prepared from adult *Rhipicephalus appendiculatus* ticks which had been infected with the Muguga stock of *Theileria parva* by feeding on infected cattle. This material was provided by Prof. Duncan Brown and colleagues at the Centre for Tropical Veterinary Medicine, University of Edinburgh. Briefly, 80 ticks infected with *T. parva* (Muguga) were fed on the ears of a rabbit. After 4 days all the ticks were still attached and were removed for preparation of sporozoite suspensions. Sterile suspensions of sporozoites were prepared as described by Brown (1983). In the experiment carried out at ILRI, sporozoites were isolated from infected tick salivary glands supplied by the ILRI Tick Unit. These were dissected from ticks infected with *T. parva* (Muguga) and pre-fed on rabbit ears for 4 days, as above. The

estimated number of infected acini was 1500. The salivary glands were crushed in a sterile homogeniser in about 1ml of cold sterile culture medium, to release the sporozoites. The suspension was centrifuged at 200xg for 5min at 4°C, and the supernatant containing the sporozoites was recovered.

2.2.3.2. *In vitro* infection of bovine PBMC with *Theileria parva* sporozoites.

Cell lines from a number of different animals were established by *in vitro* infection of PBMC with *T. parva* (Muguga) sporozoites. The PBMC were resuspended in sterile medium at 2 x 10^6 cells/ml and an equal volume of the sporozoite suspension was added. The cells were then incubated at room temperature for 4h, before washing with fresh medium to remove potentially toxic tick material, and resuspending at 4 x 10^6 cells/ml in standard culture medium.

In the experiment carried out at ILRI, 2 x 10^7 PBMC were isolated from two animals (AT107 and AT113) as described above, and pelleted by centrifugation at 200xg for 5min. The cell pellets were resuspended in 0.5ml of the sporozoite suspension (containing the equivalent of 750 infected acini) and incubated for 1h at 37°C, with gentle mixing at 10min intervals. Culture medium was added to a final volume of 5ml, and the cells were pelleted by centrifugation as above. The pellet was resuspended in 10ml culture medium, and the cells were divided between two 50ml polystyrene tissue culture flasks (Falcon, Oxford, UK), and incubated at 38°C in a humidified atmosphere of 5% CO_2 in air. The cells were examined daily for signs of transformation: when there were significant numbers of blasts in the cultures (after 3 days) the cells were irradiated and used as stimulators in the autologous *Theileria* mixed leucocyte reaction.

2.2.3.3. Establishment and maintenance of parasitized cell lines.

Three different culture conditions were used in the initial establishment of cell lines. Cells were distributed at 4 x 10^6 cells/well into 24 well cluster plates (Nunc, Roskilde, Denmark) and cultured in a total volume of 2ml of culture medium with:

a) 10% T-cell growth factors (TCGF)

b) 10% TCGF and a bovine fibroblast feeder layer

c) a bovine fibroblast feeder layer.

The TCGF consisted of conditioned medium from PBMC stimulated for 18h with 2.5μg/ml concanavilin A (ConA), prepared as described by Goddeeris and Morrison (1988), and containing 0.05% w/v α-methyl mannoside (Sigma). Bovine fibroblasts were established in the wells at 3 x 10^4 cells/well 2 days before the addition of infected PBMC, in order to provide a confluent monolayer.

The plates were incubated at 38°C in a humidified atmosphere of 5% CO_2 in air and inspected daily for signs of cell transformation. Every three days 0.5-1.0 ml of medium was removed from each well and replaced with an equal volume of fresh medium, supplemented with TCGF where necessary in accordance with the initial culture conditions. Once cell transformation was established, the medium was changed every 2-3 days. When transformed cells covered >50% of the surface of the plate, the cells were split and passed into fresh wells. Cells grown with feeder layers were seeded on to fresh feeder layers on the first passage, but TCGF was no longer added to the medium. Once the growth of transformed cells was well established, they were subcultured and maintained as continually growing cell lines in culture medium without additional growth factors. The phenotype of the cell lines was established by immunofluorescent staining with a panel of mAbs against lymphocyte differentiation antigens, including IL-A58 (immunoglobulin light chain), MM1A (CD3), CC42 (CD2), CC8 (CD4), CC63 (CD8), GB21A (γ/δ TCR), and CC15 (WC1), as described above.

2.2.3.4. Cryopreservation of parasitized cell lines.

Once cell lines were growing vigorously, aliquots of cells were stored in liquid nitrogen for future use. Cells in logarithmic phase growth were pooled, counted, pelleted by centrifugation at 200xg for 8min (at 4°C), and the supernatant discarded. The cells were resuspended at 2 x 10^6 cells/ml in 90% heat-inactivated FBS and 10% dimethylsulphoxide (DMSO; Sigma) and

1ml aliquots were transferred into polypropylene cryovials (Greiner Labortechnik Ltd., Dursley, Glous., UK). These were frozen overnight to -70°C and transferred to liquid nitrogen the following day.

2.2.4. Proliferation assays.

Proliferation assays were performed using a variety of different stimuli, responder cells, and incubation times; the details of each particular assay are outlined in the relevant chapters. Cultures were established in 96 well flat-bottomed (Corning, NY, USA) or round-bottomed plates (Nunc). Parasitized stimulator cells used in the autologous *Theileria* mixed leucocyte reaction, and PBMC or lymph node mononuclear cells used as filler cells, were exposed to gamma-radiation from a ^{137}Cs source (Gammacell 1000 Elite; Nordion International Inc., Kanata, Ontario, Canada). Parasitized cells received a radiation dose of 50 Grays (Gy), while filler cells were exposed to 20 Gy. Culture medium incorporating 2-mercaptoethanol (Sigma) was used for proliferation assays (A.4). The cultures were incubated at 38°C in a humidified atmosphere of 5% CO_2 in air. Proliferation of responding cells was measured by the incorporation of tritiated [^{3}H] thymidine (NEN Life Science Products, Stevenage, Herts., UK) or [^{125}I] iododeoxyuridine (Amersham International, Bucks., UK), added at 0.037MBq/well during the final 8h of culture. Cells were harvested onto glass microfibre filters (Wallac, Turku, Finland), using a Skatron cell harvester (Skatron Ltd., Newmarket, Suffolk, UK) and allowed to dry. For cultures incubated with [^{3}H], the filters were sealed in plastic covers, and 10ml Optiphase scintillant (LKB Ltd., Loughborough, Leics., UK) was added. The amount of incorporated radioactivity was measured by liquid scintillation counting on a Wallac 1205 beta-scintillation counter. For cultures incubated with [^{125}I] iododeoxyuridine, the filter mat discs from each well harvested were placed in 4ml polypropylene tubes (Falcon) and counted on a gamma counter (Gamma 5500, Beckman).

2.3. Techniques for histology.

2.3.1. Preparation of tissue blocks from lymph nodes.

Blocks of 5-10mm thickness were cut from the prescapular lymph nodes immediately following their removal from the animal. Since the animals received half the dose of stabilate on either side of the neck, the lymph nodes used for preparation of material for histology were those that had not been sampled by needle biopsy. Tissues were fixed by immersion in either neutral buffered formalin (NBF – B.1.1) for *in situ* hybridization or in mercuric formalin (B.1.2) for haematoxylin and eosin (H&E) staining. The blocks were then embedded in paraffin wax. Frozen tissues for use in immunocytochemistry were prepared by embedding blocks in OCT compound (Miles Inc., Elkhart, IN, U.S.A.) and freezing rapidly in liquid nitrogen. They were then stored either at -70°C or in liquid nitrogen.

2.3.2. Haematoxylin and eosin (H&E) staining.

Paraffin blocks were cut in sections 3μm thick using a 2030 rotary microtome (Reichert-Jung, Nussloch, Germany) and incubated overnight at 37°C. H&E staining was carried out using a Shandon automatic stainer (Varistain 24-3, Shandon Scientific Ltd., Bucks., UK) according to the standard staining protocol for paraffin sections (Stevens, 1982), except that xylene was substituted with Safeclear (Chemix UK Ltd., Wigan, Lancs., UK). Briefly, sections were dewaxed in Safeclear, hydrated through a graded series of alcohols to water, then stained with haematoxylin (Surgipath, St. Neots, Cambs., UK) for 3.5min, washed in tap water, differentiated with acid alcohol (0.5% hydrochloric acid in 70% alcohol), blued in 1% borax solution and washed in water. Sections were then stained with 0.5% eosin (BDH Chemicals Ltd., Poole, Dorset, UK) in distilled water for 1min, washed in tap water, dehydrated through a graded series of alcohols, cleared in Safeclear and mounted in Safemount (Chemix UK Ltd.).

2.3.3. Immunocytochemistry.

Immunocytochemistry was performed on cryostat sections. Lymph node blocks frozen in OCT compound were warmed to -20°C and cut in sections 5μm thick using a Frigocut E 2800 microtome (Reichert-Jung). The mAbs used for immunocytochemistry were MM1A, CC42, CC63, GB21A, CC149 and CC94, the *T. parva*-specific mAb, and NCL-Ki67-MM1, a mAb reactive with the Ki67 nuclear antigen expressed on proliferating cells (Novocastra Laboratories Ltd., Newcastle upon Tyne, UK). Most of these antibodies are listed in Table 2.1. Two mAbs, AV29 and TRT1 with irrelevant specificities and the isotypes $IgG2_b$ and IgG1 were used as controls to check the level of non-specific binding of mouse IgG to Fc receptors on monocytes/macrophages.

The cryostat sections were fixed for 10min in acetone, then washed with PBS. They were incubated for 30min in methanol containing 0.3% H_2O_2 to quench endogenous tissue peroxidases. The sections were washed three times with PBS over a period of 10-15 min, and then incubated with diluted normal horse serum in a humidified container for 20min at room temperature. Excess serum was tipped off the slides and the sections were covered with the primary mAb , then incubated for a further 30min at room temperature. CC42, CC63, CC149 and CC94 were available as culture supernatants from hybridomas and were used undiluted. Purified MM1A was diluted to a final concentration of 5μg/ml in PBS. GB21A, AV29, TRT1 and the *T. parva*-specific mAb (MAb5) were in ascitic fluid from mice, and were diluted 1/250 in PBS before use. Lyophilized NCL-Ki67-MM1 was reconstituted in distilled water according to the manufacturer's instructions and used at a working dilution of 1:100. Following incubation with the primary antibodies, the sections were washed three times in PBS. 100-150μl biotinylated horse anti-mouse IgG, diluted according to the manufacturer's instructions (Vectastain ABC Kit, Vector Laboratories, Peterborough, UK) was added to each section, and they were again incubated in a humidified container for 30min at room temperature. Following a further three washes in PBS, 100-150μl Vectastain ABC reagent (a solution containing a complex of Avidin DH and biotinylated horseradish peroxidase H) was applied to each section, before another 30min incubation as above. The enzyme substrate was prepared by dissolving 150mg diaminobenzidine (Sigma) in 300ml PBS containing 0.02% w/v

sodium azide and adding 6% w/v H_2O_2 to give a final concentration of 0.01%. The sections were washed three times in PBS before being transferred to the substrate solution, in which they were incubated for 10 min. They were then washed once with PBS before counter-staining in Harris haematoxylin (diluted 1/3) for 10-30s, and rinsing with tap water. The sections were dehydrated by immersion in gradually increasing concentrations of ethanol followed by Safeclear. After air-drying, they were mounted using Safeclear mounting fluid.

2.3.4. Staining for acid phosphatase.

Staining for the lysosomal enzyme acid phosphatase was performed on lymph node cryostat sections, essentially according to the method outlined by Bancroft (1982).

2.3.5. *In situ* hybridization.

2.3.5.1. Preparation of riboprobes.

Riboprobes to bovine IL-10 were synthesized and labelled with digoxigenin-11-UTP at IAH, Compton, by Wallace Bulimo, using a commercial *in vitro* transcription/labelling system (DIG RNA Labeling Kit [SP6/T7]; Boehringer Mannheim UK, Lewes, East Sussex, UK)

2.3.5.2. Unmasking of nucleic acids.

Sections of lymph nodes 3μm thick were cut using a microtome and placed on coated ribonuclease-free slides (Superfrost Plus; BDH Chemicals Ltd.). The lymph node sections were dewaxed by incubating for 5min in xylene, then hydrated by sequential transfer through a graded series of alcohols to diethyl pyrocarbonate (DEPC)-treated water (B.2.1). Nucleic acids were unmasked by digestion with proteinase K (Sigma) at 0.1mg/ml in buffer 2 (B.2.4) at 37°C for 15min. As for all incubations described below, the slides were placed in Terasaki plates (Nunc) containing TE buffer, pH8.0 (C.2.1), to prevent the sections drying out. The slides were then washed in DEPC-treated water, immersed in 100% ethanol, and air-dried.

2.3.5.3. Denaturation and hybridization of riboprobe to section.

The DIG-labelled probes were thawed at 65°C for 5min, and incorporated in a hybridization mixture for each tissue section as follows:

DIG-labelled riboprobe	xμl
Hybridization buffer (B.2.7)	35μl
Salmon sperm DNA (10mg/ml; freshly denatured – B.2.6)	2μl
TE buffer, pH8.0	yμl
Total volume	50μl

The hybridization mixtures were applied to the sections and covered carefully with a coverslip. The slides were incubated in Terasaki plates at 80°C for 30min to denature the probes, before hybridization at 55°C for 2h. Negative controls consisted of sections incubated with the DIG-labelled sense probe in the same hybridization mix.

2.3.5.4. Post-hybridization washing.

The coverslips were gently washed off with 4X SSC (B.2.2), and the slides washed twice for 5min in 4X SSC, twice for 5min in 2X SSC, and finally for 15min at 55°C in 0.1X SSC. The sections were then incubated in blocking buffer (B.2.8) at room temperature for 30min, to block non-specific binding of the antibody to the sections.

2.3.5.5. Detection of hybridized riboprobe.

Sheep anti-digoxigenin Fab' fragments conjugated to alkaline phosphatase (750U/ml; Boehringer Mannheim) were diluted 1/500 in 3% BSA solution and applied to the tissue sections. The sections were incubated at room temperature for 30min, washed twice for 5min in buffer 1 (B.2.3), and equilibrated for 2min in buffer 3 (B.2.5). The substrate solution consisted of 0.33mg/ml nitroblue tetrazolium salt (NBT; Promega UK Ltd., Southampton, Hants., UK) and 0.17mg/ml 5-bromo-4-chloro-3-indolyl phosphate (BCIP; Promega) in buffer 3. The sections were immersed in the substrate solution, and incubated in darkness until a strong colour reaction had developed in the samples hybridized with the antisense probe, while there was still minimal staining in the negative

controls (typically about 4h). The reaction was stopped by washing the slides in distilled water, and allowing them to air-dry. The sections were counterstained with 1% methyl green, washed and air-dried before mounting in a gelatin mountant (see B.2.9).

2.4. Techniques for molecular biology.

2.4.1. Isolation of total RNA.

Isolation of total RNA from lymphocytes was performed using the Ultraspec RNA Isolation Kit (Biotecx, AMS Biotechnology UK Ltd., Witney, Oxon, UK), essentially according to the protocol recommended by the manufacturers. This technique allows single-step extraction of RNA based on the guanidium-isothiocyanate method (Chomczynski and Sacchi, 1987). The cells were pelleted by centrifugation at 200xg for 5min and all the supernatant carefully removed. Cells were lysed by addition of the Ultraspec reagent (1ml per 5 x 10^6 cells), a solution containing guanidine salts and urea with phenol and other detergents (precise composition not disclosed). 1ml aliquots of the homogenate were transferred to 1.5ml microcentrifuge tubes and placed on ice for 5min to allow complete dissociation of nucleoprotein complexes. RNA was extracted by addition of 0.2ml chloroform to each tube, followed by vigorous mixing and incubation on ice for 5min, then centrifugation at 12000xg for 15min at 4°C. The upper aqueous phase was carefully transferred to a fresh tube, mixed with an equal volume of isopropanol, and placed on ice for 10min, before centrifugation at 12000xg for 15min at 4°C to precipitate the RNA. The RNA pellet was washed twice with 75% ethanol, air-dried and dissolved in 10µl DEPC-treated water.

2.4.2. Measurement of RNA concentration.

The amount of total RNA in solution was estimated by measurement of the absorbance of light from a deuterium source at wavelengths 260nm(A_{260}) and 280nm(A_{280}). Samples were diluted in DEPC-treated water (see Appendix) and transferred to quartz cuvettes for measurement of the absorbance in a calibrated spectrophotometer (Ultrospec III, Pharmacia, Uppsala, Sweden). The concentration of RNA in the sample was calculated based on the assumption that an A_{260} value of 1.0 corresponds to an RNA concentration of 40µg/ml (Sambrook *et al.*, 1989). The ratio of A_{260}:A_{280} was calculated to give an indication of the quality of the RNA preparation: values between 1.8 and 2.0 were regarded as optimal, whereas a ratio of <1.7 indicates the presence of contaminants such as protein or phenol in the RNA solution (Sambrook *et al.*, 1989).

2.4.3. Complementary DNA (cDNA) synthesis.

First strand complementary DNA (cDNA) was synthesized from 5µg total RNA using avian myeloblastoma virus reverse transcriptase (AMV-RT; supplied with the Reverse Transcription System, Promega), according to the manufacturer's instructions. The reaction components listed below were combined on ice, then incubated at 42°C for 15min, before heating to 95°C for 5min to inactivate the enzyme. The cDNA was stored at -20°C prior to use as template in the polymerase chain reaction.

10X RT buffer (C.1.1)	2µl
25mM $MgCl_2$	4µl
10mM dNTP (C.1.7)	2µl
oligo$(dT)_{15}$ (0.5µg/µl)	1µl
Recombinant ribonuclease inhibitor (rRNasin® - 39U/µl)	0.5µl
AMV-RT (25U/µl)	0.75µl
Total RNA (5µg)	xµl
DEPC-treated water	yµl
Total volume	20µl

2.4.4. Polymerase chain reaction for detection of bovine cytokine mRNA.

2.4.4.1. Synthesis of oligonucleotide primers.

Oligonucleotide primers were produced at the IAH by Miss K. Mawditt using the phosphoramidite method of synthesis on an Applied Biosystem DNA Synthesizer (Model 381A). The oligonucleotides were cleaved from glass column supports by four complete column washes with concentrated ammonium hydroxide solution (15min each) and incubated at 55°C for 16h to remove the base protecting groups. The ammonia was recovered by lyophilization in a Univap (UniScience) particle concentrator and the oligonucleotides resuspended in 0.5ml sterile double distilled water (DDW). The concentration of oligonucleotide in solution was estimated by measurement of the absorbance at 260nm as for RNA. The concentration was calculated based on the assumption that an A_{260} of 1.0 is equivalent to 20μg/ml of single-stranded oligonucleotide. The concentration in pmol/μl is given by the formula $A_{260}/0.01xN$, where N is the number of bases in the oligonucleotide.

2.4.4.2. PCR amplification of cDNA.

Amplification of cDNA was performed on a programmable thermal cycler (PTC-100; M.J. Research Inc., Watertown, Mass., U.S.A.) using *Taq* DNA polymerase (Amersham International plc, Bucks., U.K.) in the reaction buffer supplied by the manufacturers (composition not supplied). The cytokine-specific primers used for amplification were designed based on the published sequences of bovine cytokines (Collins *et al.*, 1996), and are listed in Table 2.2. A "hot-start" PCR method was used; that is, the reaction components apart from the enzyme (see below) were assembled on ice, overlaid with a drop of mineral oil and heated to 94°C for 5min, then held at 80°C while 1μl of *Taq* DNA polymerase (diluted to 1U/μl) was added. Amplification then proceeded using the following conditions: denaturation (94°C for 1min), annealing (55°C for 1min), extension (72°C for 1min) for 30 cycles, with a final extension for 7min at 72°C. Each set of reactions incorporated a negative control with cDNA replaced by DDW, and a positive control containing cDNA prepared from PBMC stimulated in culture with 5μg/ml ConA for 24h. Samples were stored at -20°C until the products could be analysed by agarose gel electrophoresis.

10X reaction buffer	2.5µl
25mM $MgCl_2$	2µl
5mM dNTP	1µl
Sense primer (10pmol/µl)	1µl
Antisense primer (10pmol/µl)	1µl
cDNA	2µl
DDW	14.5µl
Total volume	25µl

Table 2.2. Primers for the detection of bovine cytokines.

Cytokine	Primers	PCR product size (base pairs)
IL-2	5'-TGCTGCTGGATTTACAGTTGC 3'-GAGGCACTTAGTGATCAAGCT	373
IL-4	5'-GTCTCACCTACCAGCTGATC 3'-TCAGCGTACTTGTGCTCGTC	348
IL-6	5'-AGGCAGACTACTTCTGACCAC 3'-CAGCTACTTCATCCGAATAGC	505
IL-10	5'-ACAGCTCAGCACTGCTCTGTT 3'-CGTTGTCATGTAGGATTCTATG	518
IFNγ	5'-GCAAGTAGCCCAGATGTAGC 3'-GGTGACAGGTCATTCATCAC	316
TNFα	5'-ACTCAGGTCATCTTCTCAAGCC 3'-ATGATCCCAAAGTAGACCTGCC	464
β-actin	5'-CCAGACAGCACTGTGTTGGC 3'-GAGAAGCTGTGCTACGTCGC	270

2.4.4.3. Agarose gel electrophoresis of DNA.

PCR products were analysed by agarose gel electrophoresis using a midi-gel system (Hybaid, Teddington, Middlesex, UK) for the rapid analysis of DNA fragments in the 0.5-1.0 Kb size range. Aliquots (7µl) of the completed PCR reactions were diluted in 3µl 1X loading buffer (C.3.2) and examined on 1% agarose gels incorporating 0.4µg/ml ethidium bromide and prepared using 0.5X Tris-borate (TBE) buffer (C.3.1). Electrophoresis was carried out at 100V for 30min with 0.5X TBE as running buffer, and PCR products were visualized using a ultra-violet (UV) light source and photographed with a Polaroid MP4 camera or a UVP GDS500 digital camera (Mitsubushi). Gels were calibrated with 0.5µg of molecular weight DNA markers (100 bp DNA ladder; Gibco BRL, Life Technologies, Paisley, Scotland.) diluted in loading buffer and DDW to give a final volume of 10µl.

2.4.4.4. Recovery of DNA from agarose gels.

The bands containing PCR products of the predicted size were excised and the DNA recovered using the GENECLEAN II Kit (BIO 101, Vista, CA, USA) according to the manufacturer's instructions. The gel slices were weighed and dissolved in 2-3 volumes (assuming that 1g = 1ml) of a saturated (6M) sodium iodide (NaI) solution and 100µl TBE modifier at 45°C for 30min. The DNA was adhered to an aliquot of GLASSMILK (crystalline silica) suspension (5µl for up to 5µg DNA) by mixing at 4°C for 10-30min, and separated by centrifugation at 9000xg for 2min. The pellet was washed three times in NEW Wash buffer (composition not disclosed) by resuspension and centrifugation. The DNA was eluted from the silica by the addition of 10µl TE buffer, pH8.0 (C.2.1) and incubation at 55°C for 10min, followed by centrifugation at 9000xg for 1min and recovery of the supernatant.

2.4.4.5. Restriction endonuclease (RE) digestion of cytokine PCR products.

The sequence of the cytokine PCR products was confirmed by digestion with different restriction endonucleases (RE). The enzymes were selected on the basis of the published sequences, such that each PCR product was cleaved once at a specific site, yielding two fragments that could be detected by agarose gel electrophoresis. Failure to detect fragments of the predicted sizes following RE digestion would indicate that the primers

had not amplified the correct specific product. The restriction enzymes used and the predicted sizes of the fragments generated are shown in Table 3.7. (Chapter 3). 5µl of amplified DNA recovered from the agarose gel was combined with 5U of the appropriate RE in the buffer recommended by the manufacturer, made up to a final volume of 10µl with sterile DDW and incubated at 37°C for 1h. The products of the digestion were analysed by agarose gel electrophoresis as described above.

2.4.5. Anchored polymerase chain reaction.

Synthesis of complementary DNA by reverse transcription (RT), homopolymer tailing and amplification by polymerase chain reaction (PCR) were performed using the 5' RACE System Kit, manufactured by Gibco BRL. The protocols used were those recommended by the manufacturer, unless otherwise stated. Oligonucleotide primers were designed based on bovine T cell receptor sequences published by Tanaka *et al.* (1990). When designing the primers, estimates of the annealing temperature (T_m) were made using the formula:

$$T_m = T_d - 5°C$$

where $$T_d = 4 \times (G + C) + 2 \times (A + T) \text{ (in } °C)$$

The dissociation temperature, T_d, is defined as the temperature at which 50% of the hybrids formed between oligonucleotides (14-20 bases long) and immobilized DNA show decreased stability and dissociate from the hybrid (Thein and Wallace, 1986). The letters represent the numbers of each deoxynucleotide base in the primer sequence.

First strand cDNA synthesis was primed using an antisense gene-specific primer (PBC1) complementary to a conserved region near the 5' end of the TCR β chain constant region gene segments (*TCRBC*). A "nested" primer (PBC2) located 5' to PBC1 on *TCRBC* was used with the anchor primer for amplification of C-tailed cDNA. An "internal" primer (PBV2) is complementary to a conserved region at the 5' end of the bovine *TCRBV2* gene family, and was used with PBC2 in positive controls to check the yield of cDNA from first strand synthesis and purification procedures. The primer sequences are listed in Table 2.3, and the locations and orientations of the primers are illustrated in Figure 5.1. The anchor primer

was supplied as part of the 5' RACE System kit and a similar primer based on this design was synthesized at IAH, Compton.

Table 2.3. Primers used for amplification and sequencing of bovine *TCRBV* region sequences.

Primer	Sequence
PBV2	5'-CCTCTGTGACCATCGAGTG
PBC2	5'-GTTCGAACACAGCCACCTTG
PBC1	5'-GAGATCTCTGCTTCCGAGG
Anchor primer	5'-GGCCACGCGTCGACTAGTACGGGIIGGGIIGGGIIG
Modified anchor primer	5'-ACTACTACAAGCTTGGGIIGGGIIGGGIIG
P6	5' GCTTCCGGCTCGTATGTTGTGG
P7 (5' biotinylated)	5' AAAGGGGGATGTGCTGCAAGGCG
5' Sequencing primer	5'-AGCTCGGATCCACTAGTAAC
3' Sequencing primer	5'-TCTAGATGCATGCTCGAGCG

2.4.5.1. First strand cDNA synthesis.

1μg total RNA was combined with 2.5pmol of the primer PBC1 and brought to a final volume of 15μl with DEPC-treated water, then incubated at 70°C for 5-10min to denature the RNA, and chilled on ice for 1min. The remaining reaction components were added as follows:

10X buffer (C.1.2)	2.5μl
25mM $MgCl_2$	3.0μl
10mM dNTP (C.1.7)	1.0μl
0.1M dithiothreitol (DTT)	2.5μl
Total volume	24μl

The mixture was incubated at 42°C for 2min before addition of 1μl Superscript RT II (containing 200U/μl Moloney Murine Leukaemia Virus reverse transcriptase); incubation

at 42°C was then continued for a further 30min. The reaction mix was heated to 65°C for 15min to inactivate the enzyme, then cooled to 55°C before addition of 1µl *E. coli* ribonuclease H (20U/µl) and incubation for a further 10min at 55°C. A control reaction without reverse transcriptase was run in parallel to check for contamination of RNA with genomic DNA.

2.4.5.2. Purification of first strand cDNA.

Efficient purification of first strand cDNA is essential to ensure that excess dNTPs and first strand primer are not present during the tailing reaction. Purification was carried out using the GLASSMax Spin Cartridge Kit (Gibco). 120µl 6M NaI solution was added to the cDNA reaction, and then transferred to a spin cartridge and centrifuged at 11000xg for 20-30s. The cDNA is retained on the membrane of the spin column. The column was washed three times with 0.4ml of cold (4°C) dilute wash buffer (composition not disclosed) and three times with 0.4 ml of cold 70% ethanol, by centrifugation at 11000xg for 20-30s. The cDNA was eluted into a fresh tube in 50µl DDW equilibrated to 65°C, by centrifugation as before.

2.4.5.3. Homopolymer tailing of purified cDNA.

The following components of the reaction mix were combined and heated to 94°C for 3min:

10X buffer (C.1.2)	2.5µl
25mM $MgCl_2$	1.5µl
2mM dCTP	2.5µl
Purified cDNA	10.0µl
DDW	7.5µl
Total volume	24µl

The reaction was then chilled on ice before addition of 1µl terminal deoxynucleotidyl transferase (TdT-10U/µl), and incubation at 37°C for 10min, followed by 10min at 65°C to inactivate the enzyme. A control reaction that omitted TdT was run in parallel to check for non-specific annealing of the anchor primer.

2.4.5.4. Amplification of tailed cDNA.

The following components were combined in a 0.5ml microcentrifuge tube:

10X buffer (C.1.2)	5.0µl
25mM $MgCl_2$	3.0µl
10mM dNTP	1.0µl
Anchor primer (10pmol/µl)	2.0µl
PBC2 (10pmol/µl)	2.0µl
Tailed cDNA	5.0µl
DDW	31.0µl
Total volume	49.0µl

The reactions were overlaid with a drop of mineral oil, placed in a thermal cycler (PTC-100; M.J. Research, Inc., Watertown, Mass., U.S.A.) and heated to 94°C for 5min, then held at 80°C. 1µl *Taq* DNA polymerase (diluted to 2.5U/µl) was added to each reaction, and amplification was performed over 35 cycles of denaturation (94°C for 1min), annealing (55°C for 30s) and extension (72°C for 1min), with a final extension step of 72°C for 10min. In later experiments this protocol was modified by inclusion of *Taq* Extender (Stratagene) so that the final reaction composition was altered to: 5µl tailed cDNA, 5µl 10X *Taq* Extender buffer (C.1.3), 1.2µl 50mM $MgCl_2$, 1µl 10mM dNTPs, 20pmol each primer, 5U *Taq* Extender and 5U *Taq* DNA polymerase, in a total volume of 50µl. The cycling conditions were also changed to 94°C for 45s, 57°C for 30s and 72°C for 2min. PCR products were analysed by agarose gel electrophoresis as described in Section 2.4.4.3.

2.4.6. Cloning of anchored PCR products using the TA Cloning System™.

The anchored PCR product was recovered from the agarose gel as described in Section 2.4.4.4, and cloned into the *p*CR™II plasmid vector supplied with the TA Cloning Kit (Invitrogen, R&D Systems, Abingdon ,Oxon, U.K.), which allows direct non-directional cloning of PCR products without prior purification or digestion. This system takes advantage of the non-template-dependent activity of *Taq* DNA polymerase that adds a

single deoxyadenosine residue to the 3' ends of double stranded DNA molecules. These 3' A overhangs are used to insert the PCR product into the *p*CR™II vector, which contains single 3' T overhangs at the insertion site. When *Taq* Extender was included in the PCR reactions, the products generated lacked the single-base 3' A overhangs. These products were incubated with *Taq* DNA polymerase as follows, to allow addition of adenine bases: 10µl PCR product (recovered from agarose gel) was combined with 1.5µl 10X buffer (C.1.2), 0.4µl 10mM dATP, 1.25U *Taq* DNA polymerase (Gibco) and DDW to a final volume of 15µl, and incubated at 72°C for 20-30min.

2.4.6.1. Ligation reactions.

Ligation reactions were set up as follows, and incubated for 16h at 12°C:

Sterile water	yµl
10X ligation buffer (C.1.5)	1µl
*p*CR™II (25ng/µl)	2µl
PCR product (75ng)	xµl
T4 DNA ligase (4U/µl)	1µl
Total volume	10µl

2.4.6.2. Transformation of competent *E. coli.*

The ligated plasmid/inserts were transformed into OneShot INVαF' competent *E. coli* (Invitrogen; C.4.1) according to the manufacturer's protocol. A 50µl aliquot of competent cells was thawed on ice and 2µl of 0.5M β-mercaptoethanol was added. 1µl of the completed ligation reaction was added to the cells which were placed on ice for 30min, before heat shocking at 42°C for 30s and returning immediately to ice for 2min. 450µl SOC medium (C.4.4) was then added and the cells were incubated at 37°C for 1h on a rotary shaking incubator (225 rpm). 50µl or 100µl aliquots of the contents of the vial were spread on Luria-Bertani (LB) agar plates (C.4.3) and incubated overnight at 37°C. The agar plates contained 100µg/ml ampicillin and were spread with 25µl X-gal (40mg/ml 5-bromo-4-chloro-3-indoyl-β-D-galactosidase in dimethylformamide) to allow blue/white selection of colonies containing inserts.

2.4.6.3. Preparation of frozen stocks of bacterial clones.

A large number of white colonies (>100) were picked from the plates spread with transformed *E. coli.* Each individual colony was inoculated into 3ml of LB medium (C.4.2) containing 100μg/ml ampicillin, and incubated for 16h at 37°C on a rotary shaker. Aliquots of 0.7ml from each culture were mixed with 0.7ml 30% glycerol, and stored at -70°C. Prior to examination of the inserts, the bacterial clones were thawed, streaked onto LB agar plates containing 100μg/ml ampicillin and incubated overnight at 37°C to allow growth of colonies.

2.4.7. Preparation of DNA template for sequencing.

2.4.7.1. Small scale preparation of plasmid DNA.

Method A for the preparation of plasmid DNA using Qiagen columns.

Plasmid DNA was prepared using Qiagen resin tips (Tip 20; Qiagen Ltd., Dorking, Surrey, UK) according to the manufacturer's instructions. Single colonies were selected from bacterial clones and inoculated into 5ml LB broth containing 100μg/ml ampicillin, then incubated for 15h on a rotary shaker at 37°C. Cells were centrifuged at 1000xg for 15min at 4°C, the supernatant was discarded and the pellet resuspended in 300μl of buffer P1 (C.5.1). The cells were lysed by addition of 300μl of buffer P2 (C.5.3) and left at room temperature for 5min. Cellular debris and chromosomal DNA were precipitated by addition of 300μl of chilled neutralization buffer P3 (C.5.4) and incubation on ice for 10min, with occasional gentle mixing. The tubes were then centrifuged at 12000xg for 15min in a bench-top microfuge, and the supernatant was passed through a Qiagen resin tip (Tip 20) which had been equilibrated with 1ml of QBT buffer (C.5.6). The resin was washed four times with 1ml of QC buffer (C.5.7) and DNA eluted in 0.8ml of QF buffer (C.5.8). The plasmid DNA was precipitated with 0.7 volumes of isopropanol by centrifugation at 12000xg for 30min. The pellet was washed with 1ml 70% ethanol, air-dried and dissolved in 20μl of TE buffer, pH 8.0.

Method B for the preparation of plasmid DNA.

Small scale preparation of plasmid DNA was also performed according to a protocol recommended by Applied Biosystems, Inc. (ABI), Warrington, Cheshire, UK. Cultures

were prepared as described above. The cells were pelleted by centrifugation at 2000xg for 15min at 4°C, then resuspended in 200µl GTE buffer (C.5.2), before adding 300µl of lysis buffer (C.5.3). The tubes were placed on ice for 5min, then 300µl of neutralization buffer (C.5.5) was added, followed by a further 5min incubation on ice. The cellular debris was pelleted by centrifugation at 12000xg for 10min, and the supernatant was incubated at 37°C for 20min in the presence of 20µg/ml ribonuclease A to remove contaminating cellular RNA. The plasmid DNA was extracted twice with chloroform, and precipitated by adding an equal volume of isopropanol and centrifuging at 12000xg for 10min at room temperature. The pellets were washed once with 70% ethanol and air-dried before dissolving in 32µl DDW. Precipitation of plasmid DNA was repeated by addition of 8µl 4M NaCl and 40µl 13% polyethylene glycol (PEG) 8000 (Sigma), incubation on ice for 20min and centrifugation at 12000xg for 15min at 4°C. The pellet was again washed with 70% ethanol, air-dried and dissolved in 20µl TE buffer, pH8.0.

2.4.7.2. RE digestion of plasmid DNA.

The presence of inserts of the correct size (about 600bp) was confirmed by digestion with a restriction endonuclease (*Nsi*I; Stratagene Ltd.,Cambridge, U.K.) that cuts vector sequences flanking the insert. The reactions were set up as follows and incubated at 37°C for 1h. The products of RE digestion were analysed by agarose gel electrophoresis, as described for PCR products (see Section 2.4.4.3).

DNA (1-2µg)	xµl
Reaction buffer (10X; see C.1.6)	1µl
DDW	yµl
*Nsi*I (16U/µl)	0.5µl
Total volume	10µl

2.4.7.3. Measurement of DNA concentration.

The yield and purity of plasmid DNA from the miniprep procedures was assessed by measurement of the absorbance of the solution at wavelengths 260nm (A_{260}) and 280nm (A_{280}). The measurements were performed on a Ultrospec III spectrophotometer (Pharmacia) as described for RNA in Section 2.4.2. The DNA concentration was

calculated based on the assumption that an A_{260} value of 1.0 is equivalent to 50μg/ml of double-stranded DNA (Sambrook *et al.*, 1989). The quality of the DNA was assessed by calculation of the ratio A_{260}:A_{280} - a value of 1.7 - 2.0 indicated that the plasmid preparation was sufficiently pure for sequencing.

2.4.7.4. Preparation of sequencing template using magnetic beads (Dynabeads®).

Single-stranded DNA for solid-phase DNA sequencing was prepared using the Template Preparation Kit (Dynal A.S., Oslo, Norway). PCR amplification of the cloned insert was carried out using primers complementary to vector sequences flanking the cloning site, one of which is labelled with biotin at the 5' end. This generated PCR products that contain one biotinylated and one non-biotinylated strand. Biotin-labelled PCR products were immobilized on 2.8nm superparamagnetic styrene beads coated with chemically bound streptavidin (Dynabeads® M-280 Streptavidin). The non-biotinylated strand was eluted leaving single-stranded DNA bound to the beads which was used as the sequencing template.

The sequences of the oligonucleotides used as primers in the PCR reaction are given in Table 2.3. These primers were supplied by Dynal as components of the Template Preparation Kit. Additional supplies of the 5'-biotinylated oligonucleotide were obtained from Oswel DNA Service, Southampton, Hants., UK. Vent® DNA polymerase (New England Biolabs Inc., Beverly, MA, USA) was used to amplify the inserts as this enzyme contains 3' to 5' proof-reading exonuclease activity, and therefore has a lower error rate than *Taq* DNA polymerase. Single colonies were picked from bacterial clones and resuspended in 10μl of sterile DDW, then heated to 96°C for 5min to lyse the bacteria. 5μl of the bacterial lysate were combined with the following components on ice:

DDW	34µl
10X Thermopol buffer (C.1.4)	5µl
100mM $MgSO_4$	2µl
10mM dNTP	1µl
P6 (10pmol/µl)	2µl
P7 (5pmol/µl)	1µl
Total volume	49µl

The reactions were overlaid with a drop of mineral oil, placed in a thermal cycler (MTC-100) and heated to 96°C for 5min, then held at 80°C while 1µl Vent® DNA polymerase (0.5U/µl) was added. The reaction then proceeded through 25 cycles of denaturation (96°C for 30s), annealing (65°C for 1min) and extension (72°C for 2min), followed by a final extension at 72°C for 5min. Aliquots of the completed reactions were analysed by agarose gel electrophoresis to check the yield of the PCR product and the size of the insert (expected size of bands ~850bp).

The biotinylated PCR products were bound to 200µg Dynabeads® M-280 Streptavidin. The suspension of Dynabeads was placed in a magnetic particle concentrator (MPC-E; Dynal) to collect the beads, the supernatant was removed, and the beads were washed once with 20µl of Binding and Washing buffer (BW buffer – C.2.2) using the same procedure. The beads were then resuspended in 40µl BW buffer, and 40µl of the PCR reaction mix was added, followed by incubation at room temperature for 15min to allow binding of the biotinylated DNA to the Dynabeads. The Dynabead/template complex was washed with 40µl BW buffer, then resuspended in 10µl 0.1M NaOH solution and incubated for 10 min at room temperature to elute the non-biotinylated DNA strand. The Dynabead/template complex was then washed three times as follows: once with 50µl 0.1M NaOH, once with 50µl BW buffer, and once with 50µl TE buffer, pH7.5. The beads were resuspended in 10-20µl DDW before inclusion in the sequencing reaction.

2.4.8. DNA sequencing.

Sequencing was carried out using two methods adapted from Sanger's dideoxy chain termination reaction (Sanger *et al.*, 1977).

2.4.8.1. Cycle sequencing using fluorescent dye terminators.

DNA sequencing was carried out using the ABI PRISM™ Dye Terminator Cycle Sequencing Ready Reaction Kit, and an updated version of the kit incorporating AmpliTaq® DNA polymerase, FS (ABI). The reaction produces chain terminated fragments from unlabelled primers extended by AmpliTaq® DNA polymerase. Each of the dideoxynucleotides are labelled with a different fluorescent dye, to allow performance of all four base reactions simultaneously in the same tube. The kit supplies a Terminator Premix containing the dye-labelled dideoxynucleotides, deoxynucleotides (dATP, dCTP, dTTP, dITP) and AmpliTaq® DNA polymerase (C.6.1). Sequencing primers (SP_F and SP_R) designed to anneal to plasmid sequences flanking the cloning site were used to allow sequencing of both strands of the insert (see Table 2.3). The reaction components were assembled on ice as follows:

	Original kit	Kit with AmpliTaq® FS
Terminator premix	9µl	8µl
Template (0.75-1µg)	xµl	xµl
Primer (10pmol/µl)	1µl	1µl
DDW	yµl	yµl
Total volume	20µl	20µl

The reactions were overlaid with a drop of mineral oil and placed in a thermal cycler preheated to 96°C. Thermal cycling proceeded through 25 cycles of denaturation (96°C for 30s), annealing (50°C for 15s) and extension (60°C for 4min) with a rapid thermal ramp between each step. The completed reactions were placed on ice. Extension products were purified by phenol/chloroform extraction to remove unincorporated dye terminators. Briefly, 80µl DDW and 100µl chloroform were added to each reaction before extraction with 100µl phenol:chloroform:water reagent (ABI) by vortexing

thoroughly and centrifugation at 12000xg for 1min. The upper aqueous phase was transferred to a fresh tube and the phenol/chloroform extraction step was repeated. The DNA was precipitated by addition of 15µl of 2M sodium acetate, pH4.5 and 300µl of absolute ethanol and centrifugation at 12000xg for 15min at room temperature. The pellet was washed with 70% ethanol and dried under vacuum. In the updated version of the kit AmpliTaq® DNA polymerase has been replaced with a mutant form of *Taq* DNA polymerase (AmpliTaq® DNA polymerase FS) which has a greatly reduced discrimination against incorporation of dideoxynucleotides. This permits the use of much lower levels of dye labelled terminators in the reaction and removes the need for phenol/chloroform extraction to purify the extension products. For sequencing reactions performed with this enzyme, excess terminators were removed by ethanol precipitation. The entire 20µl contents of the reaction tubes were transferred to tubes containing 3µl of 2M sodium acetate, pH4.6 and 50µl of 95% ethanol, placed on ice for 10min, then centrifuged at 12000xg for 30min at room temperature. The pellets were washed with 70% ethanol and dried under vacuum. For each reaction, a mixture of 5µl deionised formamide and 1µl 50mM EDTA, pH8.0 was prepared and the pellet was redissolved in 4µl of this mixture. The samples were denatured by heating to 90°C for 2min just before loading on the gel.

2.4.8.2. DNA sequencing using Sequenase® T7 DNA polymerase.

Sequencing was also performed using the Sequenase® version 2.0 DNA sequencing kit (United States Biochemical, Cleveland, Ohio, U.S.A.). Double-stranded plasmid DNA was alkaline denatured by adding 0.1 volumes of 2M sodium hydroxide, 2mM EDTA and incubating at 37°C for 30min. The mixture was neutralized by adding 0.1 volume of 3M sodium acetate, pH5.5 and the DNA precipitated with 2 to 4 volumes of absolute ethanol, placing the sample at -70°C for 15min. After pelleting the DNA by centrifugation at 10000xg for 10min, the pellet was washed once with 70% ethanol, air-dried and dissolved in 10µl DDW. Denatured DNA (3-5µg) was mixed with 2µl of Sequenase® reaction buffer (C.6.2.1), 1µl of primer (SP_R or SP_F; 10pmol/µl) and DDW to a final volume of 10µl. The template/primer mixture was heated to 65°C for 2min and left to cool slowly to <35°C to allow annealing of the primer, and then placed on ice. The

Sequenase® enzyme was diluted to a concentration of 1.6U/µl in glycerol enzyme dilution buffer (C.6.2.5). The following components of the labelling reaction were added:

DTT (0.1M)	1µl
Labelling mix – diluted 1:5 (C.6.2.2)	2µl
[α-^{35}S]dATP (0.37MBq/µl;	
NEN Life Science Products)	0.5µl
Diluted Sequenase®	2µl
Total volume	15.5µl

The extension reaction was allowed to proceed for 5min at room temperature. To terminate the reactions, 3.5µl aliquots of the labelling reactions were added to each of four 0.5ml eppendorf tubes containing 2.5µl of each termination mixture (C.6.2.3) and prewarmed to 37°C. The reactions were incubated at 37°C for a further 5min, and stopped by the addition of 4µl of stop solution (C.6.2.4). The samples were either analysed immediately by denaturing gel electrophoresis, or stored at -20°C. Immediately before loading the samples on the gel they were heated to 70°C for 2min, then placed on ice.

2.4.9. Denaturing gel electrophoresis.

2.4.9.1. Electrophoresis of dye-terminated extension products.

A 6% polyacrylamide gel solution was prepared by dissolving 25g urea (Gibco) in 7.5ml of a 40% w/v acrylamide/bis solution (Bio-Rad Laboratories, Hemel Hempstead, Herts., UK), 5ml of 10X TBE (C.3.1) and DDW to a final volume of 50ml. The solution was deionised by addition of 1g of Amberlite monobed resin (BDH) and stirring for 5min, before being filtered through a Nalgene disposable filter (Techmate Ltd., Milton Keynes, Bucks., UK). The gel solution was polymerized by addition of 250µl of freshly prepared 10% w/v ammonium persulphate (10% APS) solution and 25µl of TEMED (N,N,N',N'-tetramethylethylenediamine – Bio-Rad), and poured immediately. The gel was poured at least 2h before the sequencing run was started. The sequencing gel was run in a 373A DNA Sequencer (ABI) at 2500V for 14h using 1X TBE as running buffer. The sequence

data was collected on a Macintosh computer running the 373A Sequence Data Collection Programme (ABI) and analysed using the 373A Sequence Analysis Programme (ABI).

2.4.9.2. Electrophoresis of ^{35}S-labelled extension products.

The products of sequencing reactions performed using Sequenase® were analysed using the Sequi-Gen™ nucleic acid sequencing cell apparatus (Bio-Rad). The glass electrophoresis plates were washed in detergent (Labdet 100, Don Whitley Scientific Ltd., Shipley, West Yorks., UK) and rinsed with DDW and ethanol. The upper plate was coated with Sigmacote™ (chlorinated organopolysiloxane; Sigma) and the plates were clamped together, separated by two 0.4mm plastic spacers along each edge. The bottom of the sequencing cell was sealed by clamping it in a casting tray containing a paper strip soaked in 10ml of 6% acrylamide gel solution to which 125µl of 10% APS and 50µl TEMED had been added. The 6% acrylamide gel solution was prepared essentially as described in section 2.4.9.1. above, except that 20X glycerol tolerant electrophoresis buffer (C.6.2.6) was substituted for 10X TBE, and the solution was neither deionised nor filtered. The solution was polymerized by the addition of 0.5ml 10% APS and 20µl TEMED and poured using a 50ml syringe. A 24-well sharks-tooth comb was inverted and placed in the top of the gel until it had set. The sequencing cell was assembled using 1X glycerol tolerant buffer as the running buffer and pre-run at 1500V for 20-30min. The comb was inserted and urea leaching from the gel was flushed out of the wells with a pasteur pipette before loading the samples. Electrophoresis was carried out at 1500V for 4-5h.

After electrophoresis, the upper siliconised plate was removed and the gel, still attached to the lower plate, was immersed in 5% acetic acid, 5% methanol (v/v) for 15-20min to remove the urea. The gel was transferred to a piece of 3MM chromatography paper (Whatman Scientific Ltd., Maidstone, Kent, UK), covered in Saran wrap, and dried on a vacuum drier (Bio-Rad) connected to a refrigerated solvent trap for 1h at 80°C. The dried gel was then exposed directly to radiographic film (Fuji RX Medical X-ray film) and developed after 1-4 days using an automatic developing machine (Xenograph). The sequence was read directly from the autoradiograph on a light box and entered into the

VAX 750 mainframe computer. The data was analysed using a number of programmes from the University of Wisconsin Genetics Computing Group (GCG) package (Devereux *et al.*, 1984).

CHAPTER THREE

THE CELLULAR IMMUNE RESPONSE IN THE REGIONAL LYMPH NODES OF CATTLE UNDERGOING PRIMARY INFECTION WITH *THEILERIA PARVA*.

3.1. Introduction.

In susceptible cattle infected with *Theileria parva*, the outcome of the infection is invariably fatal, demonstrating the failure of the immune system to mount an effective response. However, animals that recover from the infection, and cattle immunized by infection and simultaneous treatment with long-acting oxytetracycline, are resistant to challenge with a lethal dose of *T. parva*. Immunity is associated with cell-mediated immune responses, in particular with the generation of parasite-specific MHC class I-restricted $CD8^+$ cytotoxic cells (CTL), which are detected in the efferent lymph and peripheral blood of immune animals undergoing challenge (Eugui and Emery, 1981; Morrison *et al.*, 1987; McKeever *et al.*, 1994). In contrast, parasite-specific CTL are not generated at any stage during lethal infections with *T. parva*, and CTL precursors cannot be detected in the peripheral blood of naive cattle (Eugui and Emery, 1981; Taracha *et al.*, 1992). However, a massive increase in the cellularity of the lymph node draining the site of inoculation has been observed in these animals, at a time when schizont-infected cells are detected at very low levels (<1%) (Morrison *et al.*, 1981). Uninfected T lymphoblasts, comprising both $CD4^+$ and $CD8^+$ cells, form a significant proportion of cells (20-30%) in the efferent lymph at this time (Emery *et al.*, 1988). These findings suggest that naive animals mount a T cell response to *T. parva* in the drainage lymph node, but the subsequent rapid expansion of parasitized lymphoblasts indicates that this response is ineffective in controlling the infection.

The failure of naive cattle to control infections with *T. parva* may be attributable to strategies evolved by the parasite for evasion of host immune effector mechanisms. Strategies for immune evasion have been demonstrated in other parasitic infections, and involve interactions with a number of different components of the immune system. Induction by *T. parva* of an inappropriate host response would allow the parasite to

escape elimination, resulting in uncontrolled proliferation of schizont-infected cells. In *Leishmania* infections of mice and humans, susceptibility to disseminated progressive infections has been associated with inappropriate induction of $CD4^+$ T cells expressing Th2-type cytokines (IL-4, IL-5, IL-10), while individuals able to control the infection mount a Th1-type CD4 response characterized by the production of IFNγ (Heinzel *et al.*, 1991). The differentiation of naive $CD4^+$ T cells towards the Th1- or Th2-type phenotype is influenced by the cytokine environment in which initial priming occurs (Hsieh *et al.*, 1992; Seder *et al.*, 1993).

Development of *T. parva* macroschizonts takes place within lymphocytes, resulting in activation and proliferation of the infected cells. Studies with schizont-infected cell lines maintained *in vitro* have shown that they can produce IFNγ and low levels of IL-2 (Entrican *et al.*, 1991; Heussler *et al.*, 1992; Ahmed *et al.*, 1993). In addition, parasitized cells constitutively express functional IL-2 receptors (Coquerelle *et al.*, 1989; Dobbelaere *et al.*, 1990), and respond to IL-2 with increased proliferation, particularly at low cell densities (Dobbelaere *et al.*, 1988). Thus, it is possible that during the primary infection *in vivo*, cytokines secreted by responding T lymphoblasts could potentiate the growth of parasitized cells, and cytokines secreted by the infected lymphocytes may also be capable of modulating host immune reponses. Since both natural and experimental infections with *T. parva* are initiated by subcutaneous inoculation of sporozoites, immune responses will be generated initially in the local lymph node draining the site of inoculation. Indeed, the presence of large numbers of uninfected lymphoblasts in the drainage lymph nodes of cattle in the early stages of *T. parva* infection is evidence of an immune response to the parasite. The object of this chapter, therefore, was to determine the phenotype of the cells involved in the lymph node response to the parasite, and to examine the expression of a variety of cytokines in the drainage lymph node during primary infections with *T. parva*.

3.2. Materials and Methods.

3.2.1. Experimental infections.

The calves used in the experiments at Compton were castrated male Holstein-Friesians or Channel Island breeds. The Holstein-Friesians were bred at the Institute for Animal Health, Compton, and selected on the basis of their differing MHC phenotypes (see Table 3.1). The Channel Island calves were purchased from different local farms, and their MHC phenotypes were not determined. Most animals were 3 to 6 months old at the time of infection; in one experiment a 14 month old animal (3327) was used.

In initial experiments, pairs of calves were infected by subcutaneous inoculation with infective tick stabilate as described in Section 2.1. Samples of cells from the prescapular lymph node were obtained by needle biopsy at different times during the infection for detection of parasites and phenotypic analysis of the cells by flow cytometry. Four animals were euthanased at specified times after infection and the prescapular lymph nodes collected to provide larger numbers of cells for cell sorting. The remaining animals were treated on day 10 of infection by intramuscular injection of buparvaquone (Butalex®) at a dose of 20mg/kg.

In a later experiment, a group of six Channel Island calves were infected as before, and euthanased in pairs on days 5, 7 and 9 post-infection. The prescapular lymph nodes were removed to provide material for phenotypic analysis, histological examination, cell sorting and RNA isolation. Two uninfected calves of a similar age were used as controls.

The animal used for the infection and cannulation experiment carried out at ILRI was a 14 month old Boran X N'Dama heifer, which had been kept indoors under tick-free conditions. Five days after subcutaneous inoculation with infective tick stabilate, the efferent lymph duct draining the right prescapular lymph node was surgically cannulated with a dual-lumen cannula that permitted continuous infusion of Alsever's solution to the proximal tip of the cannula. Efferent lymph flowing down the lumen of the larger cannula was collected aseptically each day and the cells were separated for phenotypic analysis.

On day 15 post-infection, the cannula was removed and the animal was treated with buparvaquone, as above.

Table 3.1. MHC Phenotypes of Calves Used in Experiments.

Calf number	MHC Phenotype
3327	A10/A12
4282	A14/A11
4260	A10/A18
4291	A12/A31
5158	A18/CC1
5178	A11/A31

Serological typing for MHC class I antigens was carried out by Dr. M. Stear, Department of Veterinary Medicine, University of Glasgow, using specific alloantisera in a complement-mediated microlymphocytotoxicity test.

3.2.2. Immunofluorescent staining of lymph node cells for phenotypic analysis.

Mononuclear cells (MNC) were isolated from lymph node aspirates and from prescapular lymph nodes as described in Sections 2.2.1.2 and 2.2.1.3. The monoclonal antibodies (mAbs) used for single staining were MM1A (CD3), CC42 (CD2), CC30 (CD4), CC63 (CD8), GB21A (γδTCR), IL-A58 (surface Ig), CC-G33 (CD14) and IL-A24 (bovine monocyte/dendritic cell marker). Two-colour immunofluorescent staining was performed using the combinations of mAbs listed in Table 3.2. Three-colour immunofluorescent staining using a combination of IL-A43 (CD2), GB21A (γδTCR) and biotinylated CC63 (CD8) was carried out on lymph node cells isolated on day 9 post-infection from two animals. In some animals, PBMC were examined by single and two-colour fluorescent antibody staining using the same panel of monoclonal antibodies. Details of all monoclonal antibodies used and the staining procedures are given in Table 2.1 and Section 2.2.2.

Some of the monoclonal antibodies used in the phenotypic analysis of efferent lymph lymphocytes (ELL) were different from those described above. CH128A (CD2), IL-A12 (CD4), IL-A105 (CD8), IL-A51 (CD8) and IL-A30 (IgM) were substituted, where appropriate, in single and two-colour fluorescent antibody staining. The two-colour analysis of phenotype was extended by using CH128A and IL-A29 (WC1) in separate combinations with GB21A (γ/δ TCR).

The samples were analysed on a FACScan (Becton Dickinson). 5000 events (single staining), 10000 events (two-colour staining) or 15000 events (three-colour staining) were recorded. Statistical analysis of the data was carried out using PC LYSYS II software (Becton Dickinson).

Table 3.2. Combinations of monoclonal antibodies used in two-colour immunofluorescence analysis.

Target molecules	Monoclonal antibodies	Isotypes
CD3/CD8	MM1A/CC63	IgG1/IgG2$_a$
CD2/CD8	CC42/CC63	IgG1/IgG2$_a$
CD2/CD4	CC42/CC8	IgG1/IgG2$_a$
γ/δTCR/CD8	GB21A/CC63	IgG2$_b$/IgG2$_a$
CD4/CD8	CC30/CC63	IgG1/IgG2$_a$
CD8β/CD8α	CC58/CC63	IgG1/IgG2$_a$
CD3/MHC class II	MM1A/IL-A21	IgG1/IgG2$_a$
CD3/CD25	MM1A/CACT108A	IgG1/IgG2$_a$
γ/δTCR/CD25	GB21A/CACT108C	IgG2$_b$/IgG2$_a$
CD25/CD8	IL-A111/CC63	IgG1/IgG2$_a$
CD25/CD4	IL-A111/CC8	IgG1/IgG2$_a$

3.2.3. Isolation and culture of $CD2^-CD8^+$ T cells from the drainage lymph node.

3.2.3.1. Purification of $CD2^-CD8^+$ T cells by flow cytometry.

Lymph node cells obtained from infected animals were sorted by flow cytometry to obtain a purified population of $CD2^-CD8^+$ T cells. The cells were stained with the primary mAbs CC42 (CD2; IgG1) and CC63 (CD8; $IgG2_a$) followed by fluorescein isothiocyanate (FITC)-conjugated goat anti-mouse IgG1 and phycoerythrin (PE)-conjugated goat anti-mouse $IgG2_a$, as described in Section 2.2.2.3, and sorted on a FACStar Plus cell sorter (Becton Dickinson). In some experiments, the cells were enriched for $CD8^+$ T cells prior to sorting by incubation with magnetic beads and separation on MACS VS^+ Separation Columns (Miltenyi Biotec); the details of the protocol are given in Section 2.2.2.3. The primary mAbs were IL-A43 (CD2; $IgG2_a$) and CACT80C (CD8; IgG1) and the secondary mAbs were goat anti-mouse $IgG2_a$-PE and goat anti-mouse IgG1-FITC, allowing positive selection of $CD8^+$ cells using MACS beads coupled to an anti-FITC monoclonal antibody. Cells were selected for sorting by setting a gate on the live cells, which were distinguished from dead cells by light scattering characteristics, and gating on the $CD2^-CD8^+$ cell population (and the $CD2^+CD8^+$ population in some experiments) according to the fluorescence parameters. An example of the gates set for sorting is illustrated in Figure 3.1.

As contamination of the sorted population with γ/δ T cells had proved to be a problem during early experiments, the protocol for cell sorting was later modified to specifically exclude γ/δ T cells. This involved staining with three primary mAbs; GB21A (γ/δTCR; $IgG2_b$), IL-A45 (CD2; $IgG2_b$) and CACT80C (CD8; IgG1). The secondary mAbs were goat anti-mouse IgG1-FITC and goat anti-mouse $IgG2_b$-PE, and the $CD8^+$ population was first enriched as before, by MACS sorting with magnetic beads coupled to an anti-FITC mAb. Since both the CD2- and γδTCR-specific mAbs were of the $IgG2_b$ isotype, the $\gamma/\delta TCR^+$ cells were included in the population of cells stained by the PE-conjugated secondary antibody, and excluded from the $CD2^-CD8^+$ population gated for sorting.

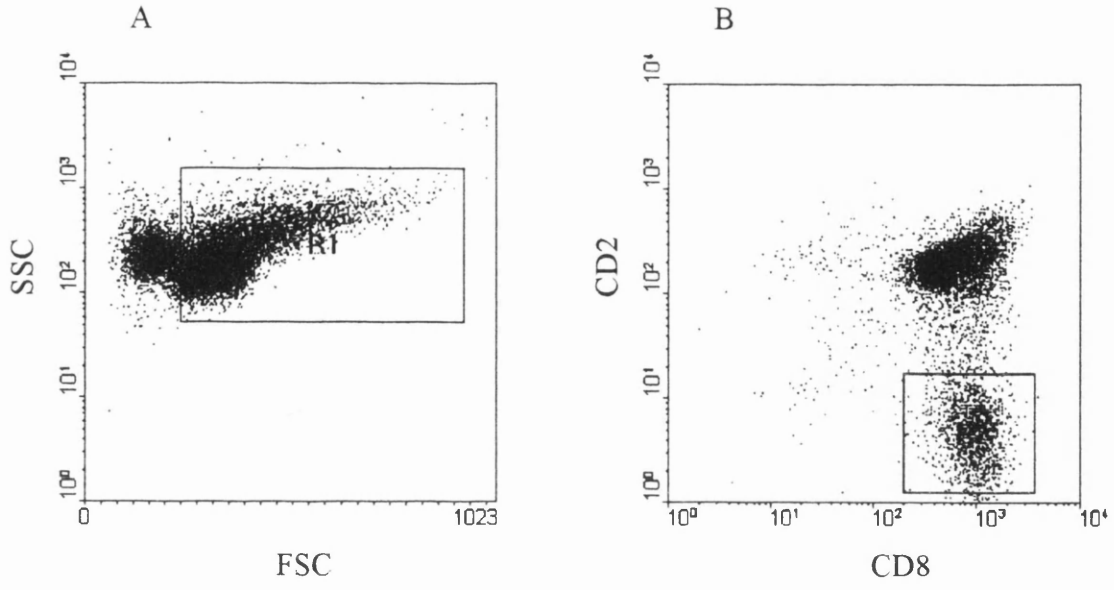

Figure 3.1. Gates to select $CD2^-CD8^+$ T cells. Mononuclear cells isolated from the prescapular lymph node of animal 5158 on day 9 of infection with *T. parva*, were stained with mAbs against CD2 (IL-A43; $IgG2_a$) and CD8 (CACT80C; IgG1). The secondary mAbs were fluorescein isothiocyanate (FITC)-conjugated goat anti-mouse IgG1 and phycoerythrin (PE)-conjugated goat anti-mouse $IgG2_a$. $CD8^+$ cells were enriched to >95% purity by incubating with anti-FITC MACS microbeads (Miltenyi Biotec) and sorting using a MidiMACS VS^+ separation column (Miltenyi). The $CD2^-CD8^+$ cells were sorted to >99% purity on a FACStar Plus cell sorter (Becton Dickinson) using two sort gates: A – forward scatter (FSC) v side scatter (SSC) gate used to distinguish live cells from dead cells and subcellular debris. B – gate set on $CD2^-CD8^+$ cells in a FITC (CD8) fluorescence (x-axis) v PE (CD2) fluorescence (y-axis) dot plot display.

3.2.3.2. Culture of sorted $CD2^-CD8^+$ T cells.

Various stimulation protocols were tried in an attempt to establish cell lines and/or clones from the sorted $CD2^-CD8^+$ T cells. Cultures were established in 96-well round-bottomed microculture plates with the sorted cells being titrated by threefold dilution at cell concentrations ranging from 300 to 0.3 cells/well. 2×10^4 irradiated (20Gy) autologous PBMC were added to each well as filler cells. The stimulators were irradiated (50Gy) autologous *T. parva*-infected leucocytes added at 5×10^3 cells/well. The culture medium was supplemented with either 10% T cell growth factors (TCGF) or 10U/ml recombinant bovine IL-2 (rboIL-2). TCGF was prepared from supernatants of cultured PBMC stimulated with ConA, essentially as described by Goddeeris and Morrison (1988), and the recombinant IL-2 was generously provided by Dr. R. A. Collins, IAH Compton. The cultures were incubated at 38°C, and regularly examined microscopically for the outgrowth of the cells.

Further experiments using a variety of stimulation protocols were carried out in an attempt to culture the $CD2^-CD8^-$ T cells. Preliminary experiments were carried out to determine optimal conditions for stimulation of purified resting $CD8^+$ T cells from uninfected animals. $CD8^+$ T cells were sorted from the PBMC of two animals using magnetic beads (see Section 2.2.2.4), distributed in 96 well round-bottomed plates at 10^5 cells/well, and cultured in medium supplemented with 10% TCGF under the following stimulation conditions:

a) Concanavilin A (ConA) at 5μg/ml.

b) ConA (5μg/ml) and 2×10^4 irradiated (20Gy) autologous PBMC/well.

c) Phorbol myristate acetate (PMA) at 50ng/ml and ionomycin at 1μg/ml.

The cultures were pulsed with tritiated thymidine and harvested after 3, 5 and 7 days to assess the level of proliferation, as described in Section 2.2.4.

In subsequent experiments, the sorted $CD2^-CD8^+$ cells were distributed at 10^4 cells/well, cultured in medium supplemented with 10% TCGF or rboIL-2, and stimulated with

a) ConA (5μg/ml) in the presence of 2×10^4 irradiated (20Gy) filler cells,

b) phorbol myristate acetate (PMA; 50ng/ml) and ionomycin (1μg/ml) in the presence or absence of 10^4 irradiated (20Gy) autologous lymph node cells as fillers, or

c) 2 x 10^4 irradiated (50Gy) MHC-matched *T. parva*-infected cells.

Proliferation was evaluated either by microscopic examination for outgrowth of the cells or by measuring [^{3}H] thymidine incorporation after 4 days in culture.

3.2.4. Histological examination of lymph node sections.

For this experiment, a group of eight Channel Island calves were used. Two control calves were killed on day 0; the other six calves were infected with *T. parva*, and pairs of calves were killed on days 5, 7 and 9 post-infection. The right prescapular lymph nodes were removed, and blocks cut from the nodes were fixed in formalin or mercuric formalin, or snap-frozen embedded in OCT compound, as described in Section 2.3.1. Sections cut from the blocks fixed with mercuric formalin were stained with haematoxylin and eosin for examination of the lymph node morphology (see Section 2.3.2).

Immunocytochemistry was performed on cryostat sections from the frozen lymph node blocks using the monoclonal antibodies MM1A (CD3), CC42 (CD2), GB21A (γδTCR), CC149 (MyD-1), CC94 (CD11b), MoAb5 (*T. parva* schizonts) and NCL-Ki67-MM1. Two mouse monoclonal antibodies with irrelevant specificities, AV29 ($IgG2_b$) and TRT1 (IgG1), were used as isotype controls. Details of the monoclonal antibodies and the staining procedure are given in Section 2.3.3 and Table 2.1. In addition, selected cryostat sections were stained for detection of the lysosomal enzyme acid phosphatase (Section 2.3.4).

Sections cut from lymph node blocks fixed with formalin were used for *in situ* hybridization with a digoxigenin (DIG)-labelled IL-10-specific riboprobe to detect expression of IL-10 mRNA, as described in Section 2.3.5.

3.2.5. Analysis of cytokine mRNA expression by polymerase chain reaction.

The expression of cytokines in the drainage lymph node during primary infection with *T. parva* was examined in the series of animals killed on days 5, 7 and 9 post-infection. Total RNA was isolated from the whole lymph node MNC population and from $CD4^+$ and $CD8^+$ T cell subpopulations separated using magnetic beads, as described in Section 2.4.1. First strand cDNA synthesis was performed on total RNA using the Reverse Transcription System (Promega) as described in Section 2.4.3, and used directly as a template for the polymerase chain reaction (PCR). Specific primers for β-actin, IL-2, IFNγ, TNFα, IL-4, IL-6 and IL-10 were used to amplify the cDNA encoding these molecules in the PCR (see Section 2.4.4). The sequences of the cytokine primers are given in Table 2.2. PCR products were analysed by electrophoresis in 1% agarose gels. Products of the predicted size were recovered from the gel and digested with restriction enzymes to verify the specificity of the PCR reaction.

3.2.6. Effect of lymph plasma from *T. parva*-infected animals on the growth of parasitized cell lines seeded at limiting dilutions.

In an experiments carried out at ILRI, a naive animal (AT115) was infected with *T. parva*, and the efferent lymphatic duct of the left prescapular lymph node was subsequently cannulated, allowing daily collection of efferent lymph over the early course of the infection. Mononuclear leucocytes were separated from efferent lymph by density gradient centrifugation; the remaining lymph plasma was removed separately and stored at -20°C. To remove the Alsever's solution used as anti-coagulant, which can inhibit immune responses, lymph plasma collected on day 7 and day 11 of infection was dialysed against RPMI 1640 medium for 18h with three changes of medium. The dialysed plasma was centrifuged at 500xg for 10 min to remove clots. As a control, normal lymph was collected by cannulation of the efferent prescapular lymphatic duct of second animal, and the lymph plasma was collected and treated in the same way as above.

A *T. parva*-infected cell line was harvested in the logarithmic growth phase. In initial experiments to determine the cell density at which continued cell growth was inhibited,

cells were seeded in 96 well round-bottomed plates at 1 x 10^4 cells/well, and titrated in two-fold dilutions to 3 x 10^2 cells/well. Triplicate dilutions of two cell lines were incubated for either 48h or 72h at 38°C in a humidified atmosphere of 5% CO_2 in air. Proliferation was measured by the incorporation of [^{125}I] iododeoxyuridine.

To determine the effect of lymph plasma from the *T. parva*-infected animal on proliferation of parasitized cells plated at limiting dilutions, cell lines were titrated as above in a series of two-fold dilutions from 5 x 10^3 cells/well to 3 x 10^2 cells/well. The dilution series were incubated in triplicate in medium containing 0%, 2.5%, 5%, 10% and 20% dialysed lymph plasma from the uninfected control animal and from an infected animal, as above. After 72h, proliferation of the cells was measured as before, by the incorporation of [^{125}I] iododeoxyuridine.

3.3. Results.

3.3.1. Kinetics of experimental infections with *Theileria parva.*

The progress of experimental infections with *Theileria parva* in 8 calves was followed by monitoring the rectal temperature, lymph node size and the number of schizonts present in smears of lymph node needle biopsies from infected animals. A rectal temperature (RT) of 39.5°C or greater was considered to indicate pyrexia. The schizont index (SI) was estimated by calculating the number of schizonts per 100 cells in lymph node smears, as described in Section 2.1.1. This information is summarized in Table 3.3. In general, the response to the stabilate was consistent in all eight animals, with only slight individual variation. Schizonts were first detected at 6-8 days post-infection, and in all but one animal the percentage of parasitized cells was 1% or less by day 8 of infection. By day 9 post-infection, the percentage of schizont-infected cells had risen above 3% in only two animals. In one calf (5178), schizonts were not detected at any point during the infection; however this was probably due to the poor quality of the lymph node smear obtained on day 8 post-infection, since in all other respects this calf appeared to be infected. There was a dramatic increase in lymph node size from day 6 of infection, so that the lymph nodes were markedly enlarged by day 8. The onset of fever was more variable, ranging from 7 to 9 days, and in two animals fever was not detected within the time-course of the experiment.

The kinetics of the infection in the animal (AT115) used in the cannulation experiment at ILRI were different, because a different stabilate was used. Schizonts were not detected in the drainage lymph node until day 9 post-infection, and the SI remained below 5% at day 12. Fever was not detected in this animal until day 13 post-infection; from days 9 to 12 of infection the rectal temperature was between 39°C and 39.5°C.

Table 3.3. Summary of the kinetics of primary infection with *T. parva* in experimental calves.

Days post-infection		0	3	6	7	8	9	10
Calf no.								
4260	RT (°C)	39.8	39.8	38.6	40.1	40.9	40.6	42.0
	SI	-	-	-	<1%	<1%	1%	6%
	LN size	-	+	++	+++	+++	+++	+++
4282	RT (°C)	39.1	38.9	38.2	38.8	39.1	38.9	39.3
	SI	-	-	-	-	<1%	<1%	5%
	LN size	-	+	++	++	+++	+++	+++
4291	RT (°C)	39.0	38.6	39.1	39.2	39.3	ND	
	SI	-	-	-	-	1%	4%	
3327	RT (°C)	38.9	38.2	38.3	40.2	40.1	ND	
	SI	-	-	-	-	<1%	5%	
5158	RT (°C)	38.9	38.8	39.2	38.6	39.2	39.6	
	SI	-	-	-	-	<1%	2%	
5178	RT (°C)	38.3	38.9	38.9	39.2	39.5		
	SI	-	-	-	-	ND		
776	RT (°C)	38.5	38.5	39.3	39.8	39.9	40.0	
	SI	-	-	-	<1%	<1%	1%	
	LN size	-	+	++	+++	+++	+++	
782	RT (°C)	38.8	38.7	40.2	39.5	40.4	40.1	
	SI	-	-	<1%	1%	1-2%	1-2%	
	LN size	-	+	++	+++	+++	+++	

Notes: RT = rectal temperature; SI = schizont index; LN = lymph node; ND = not done. Lymph node size was estimated by external palpation: + = 5-10mm diameter (cross-sectional area), ++ = 10-20mm diameter, +++ = 20-30mm diameter.

3.3.2. Changes in the phenotype of lymph node cells during primary infections with *Theileria parva.*

3.3.2.1. Indirect immunofluorescent staining using single monoclonal antibodies.

Lymph node cells were collected by needle biopsy immediately before infection, on day 3, and daily from day 6 post-infection with *T. parva*. Changes in the major subpopulations of lymphocytes during the course of the infection were monitored by flow cytometric analysis with mAbs against CD2, CD3, CD4, CD8, γδ T-cell receptor (T cells), surface immunoglobulin (B cells), CD14 and the monocyte marker recognised by IL-A24. The results of this analysis for 5 calves (4260, 4282, 4291, 5158 and 5178) are summarized in a table in Appendix D). For the T and B lymphocyte populations, defined by expression of CD3 and surface Ig respectively, no consistent trends were detected. In some animals, an early increase in the percentage of B cells was observed from day 3 to day 6 of infection, with a corresponding decrease in the proportion of T cells. There was also a tendency for the proportion of T cells to increase between days 6 and 8 post-infection. In some animals, an increase in the percentage of cells expressing the monocyte markers recognized by CC-G33 and IL-A24 was seen on days 9-10 of infection.

The changes in the $CD4^+$ and $CD8^+$ T cell subpopulations during the course of infection with *T. parva* in four animals are illustrated in Figure 3.2. To minimize the effect of fluctuations in the proportions of B cells or monocytes on the percentages of $CD4^+$ and $CD8^+$ T cells, they were expressed as a percentage of the total T cell population ($CD3^+$) rather than the total mononuclear cell population. The most consistent change in T cell subpopulations was an increase in the percentage of $CD8^+$ T cells, peaking on days 8 to 10 post-infection. This is demonstrated by a reversal in the CD4:CD8 ratio between day 0 and day 8 post-infection for most animals. Changes in the $CD4^+$ T cell subpopulation were more variable, but in some animals there was a small increase in the percentage of positive cells by days 6 or 7 post-infection, followed by a gradual decline. In one animal (5178), there was a marked increase in the percentage of $CD4^+$ T cells by day 6 and the proportion of positive cells remained elevated at day 8 post-infection. Changes in the γδ T cell subpopulation were also variable; the proportion of these cells tended to remain low throughout the observed period of the infection, and no distinct trends emerged.

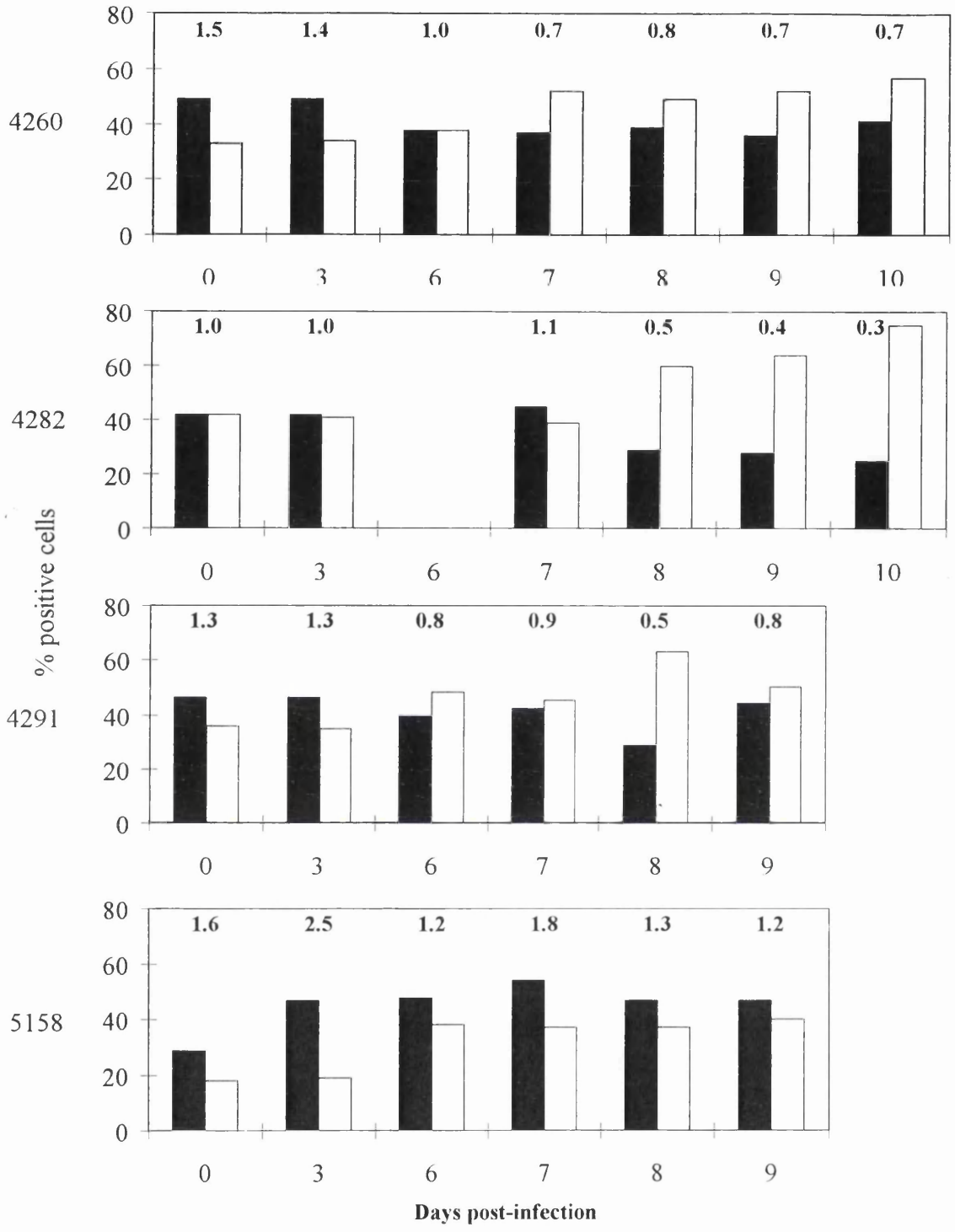

Figure 3.2. Changes in T cell subsets in the prescapular lymph nodes of four animals infected with *T. parva*. The proportions of $CD4^+$ T cells (solid bars) and $CD8^+$ T cells (open bars) are expressed as a percentage of the total T cell population i.e. the proportion of the lymph node mononuclear cell population that express CD3. The CD4:CD8 ratio is shown for each time point. When the CD4:CD8 ratios of day 0 and day 8 were compared using the Mann-Whitney U test, they were found to be significantly different ($p<0.05$). A non-parametric test was used because there were insufficient data points to determine whether the values fall into a normal distribution.

3.3.2.2. Two-colour immunofluorescent staining.

An example of the results of two-colour analysis of the $CD8^+$ lymphocyte population from animal 4282 are illustrated in Figure 3.3. The results of the analysis over the course of the infection in this animal and four others are summarised in Table 3.4. The most notable change was the emergence of a population of $CD2^-CD8^+$ T cells (Figure 3.3; C) which appeared initially on day 7 or 8 of infection. In the majority of the animals examined the appearance of this population coincided with the time at which schizonts were first detected in the drainage lymph node, and with the reversal of the CD4:CD8 ratio. For example, for animal 4291, in which schizonts were detected initally on day 8 post-infection, the CD4:CD8 ratio at this time was 0.5 (compared to 0.9 on the previous day, and 1.3 on day 0) and the percentage of $CD2^-CD8^+$ cells was 17% (compared to 2% on the previous day). The $CD2^-CD8^+$ cells expressed CD3 (Figure 3.3; B), indicating that they express T cell receptors. There was a small increase in the percentage of $\gamma\delta TCR^+$ T cells co-expressing CD8 (Figure 3.3; D), which may also be $CD2^-$; however, the proportion of these cells at day 8 was 7% of the total lymph node population compared to the $CD2^-CD8^+$ T cells which comprised 30% of the population at this time. This suggests that the majority of the $CD2^-CD8^+$ T cells express the α/β TCR. This was supported by three-colour fluorescent antibody staining on day 9 of infection, with antibodies to CD2 (IL-A43), γδTCR (GB21A) and CD8 (CC63), as illustrated in Figure 3.4. After gating on the $CD8^+$ cells, the expression of CD2 and γδTCR was analysed. In animals 4282 and 4260, only 3% and 2% respectively of the total lymph node population was $\gamma\delta TCR^+CD2^-CD8^+$, compared to 19% (4282) and 10% (4260) with the phenotype $\gamma\delta TCR^-CD2^-CD8^+$.

On the vast majority of the $CD8^+$ T lymphocytes the CD8 molecule was expressed as the $\alpha\beta$ heterodimeric form of the molecule, as demonstrated by staining with mAbs specific for the α and β chains (Figure 3.3; E). The percentage of T cells co-expressing CD4 and CD8 (Figure 3.3; F) remained very low during the first 9 days of the infection, but a small increase was observed on day 10 in animals 4260 and 4282 (see Table 3.4). Examination of $CD4^+$ T lymphocytes by two-colour immunofluorescent staining for CD2 and CD4 showed no evidence for the emergence of a $CD2^-CD4^+$ population during infection, as illustrated in Figure 3.5.

Two-colour staining with antibodies against T cell-specific antigens and CD25 (the α chain of the IL-2 receptor) was performed to assess the extent of T cell activation in the lymph node. The results were disappointing, due to low fluorescence intensity of staining on less than 5% of lymph node cells with both the monoclonals to CD25 (IL-A111 and CACT108A) on days 8-10 of infection, when there was a significant blast response in the node. However, during infection there was significant up-regulation of MHC class II expression (another indicator of T cell activation) on $CD3^+$ cells in the lymph node, as shown in Figure 3.6. In the resting lymph node, 3% of the cells co-expressed CD3 and MHC class II molecules, while on day 8 post-infection 16% of the total lymph node population and 21% of the blast cell population were $CD3^+$MHC class II^+.

To focus on the cells participating in the immune response to *T. parva,* gates were set on the larger cells, i.e. those with high forward scatter (FSC^{hi}), as shown in Figure 3.3 in the right-hand column. Since lymphoblasts are much larger than resting lymphocytes, this population contains most of the activated cells. Figure 3.7 illustrates the composition of this population in 3 animals (4260, 4282 and 4291) on day 8 of infection. The majority of cells falling within the high forward scatter gate were $CD8^+$ T cells (61%-85%), and in each animal more than half of these lacked expression of CD2. The percentage of γδ T cells in the blast cell population was low (8%-11%); however most of the activated γδ T cells co-expressed CD8 (see Figure 3.3; D). The proportions of activated $CD4^+$ T cells and B cells were also low, ranging from 10% to 19% and 10% to 13% of the FSC^{hi} population respectively.

Table 3.4. Results of two-colour immmunofluorescent staining of $CD8^+$ cells in lymph nodes of calves infected with *T. parva*.

Phenotype	Calf number	Days post-infection					
		0	6	7	8	9	10
		Percentage positive cells					
$CD3^+CD8^+$	4260	ND	ND	29	36	29	30
	4282	33	ND	33	52	45	59
	4291	22	36	36	45	ND	-
	5158	11	23	14	13	18	-
	5178	15	20	26	30	-	-
$CD2^+CD8^+$	4260	ND	ND	22	26	18	19
	4282	31	ND	32	27	26	29
	4291	20	36	33	28	21	-
	5158	8	12	15	9	9	-
	5178	12	19	20	25	-	-
$CD2^-CD8^+$	4260	ND	ND	10	11	9	13
	4282	3	ND	2	25	20	30
	4291	2	2	2	17	6	-
	5158	3	0	1	4	6	-
	5178	1	1	5	2	-	-
$\gamma\delta TCR^+CD8^+$	4260	ND	ND	2	3	ND	5
	4282	2	ND	1	5	ND	7
	4291	2	2	2	3	5	-
	5158	1	1	2	1	1	-
	5178	1	2	ND	2	-	-
$CD8\alpha^+CD8\beta^+$	4260	ND	ND	27	ND	26	22
	4282	31	ND	31	48	43	51
	4291	ND	33	33	39	26	-
	5158	11	14	ND	13	2	-
	5178	9	18	ND	29	-	-
$CD4^+CD8^+$	4260	ND	ND	1	2	2	6
	4282	2	ND	1	3	2	4
	4291	ND	1	1	3	3	-
	5158	1	ND	1	2	2	-
	5178	2	ND	1	2	-	-

Notes: ND = not done

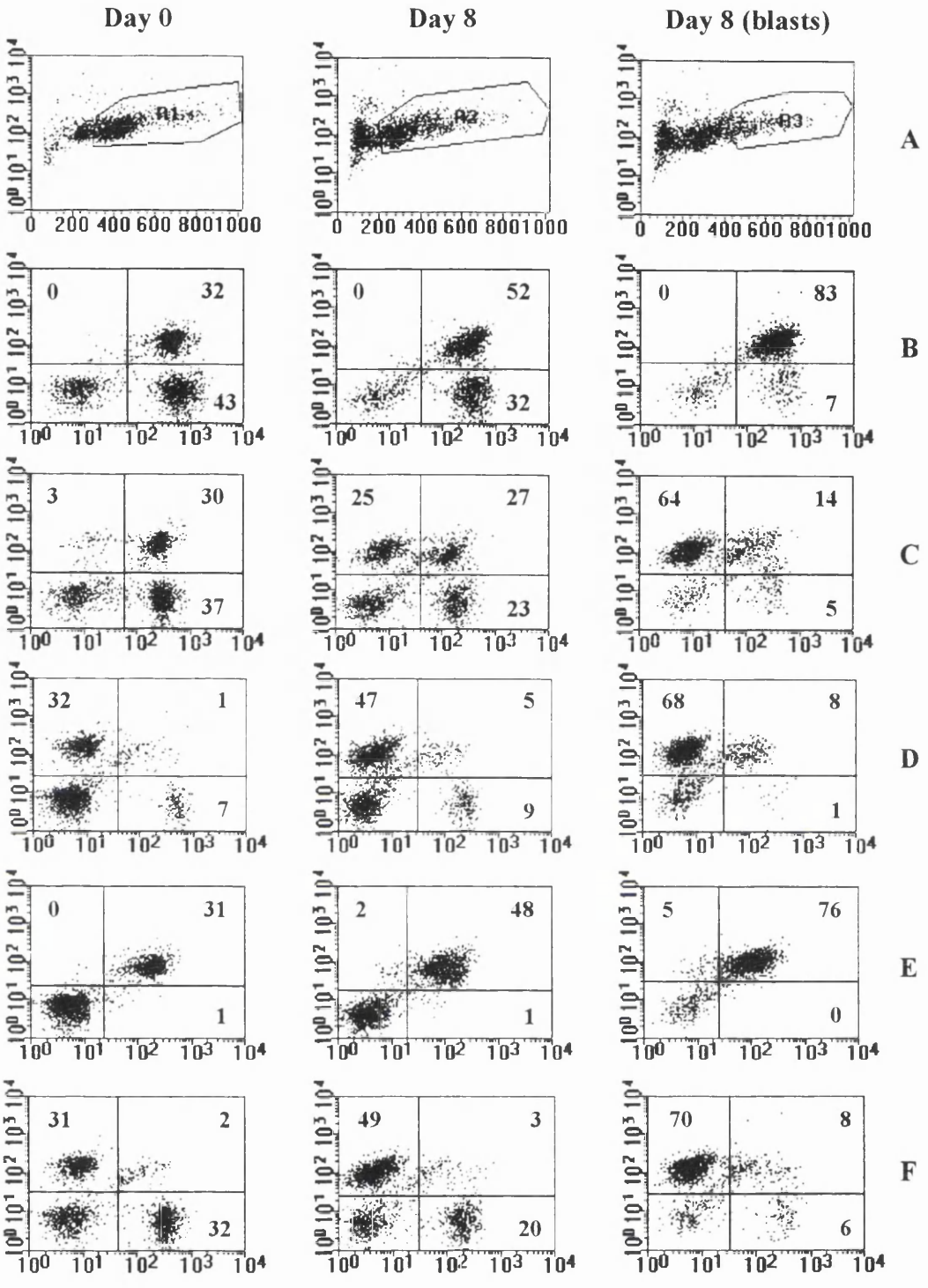

Figure 3.3. Changes in the phenotype of $CD8^+$ T lymphocytes in the drainage lymph node of calf 4282 during primary infection with *T. parva*. A: dot-plots showing forward scatter (x-axis) against side scatter (y-axis) and the gates set for analysis. B-F:dot plots showing the expression of CD3 (B), CD2 (C), γδTCR (D), CD8 β-chain (E), and CD4 (F) (x-axes), on cells expressing the CD8 α-chain (y-axes). The figures indicate the percentage of positive cells within each quadrant.

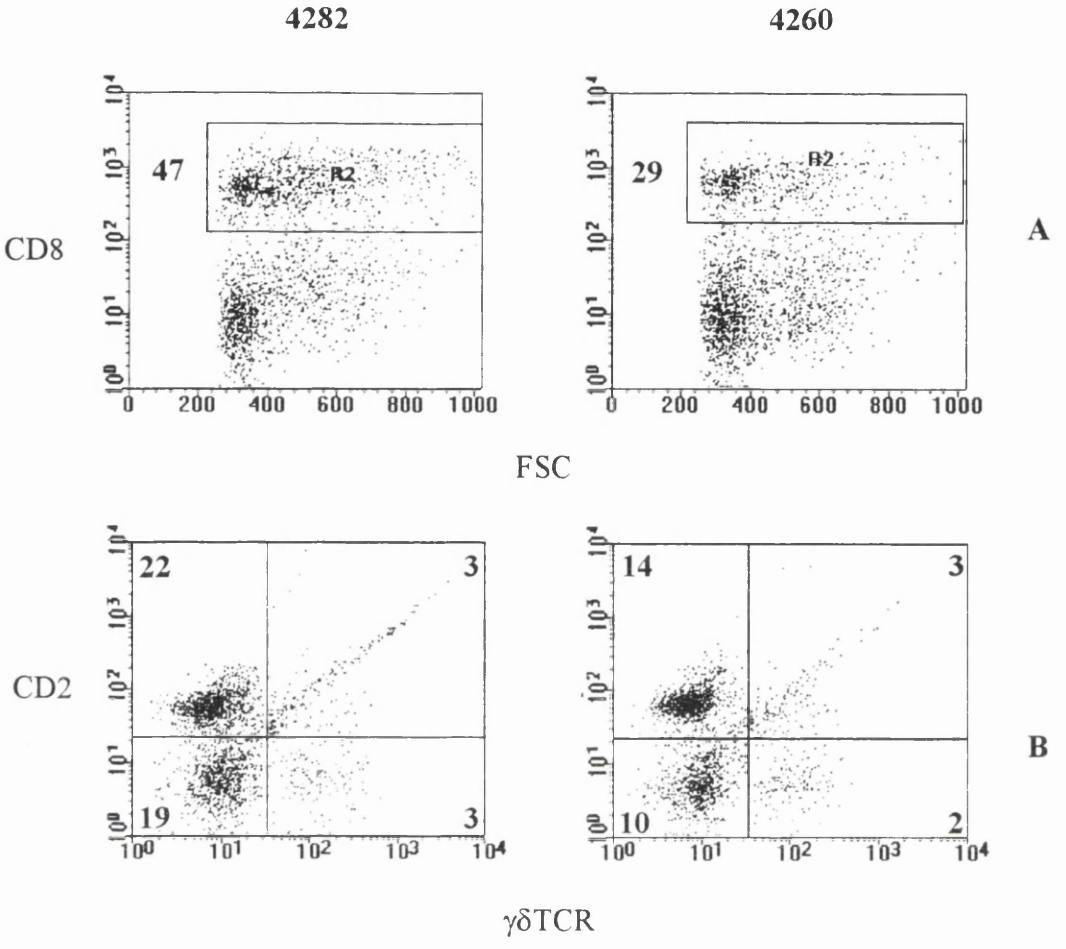

Figure 3.4. Three-colour immunofluorescent staining of CD8+ T cells isolated from the prescapular lymph nodes of animals 4260 and 4282 on day 9 post-infection. mAbs against CD2 (IL-A43; $IgG2_a$) and γ/δTCR (GB21A; $IgG2_b$) were used in combination with a biotinylated anti-CD8 mAb (CC63). The secondary mAbs were fluorescein isothiocyanate (FITC)-conjugated goat anti-mouse $IgG2_b$ and phycoerythrin (PE)-conjugated goat anti-mouse $IgG2_a$. The biotinylated mAb was revealed by staining with Streptavidin-Cy-Chrome™ (Pharmingen). A: a gate was set on the $CD8^+$ cells; the percentage of lymph node cells falling within the gate is indicated. B: dot-plots showing the distribution of cells expressing CD2 and γδTCR within the $CD8^+$ population. The figures in each quadrant indicate the percentage of the total lymph node population falling within those quadrants.

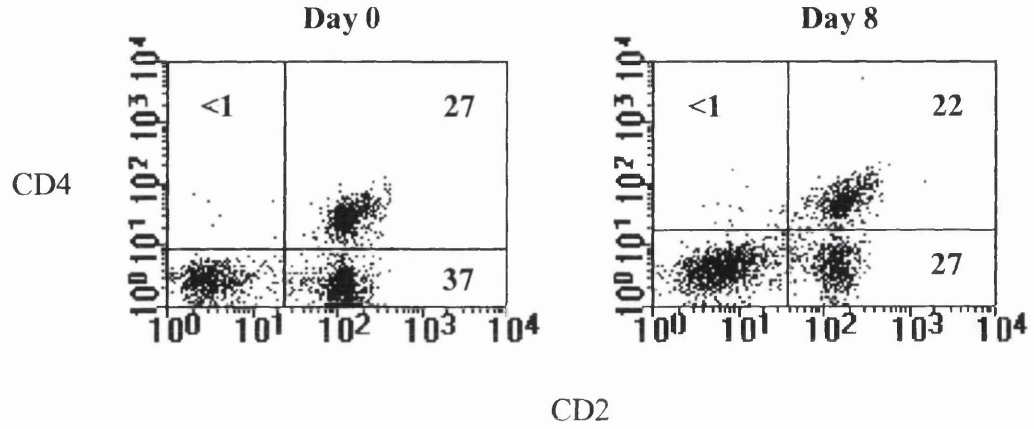

Figure 3.5. Expression of CD2 on $CD4^+$ lymphocytes is unaltered during primary infection with *T. parva*. The dot-plots show the results of two-colour staining with antibodies against CD2 (x-axes) and CD4 (y-axes) of drainage lymph node cells from calf 4282 on days 0 and 8 post-infection.

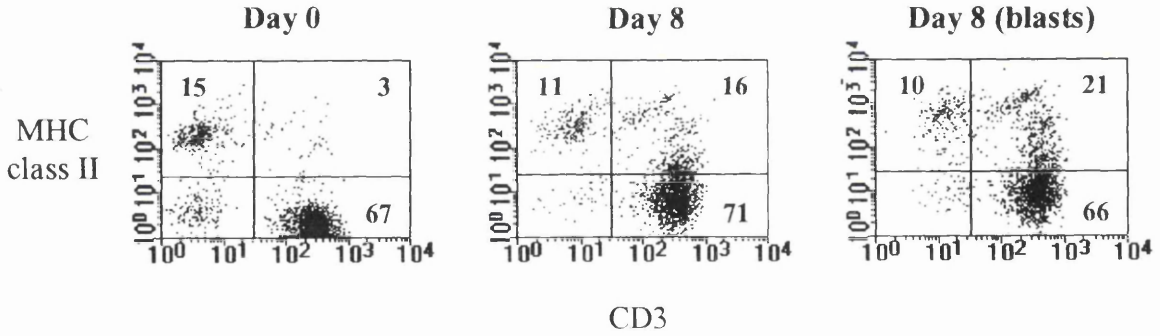

Figure 3.6. Upregulation of activation markers on T lymphocytes during primary infection with *T. parva*. The dot-plots show the results of two-colour staining with antibodies against CD3 (x-axes) and MHC class II molecules (y-axes) on drainage lymph node cells from animal 4282 on days 0 and 8 post-infection. The blasting cells on day 8 of infection were selected by gating on the cells with high forward scatter. The cell populations and gates are identical to those illustrated in Figure 3.3.

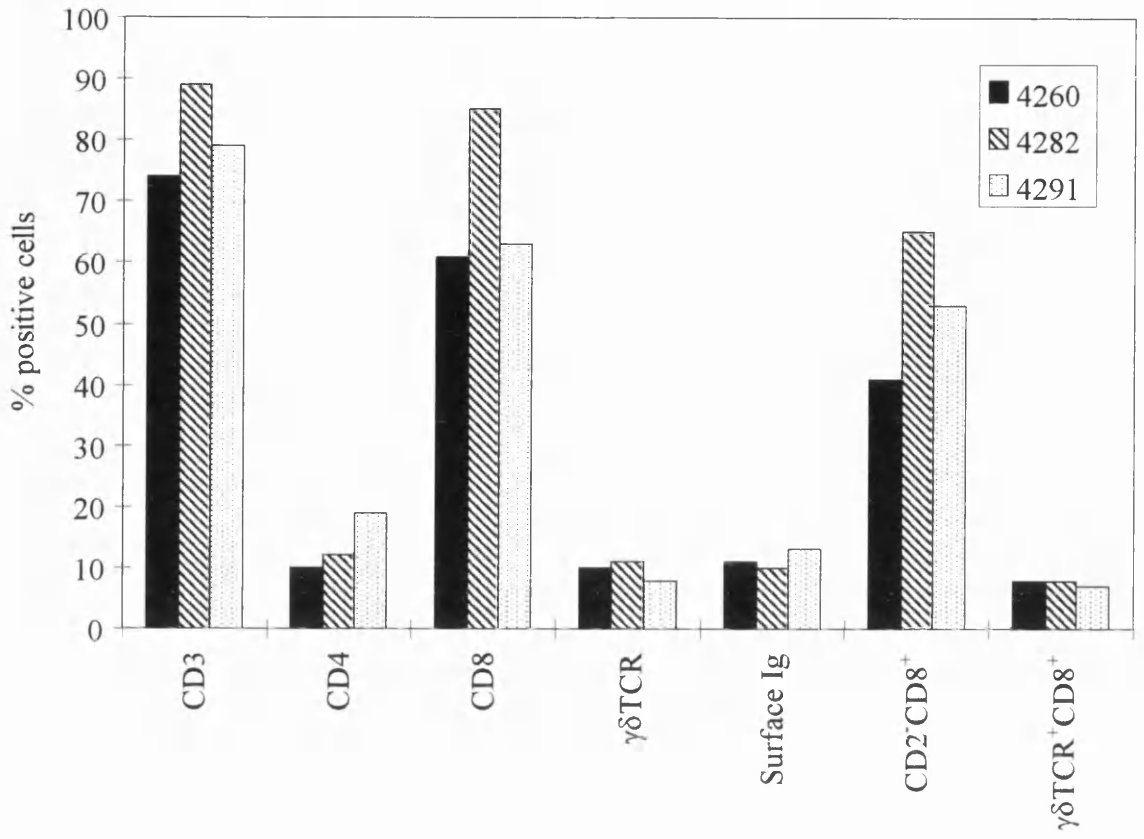

Figure 3.7. Surface phenotype of the lymphoblast population in the prescapular lymph nodes of three animals (4260, 4282 and 4291) on day 8 of infection with *T. parva*. Mononuclear cells isolated from lymph node suspensions were stained with mAbs to the lymphocyte surface markers indicated, and fluorochrome-conjugated isotype-specific goat anti-mouse IgG secondary mAbs. The samples were analysed on a FACScan (Becton Dickinson) and statistical analysis was performed using PC Lysys II software. The blasting cells were selected by gating on cells with high forward light scatter as illustrated in Figure 3.3.

3.3.2.3. Phenotypic analysis of efferent lymph lymphocytes during primary infection with *T. parva.*

To determine whether the changes in phenotype of the drainage lymph node cells were reflected in efferent lymph lymphocytes, cannulation of the prescapular efferent lymphatic duct was performed in an animal (AT115) undergoing primary infection with *T. parva*. B cells (surface Ig^+) and monocytes (IL-$A24^+$) formed a very low proportion of ELL (less than 2% respectively) from days 7 to 13 post-infection. The major changes in T cell subpopulations are illustrated in Figure 3.8. The percentage of $CD8^+$ T cells increased from 22% on day 7 post-infection to 72% of ELL on day 12. $CD2^-CD8^+$ T cells were initially detected on day 10, and formed 23% of ELL on day 11, thereafter their numbers declined rapidly. In this animal, there was also a significant increase in the proportion of γ/δ T cells that co-expressed CD8; this became obvious a day after the increase in the $CD2^-CD8^+$ population. The percentage of $\gamma\delta TCR^+CD8^+$ cells peaked at 16% on day 12 post-infection, when the total percentage of γ/δ T cells was 19%; thus CD8 was expressed on the majority of γ/δ T cells at this time. The proportion of $\gamma\delta TCR^+CD2^+$ cells was 9% on day 12 so, assuming that $\gamma\delta TCR^+CD2^+$ cells also express CD8, approximately 38% of the $CD2^-CD8^+$ T cells were $\gamma\delta TCR^+$ at this time.

3.3.2.4. Phenotypic analysis of PBMC during primary infection with *T. parva.*

In three animals, the phenotype of the PBMC during infection was examined using the same panel of monoclonal antibodies for single and two-colour immunofluorescence analysis. The results for the different mononuclear cell subpopulations ($CD4^+$ T cells, $CD8^+$ T cells, γ/δ T cells, B cells, and monocytes) are summarized in a table in Appendix E. The changes in the proportions of T cells ($CD3^+$), B cells and monocytes are illustrated in Figure 3.9. From day 0 to day 7 of infection there was little change in the composition of the PBMC population, apart from a moderate increase in the proportion of γ/δ T cells in two animals (4260 and 4282); thereafter the proportion of T cells ($CD3^+$) gradually decreased, accompanied by an increase in the percentage of monocytes. As total and differential WBC counts were not performed, it is unclear whether this reflects an increase in the absolute numbers of monocytes, or selective depletion of T lymphocytes. At no point during the infection were $CD2^-CD8^+$ T cells detected in the peripheral blood.

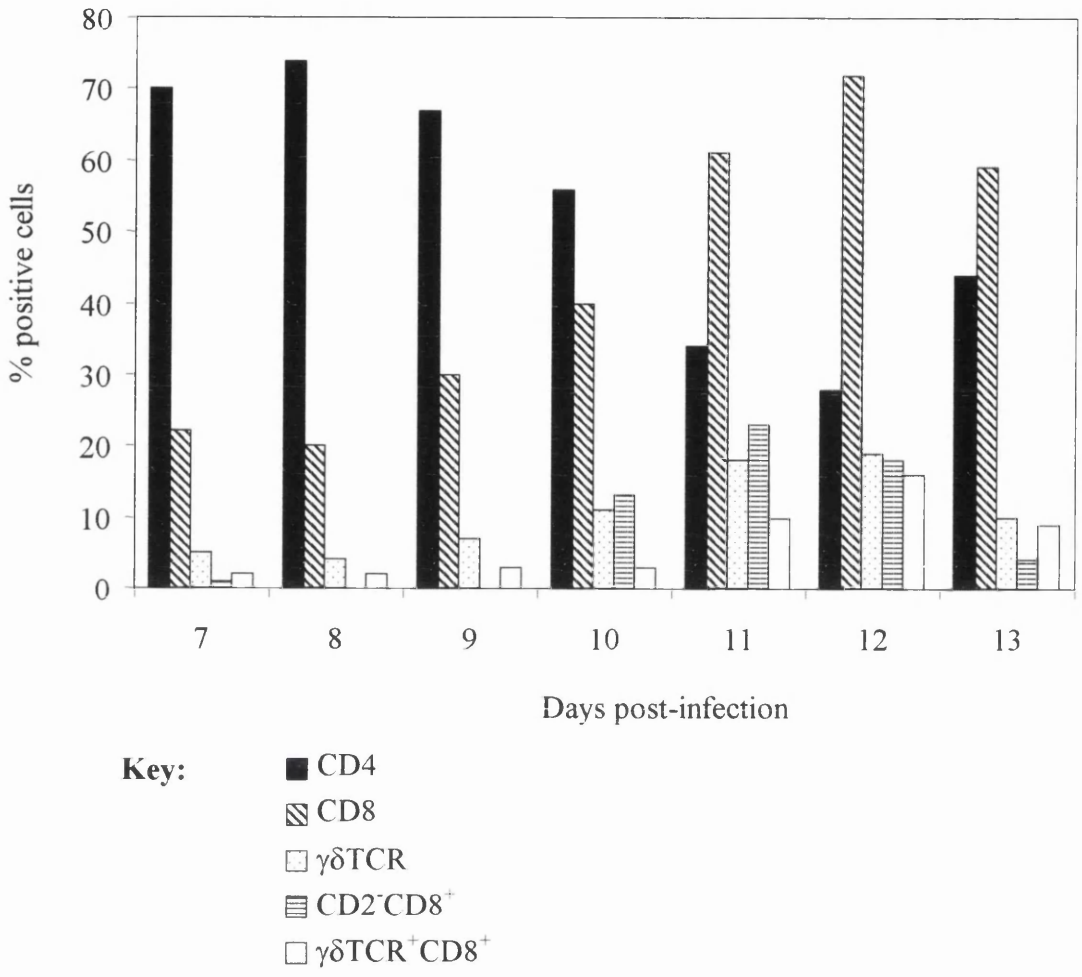

Figure 3.8. Changes in T cell subsets in the efferent lymph draining the prescapular lymph node of an animal (AT115) infected with *T. parva.* Mononuclear cells isolated from efferent lymph were stained with mAbs against CD4, CD8, γδ TCR and fluorescein (FITC)-conjugated goat anti-mouse IgG. Two colour staining was performed with combinations of mAbs against CD2 and CD8 or γδ TCR and CD8 followed by FITC- and phycoerythrin-coupled isotype-specific goat anti-mouse IgG mAbs. The samples were analysed on a FACScan. The proportions of the different T cell subsets are expressed as a percentage of the total efferent lymph lymphocyte population.

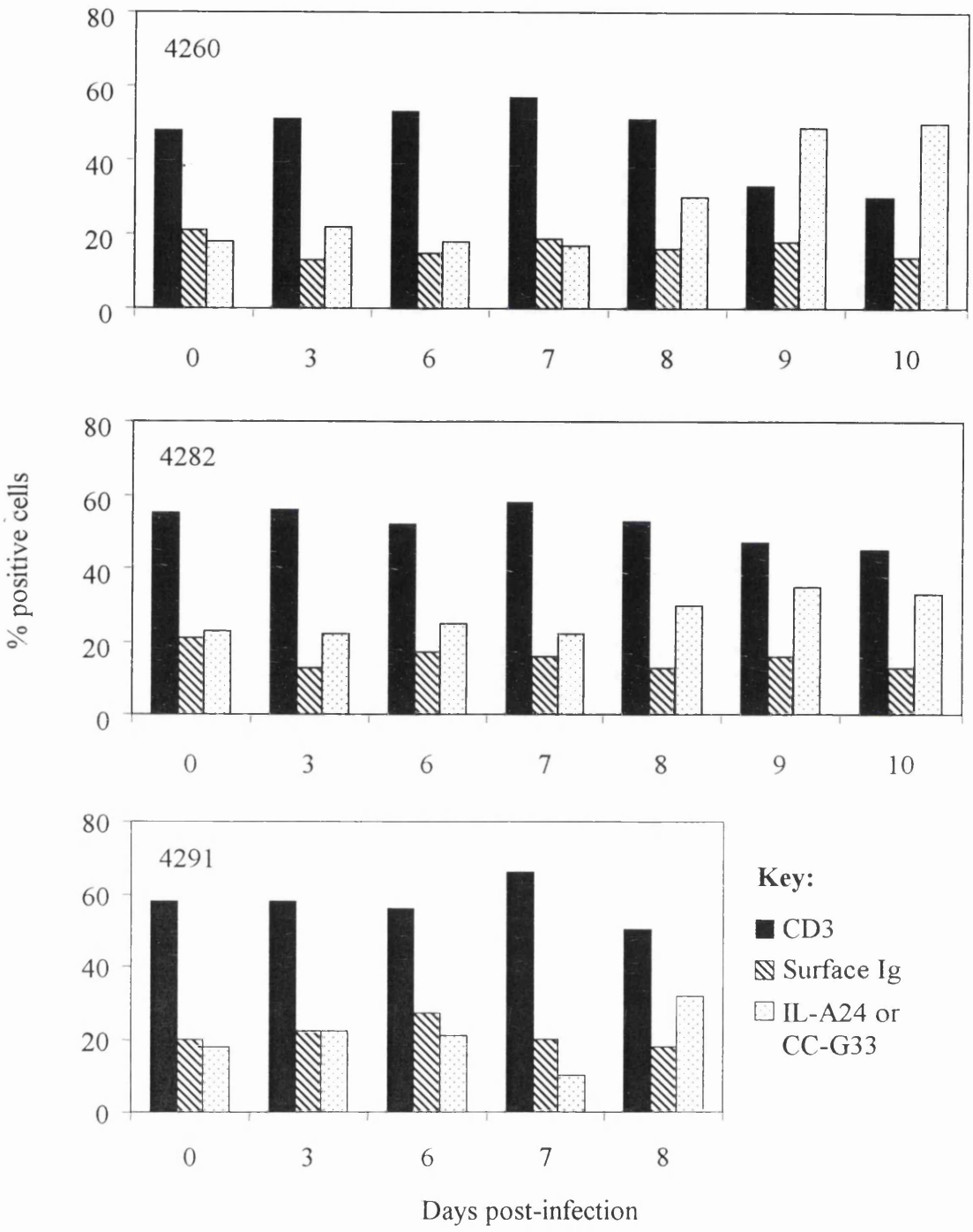

Figure 3.9. Changes in the phenotype of PBMC in three animals (4260, 4282, 4291) during infection with *T. parva*. Mononuclear cells isolated from peripheral blood were stained with mAbs against CD3 (T cell marker), surface immunoglobulin (B cell marker) and a molecule expressed on monocytes (recognized by IL-A24), and secondary fluorescein isothiocyanate- or phycoerythrin-conjugated isotype-specific goat anti-mouse IgG mAbs. The samples were analysed on a FACScan and the results are expressed as the percentage of positively staining cells in the whole population.

3.3.3. *In vitro* culture of sorted $CD2^-CD8^+$ T lymphocytes.

As relatively low numbers of $CD2^-CD8^+$ T cells could be obtained from the drainage lymph node by cell sorting, attempts were made to expand and maintain this population *in vitro*, with the aim of generating cell lines or clones that could be used in functional assays.

Initially, the sorted cells were cultured at limiting dilution with irradiated autologous parasitized cells as stimulators, in medium supplemented with TCGF or rboIL-2. Although proliferation was observed in the wells containing 100-300 cells, phenotypic analysis of cells derived from two such wells showed that one population consisted of γδ T cells and the other of $CD2^-CD3^-CD8^+$ cells. They were therefore considered to represent outgrowth of contaminating cells in the sorted population.

Subsequently, other stimuli, i.e. ConA and PMA/ionomycin, were used in addition to autologous parasitized cells. In preliminary experiments, these mitogens, in combination with TCGF, were shown to stimulate proliferation of resting $CD8^+$ T cells sorted from PBMC of uninfected animals (see Figure 3.10). However, there was no significant proliferation of the sorted $CD2^-CD8^+$ T cells, as assessed by microscopic examination of the cultures. Quantitative analysis of the proliferative response by measurement of the incorporation of tritiated thymidine was precluded by the small numbers of cells that were available in this experiment.

The apparent unresponsiveness of the $CD2^-CD8^+$ T cells to *in vitro* stimulation was subsequently confirmed in an experiment in which proliferation was assayed by incorporation of [^{3}H]-labelled thymidine. Lymph node cells isolated from a calf on day 8 post-infection with *T. parva* were sorted into two $CD8^+$ populations one of which was $\gamma/\delta TCR^-CD2^-$ and the other $\gamma/\delta TCR^+$ and/or $CD2^+$ (see section 3.2.3.1), and cultured in the presence of PMA and ionomycin, in combination with irradiated lymph node filler cells from the same calf and/or rboIL-2. Normal $CD8^+$ T cells sorted from the peripheral blood of an uninfected animal were cultured under identical conditions as an additional control. The results are illustrated in Figure 3.11. There was no significant proliferative

response of the $CD2^-CD8^+$ α/β T cells to PMA/ionomycin under any of the different culture conditions. In contrast, both the $CD2^+CD8^+$ lymph node cells (containing α/β and γ/δ T cells) and the peripheral blood $CD8^+$ T cells showed proliferative responses, although much stronger proliferation was induced in the latter population. The presence of filler cells and/or rboIL-2 did not significantly enhance the proliferative responses of these two populations to PMA/ionomycin.

The results indicate that the $CD2^-CD8^+$ population of cells do not proliferate in response to stimuli that elicit a strong proliferative response in resting $CD8^+$ T cells. The lack of growth of $CD2^-CD8^+$ T cells also indicates that this population does not contain parasitized cells, which in the presence of IL-2 would be expected eventually to overgrow the cultures.

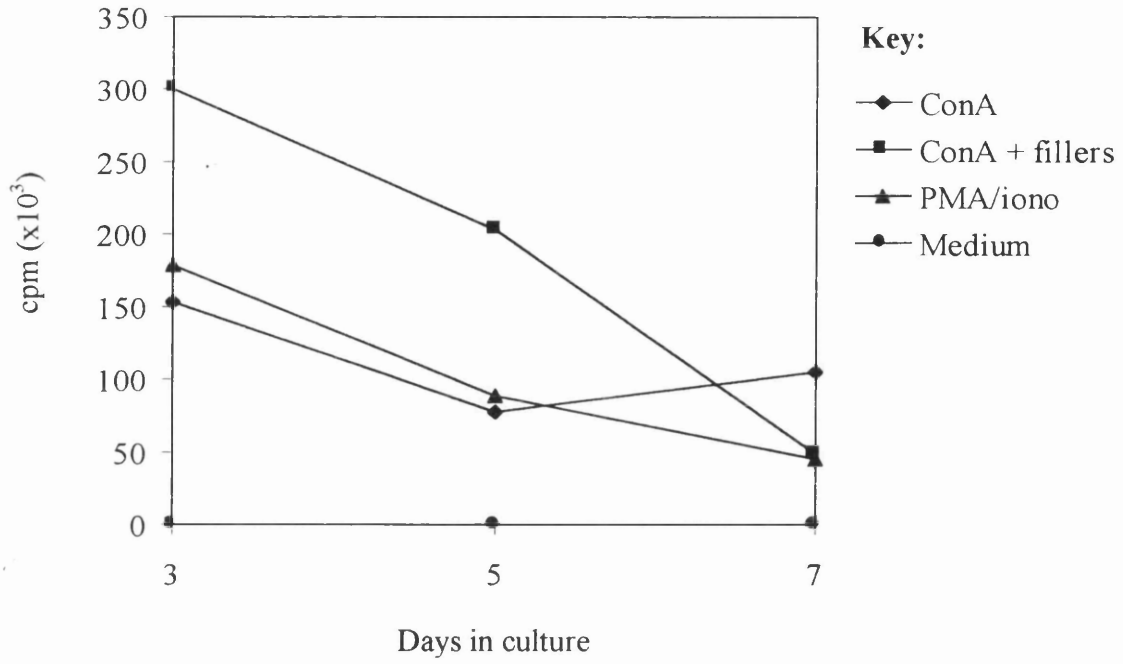

Figure 3.10. Proliferative responses of $CD8^+$ T cells. $CD8^+$ T cells were isolated from peripheral blood mononuclear cells (PBM) at >95% purity by positive selection with an anti-CD8 mAb (CC63; $IgG2_a$), incubation with anti-mouse IgG MACS microbeads (Miltenyi Biotec), and separation on a MiniMACS column (Miltenyi). The sorted cells were distributed at 10^5 cells/well in a 96 well flat-bottomed plate and stimulated either with concanavalin A (ConA) at 5μg/ml in the presence or absence of 10^4 irradiated autologous PBM as fillers, or phorbol myristate acetate (PMA) and ionomycin (iono) at 50ng/ml and 1μg/ml respectively. The cultures were incubated at 38°C and proliferation was assessed by the incorporation of tritiated thymidine after 3, 5 and 7 days in culture. The results are expressed as counts per minute (cpm) and the values represent the mean of triplicate wells.

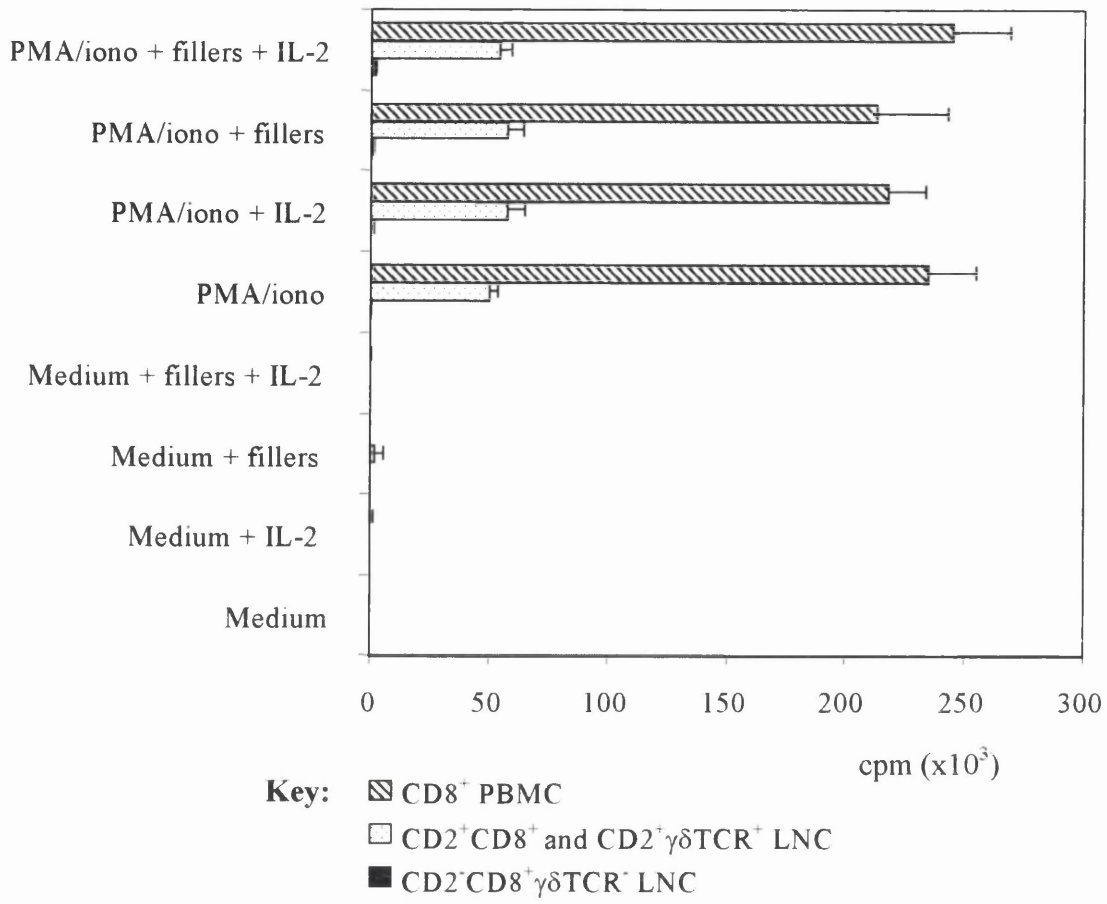

Figure 3.11. $CD2^-CD8^+\gamma/\delta TCR^-$ cells isolated from the prescapular lymph node of an animal (6294) infected with *T. parva* do not proliferate in response to stimulation with phorbol myristate acetate and ionomycin (PMA/iono). Mononuclear cells isolated from a lymph node suspension (LNC) were stained with mAbs against CD2 (IL-A45; $IgG2_b$), γ/δ TCR (GB21A; $IgG2_b$) and CD8 (CACT80C; IgG1). The secondary mAbs were fluorescein isothiocyanate (FITC)-conjugated goat anti-mouse IgG1 and phycoerythrin (PE)-conjugated goat anti-mouse $IgG2_b$. $CD8^+$ cells were enriched to >95% purity by incubating with anti-FITC MACS microbeads (Miltenyi Biotec) and sorting on a MACS VS^+ separation column (Miltenyi). The $CD8^+$ cells were sorted into $CD2^-\gamma/\delta TCR^-$ and $CD2^+$ and/or $\gamma/\delta TCR^+$ populations to >99% purity on a FACStar Plus cell sorter (Becton Dickinson). $CD8^+$ T cells were isolated at >95% purity from peripheral blood mononuclear cells (PBM) of an uninfected animal by positive selection with an anti-CD8 mAb (CC63; $IgG2_a$), incubation with anti-mouse IgG MACS beads (Miltenyi) and sorting on a MiniMACS column (Miltenyi). Cells from the three populations were distributed at 10^4 cells/well and stimulated with PMA (50ng/ml) and ionomycin (1μg/ml) in the presence or absence of 10^4 filler cells (irradiated LNC) and/or recombinant bovine IL-2 (10U/ml). Proliferation was measured after incubation of the cultures at 38°C for 4 days by incorporation of tritiated thymidine. The results are expressed as counts per minute (cpm) and represent the mean values of triplicate cultures.

3.3.4. Histological examination of lymph node sections.

Blocks cut from the prescapular lymph nodes of calves infected with *T. parva*, and from uninfected control calves were used to prepare sections for examination of changes in cellular composition and cytokine expression during infection, in relation to the histological appearance of the lymph node.

3.3.4.1. Histological examination of sections stained with haematoxylin and eosin.

The morphological features of normal lymph nodes obtained from two uninfected control animals are illustrated in Figure 3.12. The cortex and paracortex contained mainly small resting lymphocytes, with the occasional isolated lymphoblast (Figure 3.12.A). A proportion of the B cell follicles contained active germinal centres. These secondary follicles had an outer narrow rim of small resting lymphocytes, surrounding the large activated lymphoblasts of the germinal centre. The lymphoblasts had large pale nuclei with prominent nucleoli, and mitotic figures were frequently observed. Mature germinal centres were divided into light and dark zones; the latter containing more actively proliferating cells (Figure 3.12.D). The medullary cords were populated by resting lymphocytes with some lymphoblasts, and the sinuses contained relatively few cells, most of which were small lymphocytes. (Figure 3.12.F). Small foci of polymorphonuclear cells were seen occasionally in the paracortex, at the cortico-medullary junction and in the medullary cords. On day 5 of infection, the morphology of the lymph node cortex and paracortex was essentially the same as in the resting node. In one animal, there were numerous large secondary B cell follicles. In both animals, there was a notable increase in the cellularity of the medulla, with expansion of the medullary cords and much greater numbers of cells in the sinuses. The frequency of lymphoblasts was increased, especially within the sinuses, and mitotic figures were occasionally observed.

On day 7 of infection, there was a marked increase in the number of activated cells within the medulla, particularly in the sinuses. There were many large dark-staining lymphoblasts (Figure 3.12.G). Lymphoblasts were also found within the medullary cords and at the cortico-medullary junction. In one animal (786), increased numbers of blasts were also noted in some areas of the paracortex (Figure 3.12.B).

By day 9 of infection, lymphocyte activation was widespread throughout the lymph node. This was particularly notable in one of the animals (782), in which lymphoblasts were predominant in the cortex, paracortex, and medulla, with numerous mitotic figures visible (Figure 3.12.C,H). In this animal, significant numbers of polymorphonuclear cells were also observed in all regions. Although B cell follicles could still be distinguished, germinal centres were not seen in the lymph nodes at this stage of the infection (Figure 3.12.E).

A. Paracortex – normal prescapular lymph node. There are numerous small resting lymphocytes. A high endothelial venule (HEV) is present on the right of the picture. x128.

B. Paracortex – prescapular lymph node (calf 786); 7 days post-infection with *Theileria parva*. There are a number of large lymphoblasts present (arrowed), which can be distinguished by the pale staining nuclei containing prominent nucleoli. x310.

C. Paracortex – prescapular lymph node (calf 782); 9 days post-infection with *T. parva*. There are numerous lymphoblasts present. A primary B cell follicle, containing predominantly small resting lymphocytes, is present on the right of the picture. x80.

Figure 3.12. Sections of bovine lymph node stained with haematoxylin and eosin.

A.

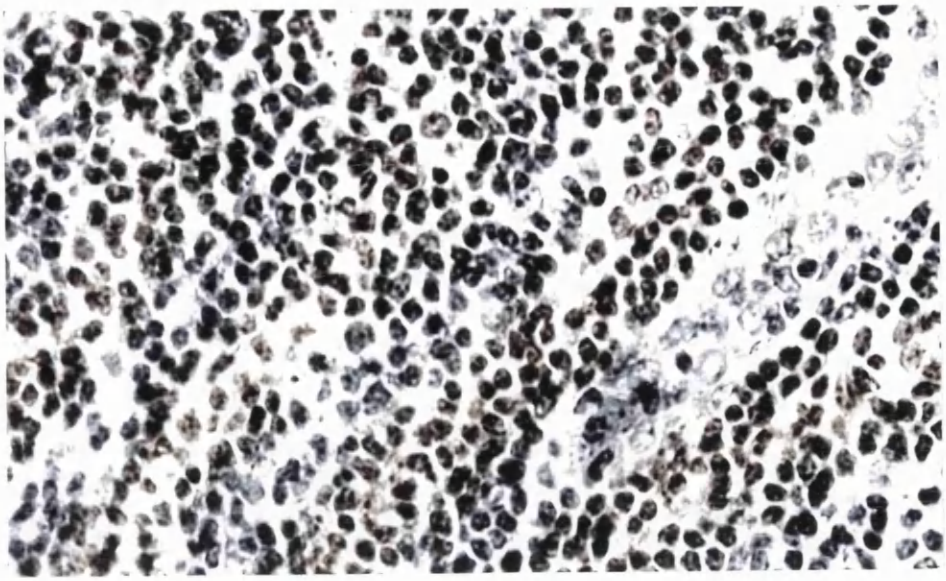

B.

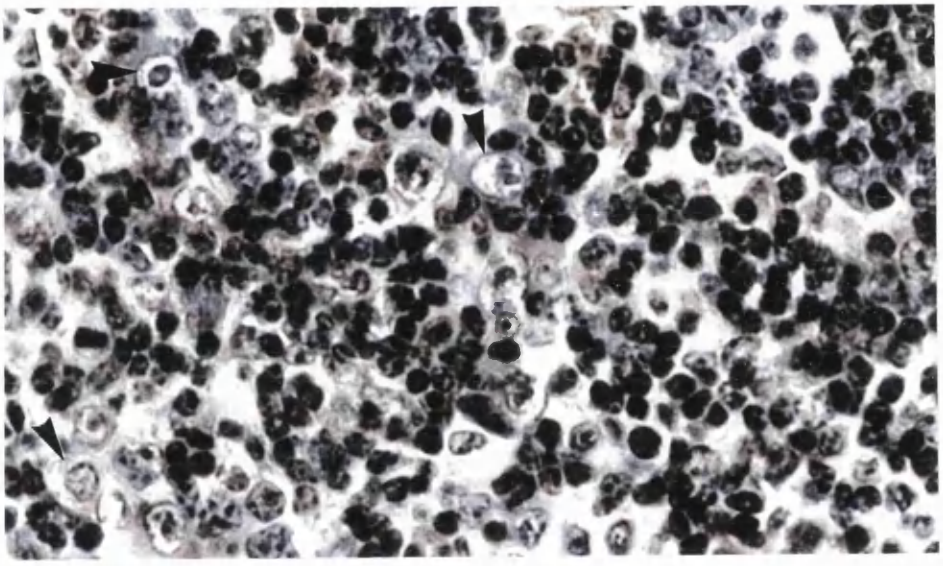

C.

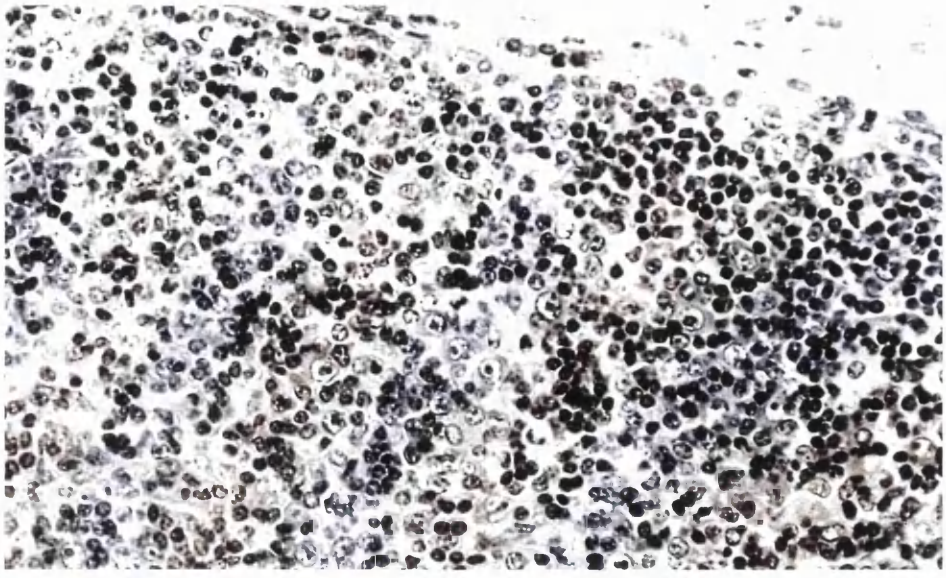

D. Dark zone of a germinal centre – normal prescapular lymph node (calf 784). The rim of the germinal centre (GC) is indicated by filled arrows. The dark zone of the GC contains numerous lymphoblasts and mitotic figures (open arrows), indicating active cell division. x128.

E. Primary follicle and paracortex – prescapular lymph node (calf 776); 9 days post-infection with *T. parva*. The paracortex contains numerous lymphoblasts, while the B cell follicle at the top of the picture is composed mainly of small resting lymphocytes. x128.

Figure 3.12. (cont.) Sections of bovine lymph node stained with haematoxylin and eosin

D.

E.

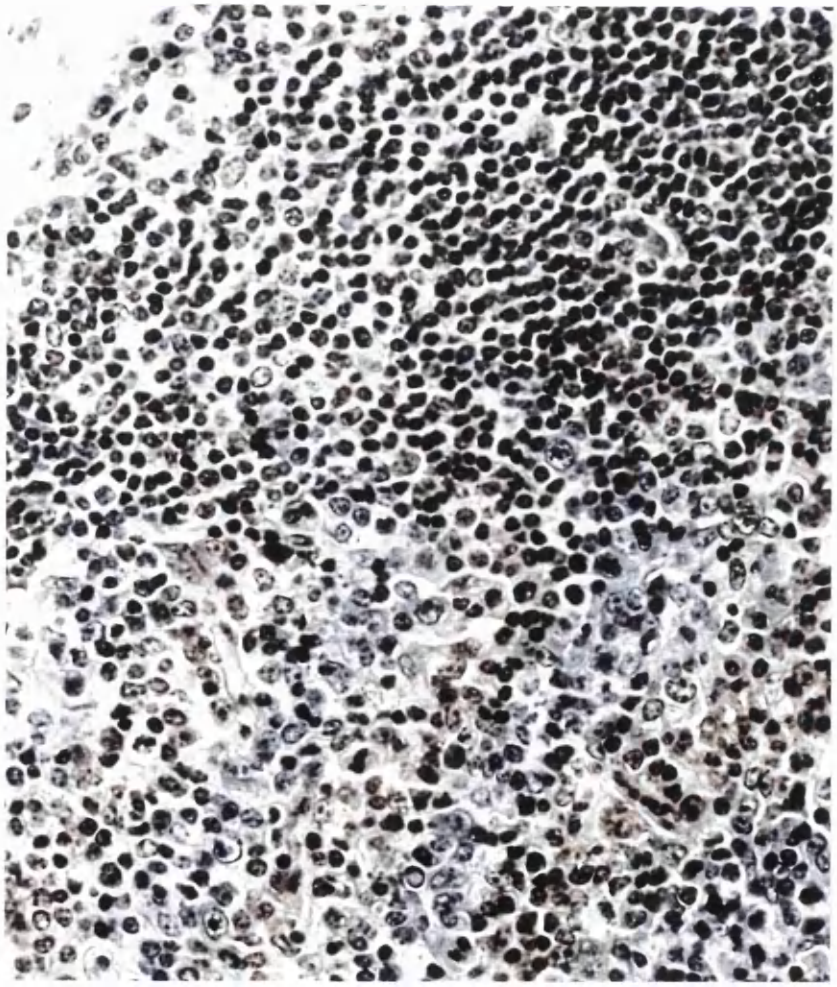

F. Medulla – normal prescapular lymph node. The majority of the cells forming the medullary cords (C) or present within the sinuses (S) have the morphology of small resting lymphocytes. x80.

G. Medulla – prescapular lymph node (calf 783); 7 days post-infection with *T. parva*. There are numerous large lymphoblasts with darkly stained cytoplasm in the medullary sinus. A few lymphoblasts are also seen within the medullary cords. x80.

H. Medulla – prescapular lymph node (calf 782); 9 days post-infection with *T. parva*. There are numerous lymphoblasts in the medullary sinuses and cords. x80.

Figure 3.12. (cont.) Sections of bovine lymph node stained with haematoxylin and eosin.

F.

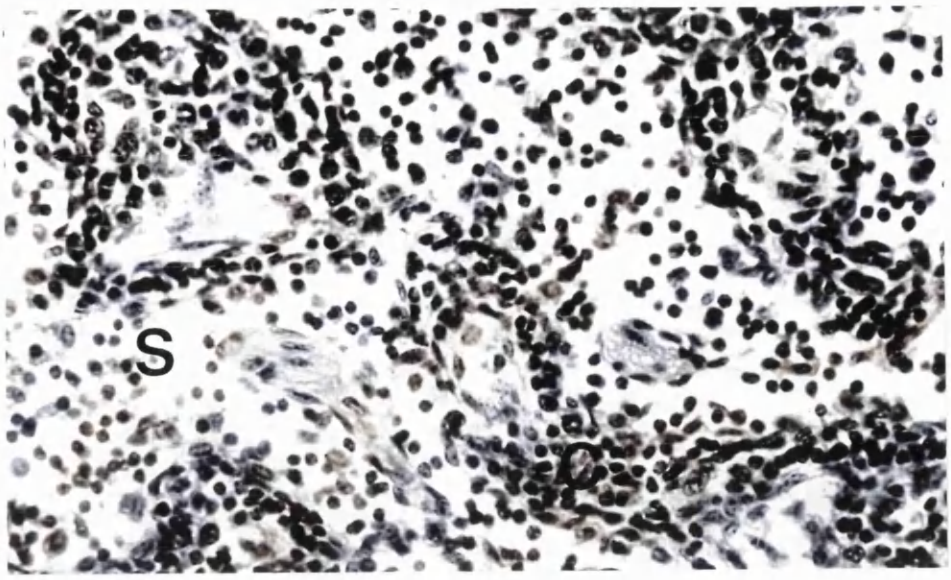

G.

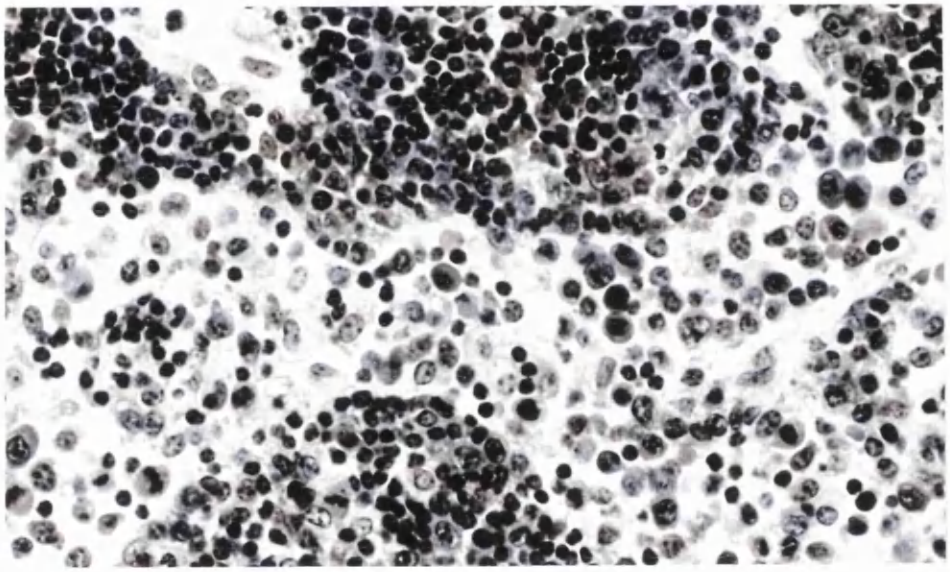

H.

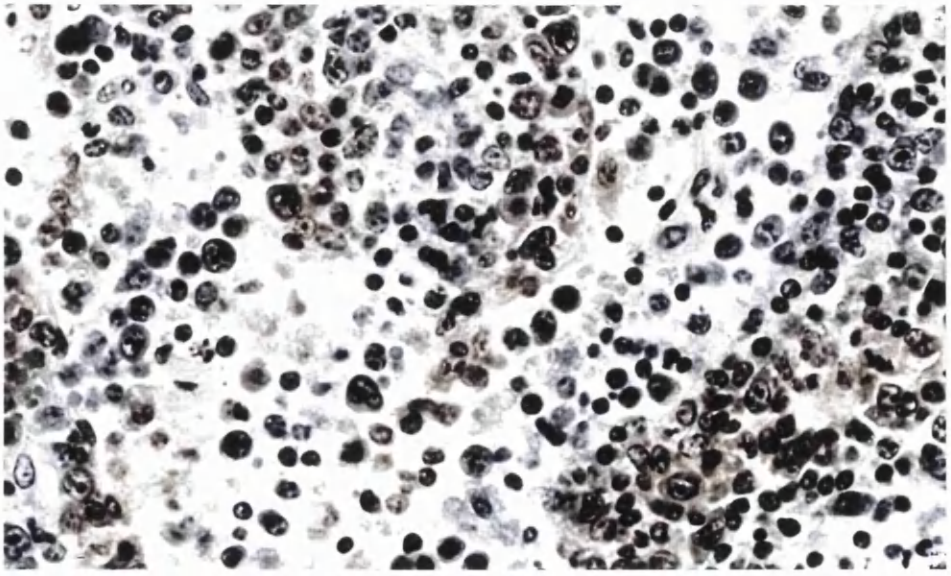

3.3.4.2. Examination of lymph node sections by immunocytochemistry.

To obtain direct quantitative confirmation of the presence of actively proliferating cells within the lymph node, cryostat sections were stained with a monoclonal antibody against Ki67, a nuclear antigen expressed by proliferating cells in the late G1, S, M and G2 phases of the cell cycle (Gerdes *et al.*, 1984). The pattern of cell activation was compared with the distribution of the parasite within the lymph node, revealed by staining with a mAb specific for a schizont antigen of *T. parva*. A quantitative estimate of the numbers of positive cells in different parts of the lymph node was made by counting the positive cells in five different fields for each region, using an eyepiece graticule. These results are summarized in Tables 3.5. and 3.6., and the staining patterns are illustrated in Figure 3.13.

The results obtained by staining with the anti-Ki67 monoclonal antibody reflect the observations made on the H&E-stained sections. An increase in the numbers of activated cells was found initially within the medullary cords and sinuses, and at the cortico-medullary junction on days 5 and 7 post-infection, and by day 9 there was a substantial increase of Ki67-positive cells in the cortex and paracortex (Figure 3.13.I.B). Isolated schizonts were detected initially within the medullary cords on day 5 post-infection, and by day 7 could be seen in low numbers in all regions of the lymph node. On day 9, there was a dramatic increase in the number of schizonts, correlating with the increased numbers of activated cells. With the exception of the B cell follicles, which contained very few parasites, this increase in parasitized cells occurred throughout the lymph node, as shown in Figure 3.13.II.A,B. However, the individual schizonts were scattered, rather than occurring in clusters, suggesting that the increase in parasitized cells was due to continual migration into the node. Alternatively, the parasitized cells may rapidly become separated following cell division.

Table 3.5. The numbers and distribution of Ki67-positive cells in the drainage lymph node during primary infection with *T. parva*.

Stage of infection	Day 0		Day 5		Day 7		Day 9	
Calf number	**781**	**784**	**788**	**789**	**783**	**786**	**776**	**782**
Primary follicles	-	8(7)	29(14)	25(5)	23(7)	7(5)	26(15)	22(8)
Outer cortex	15(4)	25(8)	23(9)	17(6)	54(25)	25(11)	70(28)	57(5)
Paracortex	17(3)	20(9)	17(1)	23(6)	42(12)	31(3)	73(14)	79(15)
C-M junction	13(3)	16(7)	33(13)	55(22)	57(19)	35(8)	52(11)	75(5)
Medullary cords	5(3)	4(2)	20(11)	34(35)	27(7)	23(4)	30(16)	24(16)
Medullary sinuses	1(1)	0	7(4)	11(3)	19(10)	42(7)	6(6)	10(11)

Table 3.6. The numbers and distribution of schizonts in the drainage lymph node during primary infection with *T. parva*.

Stage of infection	Day 5		Day 7		Day 9	
Calf number	**788**	**789**	**783**	**786**	**776**	**782**
Primary follicles	0	0	<1	<1	3(2)	3(2)
Outer cortex	0	0	0	2	27(17)	14(4)
Paracortex	0	0	1	2	23(6)	20(7)
C-M junction	0	0	1	1	23(10)	29(7)
Medullary cords	<1	0	1	3	19(6)	26(6)
Medullary sinuses	0	0	0	1	12(5)	16(1)

Notes: The figures are the average of the numbers of positively-stained cells counted in 5 fields from each region of the lymph node, using an eyepiece graticule and the X25 objective. Figures in parentheses are the standard deviations.
C-M = cortico-medullary

A.

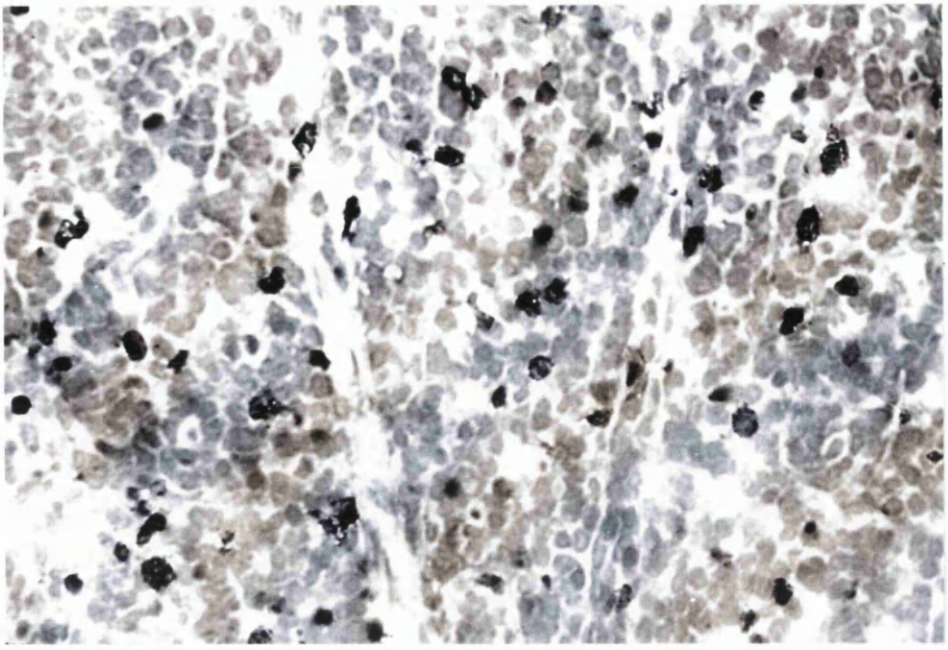

A. Paracortex – normal prescapular lymph node (784). Cells positive for the Ki67 antigen are found in small numbers throughout the paracortex. x80.

B.

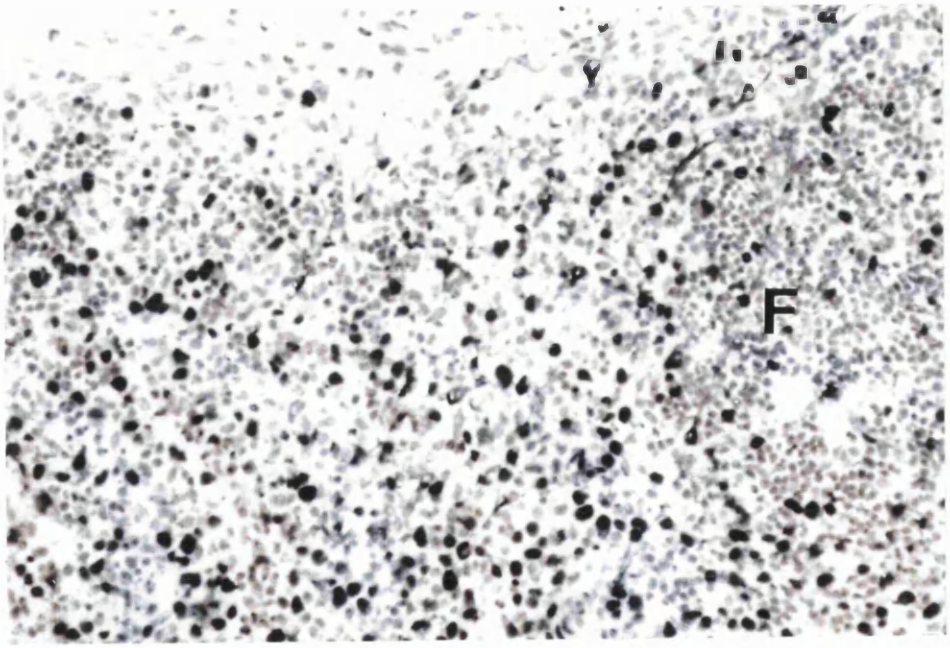

B. Cortex – prescapular lymph node (782); 9 days post-infection with *T. parva*. Large numbers of positive cells are found throughout the paracortex. The primary follicles (F) on the right and left of the picture contain only a few positive cells. x32.

Figure 3.13. I. Sections of bovine lymph node stained by immunoperoxidase with the monoclonal antibody NCL-Ki67-MM1 (anti-Ki67).

C.

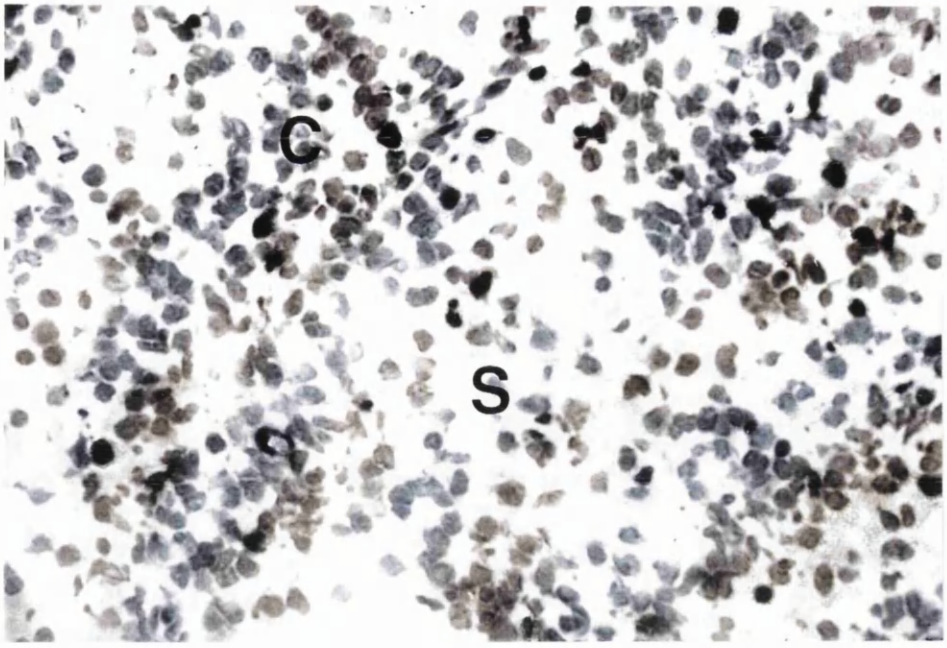

C. Medulla – normal prescapular lymph node (784). Very small numbers of cells positive for Ki67 are scattered in the medullary cords (C) and sinuses (S). x80.

D.

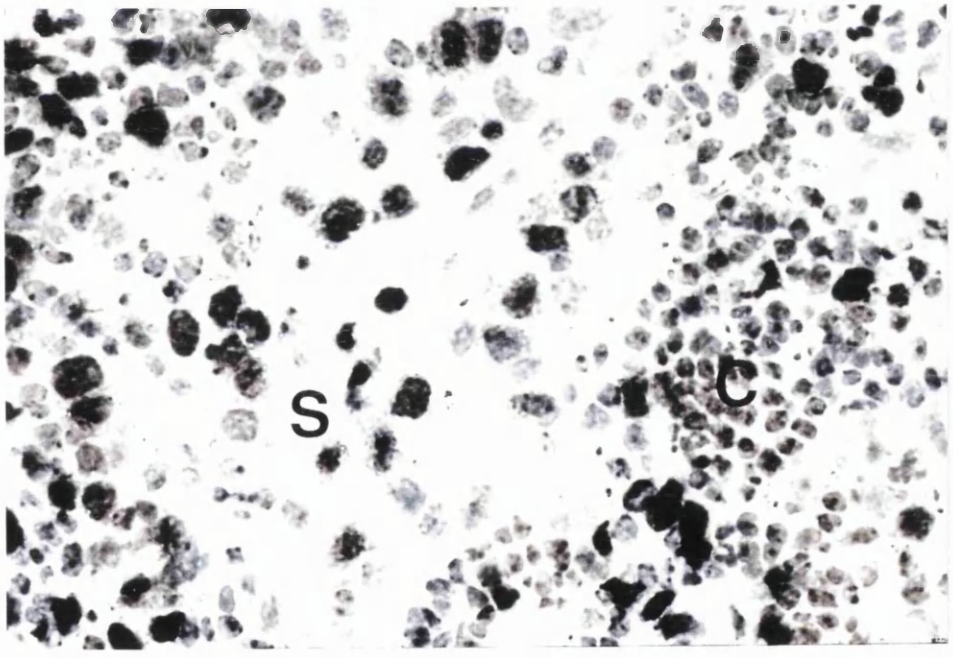

D. Medulla – prescapular lymph node (782); 9 days post-infection with *T. parva*. Large numbers of cells expressing Ki67 are found in both the medullary cords (C) and sinuses (S). x80.

Figure 3.13. I. (cont.) Sections of bovine lymph node stained by immunoperoxidase with the monoclonal antibody NCL-Ki67-MM1 (anti-Ki67).

A. Cortex – prescapular lymph node (782); 9 days post-infection with *T. parva*. Individual schizonts are clearly visible scattered throughout the paracortex; a few schizonts are also present in the primary follicle (F). x32.

B. Medulla – prescapular lymph node (782); 9 days post-infection with *T. parva*. Parasitized cells are present within the medullary cords (C) and sinuses (S). x80.

Figure 3.13. II. Sections of bovine lymph node stained by immunoperoxidase with MAb5 (against the polymorphic immunodominant molecule of *T. parva*).

A.

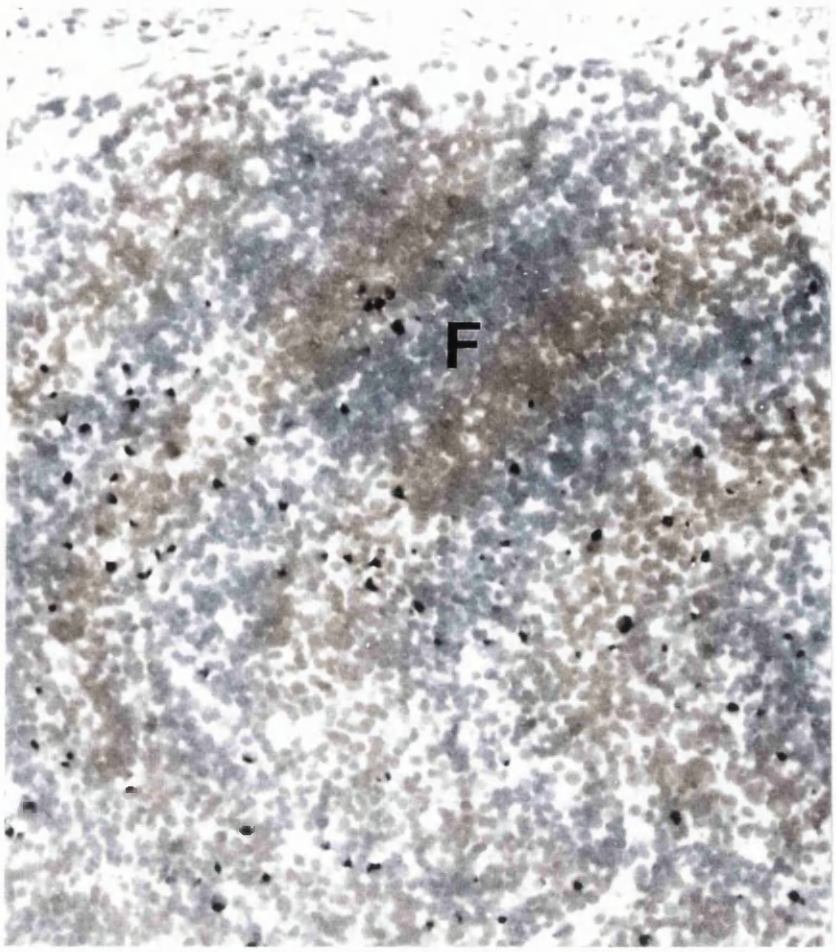

B.

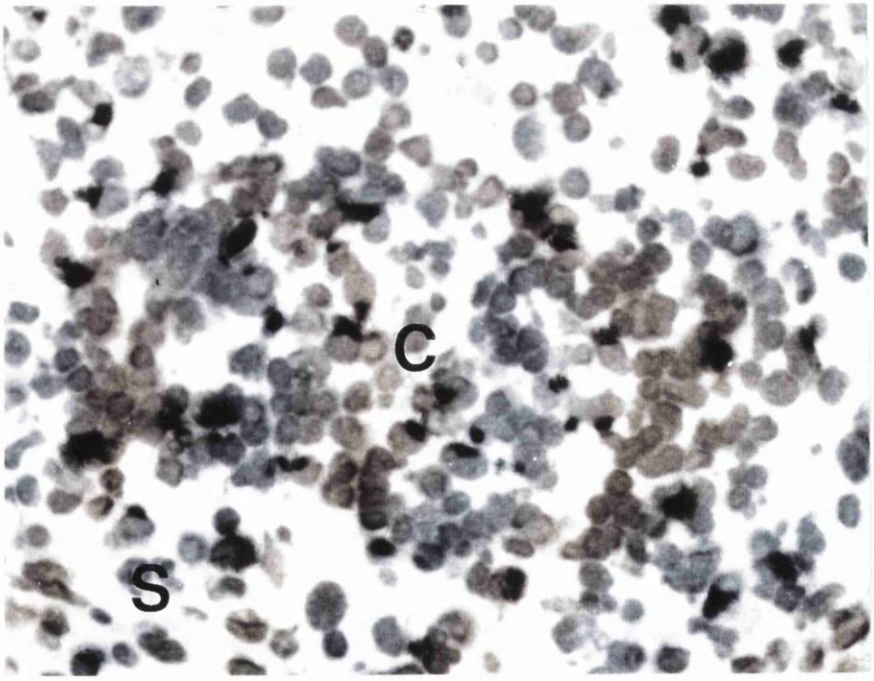

In control animals, large numbers of $CD3^+$ and $CD8^+$ T cells were found in the paracortex, with smaller numbers scattered in the medullary cords and a few positive cells within the medullary sinuses (Figure 3.14.A,B). By day 7 post-infection, the distribution of $CD3^+$ and $CD8^+$ cells within the paracortex was very similar to the controls; however, large numbers of $CD3^+$ cells and smaller numbers of $CD8^+$ T cells were also found in the medullary cords and sinuses (Figure 3.14.C,D). Similar patterns of staining with these T cell-specific mAbs were observed on day 9 post-infection. These findings suggest that many of the lymphoblasts in the medulla on days 7 and 9 post-infection are T cells, but not all of them express CD8.

The cryostat sections were also stained with two antibodies specific for molecules expressed on bovine myeloid cells: CC149 which binds to MyD-1, a molecule expressed on a subset of dendritic cells and monocytes, and CC94 which binds to CD11b (expressed on monocytes and a small subset of B cells). In the resting node, small numbers of cells that stained with CC149 were found in the paracortex (Figure 3.15.A). CC94 did not stain cells within the cortex or paracortex, but there were foci of positive cells near the cortico-medullary junction. Both antibodies stained small numbers of cells within the medullary cords and sinuses (Figure 3.15.B). By day 5 post-infection, there was little change in the numbers and distribution of cells stained by CC149 and CC94. However on day 7, there was an increased numbers of cells staining with CC149 and CC94 in the cortex and large numbers of cells positive for both markers within the medullary cords and sinuses. These changes were particularly marked in calf 786 (see Figure 3.15.C,D). By day 9 post-infection, numerous cells within the cortex and paracortex stained with both antibodies (Figure 3.15.E,F) and occasional positive cells were seen in B cell follicles. To determine whether the increased numbers of cells recognized by both CC149 and CC94 represent monocytes/macrophages, cryostat sections were stained for the lysosomal enzyme, acid phosphatase. In the lymph nodes of uninfected animals, positive cells were largely confined to the medulla; very few were seen in the paracortex, as shown in Figure 3.16.A,B. From day 7 to day 9 of infection there was a progressive increase in positive cells the paracortex (Figure 3.16.,C). These changes parallel the findings with CC149 and CC94 and indicate that the cells identified by these monoclonal antibodies have a well-developed lysosomal system, suggesting that they are macrophages.

A.

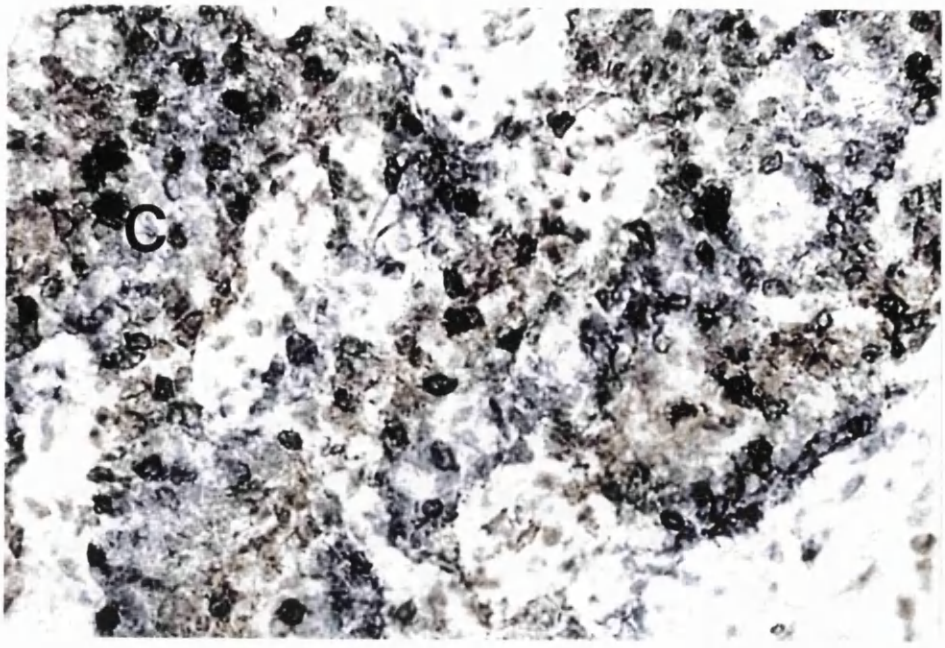

A. Medulla – normal prescapular lymph node stained with MM1A. Small numbers of positive cells are found, mainly within the medullary cords (C). x80.

B.

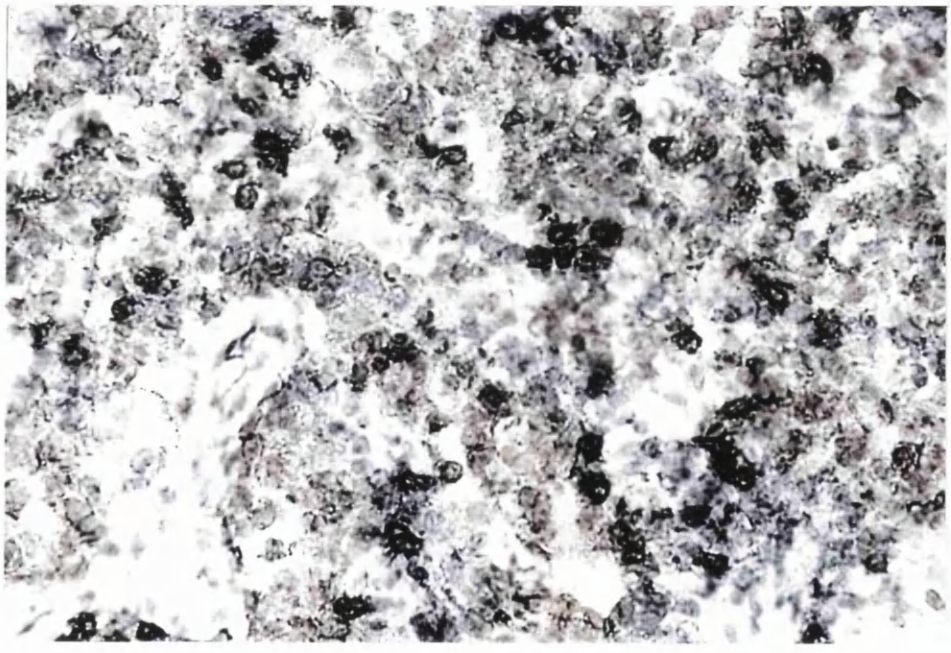

B. Medulla –normal prescapular lymph node stained with CC63. The appearance is similar to that of the section stained with MM1A, with small numbers of positive cells located in the medullary cords. x80.

Figure 3.14. Sections of bovine lymph node stained by immunoperoxidase with MM1A (anti-CD3) and CC63 (anti-CD8).

C.

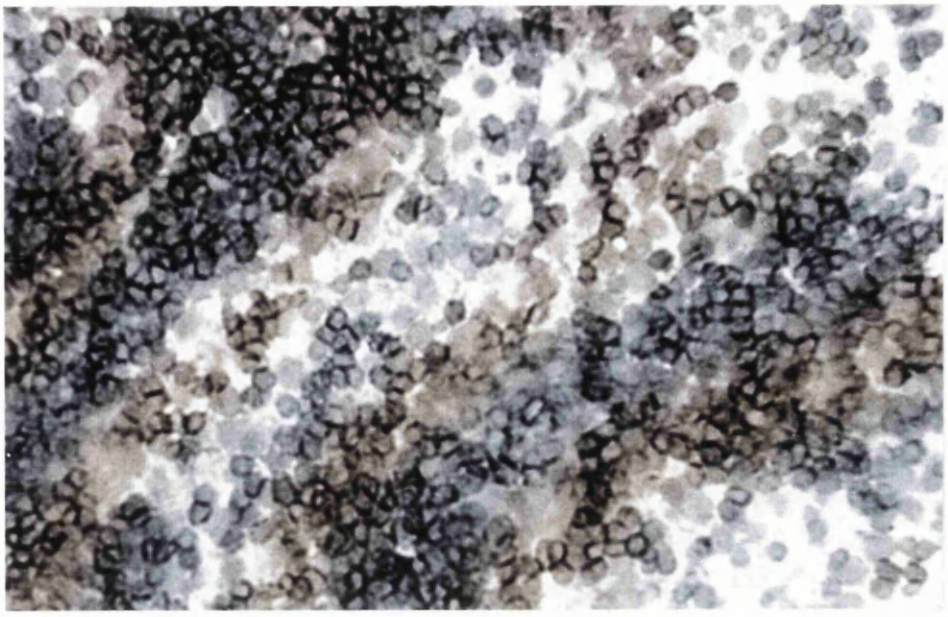

C. Medulla – prescapular lymph node (calf 783) stained with MM1A; 7 days post-infection with *T. parva*. There are large numbers of positively stained cells within the medullary cords and sinuses. x80.

D.

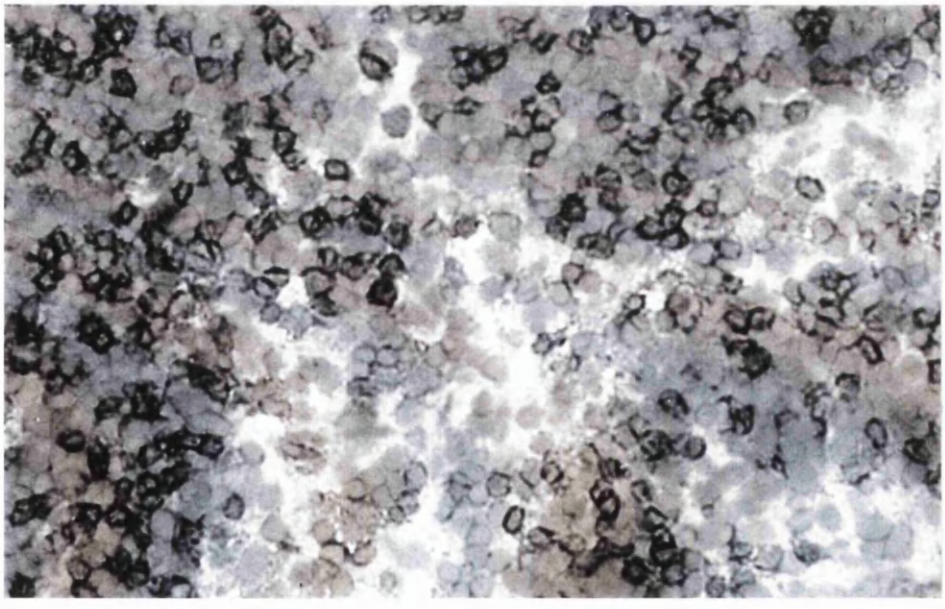

D. Medulla – prescapular lymph node (calf 783) stained with CC63; 7 days post-infection with *T. parva*. $CD8^+$ cells are less numerous than $CD3^+$ cells in the medullary cords. x80.

Figure 3.14. (cont.) Sections of bovine lymph node stained by immunoperoxidase with MM1A (anti-CD3) and CC63 (anti-CD8).

A.

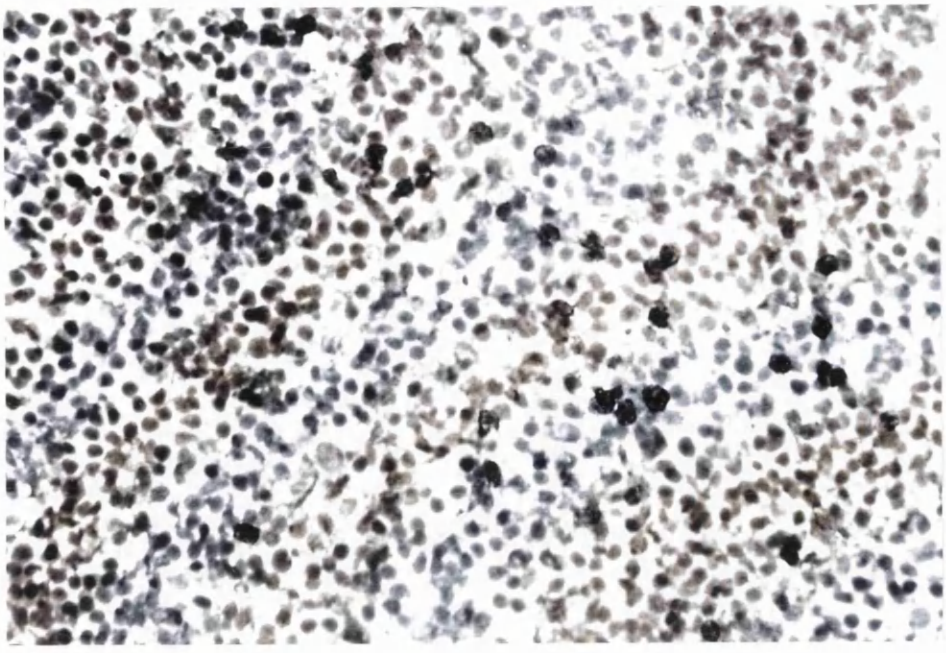

A. Paracortex – normal prescapular lymph node (784) stained with CC149. Small foci of positively staining cells were found scattered in the paracortex. x80.

B.

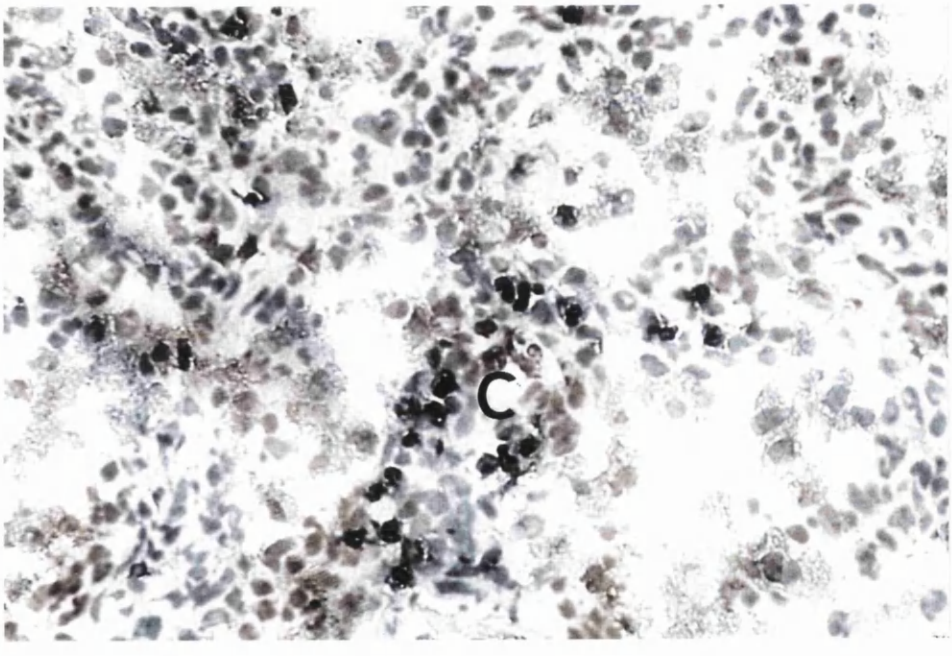

B. Medulla – normal prescapular lymph node (784) stained with CC94. Small numbers of positively staining cells were found in the medullary cords (C). x80.

Figure 3.15. Sections of bovine lymph node stained by immunoperoxidase with CC94 (anti-CD11b) and CC149 (anti-MyD-1).

C.

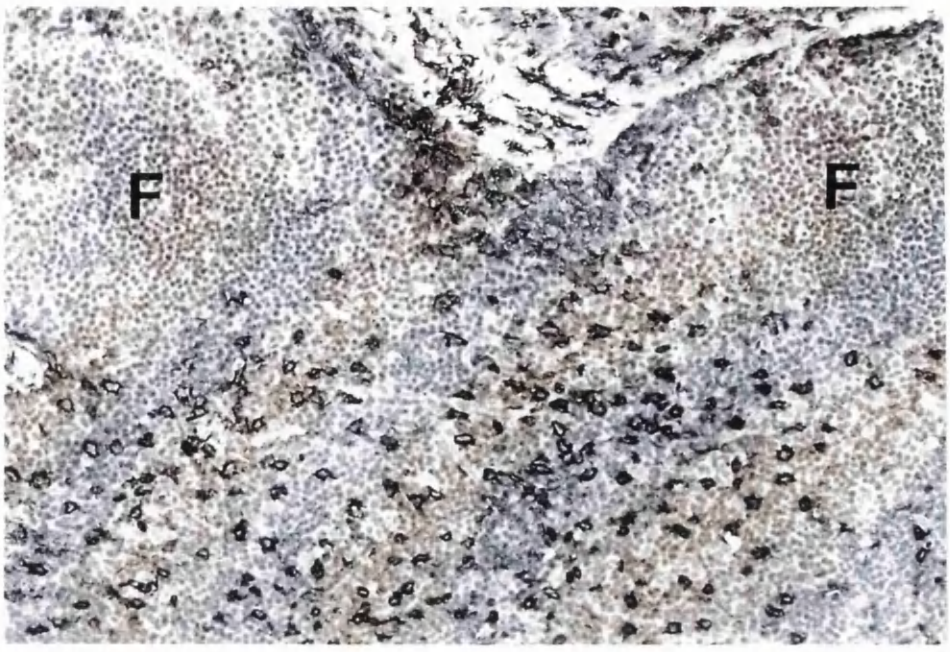

C. Cortex – prescapular lymph node (calf 786) stained with CC149; 7 days post-infection with *T. parva*. Large numbers of positive cells are found throughout the paracortex, but not within the primary follicles (F). x32.

D.

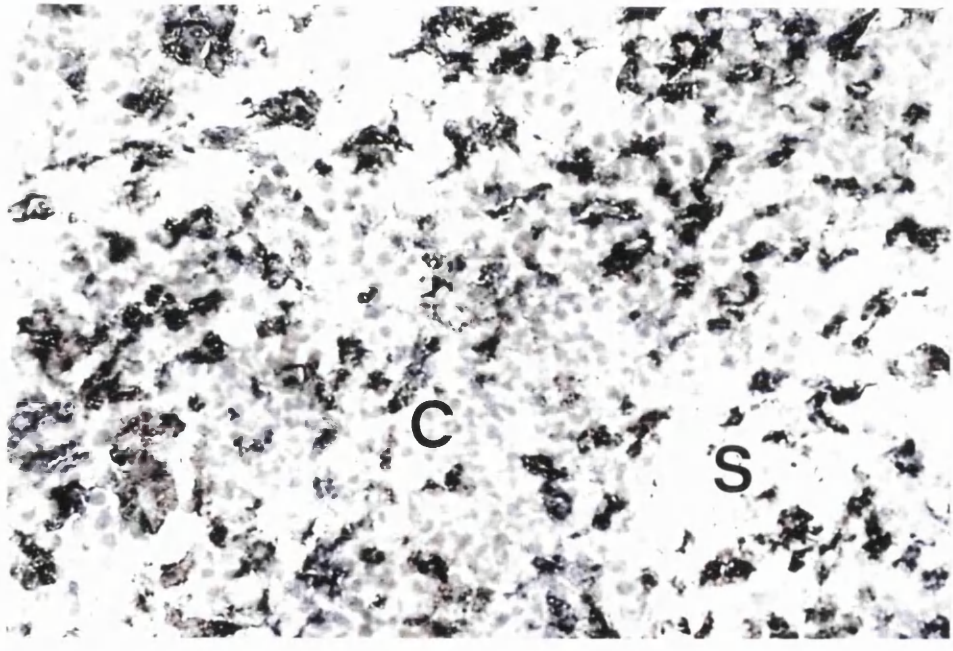

D. Medulla – prescapular lymph node (calf 786) stained with CC149; 7 days post-infection with *T. parva*. Large numbers of positive cells are present within the medullary cords (C) and sinuses (S). x80.

Figure 3.15. (cont) Sections of bovine lymph node stained by immunoperoxidase with CC94 (anti-CD11b) and CC149 (anti-MyD-1).

E.

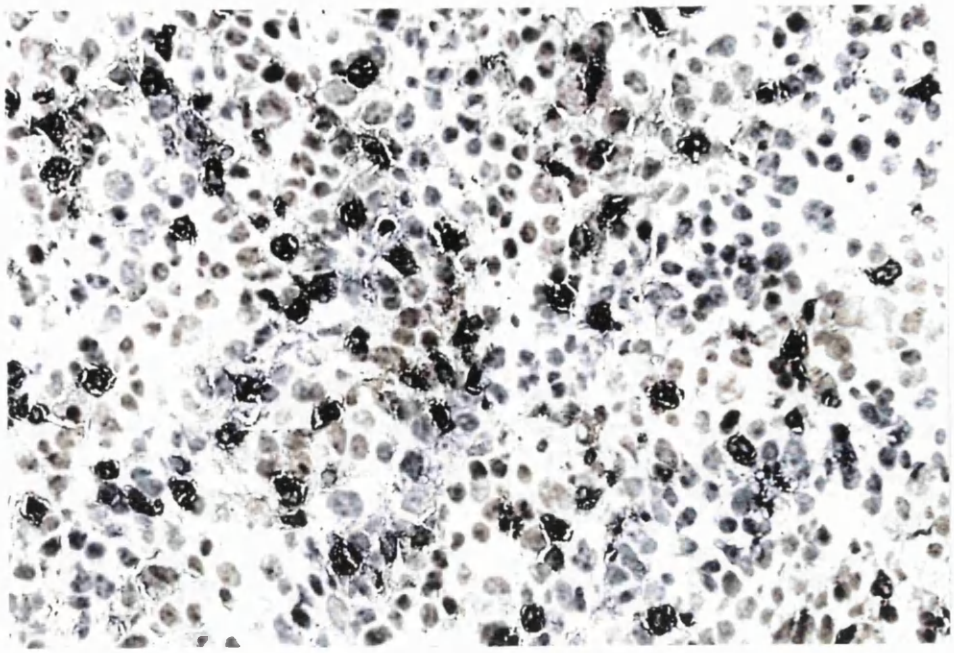

E. Paracortex – prescapular lymph node (calf 776) stained with CC94; 9 days post-infection with *T. parva*. Large numbers of positively staining cells are found throughout the paracortex. x80.

F.

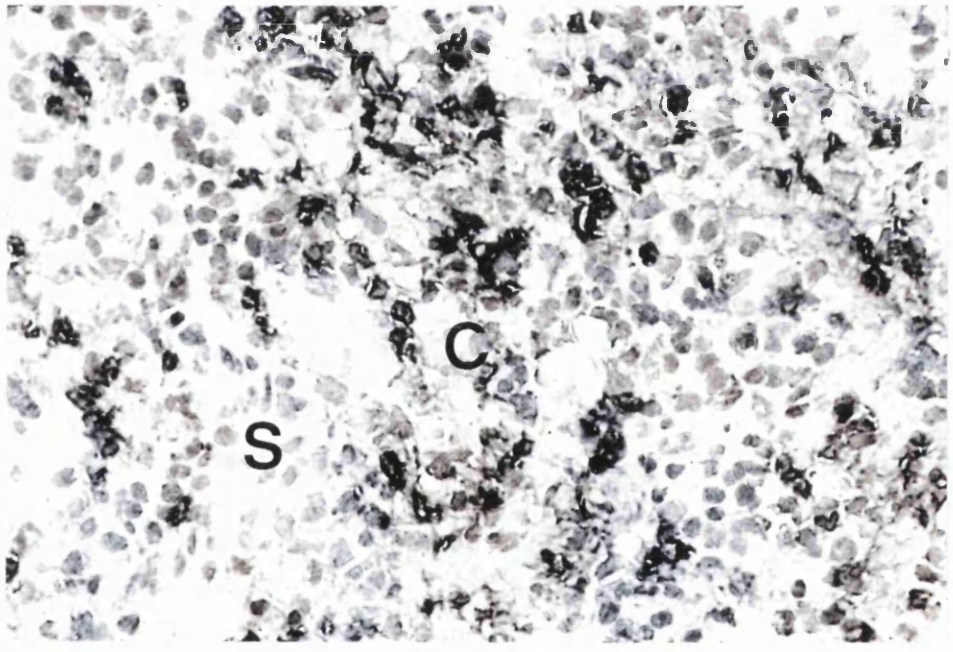

F. Medulla – prescapular lymph node (calf 776) stained with CC94; 9 days post-infection with *T. parva*. Positively stained cells are located mainly within the medullary cords (C). x80.

Figure 3.15. (cont.) Sections of bovine lymph node stained by immunoperoxidase with CC94 (anti-CD11b) and CC149 (anti-MyD-1)

A. Medulla – normal prescapular lymph node (calf 784). Positively staining cells (pink) are confined mainly to the medullary sinuses (S). Counter-stained with methyl green. x80.

B. Cortex – normal prescapular lymph node (calf 784). A few small positively stained cells are scattered in the paracortex. x80.

C. Cortex – prescapular lymph node (calf 5158); day 9 post-infection with *T. parva*. Numerous large positively stained cells are present throughout the paracortex, but not within the primary follicle (F) on the left of the picture. x80.

Figure 3.16. Sections of bovine lymph node stained for acid phosphatase.

A.

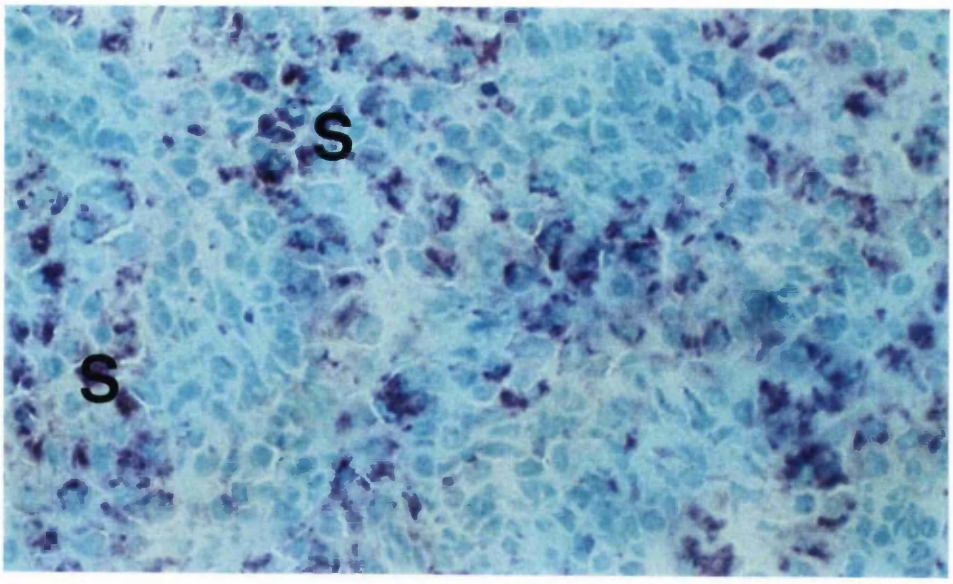

B.

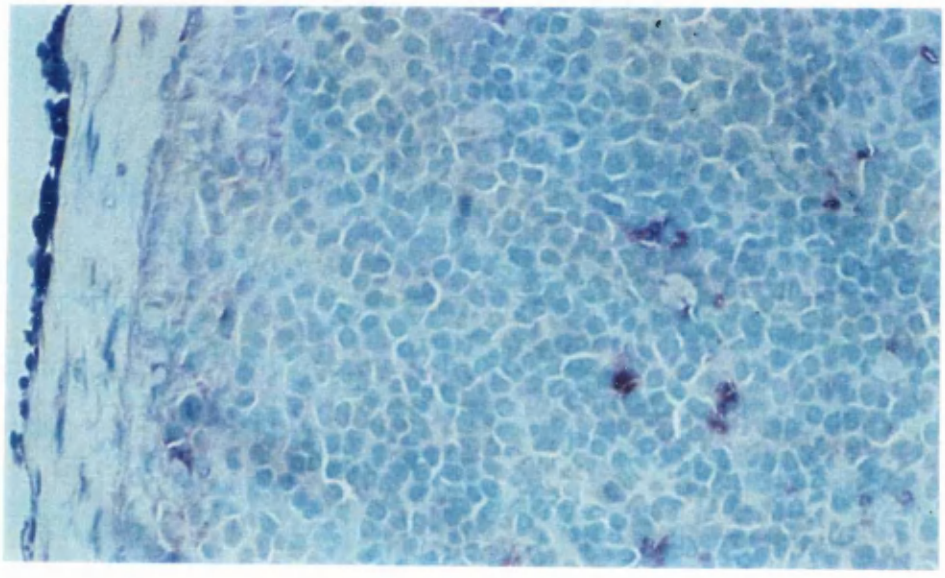

C.

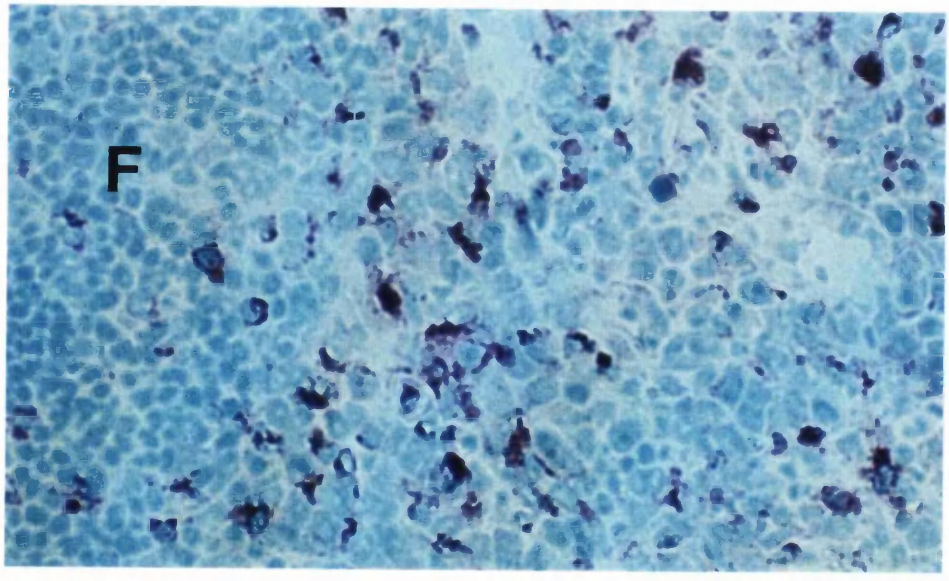

3.3.5. Cytokine expression in the drainage lymph node during primary infection with *T. parva.*

3.3.5.1. Detection of cytokine transcripts by RT-PCR.

To identify the cytokines expressed in the lymph node during infection with *T. parva,* RNA was extracted from freshly isolated lymph node cells (the whole MNC population and sorted $CD4^-$ and $CD8^+$ subpopulations) at different time points and used as a template for RT-PCR. Amplification using bovine β-actin-specific primers was performed in each case to verify the efficiency of cDNA synthesis by reverse transcription (Figure 3.18). The specificity of the cytokine PCR products was checked by digestion with restriction endonucleases to produce fragments of the sizes predicted from published sequences of bovine cytokines (see Table 3.7 and Figure 3.17).

Transcripts for IL-2, IFNγ, TNFα and IL-10 were detected in both the whole lymph node MNC population and the $CD4^+$ and $CD8^+$ T cell subpopulations of the control animals; no transcripts for IL-4 and IL-6 were found in these samples. Transcripts for all six cytokines are present in the whole MNC population and $CD4^+$ T cells on days 5, 7 and 9 of infection with *T. parva.* There was insufficient RNA from the $CD8^+$ T cells to perform RT-PCR at each time point; however at day 7 transcripts for all cytokines except IL-4 were detected. Figure 3.18 illustrates the results of RT-PCR on the whole lymph node MNC population; these are also representative of the results obtained from sorted $CD4^+$ T cells.

Table 3.7. Predicted sizes of fragments generated by restriction enzyme digestion of cytokine PCR products.

Cytokine	PCR product size (bp)	Restriction enzyme	Sizes of fragments (bp)
IL-2	373	*Xba* I	149, 224
IFNγ	316	*Eco* RV	164, 152
TNFα	464	*Bgl* I	355, 109
IL-4	348	*Pst* I	141, 207
IL-6	505	*Bgl* II	352, 153
IL-10	518	*Bst* EII	223, 295

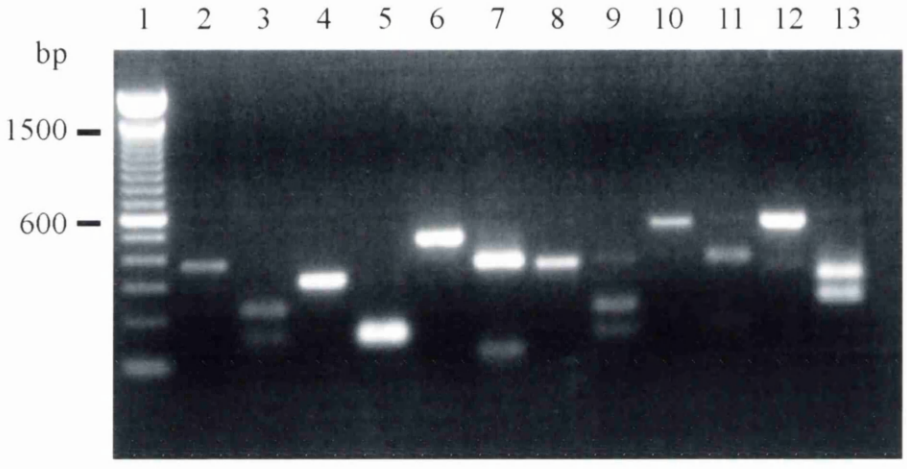

Key

Lane 1:	100bp DNA ladder		
Lane 2:	IL-2	Lane 8:	IL-4
Lane 3:	IL-2/*Xba* I	Lane 9:	IL-4/*Pst* I
Lane 4:	IFNγ	Lane 10:	IL-6
Lane 5:	IFNγ/*Eco* RV	Lane 11:	IL-6/*Bgl* II
Lane 6:	TNFα	Lane 12:	IL-10
Lane 7:	TNFα/*Bgl* I	Lane 13:	IL-10/*Bst* EII

Figure 3.17. Verification of the specificity of cytokine-specific primers by restriction enzyme digestion of the PCR products. cDNA from ConA-stimulated peripheral blood mononuclear cells was the substrate for amplification. The sizes of the fragments generated by digestion with restriction enzymes were predicted from the published sequences of bovine cytokines and are shown in Table 3.7.

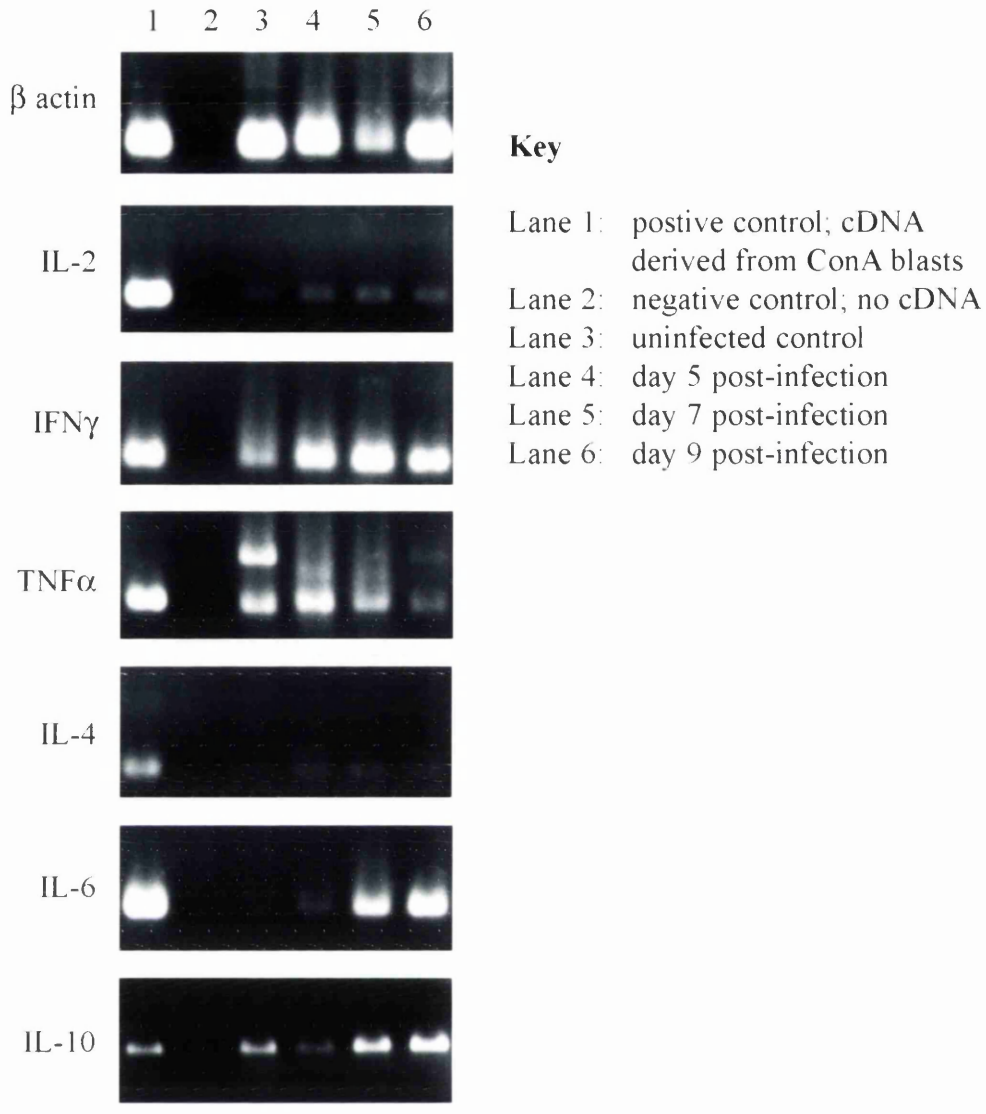

Figure 3.18. Cytokine transcripts detected by RT-PCR in the mononuclear cell (MNC) population of the drainage lymph node during primary infection with *Theileria parva*.

3.3.5.2. Expression of IL-10 mRNA in the drainage lymph node of infected calves.

Examination of cytokine mRNA expression by *in situ* hybridization (ISH) can provide more useful information than RT-PCR alone, as ISH allows direct assessment of the numbers of cells expressing the cytokine and their anatomical location. Digoxigenin-labelled antisense and sense riboprobes specific for bovine IL-10 were available at the time these experiments were performed, and were used to examine the expression of IL-10 mRNA in the drainage lymph nodes of *T. parva*-infected animals. Expression of this cytokine was detected in the lymph node of one of the control animals (784); a few strongly positive cells were observed within the medullary sinuses (Figure 3.19.A). In the other uninfected calf, 781, the appearance of the sections stained with the antisense probe was not significantly different from that of the negative control which was hybridized with the sense probe. At day 5 post-infection, the pattern of expression of IL-10 mRNA was not significantly altered. By day 7 post-infection, there was a marked increase in IL-10 mRNA expression which was confined almost exclusively to cells within the medulla (Figure 3.19.B,C). In the medulla, large numbers of positive cells were found predominantly within the sinuses. The flattened cells lining the sinuses were also positive for IL-10 mRNA. The pattern of mRNA expression on day 9 post-infection was essentially the same as at day 7, with the majority of positively staining cells confined to the medulla (Figure 3.19.D,E). There was considerable cell-to-cell variation in the intensity of the staining, with the most strongly staining cells located in the sinuses. No positive cells were seen in the outer cortex, paracortex, follicles and germinal centres, or within the subcapsular sinus or trabecular sinuses at day 7 or day 9 post-infection.

A.

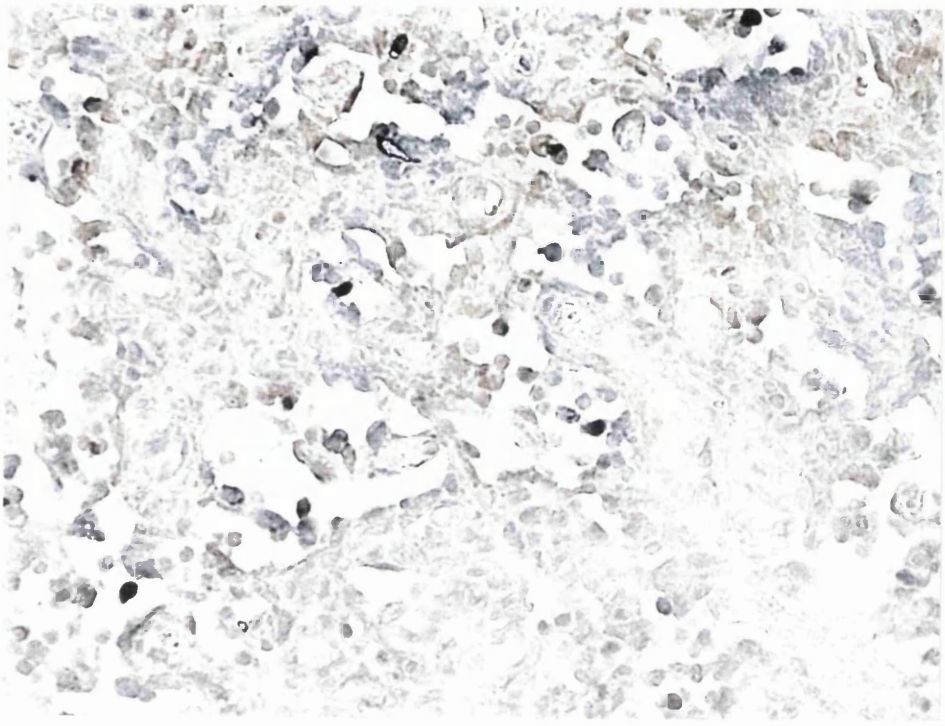

Figure 3.19. Sections of bovine lymph node stained by *in situ* hybridization with a digoxigenin-labelled riboprobe to bovine IL-10.

A. Medulla – normal prescapular lymph node (calf 784); stained with the antisense IL-10 probe. A very small number of positive cells are present in the medullary sinuses. x80.

B.

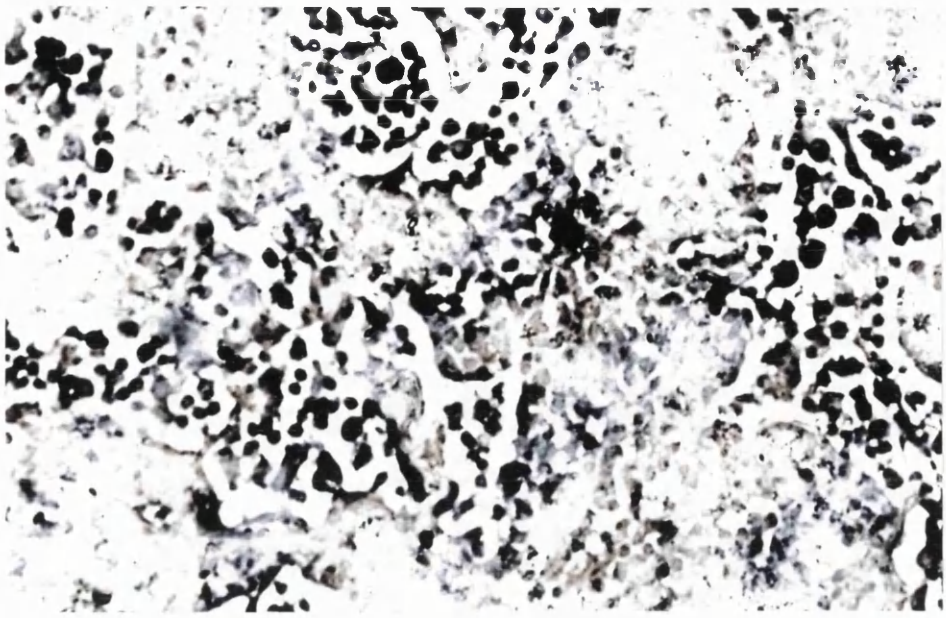

B. Medulla – prescapular lymph node (calf 783) stained with the antisense IL-10 probe; 7 days post-infection with *T. parva*. Large numbers of intensely stained cells are present within the medullary sinuses, but are much less numerous in the medullary cords. x80.

C.

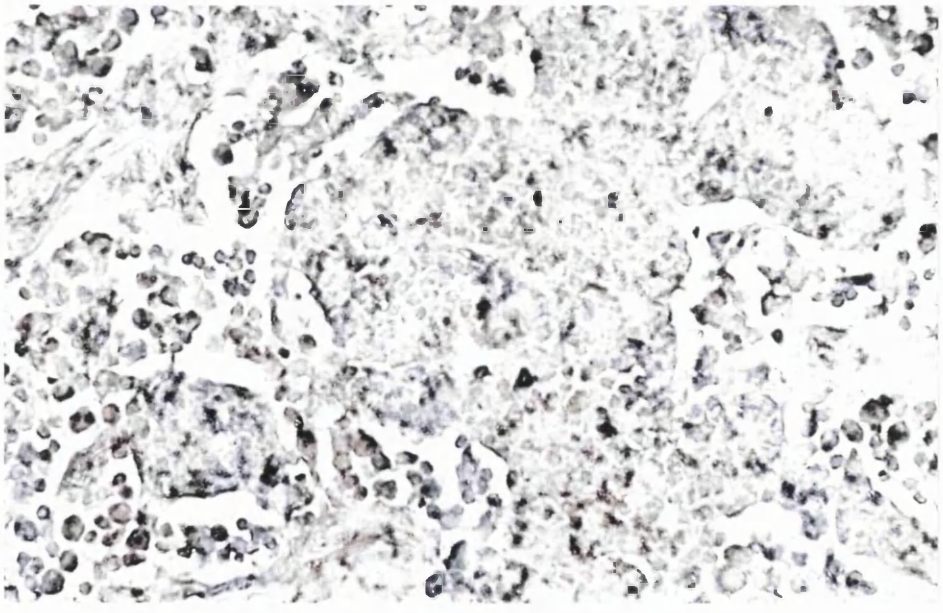

C. Medulla – prescapular lymph node (calf 783) stained with the sense IL-10 probe; 7 days post-infection with *T. parva*. This is taken from the same region as the section shown above to serve as a control for the specific binding of the IL-10 riboprobe. x80.

Figure 3.19. (cont.) Sections of bovine lymph node stained by *in situ* hybridization with a digoxigenin-labelled riboprobe to bovine IL-10.

D.

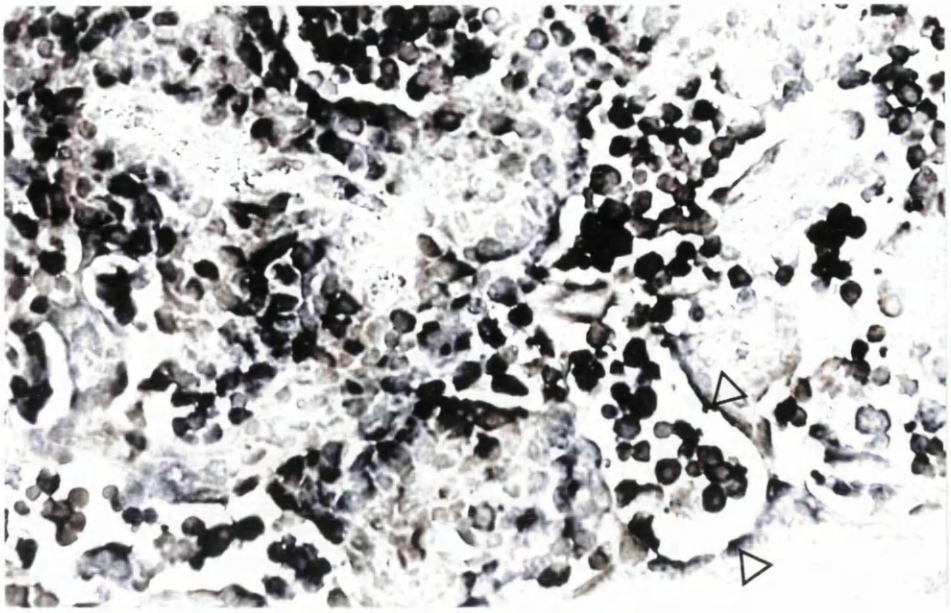

D. Medulla – prescapular lymph node (calf 776) stained with the IL-10 anti-sense probe; day 9 post-infection with *T. parva*. Large numbers of positively stained cells are present within the medullary sinuses, and the flattened cells lining the sinuses are also stained (open arrows). Small numbers of positive cells are also present in the medullary cords. x80.

E.

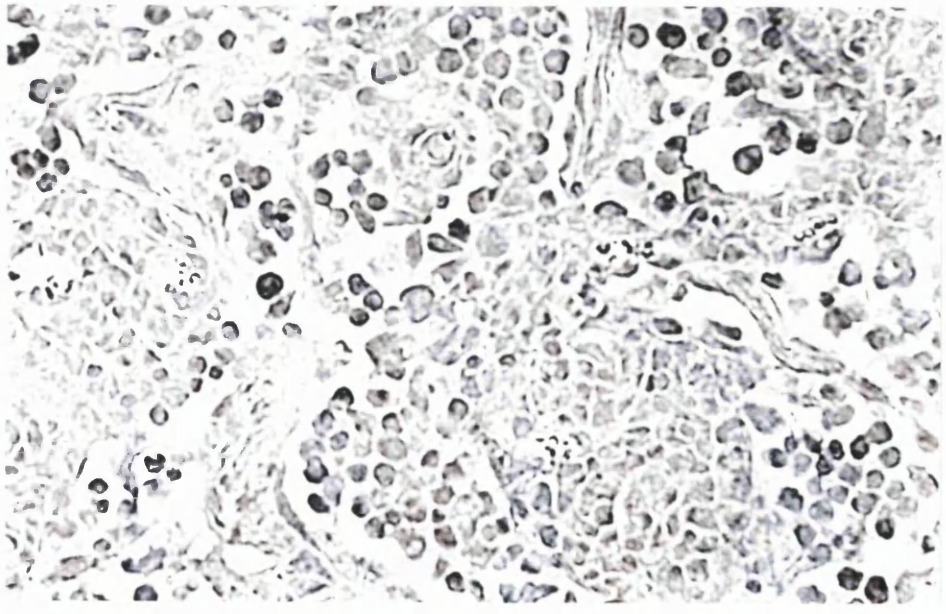

E. Medulla – prescapular lymph node (calf 776) stained with the IL-10 sense probe; day 9 post-infection with *T. parva*. This is taken from the same region as the section shown above. x80.

Figure 3.19. (cont.) Sections of bovine lymph node stained by *in situ* hybridization with a digoxigenin-labelled riboprobe to bovine IL-10.

3.3.6. Effect of lymph plasma from a *T. parva*-infected animal on the growth of parasitized cell lines seeded at limiting dilutions.

The immune response provoked during primary infections with *T. parva* may benefit the parasite by secretion of cytokines from activated lymphocytes which could act as growth factors for parasitized cells, enhancing their proliferation. To test whether substances capable of enhancing proliferation of *T. parva*-infected cells were produced during infection, plasma was separated from efferent lymph draining from the prescapular lymph node of an infected calf (AT115) on days 7 and 11 of infection. At day 7 in this animal, no response was evident, while at day 11 approximately 30% of efferent lymph lymphocytes were blasting, and the proportion of $CD2^{-}CD8^{+}$ T cells reached its peak (23%). The percentage of parasitized cells in the efferent lymph was <2% at day 11. Different concentrations of lymph plasma were included in the culture medium of a *T. parva*-infected cell line over a range of cell concentrations that had been shown to be suboptimal for maintenance of proliferation (see Figure 3.20). As illustrated in Figure 3.21, lymph plasma isolated from an uninfected animal had no effect on the proliferation of the cell line. However, day 7 lymph plasma from the infected animal produced a dose-dependent enhancement in the proliferation of parasitized cells seeded at 2.5×10^3 and 5×10^3 cells/well. Lymph plasma isolated on day 11 of infection produced even greater enhancement of proliferation at the same cell concentrations; however this effect was more marked with the lower concentrations of lymph (2.5% and 5%), and least pronounced when lymph formed 20% of the culture medium.

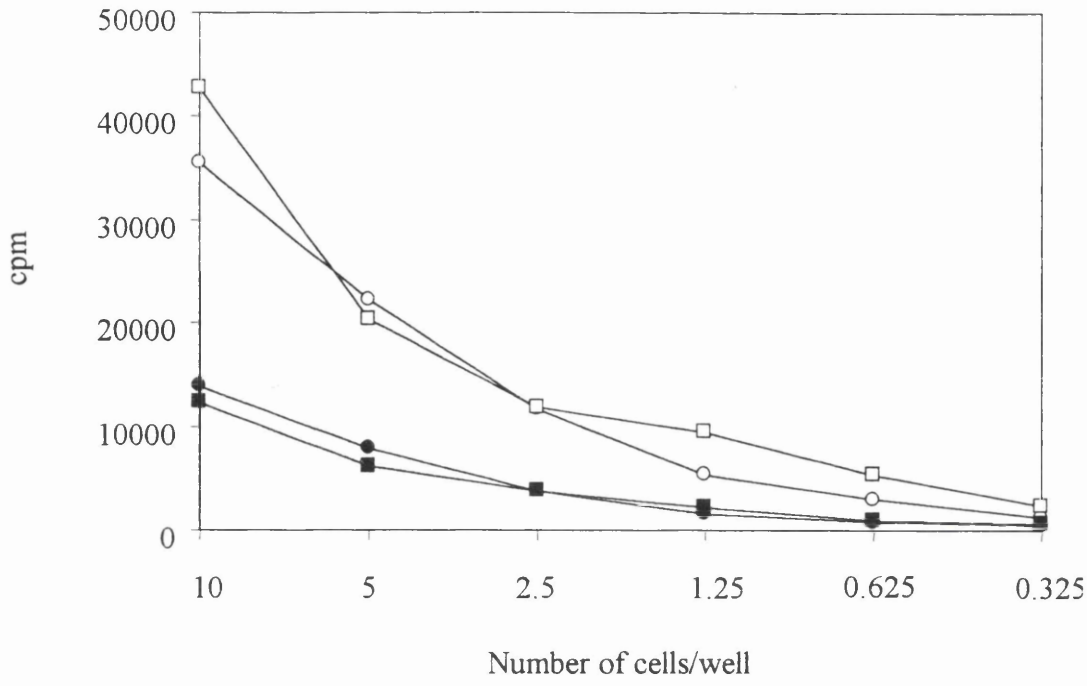

Figure 3.20. Titration of *T. parva*-infected cell lines to determine the cell density that is critical for maintenance of cell proliferation. Two cell lines, AT107 (circles) and AT112 (squares), were seeded at doubling dilutions from $1x10^4$ to $3x10^2$ cells/well, and incubated at 38°C for 48h (closed symbols) or 72h (open symbols). Proliferation was assessed by the incorporation of [^{125}I] iododeoxyuridine. The results are expressed as counts per minute (cpm), and represent the mean values of triplicate cultures.

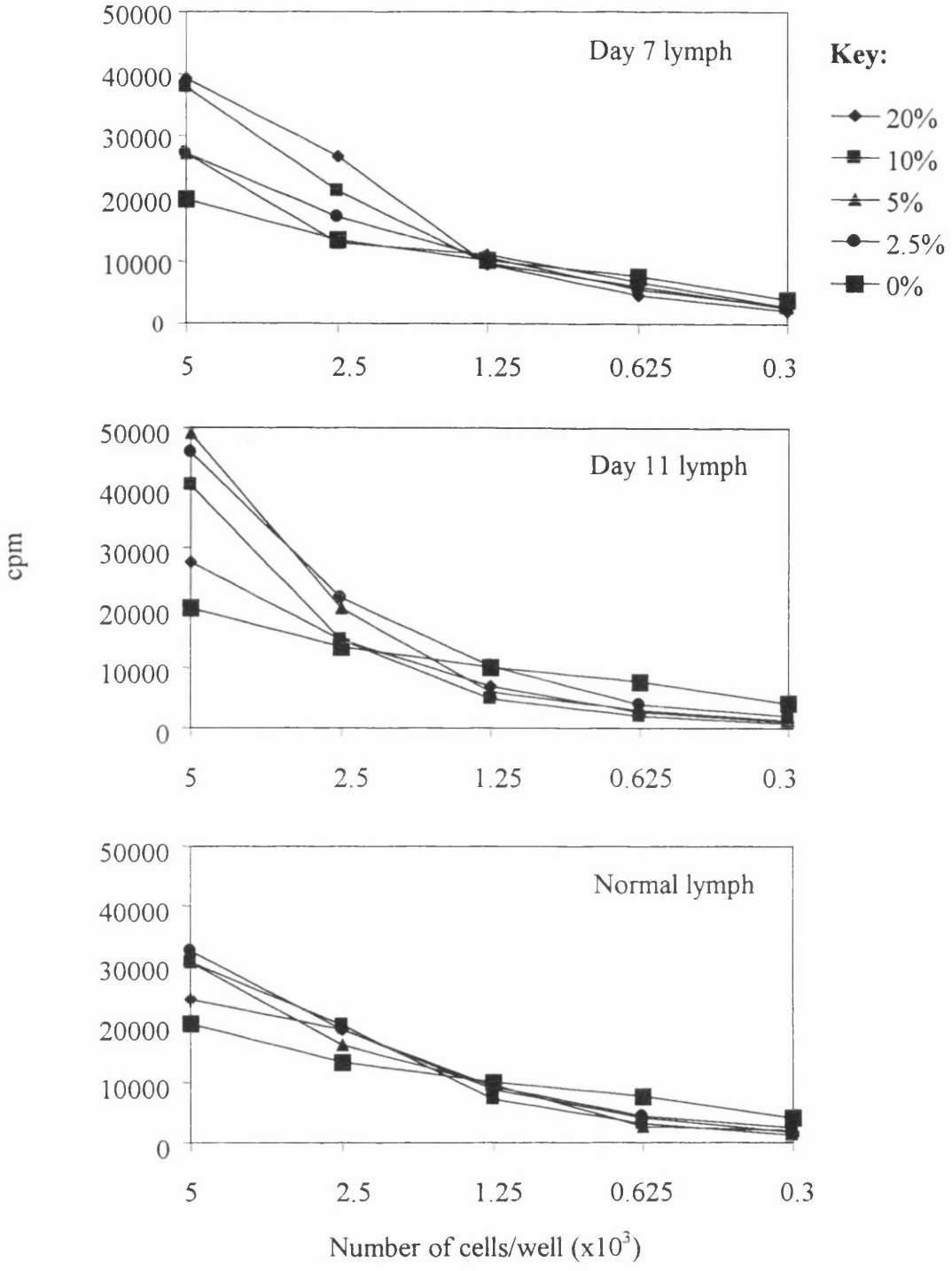

Figure 3.21. The effect of lymph plasma from an animal (AT115) infected with *T. parva* on the proliferation of a parasitized cell line seeded at limiting dilution. Cell-free lymph plasma was prepared from efferent lymph draining the prescapular lymph node on days 7 and 11 post-infection, and dialysed to remove Alsever's solution used as anticoagulant. The lymph plasma was included in the culture medium of parasitized cells seeded at doubling dilutions from $5x10^3$ to $3x10^2$ cells/well, at concentrations of 20%, 10%, 5% and 2.5% (v/v). The cultures were incubated at 38°C for 3 days and proliferation was assessed by the incorporation of [^{125}I]iododeoxyuridine. The results are expressed in counts per minute (cpm) and represent the mean values of triplicate cultures.

3.4. Discussion.

The results presented in this chapter indicate that a major T cell response, principally involving $CD8^+$ T cells, occurs in the drainage lymph nodes of calves undergoing primary infections with *Theileria parva*. The response coincides with the initial detection of parasites within the lymph node, and occurs at a time when parasite numbers are increasing rapidly. In previous studies, T cell responses have been shown to play an important role in immunity to *T. parva*. After immunization or challenge of animals with *T. parva*, MHC class I-restricted $CD8^+$ cytotoxic T cells (CTL) were detected in PBMC and ELL, and CTL precursors (CTLp) could be detected in the PBMC of immune animals by limiting dilution analysis (Eugui and Emery, 1981; Morrison *et al.*, 1987; Taracha *et al.*, 1992). In contrast, CTLp were undetectable in the PBMC of naive animals, and CTL capable of killing autologous infected targets were not detected during the course of lethal primary infections, although cytotoxic activity against allogeneic infected cells and xenogeneic targets was observed in the late stages of the infection (Eugui and Emery, 1981; Taracha *et al.*, 1992). $CD2^-CD8^+$ and $CD2^+CD8^+$ cells sorted from the efferent lymph of animals undergoing lethal infections, and tested for cytotoxic activity in a limiting dilution assay had a very low frequency of CTLp (less than 1:20000) (Taracha, 1991). The response involving $CD8^+$ T cells in the drainage lymph node during primary infections may thus represent a host immune response which is ineffective in controlling parasite replication. The failure to clear the infection may be the result of a strategy employed by the parasite to evade the host immune response, for example, non-specific T cell activation, which would promote parasite survival.

The unusual phenotype ($CD2^-CD3^+CD8^+$) of a large proportion of the T cells involved in the primary response to the parasite, and the failure to detect parasite-specific cytotoxic activity at this stage of the infection, suggests that these are not conventional CTL. *Theileria*-specific CTL clones have been shown to express both CD2 and CD8 (Morrison *et al.*, 1988). Almost all mature T cells in the periphery, with the exception of γ/δ T cells, express CD2. However, analysis of the $CD2^-CD8^+$ population by three-colour fluorescent antibody staining revealed that the majority of these cells are negative for the γ/δ TCR, and since they are $CD3^+$, they are assumed to express an α/β TCR. In the

infected animals examined, these cells reach a maximal percentage ranging from 5% to 30% of the total lymph node cell population, compared to 3% or less in resting nodes. The histological and immunocytochemical examination of lymph node sections from infected animals provided evidence that these cells are probably accumulating in the medulla or corticomedullary junction regions.

The $CD2^-CD3^+CD8^+$ population may arise as a result of downregulation of CD2 expression on the surface of activated $CD8^+$ lymphocytes, or from expansion of a small pre-existing population of T lymphocytes with this phenotype. The division of the $CD8^+$ T cells of infected animals into distinct CD2-negative and CD2-positive subpopulations argues against the downregulation of CD2 expression at the cell surface, as this might be expected to produce a gradation of mean fluorescence intensity such as occurs during modulation of CD2 expression by monoclonal antibodies (Gückel *et al.*, 1991). On the other hand, the possibility that the parasite has evolved a mechanism to rapidly block expression of CD2 on CD8 T cells cannot be discounted. CD2 appears to have important functions in the activation and expression of effector functions in $CD8^+$ cytotoxic cells (de Waal-Malefyt *et al.*, 1993); therefore loss of CD2 from these cells could confer a survival advantage on the parasite by preventing expression of cytolytic activity against parasitized lymphocytes. However $CD2^-CD4^+$ T cells were not detected during the infection, and it is difficult to conceive how CD2 could be selectively down-regulated on CD8 T cells and not on activated CD4 T cells. Therefore, it seems more likely that the appearance of $CD2^-CD3^+CD8^+$ T cells represents expansion of a small pre-existing population of these cells. $CD2^-CD8^+$ can form 1-3% of the MNC population in the normal resting lymph node, but are not detected in peripheral blood. Some of these cells in the resting node may be γ/δ T lymphocytes, as small numbers of $\gamma\delta TCR^+CD8^+$ cells are also found.

The existence of a minor subpopulation of bovine $CD2^-CD3^+CD8^+$ (assumed $\alpha\beta TCR^+$) lymphocytes that can be selectively activated during infection has not been previously reported. Cells with this phenotype have not been described in peripheral lymphoid compartments of other species, although a subset of $\alpha/\beta TCR^+CD2^-CD8^+$ intestinal intraepithelial lymphocytes (IEL) has been noted in mice. (Van Houten *et al.*, 1993). In

man $CD2^-CD3^+\alpha\beta TCR^+$ T cells were shown to comprise less than 1% of PBMC in adults; however phenotypic analysis of a small number of clones derived from this population showed that they expressed CD4 rather than CD8 (Kabelitz *et al.*, 1989). The functions of these cells and their stimulatory requirements are thus unknown, and attempts to address these questions in the present study by culturing the cells *in vitro* were unsuccessful. Although a variety of stimuli, including autologous parasitized stimulators, PMA and ionomycin, and ConA were used, the cells appeared refractory and failed to demonstrate significant proliferative responses. This may reflect a requirement for CD2-mediated costimulation of the CD3/TCR signalling pathway. There is evidence that in addition to acting as a cell adhesion molecule, CD2 can play an important role in T cell activation. $CD2^-$ mutants of the human Jurkat leukaemia cell line stimulated via CD3/TCR produce much less IL-2 than the parental cells; transfection of CD2 restored IL-2 production (Makni *et al.*, 1991). In addition, down-regulation of CD2 expression *in vivo* by injection of mice with an anti-CD2 monoclonal antibody has been shown to result in profound inhibition of T cell-mediated immune responses (Gückel *et al.*, 1991). The $CD2^-\alpha\beta TCR^+$ subset of murine intestinal intraepithelial lymphocytes show greatly reduced proliferative responses to PMA/ionomycin and anti-CD3 monoclonal antibody in comparison with their $CD2^+$ counterparts (Van Houten *et al.*, 1993). Recently it has been shown that interaction between CD2 and its ligand CD58 is required for optimal stimulation of T cell proliferation by IL-12 (Gollob *et al.*, 1995,1996). However, for the $CD2^-CD8^+$ T cells to be expanded during infection with *T. parva*, they must be activated *in vivo* by a CD2-independent mechanism. The inclusion of exogenous IL-2 in the cultures would be expected to replace the need for co-stimulation of the CD3/TCR signalling pathway. It may be that *in vivo* these cells have stimulatory requirements distinct from those of conventional $CD8^+\alpha\beta TCR^+$ T cells, which are not adequately reproduced by the *in vitro* culture conditions used. Alternatively, since most of the sorted $CD2^-CD8^+$ T cells have already been activated *in vivo,* it is possible that the activation process has rendered them anergic, or that further stimulation induces programmed cell death. It has been shown in several systems that the same stimuli which activate resting T cells can trigger apoptosis in activated T cells (Wesselborg *et al.*, 1993; Pohl *et al.*, 1995). Interestingly, apoptosis and anergy are commonly observed following *in vivo* T cell activation by superantigens (Webb *et al.*, 1990; MacDonald *et*

al., 1991). However, in the experiments that were carried out in the current study, insufficient numbers of the purified cells were obtained to test for the induction of apoptosis.

The expansion of lymphocyte subsets of unusual phenotype has been demonstrated during some chronic infections. In mice infected with the cestode parasite *Mesocestoides corti,* increased numbers of cells with the morphology of large granular lymphocytes were found in the liver and spleen. These cells expressed Thy-1 and low levels of CD4, but were negative for CD3 and other T and B cell markers. Cell lines with this phenotype produced by *in vitro* stimulation of splenocytes by *M. corti* hsp70 produced IL-6 constitutively and could be induced to secrete IL-2; however no cytolytic activity was detected (Estes *et al.*, 1993). An atypical subset of human $CD8^+\alpha\beta TCR^+$ T cells is significantly expanded in HIV-infected individuals (Lewis *et al.*, 1985), CMV-infected patients (Wang *et al.*, 1993a) and transplant recipients. These cells, which are also found in low numbers in the blood of normal donors, are $CD28^-$ and express CD57, a molecule also found on human NK cells; they express levels of CD2 equivalent to those found on the cell surface of $CD8^+CD28^+CD57^-$ T cells (Azuma *et al.*, 1993). They show poor proliferative responses to a variety of stimuli (Rüthlein *et al.*, 1988; Azuma *et al.*, 1993), and mediate suppression of humoral and cellular immune responses, including cytotoxic T cell responses (Clement *et al.*, 1984; Wang *et al.*, 1994). In addition, this population appears more susceptible to apoptosis when cultured *ex vivo* (Lewis *et al.*, 1994). In both these examples, the effector function of these unusual cells *in vivo* is unknown.

Although the cytotoxic potential of the novel $CD2^-CD8^+$ population was not directly tested, their expression of CD3 makes it unlikely that they represent natural killer (NK) cells, which do not express a TCR. Bovine NK cells are poorly characterized in terms of phenotype, however non-specific cytotoxic activity of bovine PBMC against virus-infected and tumour cell targets has been demonstrated following treatment with IL-2 (Campos *et al.*, 1992). Two cloned cell lines derived from the PBMC of an animal immunized with *T. parva* by stimulation with TCGF and irradiated parasitized cells displayed non-MHC-restricted cytotoxic activity against infected and uninfected lymphoblasts (Goddeeris *et al.*, 1991). Phenotypic characterization of these clones

showed that neither expressed CD3 mRNA; one expressed CD2 only and the other expressed homodimeric CD8α. Attempts to identify the cell in bovine PBMC that mediates non-specific IL-2-activated killing of tumour cells demonstrated that most of this activity resided in a non-adherent population of $CD2^+CD4^-CD8^-$ lymphocytes (Campos *et al.*, 1992). In contrast, a population of bovine lymphocytes with NK activity against virus-infected and non-infected embryonic kidney cells were shown to be negative for CD2, CD4, CD8 and WC1, but expressed CD3, CD45 and Fc receptors; this population may represent a subset of γ/δ T cells (Amadori *et al.*, 1992).

The role of T cell-derived cytokines in determining the outcome of parasitic infections of mice has been well documented. The polarization of $CD4^+$ T cell responses towards dominance of cells producing either Th1-type (IL-2, IFNγ) or Th2-type (IL-4, IL-5) cytokines appears to be influenced by the conditions under which initial priming of naive $CD4^+$ T cells occurs. Studies using $CD4^+$ T cells from TCR transgenic mice established the importance of certain cytokines in the local microenvironment for promoting Th subset differentiation *in vitro* (Hsieh *et al.*, 1992; Seder *et al.*, 1993). The influence of cytokines on the differentiation of Th subsets during *in vivo* infection with an intracellular pathogen has been extensively studied using the model of *Leishmania major* infection in mice. In susceptible BALB/c mice, IL-4 plays a key role in initiating a Th2-type response which fails to clear the infection, while the induction of IL-12 in resistant strains of mice is essential for the development of protective Th1-type responses (Mattner *et al.*, 1996). Intracellular pathogens that have evolved mechanisms capable of diverting the $CD4^+$ T cell response towards a Th2-type phenotype would be expected to have a selective advantage due to their ability to evade elimination by the host. However, examination of cytokine mRNA expression in the drainage lymph nodes of naive cattle infected with *T. parva* revealed no bias in the expression of Th1- or Th2-type cytokines by $CD4^+$ T cells, with transcripts for IL-2, IFNγ, IL-4, IL-6, IL-10 and TNFα consistently detected at days 5, 7 and 9 post-infection. This is perhaps not surprising in view of the evidence that, during the first few days after infection with *L. major*, $CD4^+$ T cells in the drainage lymph nodes of both susceptible and resistant mice express IL-2, IL-4 and IFNγ at the mRNA and protein level (Morris *et al.*, 1992; Reiner *et al.*, 1994). In the present study, the relative levels of expression of the different cytokines were not

quantified and it is therefore difficult to draw any conclusions about the potential role of cytokines in promoting a bias towards a either a Th1- or Th2-type response in primary infections with *T. parva*. Interpretation of the results of RT-PCR was also made difficult by the finding that transcripts for IL-2, IFNγ, IL-10 and TNFα were expressed in the lymph nodes of both uninfected control animals. This reflects the sensitivity of the RT-PCR technique, and presumably is the result of background immunological activity in the lymph nodes.

Examination of the distribution of cells expressing IL-10 mRNA in the drainage lymph nodes of infected calves found that the most intensely staining cells on days 7 and 9 post-infection were concentrated within the medullary sinuses, although numerous cells in the medullary cords were also postively stained. It is likely that IL-10 is being expressed by T cells and/or macrophages/monocytes, as these form the predominant cell types within the medulla at this time. These findings alone do not provide any direct information about the role of IL-10 in the primary immune response to *T. parva*. IL-10 was initially recognized as a soluble factor produced by murine $CD4^+$ Th2-type clones that selectively inhibited cytokine synthesis (IL-2 and IFNγ) of Th1-type clones (Fiorentino *et al.*, 1989). In humans and cattle, IL-10 is produced by Th0-, Th1- and Th2-type clones and down-regulates proliferation of all subsets indirectly, by inhibition of the costimulatory function of macrophages (Del Prete *et al.*, 1993; Brown *et al.*, 1994; Ding *et al.*, 1993). Human recombinant IL-10 was also shown to directly inhibit proliferation of a bovine $CD8^+$ clone (Brown *et al.*, 1994). In addition, IL-10 down-regulates the functions of activated human and murine macrophages by inhibiting the synthesis of pro-inflammatory cytokines such as IL-12, IL-1, TNFα and IL-6, and production of reactive oxygen and nitrogen intermediates (de Waal Malefyt *et al.*, 1991; Gazzinelli *et al.*, 1992a). In mice, IL-10 has been shown to play a role in the transient down-regulation of T cell responses that occurs during the acute phase of *Toxoplasma gondii* infection (Khan *et al.*, 1995). Transient immunosuppression is a common feature of the acute phase of many parasitic infections, and is thought to benefit the parasite by allowing it to evade host immune responses and establish persistent infections. However, since many parasites induce strong cell-mediated responses, the immunosuppression may also benefit the host by protecting against the deleterious effects of excessive production of pro-inflammatory

cytokines. The influence of IL-10 on the outcome of infection depends on complex interactions with other components of the immune reponse and cannot be predicted from examination of the level of expression of this cytokine alone.

The role of cytokines in the pathogenesis of *Theileria parva* infections is further complicated by the fact that the parasite invades lymphocytes and results in their activation, such that these cells are responsive to cytokines and can themselves produce certain cytokines. *In vitro* studies have established that *T. parva*-infected cell lines constitutively express high-affinity IL-2 receptors, and that cell lines seeded at low densities proliferate in response to exogenous IL-2 (Coquerelle *et al.*, 1989; Dobbelaere *et al.*, 1990,1991). Thus, *in vivo*, IL-2 produced by T cells activated in the primary response may contribute to parasite survival by promoting proliferation of infected cells. To determine whether soluble growth factors for parasitized cells were produced during the *in vivo* response to *T. parva*, lymph plasma obtained from an infected animal was included in the culture medium of a parasitized cell line seeded at limiting dilution. Enhanced proliferation, proportional to the concentration of lymph in the culture medium, was observed at cell densities greater than 6.25×10^3 cells/ml with lymph collected on day 7 post-infection. With lymph collected on day 11, the greatest enhancement in proliferation was found with the lower concentrations of lymph plasma. This may be due to a tendency of the lymph plasma to form clots in the cultures at higher concentrations, which was observed with day 11 lymph, or may reflect the presence of molecules that inhibit growth of parasitized cells at higher concentrations. These preliminary results suggest that soluble growth factors for parasitized lymphocytes are produced in the drainage lymph node during primary infections with *T. parva*. However, since this experiment was carried out using only one animal, confirmation of this observation is required, and further studies will be needed to establish the precise nature of the stimulatory factors and whether they play a role in the pathogenesis of the infection. Previous studies have examined the influence of recombinant cytokines, including IL-1, IL-2, IFNγ, IFNα and TNFα, on the establishment and proliferation of *T. parva*-infected cell lines. IL-2 was the only cytokine that consistently enhanced the proliferation of established cell lines; none of the cytokines tested had an inhibitory effect (DeMartini and Baldwin, 1991; Preston *et al.*, 1992).

Another notable feature of the lymph node response to *T. parva* was the appearance between days 7 and 9 post-infection of large numbers of cells expressing the myeloid lineage markers recognized by the monoclonal antibodies CC149 and CC94. Staining for the enzyme acid phosphatase revealed that these cells contained a well-developed lysosomal system, suggesting that they are activated monocytes/macrophages. The results of immunocytochemistry are supported by the flow cytometric analysis, which revealed increased proportions of monocytes in the drainage lymph nodes and PBMC of some animals at this stage of the infection. A transient increase in monocytes/ macrophages in PBMC and lymph nodes of calves undergoing lethal infections with *T. parva* was previously reported by Emery *et al.* (1988). Similar observations were made in a recent study of the lymph node response to *Theileria annulata*; 8 days post-infection large numbers of monocytes/macrophages were found throughout the cortex and medulla (Campbell *et al.*, 1995). However, these may represent parasitized cells, since *T. annulata* is known to preferentially infect monocytes, and large numbers of schizonts were also present at this time. *T. parva* does not infect monocytes; in this case the appearance of these cells in the drainage lymph node is likely to reflect recruitment in response to the infection. Recruitment of monocytes from peripheral blood into tissues usually involves the release of chemokines e.g. MIP-1α, MCP-1, from a variety of cells, including activated lymphocytes, at the site of infection or inflammation (Strieter *et al.*, 1996).

Macrophages, activated via IFNγ produced by $CD4^+$ and $CD8^+$ T lymphocytes and NK cells, are an important component of cell-mediated immune responses against a variety of intracellular pathogens (Suzuki *et al.*, 1988; Gazzinelli *et al.*, 1992b). In mice, much of the microbicidal activity of macrophages is mediated by the production of toxic oxidative metabolites such as nitric oxide (NO) (Liew *et al.*, 1990). PBMC isolated from naive cattle during the course of infections with *T. parva* and *T. annulata* were shown to synthesize NO spontaneously *in vitro*, and NO appeared to inhibit the establishment of schizont-infected cell lines (Visser *et al.*, 1995). Thus, activation of macrophages may play a role in the response to primary infections with *T. parva*. The expansion of $CD2^-$ $CD8^+$ T cells within the drainage lymph node coincides with the detection of increased numbers of monocytes/macrophages, and it is possible that this population plays a role in

the recruitment and activation of monocytes from peripheral blood. Unfortunately the pattern of cytokine expression in the $CD2^-CD8^+\alpha\beta TCR^+$ population was not established, although expression of transcripts for IFNγ was detected in the whole $CD8^+$ population.

In summary, the primary response to *T. parva* in the drainage lymph node is characterized by the expansion of $CD8^+$ T cells, a large proportion of which have the unusual phenotype $CD2^-CD3^+CD8^+$, and by the appearance of large numbers monocytes/macrophages, at a time when parasite numbers are increasing rapidly. The function of the $CD2^-CD8^+$ population remains obscure, but the fact that their emergence coincides with the increase in monocytes/macrophages suggests that they may have a role in recruitment and activation of these cells. There is no direct evidence that this response contributes to the pathogenesis of the infection, but these observations suggest a number of areas that deserve further investigation. It would be interesting to try to establish the stimulus that triggers activation of the $CD2^-CD8^+\alpha\beta TCR^+$ cells, and also to investigate which cytokines they express, and if they are capable of inducing activation of monocytes. Activated monocytes/macrophages might be expected to have an inhibitory effect on parasite growth; however excessive stimulation of these cells could also have deleterious effects for the host. Further studies are required to investigate the ability of monocytes/macrophages to influence parasite growth and modulate host immune responses.

CHAPTER FOUR

ANALYSIS OF *IN VITRO* RESPONSES TO *THEILERIA PARVA.*

4.1. Introduction.

The ability to produce continuously growing schizont-infected cell lines by *in vitro* incubation of bovine PBMC with sporozoites from infected ticks has played an important role in the elucidation of immune responses to *Theileria parva.* These *T. parva*-infected cell lines are capable of stimulating potent proliferative responses in autologous PBMC from immune or naive animals, a response referred to as the autologous Theileria mixed leucocyte reaction (MLR) (Goddeeris and Morrison, 1987). The responding populations from immune animals have been shown to contain both MHC class I restricted, parasite-specific, $CD8^+$ cytotoxic T cells, and parasite-specific $CD4^+$ Th cells (Goddeeris *et al.*, 1986a,b; Baldwin *et al.*, 1987). However, cytotoxic T cells are not generated when PBMC from naive animals are stimulated by autologous parasitized cell lines, despite proliferative responses of similar magnitude to those of immune animals. The phenotype of the responding cells has not been examined in detail; however, using a mAb against immunoglobulin as a marker for B cells and peanut agglutinin (PNA) as a marker for T cells, the majority of the responding population were found to be negative for both markers (Pearson *et al.*, 1982). The proliferative response of naive PBMC is maintained even when the stimulator cells are glutaraldehyde-fixed, suggesting that they are responding to a specific cell surface component of the parasitized cells, and not to soluble mitogens or growth factors secreted by the infected cells. In addition, culture supernatants from parasitized cell lines do not produce proliferative responses in normal PBMC; in fact, when they are grown at high cell densities, the supernatants from infected T cell lines suppress proliferation in autologous and allogeneic mixed lymphocyte reactions (MLR) (Goddeeris and Morrison, 1987).

In primary T cell responses to conventional antigens, the frequency of responding cells is normally too low to be detected in antigen-specific T cell proliferative assays. The strong proliferative response to *T. parva*-infected cells of PBMC from naive individuals suggests that these cells have received a stimulus which results in activation of a high

proportion of the population. This could be due to a cross-reactive memory T cell subset, or the action of a mitogen or superantigen. Limiting dilution analysis of the response to the *Mls* superantigen (encoded by an endogenous mouse mammary tumour virus) estimated the frequency of precursors at between 1 in 30 and 1 in 20, while the frequency of cells responding to a mitogen such as ConA was between 1:10 and 1:3 (MacPhail *et al.*, 1985). The frequency of 'memory' cells responding to recall antigens such as tetanus toxin is lower, of the order of 1:5000 (Merkenschlager *et al.*, 1988).

The strong proliferative responses of PBMC from naive cattle stimulated by autologous parasitized cells *in vitro* may parallel the marked T cell response observed in the lymph nodes of infected cattle at the time of initial detection of parasites. The aim of the work described in this chapter was to examine the phenotype of the responding cells *in vitro* and, by comparison with the *in vivo* response, to determine whether the autologous *Theileria* MLR could be used to model events occurring in the lymph node. In particular, it was hoped that if $CD2^{-}CD8^{+}$ α/β T cells were also generated during the *in vitro* response, this might be a more convenient approach for the further characterization of this unusual subset of T cells.

4.2. Materials and Methods.

4.2.1. Autologous *Theileria* mixed leucocyte cultures.

4.2.1.1. Establishing the kinetics of the response.

Autologous *Theileria* mixed leucocyte cultures were established essentially as described by Goddeeris and Morrison (1987). The cultures were established in 96 well flat-bottomed microculture plates with 4 x 10^5 PBMC per well as responder cells and a variable number of irradiated autologous *T. parva*-infected leucocytes as stimulator cells. The parasitized stimulator cells were harvested from cultures during logarithmic growth and exposed to 50 Gy of gamma-radiation prior to use. The stimulator cells were titrated into the culture by two-fold dilution, starting at 4 x 10^5 cells/well. Each series of cultures was set up in triplicate or duplicate. Controls included PBMC cultured with medium alone, and dilutions of stimulators cultured alone. The cultures were incubated at 38°C in a humidified atmosphere of 5% CO_2 in air for 3-7 days. Proliferation of cells was measured by the incorporation of tritiated thymidine as described in Section 2.2.4.

4.2.1.2. Bulk cultures.

Once optimal conditions for the responder:stimulator ratio and length of culture had been established, bulk cultures were set up to examine the phenotype of the blasting cells at the peak of the response. The cultures were established in 24 well cluster plates with 4 x 10^6 PBMC per well as responders, and a responder:stimulator ratio of 10:1. Parallel cultures were established in triplicate in 96 well flat-bottomed plates with 4 x 10^5 PBMC per well as responders, to confirm that a proliferative response was occurring by measurement of incorporation of [^{3}H]thymidine or [^{125}I]iododeoxyuridine as above. Control wells containing responders or stimulators cultured alone were also included on the 96 well plate. The cultures were incubated for 5 days.

4.2.1.3. Phenotyping responding cells in the autologous *Theileria* MLR.

Cells from the bulk cultures were resuspended, and the live cells were separated by density gradient centrifugation using Histopaque or Ficoll-Paque. The cells were washed once with PBS and distributed at 2 x 10^5 cells/well in a 96 well round-bottomed microtitre plate. The cells were incubated either with single monoclonal antibodies to

CD2 (CC42 or CH128A), CD3 (MM1A), CD4 (CC30 or IL-A12), CD8 (CC63 or IL-A105), γ/δ TCR (GB21A), WC1 (CC15 or IL-A29), surface Ig (IL-A58 or IL-A30) and the monocyte marker recognized by IL-A24, or different combinations of two of these antibodies, as shown in Table 4.1. Details of monoclonal antibodies and the protocols used for single staining and two-colour indirect immunofluorescent staining are given in Table 2.1 and Section 2.2.2.1. The samples were analysed on a FACScan (Becton Dickinson) and 5000 (single staining) or 10000 (two-colour staining) events were recorded. Statistical analysis of the data was carried out using PC LYSYS II software (Becton Dickinson).

Table 4.1. Antibodies used in two-colour staining of responding lymphocytes in the autologous *Theileria* MLR.

Target molecules	Monoclonal antibodies	Isotypes
Isotype control	TRT1/TRT3	IgG1/IgG2$_a$
CD2/CD8	CC42/CC63 or CH128A/IL-A105	IgG1/IgG2$_a$
CD3/CD8	MM1A/CC63 or MM1A/IL-A105	IgG1/IgG2$_a$
γ/δTCR/CD8	GB21A/CC63 or GB21A/IL-A51	IgG2$_b$/IgG2$_a$ IgG1/IgG2$_b$
γ/δTCR/CD2	GB21A/CH128A	IgG2$_b$/IgG1
CD8β/CD8α	CC58/CC63	IgG1/IgG2$_a$
CD4/CD8	CC30/CC63	IgG1/IgG2$_a$

4.2.2. Phenotyping responding cells in cultures of lymph node cells stimulated by mitogens.

Mononuclear leucocytes were isolated from the prefemoral lymph node of a healthy five month old Channel Island calf, as described in Section 2.2.1.3. The cells were resuspended in standard culture medium and distributed at 4 x 10^6 cells/well in a 24 well cluster plate. The mitogens used to stimulate proliferation were:

a) ConA at 5μg/ml

b) Pokeweed mitogen (PWM) at 5μg/ml

c) Phorbol myristate acetate (PMA) at 50ng/ml and ionomycin at 1μg/ml.

The cultures were incubated at 38°C as above for 3 days. To confirm that a proliferative response was occurring, cultures with identical stimuli were also established in triplicate in 96 well flat-bottomed plates with 4 x 10^5 responder cells/well, and the incorporation of tritiated thymidine was measured on day 3.

Cells harvested from the bulk cultures were treated in the same way as those harvested from the autologous *Theileria* mixed leucocyte cultures. A more limited panel of monoclonal antibodies was used to analyse the phenotype of the responding cells. Single staining was performed using monoclonal antibodies recognizing CD3 (MM1A), CD4 (CC8), CD21 (CC21), and a monocyte marker (IL-A24). Two colour staining was carried out by combining the anti-CD8 mAb, CC63, with either GB21A (γ/δ TCR) or CC42 (CD2). The cells were analysed on a FACScan as described above.

4.3. Results.

4.3.1. Determination of the kinetics of the *in vitro* response to *Theileria parva*.

To ensure that autologous *Theileria* mixed leucocyte cultures were harvested when the response was at its peak, the kinetics of the response were examined. In initial experiments, cultures were established in 96 well plates with varying numbers of irradiated stimulator cells, and incubated for different lengths of time before proliferation was measured by incorporation of tritiated thymidine. After 5 days in culture, maximal proliferation was observed at responder:stimulator ratios of 8:1 to 16:1, with proliferative responses of lower magnitude being observed at higher ratios (see Figure 4.1.A). The time at which maximum proliferation occurred was more variable, but the peak response was usually found between days 4 and 6 of culture (Figure 4.1.B). Thus a responder:stimulator ratio of 10:1 and a culture period of 5 days were adopted in subsequent experiments as the conditions most likely to provide optimal stimulation of PBMC by autologous *T. parva*-infected cell lines.

4.3.2. Phenotypic analysis of responses of PBMC to *T. parva*-infected cells.

4.3.2.1. Responses of PBMC from naive cattle.

PBMC from two animals (3225 and 4197) naive to infection with *T. parva* were cultured for five days with irradiated autologous *T. parva*-infected cells. The cell surface phenotype of the stimulator cells is shown in Table 4.2. The phenotype of the cultured cells was examined by flow cytometry using antibodies to CD2, CD3, CD4, CD8, γ/δTCR, WC1 (γ/δ T cell marker), surface immunoglobulin and the monocyte marker recognized by IL-A24. Gates for analysis were set on all viable cells and on the cells with high forward scatter (FSC^{hi}), which comprise mainly blasting cells (Figure 4.2). The results are shown in Table 4.3. For both animals, there was a marked increase in the percentage of γ/δ T cells, which formed more than 50% of the total viable cell population after 5 days in culture. The majority of the $\gamma/\delta TCR^{+}$ cells expressed WC1, a high molecular weight surface marker of ruminant γ/δ T cells. There was also evidence that $CD8^{+}$ T cells were involved in the response, as their percentage increased from 6% to

23% of the total population in 4197; and they formed a substantial proportion (23%) of the blast cell population from 3225. The involvement of $CD4^+$ T cells was more difficult to assess; there was a marked decrease in the proportion of this subpopulation in 3225, while a moderate increase in the percentage of $CD4^+$ cells was seen in 4197. B cells and monocytes did not appear to participate in the proliferative response, as the proportions of these cells showed a marked decrease during the culture period.

Two-colour immunofluorescent staining of the $CD8^+$ cells in the responding population revealed that a significant response involving $CD2^-CD8^+$ α/β T cells did not occur *in vitro*. As illustrated in Figure 4.3, a small percentage of the $CD2^-$ population expressed low levels of CD8 (representing 8% of the total population for 3225, and 2% for 4197), but this subset was not enriched within the blasting population. The percentage of $\gamma/\delta TCR^+CD8^+$ cells (11% of the total population for 3225 and 6% for 4197) exceeded the percentage of $CD2^-CD8^+$ cells in both cases. This suggests that the majority of cells in the $CD2^-CD8^+$ subset may be γ/δ T cells; however three-colour cytofluorometry was not performed to confirm this possiblity.

4.3.2.2. Comparison of the reponses of PBMC from naive and immune cattle.

In one experiment, the response of PBMC from a naive animal (4197) was compared with that of an immune animal (4198). These animals were twins, homozygous at the MHC, and therefore were stimulated using the same irradiated *T. parva*-infected cell line, originally derived from 4197. The results of flow cytometric analysis of the phenotype of the responding populations for each animal are shown in Table 4.3. There were no obvious differences between the responses of the immune and naive twin; in both animals, γ/δ T cells formed the largest proportion of the blast cell population after 5 days in culture. In both animals, the percentage of $CD8^+$ T cells in the total population was also expanded at day 5, and a small increase in the proportion of $CD4^+$ T cells was also found. Two-colour immunofluorescent staining of the $CD8^+$ subpopulation during the response of the immune twin also gave results very similar to those found in the naive twin (see Figure 4.3). Thus, at the level of the phenotype of the responding cells, it was not possible to distinguish between the responses of the PBMC from immune and naive twins following stimulation *in vitro* with a *T. parva*-infected cell line.

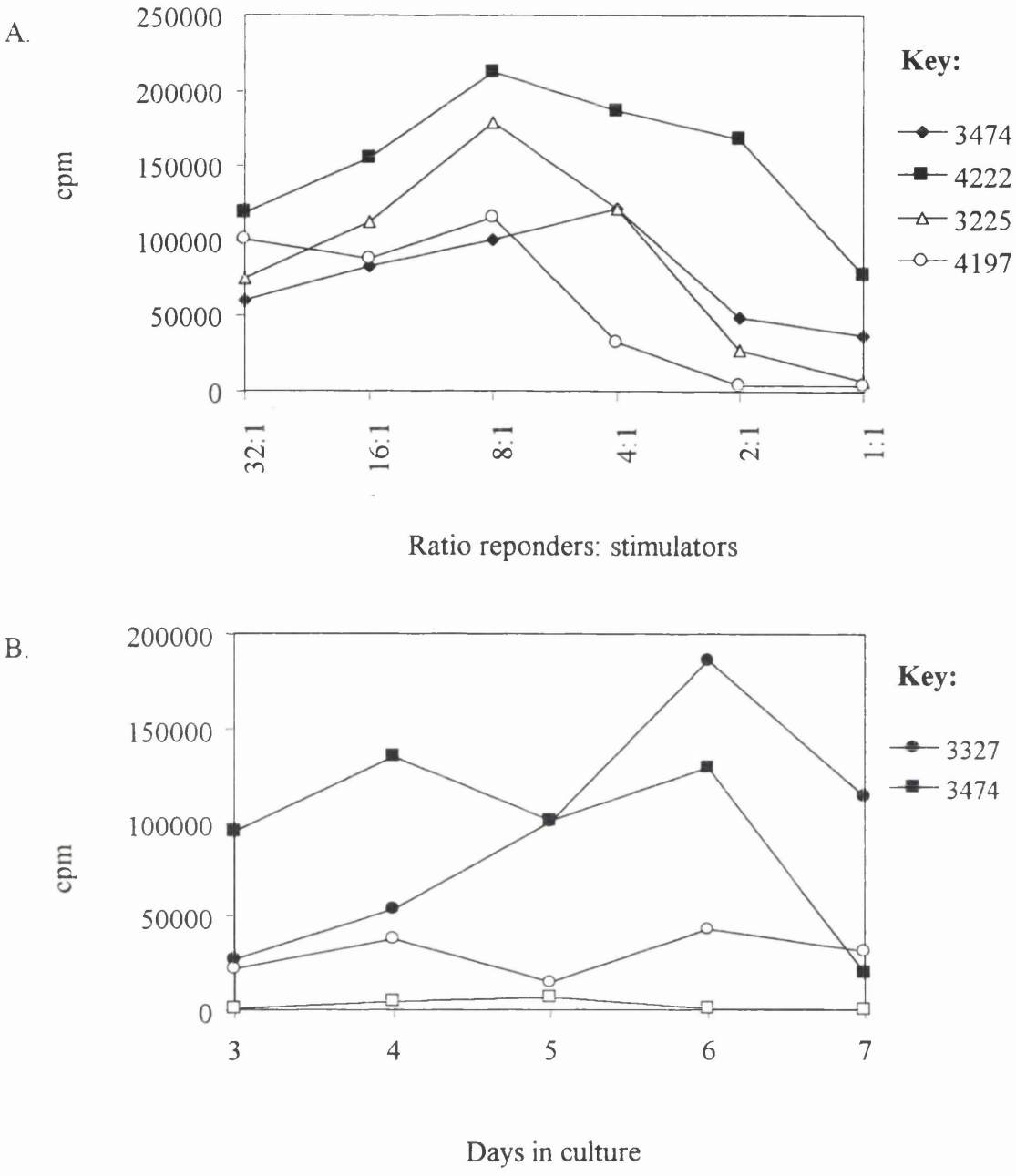

Figure 4.1. Kinetics of the autologous *Theileria* mixed leucocyte reaction. Proliferation was assessed by the incorporation of tritiated thymidine, and values are expressed as counts per minute (cpm) and represent the mean of duplicate or triplicate cultures. A: the effect of varying the ratio of responder cells (PBMC) to stimulator cells (irradiated autologous *T. parva*-infected cells) was measured for 4 animals (3474, 4222, 3225, 4197) after 5 days in culture. The background counts for PBMC cultured alone were 2095, 540, 7732, and 6058 cpm, respectively. B: the magnitude of the proliferative response was measured for 2 animals from day 3 to day 7 of culture. PBMC from 3474 and 3327 were cultured at responder:stimulator ratios of 8:1 and 16:1 respectively (closed symbols). The background counts for PBMC cultured alone are also shown (open symbols).

Table 4.2. Phenotype of parasitized cell lines used as stimulators in the autologous *Theileria* MLR.

Calf number / Phenotype	3225	4197
CD3	+	+
CD4	+/-	+
CD8	+/-	+
SIg	-	-
WC1	-	-

Notes: + = majority of cells in the cell line were positive for this marker; +/- = distinct populations of positive and negative cells; - = majority of cells were negative for this marker.

Table 4.3. Changes in leucocyte subpopulations following culture of PBMC with autologous *T. parva*-infected cells.

Calf number	3225			4197			4198		
	Day 0	Day 5		Day 0	Day 5		Day 0	Day 5	
Phenotype	Total (%)	Total (%)	FSC^{hi} (%)	Total (%)	Total (%)	FSC^{hi} (%)	Total (%)	Total (%)	FSC^{hi} (%)
CD2	46	36	37	29	48	58	30	43	54
CD3	54	88	82	56	89	76	62	87	74
CD4	20	13	9	20	22	28	14	15	18
CD8	20	19	23	6	23	28	11	24	30
γ/δTCR	26	66	66	31	54	42	ND	57	45
WC1	17	58	59	28	47	40	36	47	39
B cells	34	13	16	21	5	5	23	10	14
Monocytes	12	<1	<1	31	<1	<1	16	<1	<1

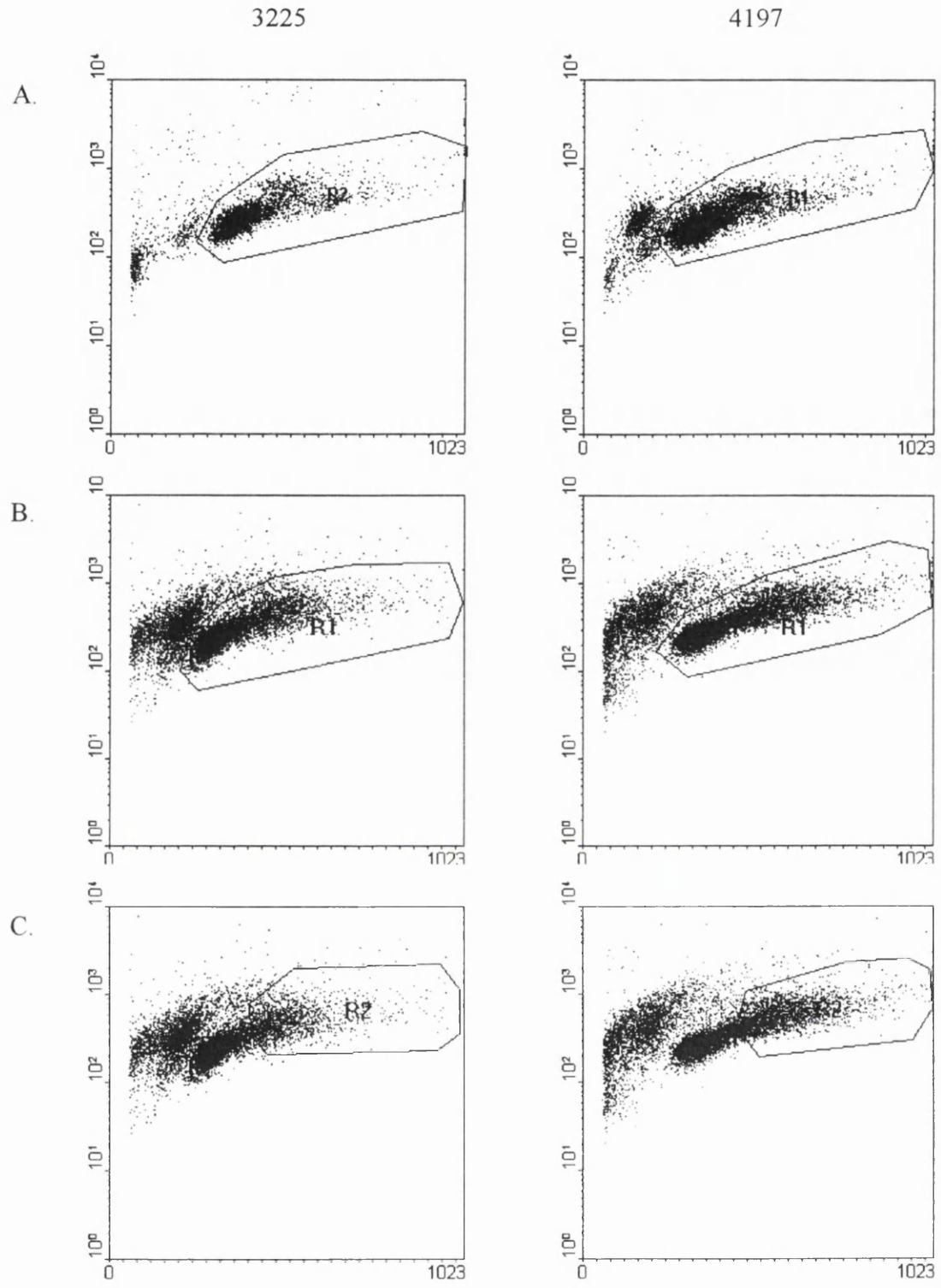

Figure 4.2. Gates set for flow cytometric analysis of responding cells in the autologous *Theileria* mixed leucocyte reaction. PBMC isolated from animals 3225 and 4197 were cultured with irradiated (50 Grays) autologous parasitized cells at a responder:stimulator ratio of 10:1. After 5 days, the viable cells were separated by density gradient centrifugation, stained with monoclonal antibodies and analysed on a FACScan (Becton Dickinson). The dot-plots show forward light scatter (x-axis) against side scatter (y-axis). Gates for analysis were set by comparison with day 0 PBMC (A) to focus either on the entire population of viable lymphocytes (B) or on cells with high forward scatter (FSC^{hi} – C), which comprise mainly blast cells.

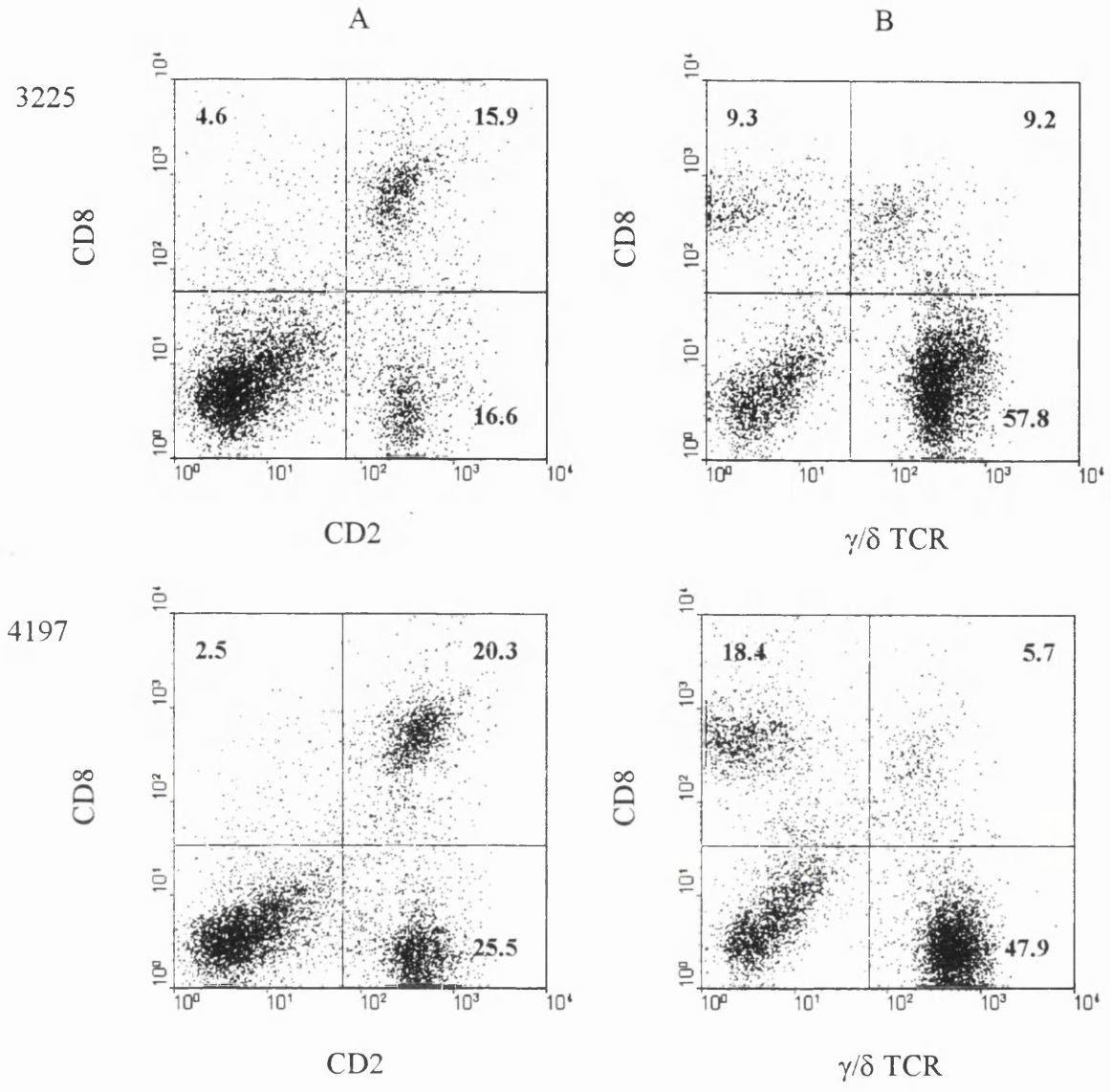

Figure 4.3. Two-colour immunofluorescent staining of $CD8^+$ T cells in the autologous *Theileria* mixed leucocyte reaction. PBMC from animals 3225 and 4197 were cultured for 5 days in the presence of irradiated (50 Gy) autologous parasitized cells at a responder: stimulator ratio of 10:1. The viable cells were separated by density gradient centrifugation and stained with either CC42 (CD2; IgG1) or GB21A (γ/δ TCR; $IgG2_b$) in combination with CC63 (CD8; $IgG2_a$). The secondary mAbs were fluorescein isothiocyanate (FITC)-conjugated goat anti-mouse IgG1 or FITC-conjugated goat anti-mouse $IgG2_b$ with phycoerythrin (PE)-conjugated goat anti-mouse $IgG2_a$. The samples were analysed on a FACScan (Becton Dickinson). The dot-plots show the patterns of staining for cells falling within the gate set on the total live cell population (see Figure 4.2.A). The $CD8^+$ cells are shown on the y-axes and the $CD2^+$ cells (A) and γ/δ TCR^+ cells (B) on the x-axes. The figures on the dot-plots are the percentages of gated cells that fall within each quadrant.

4.3.3. Effect of different *T. parva*-infected stimulator populations on the phenotype of responding cells.

The continuous growth of *T. parva*-infected cell lines *in vitro* probably involves the selective outgrowth of the most rapidly proliferating cells and, following numerous passages, the phenotype of the cells may be significantly different from that of freshly infected lymphocytes. To investigate whether the nature of the stimulator cell population can influence the *in vitro* response to *T. parva*, the phenotype of cells responding either to freshly infected PBMC or to established cell lines was compared. PBMC from two naive animals (AT113 and AT107) were incubated with large numbers of sporozoites prepared from infected tick salivary glands, as described in Section 2.2.4.2. The cell cultures were examined microscopically every day until a significant blast population was observed (after 3 days), indicating that the infected cells were undergoing transformation and beginning to proliferate. The cells were harvested, irradiated and used as stimulators in autologous *Theileria* MLC, while parallel cultures were set up using established *T. parva*-infected cell lines from the same animals as stimulators. For simplicity, the freshly-infected PBMC and the established cell lines are referred to as stimulator populations A and B, respectively.

The phenotype of the stimulator populations was determined using a panel of monoclonal antibodies to CD2, CD3, CD4, CD8, γ/δTCR, surface Ig, and the monocyte marker recognized by IL-A24. The results are shown in Table 4.4. For both animals, the phenotypes of the stimulator cells were quite different. In freshly-infected PBMC from both individuals, all the major lymphocyte subsets were represented among the blasting (infected) cell population, including B cells and γ/δ T cells. The long-term parasitized cell line established from AT107 was negative for all the leucocyte differentiation antigens, apart from small numbers of cells expressing very low levels of surface Ig and the monocyte marker. This phenotype is found in cell lines derived from infected B lymphocytes, but is unusual in bulk cell lines derived from unfractionated PBMC. The majority of cells in the parasitized line established from AT113 expressed the T cell markers CD2, CD3 and CD4.

Despite the differences in the phenotypes of the stimulator populations, the responses they provoked in autologous PBMC were remarkably similar. As shown in Table 4.5, the response of PBMC from AT113 and AT107 to both stimulator populations was dominated by γ/δ T cells, which constituted at least 45% of the total viable population after 5 days in culture. In addition, γ/δ T cells were enriched in the blast cell population (high FSC) of three of the four cultures, the proportion being approximately 10% greater than in the total population in cultures stimulated with AT107A, AT113A and AT113B. Increases in the percentage of $CD8^+$ T cells in the total and blast cell populations were most marked in the cultures stimulated with freshly infected PBMC. In cultures stimulated with AT107A and AT113A, $CD8^+$ T cells were expanded from 16% of PBMC in both animals at day 0 to 36% and 22%, respectively, of the total viable cell population at day 5. $CD8^+$ T cells were also enriched in the blast cell populations of these cultures, forming 51% (AT107A) and 28% (AT113A) of blasts at day 5. The percentage of $CD4^+$ T cells in the total population was decreased after 5 days in culture in comparison to the starting population; however $CD4^+$ T cells formed a significant proportion (34%) of the blast cell population in the culture stimulated with AT107B.

As in the previous experiments, two-colour flow cytometric analysis of the $CD8^+$ T cells in these cultures provided no evidence for the involvement of $CD2^-CD8^+$ α/β T cells in the *in vitro* response of PBMC to *T. parva*. The results are illustrated in Figure 4.4. For both animals, regardless of the stimulator population used, all $CD8^+$ T cells in the responding populations also expressed CD2. Expression of CD2 and CD8 on γ/δTCR^+ cells was also examined (Figure 4.5). CD2 was expressed on approximately 40% of γ/δ TCR^+ cells in resting PBMC from both animals, while CD8 was expressed on 30% and 20% of γ/δTCR^+ cells from AT107 and AT113, respectively. Increased percentages of γ/δTCR^+CD2^+ and γ/δTCR^+CD8^+ cells were found in the total viable cell populations of day 5 cultures, as would be expected from the general increase in the proportion of γ/δ T cells. The percentages of these subsets were higher in the blast cell populations than in the total population in all cultures except that stimulated by AT113A. In all cases, the proportion of γ/δ T cells co-expressing CD2 exceeded the proportion that co-expressed CD8.

Table 4.4. The phenotype of *T. parva*-infected cell populations used to stimulate PBMC from AT107 and AT113.

Calf number	AT107		AT113	
Stimulator population	A	B	A	B
Phenotype	(%)	(%)	(%)	(%)
CD2	56	0	59	91
CD3	64	0	65	90
CD4	32	0	42	75
CD8	12	0	11	1
γ/δTCR	10	0	7	0
Surface Ig	23	1	27	0
Monocytes	7	7	5	0

Table 4.5. Effect of different stimulator populations on the phenotype of responding cells in the autologous *Theileria* MLR.

Calf number	AT107					AT113				
Stimulator population	Day 0	Day 5 -A		Day 5 - B		Day 0	Day 5 -A		Day 5 -B	
Phenotype	(%)	Total (%)	FSC^{hi} (%)	Total (%)	FSC^{hi} (%)	(%)	Total (%)	FSC^{hi} (%)	Total (%)	FSC^{hi} (%)
CD2	59	53	62	41	60	55	55	58	49	48
CD3	56	75	85	83	90	61	84	85	82	78
CD4	28	11	15	19	34	33	16	14	20	20
CD8	16	36	51	15	20	16	22	28	17	20
γ/δTCR	24	45	53	58	58	14	58	67	50	60
Surface Ig	21	10	10	7	8	14	9	10	13	17
Monocyte	5	2	4	1	1	13	2	3	3	5

Notes: PBMC from AT107 and AT113 were cultured with two different stimulator cell populations; recently-infected PBMC (stimulator population A) or *T. parva*-infected cell lines after multiple passages (stimulator population B).

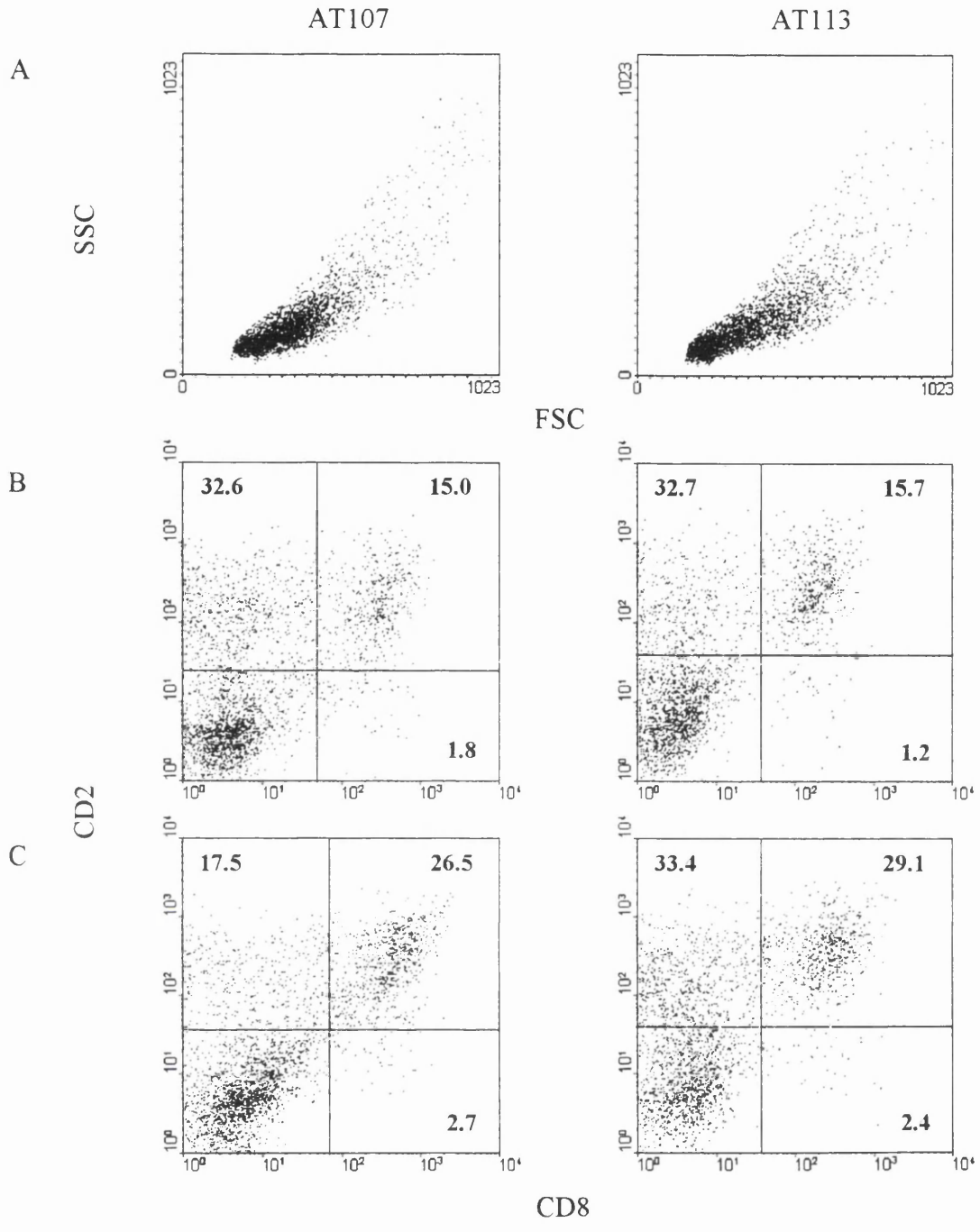

Figure 4.4. Two-colour immunofluorescent staining for CD2 and CD8 on responding cells in the autologous Theileria MLR. PBMC from animals AT107 and AT113 were cultured for 5 days in the presence of two different stimulator cell populations; an established autologous parasitized cell line (B) or PBMC infected three days previously with *T. parva* sporozoites (C). Cells harvested from the cultures were stained with the mAbs CC42 (CD2; IgG1) and CC63 (CD8; IgG2a) followed by phycoerythrin (PE)-conjugated goat anti-mouse IgG1 and fluorescein-isothiocyanate (FITC)-conjugated goat anti-mouse $IgG2_a$, and analysed on a FACScan. Gates were set on the live cells as they were analysed, and the gated populations are illustrated in A. The dot-plots show the pattern of staining for CD2 (y-axes) and CD8 (x-axes) within these populations. The percentages of cells that fall within each quadrant are shown.

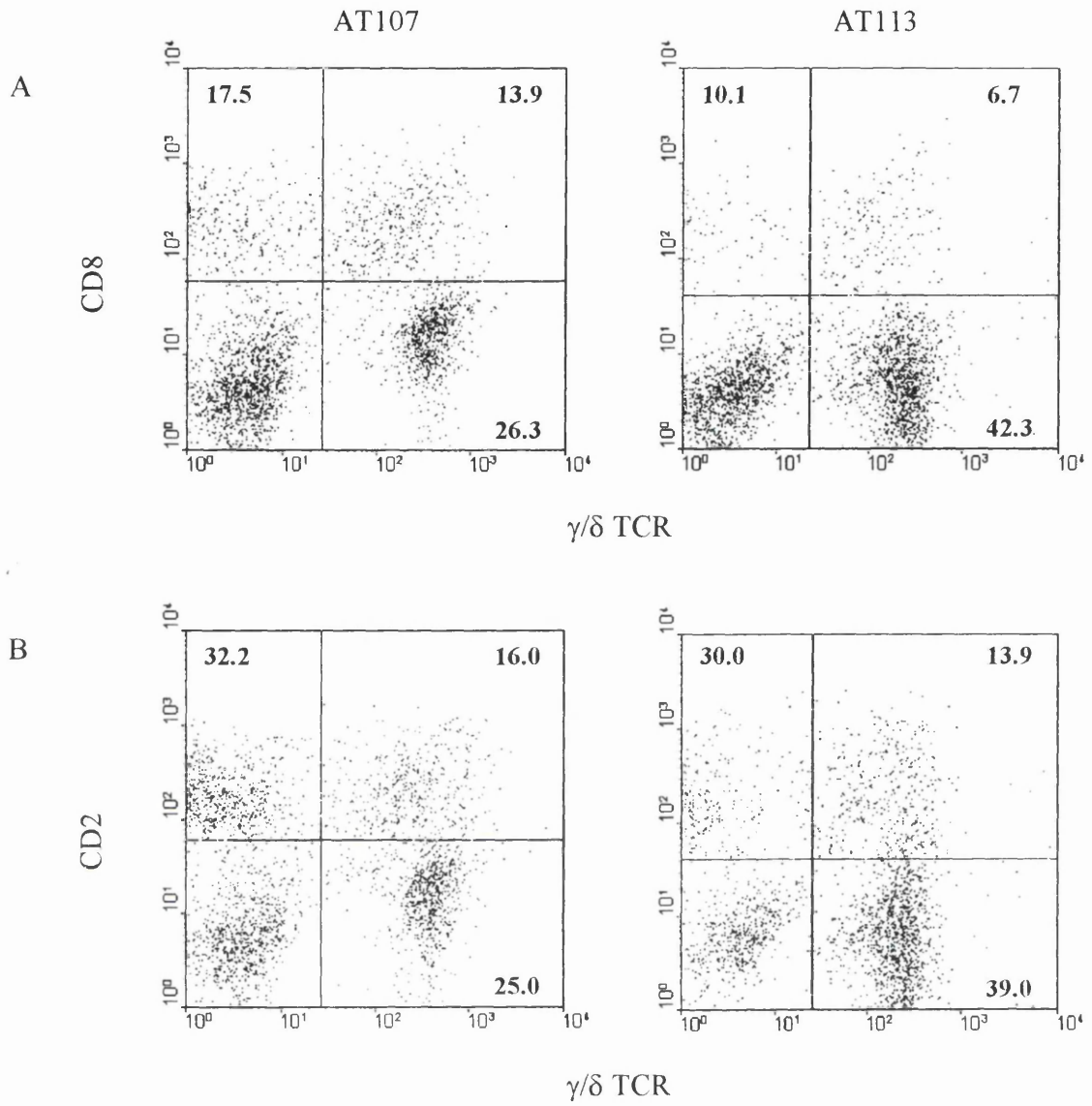

Figure 4.5. Two-colour immunofluorescent staining of γ/δ T cells in the autologous *Theileria* MLR. The cultures were set up as described in the legend to Figure 4.4. Acutely infected autologous PBMC were used as the stimulator cells for AT107, and an established autologous parasitized cell line provided the stimulator dells for AT113. Cells harvested from the cultures were stained either with CH128A (CD2; IgG1) or IL-A51 (CD8; IgG1) in combination with GB21A (γ/δ TCR; $IgG2_b$). The secondary mAbs were fluorescein isothiocyanate (FITC)-conjugated goat anti-mouse $IgG2_b$ and phycoerythrin (PE)-conjugated goat anti-mouse IgG1. The samples were analysed on a FACScan and live cells were gated for analysis as illustrated in Figure 4.4. The dot-plots show the pattern of staining of CD8 (A) and CD2 (B) (y-axes) on γ/δ TCR^+ cells (x-axes). The percentages of cells falling within each quadrant are shown on the dot-plots.

4.3.4. Phenotype of lymph node cells responding to mitogenic stimulation.

One possible explanation for the failure to observe expansion of $CD2^-CD8^+$ α/β T cells during the *in vitro* response to *T. parva* may be that the precursors of this subset are not found in peripheral blood, but are localized in the lymph nodes. To investigate this possibility, mononuclear leucocytes isolated from the prescapular lymph node of a healthy calf were cultured in the presence of different mitogens. The stimuli used were Concanavalin A (ConA), pokeweed mitogen (PWM) and phorbol myristate acetate in combination with ionomycin (PMA/iono). The phenotypes of the total viable cell populations after 3 days in culture are shown in Table 4.6. With each of the stimuli, the vast majority of cells in the cultures at this stage were T cells, predominantly $CD4^+$ and $CD8^+$ α/β T cells. γ/δ T cells were also expanded at day 3, but did not exceed 17% of the total population in any of the cultures. $CD2^-CD8^+$ T cells were not found in lymph node cells before stimulation; however, a very small percentage of cells (1-3%) with this phenotype were detected in cultures stimulated with all three mitogens, as shown in Table 4.6. These could be equivalent to the subset observed in the drainage lymph node during the *in vivo* response to *T. parva* but, lacking a parasite-specific stimulus, they may not be expanded to the same extent. However, the possibility that they are $\gamma/\delta TCR^+CD2^-$ $CD8^+$ cells cannot be excluded without three-colour cytofluorometric analysis. Unfortunately, an autologous *T. parva*-infected cell line was not available for this animal, so the effect of stimulation with parasitized cells could not be assessed.

Table 4.6. Phenotype of lymph node cells responding to stimulation with various mitogens.

Phenotype	Day 0 (%)	Day 3 (%)		
		ConA	PWM	PMA/iono
CD2	75	83	88	84
CD3	78	92	88	86
CD4	45	49	47	42
CD8	25	39	42	44
γ/δTCR	9	17	10	17
CD21	23	16	15	5
Monocyte	6	7	5	2
$CD2^-CD8^+$	0	1	2	3
$\gamma/\delta TCR^+CD8^+$	5	9	6	12

4.4. Discussion.

The results presented in this chapter show that, following in *vitro* stimulation of PBMC from naive cattle with autologous *T. parva*-infected cell lines, a large percentage of the responding population were γ/δ T cells. This was a consistent finding, regardless of the phenotype of the stimulator cells. Although $CD8^+$ T cells were also moderately expanded in the cultures, there was no evidence for the emergence of the $CD2^-CD8^+$ α/β T cell subset found during the *in vivo* response to *T. parva*.

A similar response was observed when PBMC from unexposed cattle were cultured with cell lines infected with *Theileria annulata* (Collins *et al.*, 1996). The majority of the responding population after five days in culture was γ/δ T cells. $CD8^+$ T cells also formed a significant proportion of the blasting population, but the percentage of responding $CD4^+$ T cells was low, in contrast to the present study, where in some cases $CD4^+$ T cells formed 20% or more of the blast cell population. However, highly purified γ/δ T cells could not respond to *T. annulata*-infected cells in the absence of exogenous IL-2, suggesting that cooperation with $CD4^+$ T cells may be necessary for this response to occur. Strong *in vitro* proliferative responses of PBMC from naive individuals to other parasites, including *Plasmodium falciparum* (Jones *et al.*, 1990), *Trypanosoma cruzi* (Piuvezam *et al.*, 1993) and *Borrelia burgdorferi* (Roessner *et al.*, 1994), have also been reported. The response of human PBMC to *P. falciparum* has been studied in some detail. Responding cells from individuals not previously exposed to malaria are confined to the subset of PBMC that express CD45RO, a cell surface marker associated with memory cells (Jones *et al.*, 1990; Currier *et al.*, 1992). The strong proliferative response is thought to be due to activation of cross-reactive memory T cells which have arisen as a result of exposure to environmental organisms (Currier *et al.*, 1995). However, γ/δ T cells bearing the Vγ9/Vδ2 TCR also form a substantial proportion of the responding population (Goodier *et al.*, 1992; Behr and Dubois, 1992). The response of the γ/δ T cells is dependent on the presence of $CD4^+$ T cells, but this requirement can be overcome by addition of exogenous IL-2, IL-4 or IL-5 (Elloso *et al.*, 1996). Thus the *in vitro* response of human PBMC to *P. falciparum*-infected erythrocytes shares some similiarities with the response of bovine PBMC to *T. annulata* (Collins *et al.*, 1996). The

nature of the stimulatory component(s) of these parasites for γ/δ T cells has not yet been identified. Reported ligands for the γ/δ TCR include classical and non-classical MHC class I and class II molecules (Kronenberg, 1994). However, human Vγ9/Vδ2TCR$^+$ cells that respond to mycobacteria have been shown to be stimulated by low molecular weight non-peptide ligands independently of MHC molecules. The most potent of these molecules are phosphorylated thymidine- and uridine-containing compounds and prenyl pyrophosphate derivatives e.g. isopentenyl pyrophosphate (Porcelli *et al.*, 1996).

In one experiment, PBMC from a pair of MHC-identical twins, one of which had been immunized against *T. parva*, were stimulated with a parasitized line derived from animal 4197. The responses were indistinguishable based on the phenotype of the responding cells, with γ/δ T cells forming the majority of the blast cell population in the immune as well as the naive animal. The effector function of the responding cells was not examined in the present study; however it has previously been established that repeated stimulation of PBMC from immune animals results in enrichment of MHC class I restricted CD8$^+$ cytotoxic T cells and MHC class II restricted CD4$^+$ T cells with specificity for parasite antigens (Goddeeris *et al.*, 1986a; Baldwin *et al.*, 1987). In contrast, the levels of cytotoxicity generated in PBMC from naive cattle were lower and the effectors were not MHC restricted. In some instances, no cytotoxic activity was observed or the culture failed to proliferate following the primary stimulation (Goddeeris *et al.*, 1986a). Thus, although in the present study the cultures from immune and naive animals were phenotypically identical after primary stimulation, these previous studies indicate that they differ at the functional level. The enhancement of MHC class I restricted cytotoxicity following repeated stimulation of immune PBMC may reflect selective outgrowth of parasite-specific CD8$^+$ T cells at the expense of the γ/δ T cells.

The potent proliferative response of PBMC to stimulation with *T. parva*-infected cells *in vitro* clearly does not reflect the processes leading to widespread lymphocyte activation in the drainage lymph nodes of infected cattle. Although there was a small increase in the proportion of γ/δ T cells between days 8 and 12 of infection in some animals, they did not form the majority of the responding population as they did in the *in vitro* cultures. Also, the CD2$^-$CD8$^+$ α/β T cell subset that was consistently found among the responding

population *in vivo* did not appear in the *in vitro* cultures. There are several possible reasons for these differences. Under *in vitro* culture conditions, the bovine γ/δ T cells may have an increased sensitivity to activation signals. The majority of γ/δ T cells in the peripheral blood of cattle and sheep express WC1, a polymorphic glycoprotein that belongs to a family of molecules which includes the macrophage type 1 scavenger receptor, CD5 and CD6 (Wijngaard *et al.*, 1992,1994). The function of this molecule *in vivo* is unknown; however, recent studies have demonstrated that mAbs to WC1 inhibit the proliferation of ovine and bovine IL-2-dependent γ/δ T cell lines *in vitro*, causing cell cycle arrest in G0/G1 phase. The growth arrest could be reversed by signalling through the TCR in the presence of IL-2 (Takamatsu *et al.*, 1997). In view of these findings *in vitro*, it is tempting to speculate that, *in vivo*, WC1 may function to inhibit non-specific activation of γ/δ T cells. The ligand for WC1 *in vivo* has not been identified; however, if the ligand were absent under *in vitro* culture conditions, the removal of inhibition might result in increased sensitivity of γ/δ T cells to non-specific stimuli. The failure to activate $CD2^{-}CD8^{+}$ T cells during *in vitro* stimulation may reflect a lack of precursors for these cells in peripheral blood. However, when mononuclear leucocytes isolated from a peripheral lymph node were stimulated *in vitro* with a number of different mitogens, only very low numbers of $CD2^{-}CD8^{+}$ (2-3%) cells were found among the responding cells. This may reflect the need for a parasite-specific stimulus to preferentially activate or expand this particular cell type.

Another possible reason for the differences observed between the *in vitro* and *in vivo* responses may occur at the level of the antigen presenting cells, and cell-cell interactions involved in the initiation of the responses. Following infection with *T. parva*, lymphocytes undergo a number of phenotypic changes; T lymphocytes acquire expression of MHC class II molecules, B lymphocytes modulate surface expression of immunoglobulin and both subsets upregulate molecules associated with activated T cells (Naessens *et al.*, 1985; Baldwin *et al.*, 1988). Parasitized cell lines maintained *in vitro* secrete IFNγ and low levels of IL-2 (Brown and Logan, 1986; Entrican *et al.*, 1991) and express mRNA for various cytokines, including IL-2, IL-6, IL-10, IFNγ, and TNFα (Heussler *et al.*, 1992; McKeever *et al.*, 1997). In humans, activated T cells have been shown to express costimulatory molecules such as B7 (CD80/CD86) and are capable of

presenting antigen to other T cells (Lanzavecchia *et al.*, 1988; Azuma *et al.*, 1993b). Thus in autologous *Theileria* mixed lymphocyte cultures, parasite antigens may be presented by the parasitized cells themselves or by monocytes present in PBMC. However, continuously growing cell lines represent the outgrowth of the most rapidly proliferating cells and thus may become modified during prolonged culture *in vitro*, so that they differ in their stimulatory properties from the parasitized cells responsible for initiating the primary immune response *in vivo*. Indeed, susceptible cattle infected with autologous parasitized cell lines after multiple passages *in vitro*, show mild or inapparent clinical reactions indicating that prolonged culture produces changes that result in reduced pathogenicity of the infected cells (Morrison *et al.*, 1996). For this reason, PBMC from naive cattle were stimulated with freshly infected lymphocytes, which is more likely to reflect the situation *in vivo* if such cells were responsible for initiating the lymph node response. The responses were indistinguishable from those provoked by long-term parasitized cell lines, suggesting that the differences between the *in vitro* and *in vivo* responses do not simply reflect modification of the cultured stimulator cells, but that signals or cytokines from other cell types in the lymph node environment are not being provided *in vitro*.

Although cells expressing MHC class II molecules, including B cells, macrophages and dendritic cells, can all function as accessory cells during T cell activation, a number of studies have indicated that dendritic cells may be the major antigen-presenting cell involved in initiating responses of naive resting T cells (Inaba *et al.*, 1990). *In vitro* studies of the cellular targets for *T. parva* infections have shown that parasitized cell lines can be established from purified populations of B lymphocytes and both γ/δ and α/β T lymphocytes, but not monocytes (Baldwin *et al.*, 1988). However there is evidence that both macrophages and afferent lymph veiled cells (equivalent to dendritic cells) can be infected by sporozoites *in vitro* but do not become "transformed" i.e. undergo continuous replication, perhaps because they are not permissive for parasite differentiation (Shaw *et al.*, 1993; D. McKeever, personal communication). In addition, sporozoites are phagocytosed by macrophages (Fawcett and Stagg, 1986). However, it is not known to what extent macrophages and dendritic cells are infected *in vivo*, and whether such cells contribute to initiation of the immune response. Parasitized

lymphocytes can provide adequate signals for the activation of memory T cells, as shown by the generation of parasite-specific cytotoxic and T helper cells when PBMC from immune animals are stimulated *in vitro* with autologous infected cell lines (Goddeeris *et al.*, 1986a; Baldwin *et al.*, 1987). They are also capable of inducing T cell proliferative responses in PBMC from naive animals, although CTLs are not generated, perhaps due to the low frequency of precursors (Goddeeris and Morrison, 1987). Thus it is reasonable to assume that schizont-infected lymphocytes can also function as antigen-presenting cells *in vivo*. However, they may not provide appropriate stimuli for activation of parasite-specific effector function in naive T cells. This could be due to lack of co-stimulatory function and/or secretion of appropriate cytokines. For example, it has been demonstrated in mice that presentation of antigen by either resting or activated B cells induces tolerance in naive T cells, but results in activation of memory T cells (Fuchs and Matzinger, 1992).

In summary, *in vitro* stimulation of PBMC with *T. parva*-infected cell lines produces a responding population which is phenotypically distinct from the blast cell population in the drainage lymph node during the primary *in vivo* response. The inability to detect $CD2^{-}CD8^{+}$ T cells among the responding population *in vitro* prohibited further studies to determine the stimulatory requirements and function of these cells *in vitro*. In future work, it would be useful to investigate which cells are responsible for initiation of the immune response *in vivo*. Further *in vitro* studies using lymph node cells rather than PBMC may yield more information about the $CD2^{-}CD8^{+}$ subset.

CHAPTER FIVE

CLONING, SEQUENCING AND CLASSIFICATION OF BOVINE *TCRBV* GENES.

5.1. Introduction.

The T cell antigen receptor consists of a polymorphic, disulphide-linked heterodimer associated with a complex of invariant CD3 molecules. The function of the heterodimer is antigen recognition, while the components of CD3 are involved in signal transduction. The α and β (or γ and δ) chains that make up the heterodimer are encoded by separate variable (*V*), diversity (*D* - β and δ chains only), joining (*J*) and constant (*C*) gene segments which are assembled by somatic recombination, as for immunoglobulin heavy and light chains, during T cell differentiation. The V regions of the TCR polypeptides contain three regions of relatively greater variability which correspond to immunoglobulin hypervariable regions (complementarity determining regions or CDRs), and which are brought together by protein folding and V domain packing to form the site which interacts with antigenic peptides bound to MHC molecules. Compared to immunoglobulins, the number of different *AV* and *BV* genes used by the TCR is relatively small; however, there is potential for enormous diversity in the junctional region comprising CDR3. Various models of the interactions between the α/β TCR and peptide/MHC complexes predicted that CDR1 and CDR2 of Vα and Vβ would contact residues on the α_1 and α_2 domains of the MHC molecule, while the CDR3 loops would interact with the bound peptide (Davis and Bjorkman, 1988; Chothia *et al.*, 1988). This model has recently been confirmed by structural analysis of a crystallized ternary complex of TCR, MHC class I molecule and peptide (Garcia *et al.*, 1996).

The specificity of the TCRs on T cells is determined by the combination of Vα and Vβ elements. Studies with T cell clones that react with a defined peptide/MHC combination have shown that in some cases the TCRs express a limited repertoire of *V* and *J* gene segments and restricted junctional sequences (Hedrick *et al.*, 1988; Moss *et al.*, 1991), while in others a diverse repertoire of *TCRV* and *J* genes are used, with no apparent

conservation of junctional sequences (Taylor *et al.*, 1990; Casanova *et al.*, 1991). In contrast, T cell responses to superantigens are characterized by polyclonal activation of T cells bearing a restricted subset of Vβ elements and diverse junctional sequences, irrespective of the paired Vα domain or the MHC molecule involved in antigen presentation (Kappler *et al.*, 1989; Mollick *et al.*, 1989). The explanation for this is that superantigens are not degraded into peptide fragments which are presented in the antigen-binding groove of MHC molecules (Yagi *et al.*, 1988); instead, they bind directly to a number of different MHC class II molecules, and make contact only with residues on the solvent-exposed lateral face of the TCR Vβ domain (Scholl *et al.*, 1989; Choi *et al.*, 1990a).

One of the major aims of this project was to examine the repertoire of *TCRBV* genes expressed by T cells participating in the primary immune response to *Theileria parva* infection in cattle, to determine whether a superantigen could be driving the response. The Vβ-specific expansion of T cells without clonal restriction or conserved CDR3 motifs, in individuals of differing MHC phenotypes, is evidence of stimulation by a superantigen.

The extent of the bovine *TCRBV* repertoire has not yet been determined. In mice and humans, the repertoire of *TCRBV* gene segments was predicted to be limited in comparison to that of immunoglobulins, based on the numbers of sequences isolated from cDNA libraries and the number of bands hybridizing to *BV*-specific probes in Southern blots of genomic DNA (Barth *et al.*, 1985; Behlke *et al.*, 1985; Kimura *et al.*, 1987). Mapping and sequencing of germline *BV* segments has confirmed that previous estimates of the size of the repertoire were accurate. In humans, 65 unique *TCRBV* gene segments have been identified following sequencing of the entire *TCRB* locus, of which 46 appear to be functional (Rowen *et al.*, 1996). Based on the requirement of greater than 75% nucleotide sequence homology for cross-hybridization, *BV* sequences have been divided into subfamilies of sequences that share greater that 75% identity at the nucleotide level. In humans, thirty-four subfamilies have been defined, of which twenty-four contain functional gene segments, while in the mouse, twenty-five subfamilies have been identified at the genomic level but only twenty contain functional *TCRBV* genes.

Several of the human *TCRBV* subfamilies contain multiple members, but most of the murine *TCRBV* subfamilies have only a single member. In both species, the *V* gene segments show limited polymorphism, with alleles usually differing by less than five nucleotides (Arden *et al.*, 1995a,b).

Tanaka *et al.* (1990) identified twelve distinct *TCRBV* sequences in clones from a cDNA library derived from bovine PBMC. They classified the sequences into nine subfamilies, each of which was shown to have significant homology at the nucleotide and protein level to representative human *TCRBV* subfamily members. They were unable to demonstrate *BV*-associated polymorphisms in Southern blot analysis of genomic DNA; in addition, they reported that a limited number of bands were detected on the blots with each *BV*-specific probe, suggesting that each bovine *TCRBV* subfamily contains relatively few members.

To facilitate interpretation of the pattern of *TCRBV* gene usage found in T cells responding to *T. parva*, it was important initially to establish the frequency with which different *TCRBV* subfamilies were expressed in normal individuals. In the absence of monoclonal antibodies to specific bovine TCR Vβ regions, examination of the expression of *TCRBV* genes was feasible only at the mRNA level. As sequence data for only nine bovine *TCRBV* subfamilies was available, the approach used for repertoire analysis was to amplify all *TCRBV* cDNA transcripts by anchored PCR. This technique permits amplification all the *TCRBV* genes expressed by the T cell population, including those for which the sequences are unknown, using a single pair of primers. This approach has previously been used in several studies of the human TCR repertoire, in which many new *V* gene segments were identified (Robinson, 1991; Plaza *et al.*, 1991; Ferradini *et al.*, 1991). In this chapter, the sequences of cDNA clones derived by this technique are analysed and classified into different *TCRBV* subfamilies.

5.2. Materials and Methods.

5.2.1. Cellular sources of RNA.

To provide material for analysis of the normal T cell receptor repertoire of peripheral lymph nodes, a prefemoral lymph node was surgically removed from one experimental animal (calf 3327). The mononuclear leucocytes were isolated from the lymph node as described in Section 2.2.1.3, and used to prepare total RNA without further fractionation. The same animal was later infected with *Theileria parva*, as described previously, and a prescapular lymph node draining the site of inoculation was removed after euthanasia on day 9 of infection. Mononuclear leucocytes isolated from the lymph node of the infected calf by density gradient centrifugation were stained with monoclonal antibodies to CD3 (MM1A) and MHC class II (IL-A21) for sorting on a FACStar cell sorter, using the procedure outlined in Section 2.2.3.3. To isolate activated T cells, cells were selected for sorting on the basis of their co-expression of both markers. In a subsequent experiment, $CD2^-CD8^-$ T cells were sorted from the drainage lymph node of another animal (5158) on day 9 of infection with *T. parva*, as described in Section 2.2.3.3. Briefly, the separated mononuclear leukocytes were stained with monoclonal antibodies to CD2 (IL-A43; $IgG2_a$) and CD8 (CACT80C; IgG1), and secondary goat anti-mouse $IgG2_a$-PE and goat anti-mouse IgG1-FITC antibodies. The $CD8^+$ population was enriched by staining with an anti-FITC mAb coupled to magnetic beads and separation on a MACS VS^+ Separation Column. The $CD2^-CD8^+$ subset was subsequently purified on a FACStar cell sorter. In all cases, total RNA was isolated from the lymphocyte populations using the Ultraspec RNA Isolation Kit (Biotecx) as described in Section 2.4.1.

5.2.2. Amplification and cloning of bovine *TCRBV* cDNA transcripts.

The strategy for amplification of bovine *TCRBV* sequences using the anchored PCR is illustrated in Figure 5.1. The details of the protocols are given in Section 2.4.5. Synthesis of cDNA was performed by reverse transcription of mRNA using an antisense oligonucleotide (PBC1) specific for a conserved region at the 5' end of the bovine

BC gene segments. After digestion of mRNA by RNase H, cDNA was purified to remove excess primer and dNTPs, before addition of a homopolymer tail of dC nucleotides to the 3' end of the cDNA by the enzyme terminal deoxynucleotidyl transferase (TdT). The tailed cDNA was amplified by PCR using a second *BC*-specific primer (PBC2) and an anchor primer complementary to the poly-dC tail. As a positive control to verify that *TCRBV* sequences were present after each step in the procedure, PCR amplification was also performed using the *BC*-specific primer with an internal primer (PBV2), which is complementary to a conserved region near the 5' end of the published sequences for *TCRBV2* gene segments (Tanaka *et al.*, 1990). The specificity of the primers was checked by performing an amplification reaction using cDNA prepared from a bovine γ/δ T cell line. As illustrated in Figure 5.2., a distinct band of ~350 bp (the expected size of the PCR product) was obtained when cDNA from ConA blasts was the target for amplification, whereas the primers failed to amplify any sequences from the cDNA of γ/δ T cells. The sequences of all the oligonucleotide primers are shown in Table 2.3. in Chapter 2.

The products of the anchored PCR were separated by electrophoresis on a 1% agarose gel; a band corresponding to the size expected for *TCRBV* sequences (approximately 500bp) was excised and the DNA recovered using the GENECLEAN II Kit (BIO 101), as described in Section 2.4.4.4. The purified DNA was cloned directly into the *p*CR™II plasmid vector supplied with the TA Cloning Kit (Invitrogen), products of the ligation reaction were transformed into competent *E. coli* cells (OneShot INVαF'; Invitrogen) and the bacteria were plated on LB agar containing 100μg/ml ampicillin. Details of the protocols used for cloning and transformation are given in Section 2.4.6. Large numbers of white colonies (>100) were picked from the agar plates from each transformation. These clones were grown in liquid LB medium overnight and aliquots of the cultures were stored at -70°C in 15% glycerol until required for sequence analysis. Details of the reagents and methods used for anchored PCR and cloning are given in Chapter 2. Clones derived from the two different animals, 3327 and 5158, were numbered and given the prefixes C and D respectively; clones derived from the infected lymph node of 3327 were given the prefix IC.

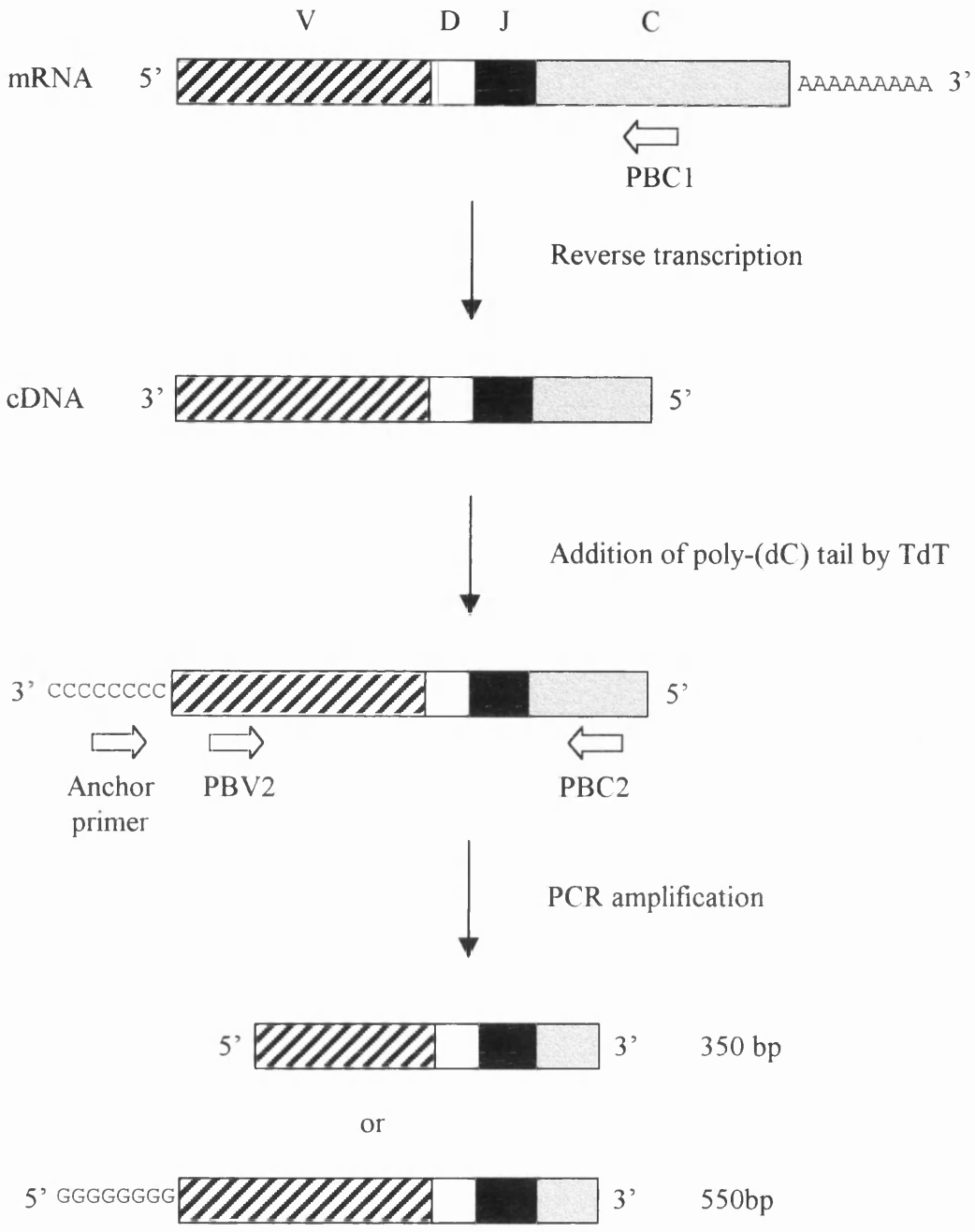

Figure 5.1. Schematic representation of the strategy used for amplification of bovine *TCRBV* sequences by anchored polymerase chain reaction (A-PCR). Reverse transcription of mRNA was primed with an oligonuleotide (PBC1) complementary to the bovine *TCRBC* genes. A poly-(dC) tail was added to the 3' end of the cDNA by terminal deoxynucleotidyl transferase (TdT). The *TCRBV* sequences were amplified with the anchor primer and a second *TCRBC*-specific primer (PBC2) to give a 550 base pair (bp) product. To check the efficiency of cDNA synthesis, amplification was also performed with PBC2 and a primer complementary to bovine *TCRBV2* genes (PBV2), to give a 350bp product.

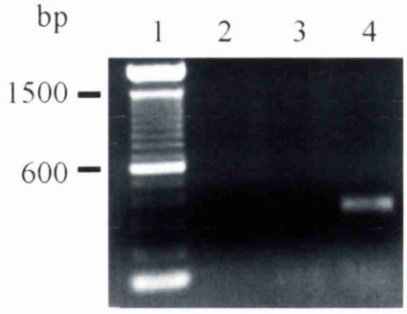

Key:

Lane 1: 100 bp DNA ladder
Lane 2: negative control; no cDNA
Lane 3: cDNA from γδ T cell line
Lane 4: cDNA from PBMC stimulated with ConA

Figure 5.2. Verification of the specificity of the internal control primer PBV2 (complementary to bovine *TCRBV2* subfamily members) for α/β T cells. cDNA prepared from a γ/δ T cell line and from Con-A stimulated PBMC were subjected to the same amplification protocol using PBV2 and the *TCRBC*-specific primer PBC2.

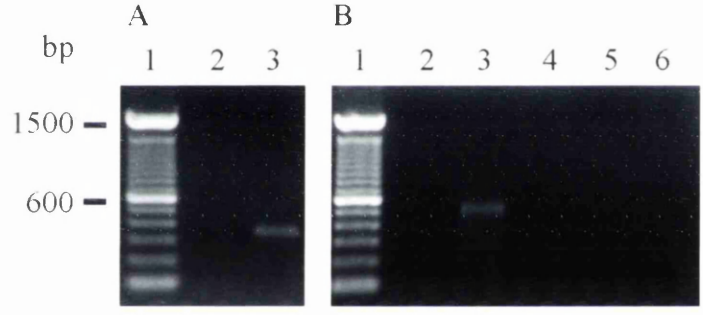

Key:

A
Lane 1: 100 bp DNA ladder
Lane 2: negative control; no cDNA
Lane 3: untailed cDNA
B
Lane 1: 100 bp DNA ladder
Lane 2: negative control; cDNA synthesis reaction without RT
Lane 3: d(C) tailed cDNA
Lane 4: negative control; tailing reaction without TdT
Lane 5: negative control; anchor primer only
Lane 6: negative control; PBC2 only

Figure 5.3.

A. Demonstration of the efficiency of reverse transcription by amplification of cDNA with the primers PBV2 and PBC2.

B. Demonstration of the specificity of the anchor primer and PBC2 for amplification of d(C)-tailed cDNA encoding bovine *TCRBV* sequences in the anchored PCR.

5.2.3. Preparation of DNA template for sequencing.

Two different methods were used to prepare plasmid DNA from bacterial clones for sequencing, as outlined in Section 2.4.7.1. However, the DNA from these preparations was not consistently of sufficiently high quality for automated cycle sequencing. Thus, most cycle sequencing reactions were performed using single stranded DNA immobilized on magnetic beads (Dynabeads®), which proved to be a reliable and efficient method for generating high quality sequencing template (see Section 2.4.7.4). The template used for sequencing reactions with Sequenase® T7 DNA polymerase was alkaline-denatured plasmid DNA prepared using Qiagen Tip 20 resin columns (see Section 2.4.7.1). Sequencing reactions and denaturing gel electrophoresis of the extension products were performed as described in Sections 2.4.8 and 2.4.9.

5.2.4. Analysis of sequence data.

Products of cycle sequencing incorporating fluorescent dye terminators were electrophoresed in a 373A DNA Sequencer (Applied Biosystems, Inc.), and the sequence data was collected on a Macintosh computer running the 373A Sequence Data Collection Programme (ABI) and analysed using the 373A Sequence Analysis Programme (ABI). Sequences were checked and edited using the Seqed or Sequence Navigator (ABI) programmes, before being transferred to the VAX 750 mainframe computer. Sequence information from reactions performed using Sequenase was read directly from autoradiographs and entered into the VAX 750 mainframe computer. The sequence data was analysed using the GAP, BESTFIT, FASTA, PILEUP and LINEUP programs from the University of Wisconsin Genetic Computing Group (GCG) package (Devereux *et al.*, 1984).

5.3. Results.

5.3.1. Amplification of *TCRBC*-specific cDNA.

5.3.1.1. Optimization of the anchored PCR.

The method which was initially adopted for amplification of *TCRBV* sequences was based on that described by Thiesen *et al.* (1990). This entailed reverse transcription of mRNA using an oligo-dT primer, addition of a poly(dG) tail by TdT and PCR amplification with a bovine *TCRBC*-specific 3' primer and a 5' primer complementary to the homopolymer tail with additional 5' sequence containing restriction sites for cloning. Solvent extraction and ethanol precipitation of the DNA was necessary after each stage in the procedure, to remove excess dNTPs and first-strand synthesis primer before the tailing reaction, and to remove the cobalt-containing TdT buffer before amplification. The considerable loss of DNA following repeated precipitation and problems with the tailing reaction resulted in failure to amplify *TCRBV* sequences using this method.

The second approach was a simplified protocol based on the 5' RACE System Kit supplied by Gibco. This system represents a considerable improvement over the original method for two major reasons. First, the requirement for repeated extraction and precipitation of the cDNA is removed by the use of GLASSMax spin columns for purification of first strand cDNA, and by performing tailing and amplification reactions in the same buffer. Second, the anchor primer is designed with selective placement of deoxyinosine residues in the 3' region to create a melting temperature (T_m) for the anchor region which is comparable to that of a typical 20-mer primer with 50% GC content. Deoxyinosine has the capacity to base pair with all four nucleotides with varying affinities, the most stable conformation being achieved by I:C pairs. This design maximizes specific priming from the poly(dC) tail, and establishes a relationship of a "balanced" T_m with that of the 3' *TCRBC*-specific primer (required for efficient PCR amplification). The improved specificity and reduced T_m of this primer removes the need for amplification with mixtures of anchor and adapter primers (complementary to the 5' region of the anchor primer), as is the case in most protocols for anchored PCR.

Some modifications of the protocol recommended by the manufacturers were necessary to obtain optimal results using the kit. Initially, problems were encountered with the tailing reaction. The magnesium concentration during this reaction is critical; concentrations of Mg^{2+} above 1.5mM inhibit the length of the tail and the percentage of molecules tailed. The supplied buffer contained magnesium chloride, and it was found that by substituting a Mg^{2+}-free buffer and adding $MgCl_2$ separately (allowing more accurate control of the Mg^{2+} concentration), a product of the expected size (500bp) could be generated by the anchored PCR. However, the efficiency of the PCR reaction was poor, and a second round of amplification with the anchor primer and a "nested" *TCRBC*-specific primer was necessary to generate sufficient DNA for cloning. Sequencing of three clones derived from this product revealed that they contained identical *BV* gene segments and junctional sequences, strongly suggesting that a bias had occurred during amplification. Subsequently, the anchored PCR was performed using a modified anchor primer synthesized at IAH, Compton, and generously supplied by Dr. Sean McCarthy. This primer had an identical 3' region (containing deoxyinosine residues) to the anchor primer supplied with the kit, but a shorter 5' region containing only one restriction site (compared with 3 restriction sites and a cloning region in the kit primer). Thus, the T_m for the whole primer is lower, resulting in more efficient PCR amplification. Using this primer, a strong band of 500bp was obtained after a single round of amplification (35 cycles), as shown in Figure 5.3. Sequencing of clones derived from this PCR product revealed a wide range of different *TCRBV* genes and diverse junctional sequences, with no obvious biases.

5.3.1.2. Analysis of the cloned inserts derived from the anchored PCR.

In initial experiments, restriction enzyme digestion of plasmid DNA followed by analysis by agarose gel electrophoresis revealed that the proportion of clones containing inserts of ~500bp was disappointingly low; only 12 of the 39 clones (31%) examined had full-length inserts. In addition, a number of clones contained inserts of approximately 300bp, although a band of this molecular weight was not observed following agarose gel electrophoresis of the PCR product. Size selection of the PCR product by excision of the 500bp band from the agarose gel and purification of the DNA prior to ligation into the *p*CR™II vector resulted in a marked reduction in the frequency of isolation of clones

without inserts. Unexpectedly, however, some clones still contained 300bp inserts, the proportion varying for different PCR reactions from 0-27%.

Sequence information was obtained from 134 clones containing full-length inserts; these clones were derived from the anchor PCR amplification of *TCRB* chain transcripts from the three different lymphocyte populations described in 5.2.1. Seventeen clones contained sequences unrelated to *TCRB* genes and have probably arisen as a result of PCR artefact. Sequencing of a small number of the shorter inserts revealed that they also contained no *TCRB* gene segments. One clone contained *TCRBC* sequence, and another contained rearranged *BJ-BC* gene segments. These are probably the result of amplification of germline sequences, or in the case of the rearranged sequence, from a *BD-BJ-BC* transcript. One clone included a full-length *TCRBV* gene segment but no *BD*, *BJ* or *BC* sequences. In three clones, truncated rearranged *TCRB* sequences including between 125bp-250bp of the *BV* gene segment were found.

The remaining 111 clones contained rearranged *TCRBV-BD-BJ-BC* transcripts. Among these sequences, nine reoccurred; (i.e., they were identical to another sequence throughout the *V-D-J* region), including three copies of one sequence, and three identical pairs. Interestingly, these duplicated sequences were found only in the clones derived from the activated T cell populations, which would be more likely to include clonally expanded T cells and hence yield more than one copy of the *V-D-J* rearrangement expressed by these cells.

5.3.2. Classification of *TCRBV* gene segments.

The clones containing rearranged *TCRB* transcripts were sequenced at least twice. Unfortunately, it proved difficult to obtain good quality sequence from the 5' end of the clones using cycle sequencing and the automated sequencer, probably because of "slippage" of the *Taq* DNA polymerase on the homopolymer dC tail. All clones were therefore sequenced in one direction (3'-5'), and in many cases this was sufficient to obtain sequence for almost the entire *TCRBV* gene segment. A number of clones representing new bovine *TCRBV* subfamilies or subfamily members were selected and

sequence from the 5' end of the *V* gene was obtained by conventional manual sequencing using Sequenase®. The extent of the leader sequence varied between clones; in some cases it was truncated while in other clones the translational start codon could be identified. Three clones contained deletions or insertions of one or more bases within the *TCRBV* sequences which caused an alteration in the reading frame of the transcript; these are probably artefacts that have arisen during the amplification or sequencing reactions.

The remaining 103 sequences were classified into *TCRBV* families by screening them for nucleotide sequence homology to bovine and human *TCRBV* sequences in the GenEMBL database, using the FASTA programme. The sequences were first edited to remove leader, *BD*, *BJ* and *BC* sequences. The 3' end of the V gene segments were assigned as three codons after the conserved cysteine residue at position 92, according to convention. Where sequences differed by no more than five nucleotide substitutions, they were considered to be products of a single gene locus. This was based on the observations of Arden *et al.* (1995a,b) who, in an extensive analysis of all published human and murine TCR sequences derived from genomic or cDNA, noted that alleles of *V* gene segments rarely differ by more than 5 nucleotides, while genes from different loci usually differ by at least 10 nucleotides. In the present study the numbers of variant sequences in each group were generally too small to distinguish whether nucleotide substitutions were genuine allelic differences or had arisen through misincorporation of nucleotides by *Taq* DNA polymerase. However, to minimize the sequence errors introduced by *Taq* DNA polymerase, consensus sequences from at least three different clones were derived, where possible, for comparison with other sequences. Sequences sharing greater than 75% identity at the nucleotide level are defined as being members of the same subfamily. Tanaka *et al.*, (1990) defined nine bovine *TCRBV* subfamilies based on comparison of cDNA sequences with their human counterparts. Their clones, which were numbered and had the prefix BTB, are referred to in the text below; the sequence comparisons leading to the classification of these clones into subfamilies are shown in Table 5.1.

Only nineteen clones contained nucleotide sequences identical or almost identical to the published bovine *TCRBV* sequences. Four clones contained sequences that were almost

identical to BTB18 (bovine *BV1*) at the nucleotide level; however, the deduced peptide sequences were only 88.6% identical. This was due to a frame-shift between bases 165 or 170 and base 191 of the nucleotide sequence which caused an alteration in the reading frame of the transcript. However, these transcripts were apparently functional, since the frame-shift did not result in the introduction of a stop codon or mutation of any functionally important conserved residues, as shown in Figure 5.4. Similarly, four clones contained sequences identical to BTB4 (bovine *BV2*) apart from a dinucleotide insertion near the 5' end of the V gene, causing a shift in the reading frame. This resulted in a divergence of the deduced peptide sequences over the first 10 amino acid residues of the V region, so that the percentage identity of the sequences was only 92.5%.

The remaining eleven clones contained sequences identical, or almost identical to BTB10 (*BV2*), BTB91 (*BV3*), BTB27 (*BV7*), BTB13 (*BV12*), BTB22 and BTB45 (both *BV15*). Some sequences differed from the published sequences by one or two nucleotides; however, it could not be established whether these differences were genuine or due to PCR error because the number of clones that matched each sequence was too low to establish consensus sequences. The two clones corresponding to BTB13 contained the entire sequence of this *V* gene; the published sequence of this clone is truncated.

5.3.2.1. New *TCRBV* subfamily members.

A large number of sequences were identified that, although different from the published bovine sequences, shared greater than 75% identity at the nucleotide level, and were classified as new subfamily members. Comparisons of the nucleotide and protein sequences of all new subfamily members to published human and bovine sequences are shown in Table 5.1.

Thirty-seven clones were classified as belonging to the bovine *BV1* subfamily, as they shared >75% nucleotide sequence similarity with BTB18, including the clones that were almost identical (see above). These sequences formed 9 groups of identical or closely related sequences and two single sequences that were distinct from these groups, as illustrated in Figure 5.4. As shown, alignment of the sequences with BTB18 results in a frameshift in each new sequence as mentioned above, suggesting that the published sequence contains an error. This will be discussed more fully later. The results of this

analysis suggest that the bovine *BV1* subfamily contains at least 11 members. The nucleotide sequences of the different subfamily members were compared to one another and the results of this analysis are presented in Table 5.2. The percentage similarity of the nucleotide sequences ranged from 79.3% to 95.4%; however the majority of the sequences show 80%-90% nucleotide identity to one another. The amino acid identity between different subfamily members ranged from 64.2% to 91.0%. It is interesting that many of the differences in the predicted amino acid sequence of the different subfamily members are concentrated within the CDR2 region, which is predicted to interact mainly with residues on the MHC molecule.

Twenty sequences with >75% similarity to BTB1, BTB4 and BTB10, including those mentioned above, were classified as belonging to the bovine *BV2* subfamily. These sequences fell into 5 groups of identical or almost identical sequences, with two additional distinct single sequences. Alignments of the nucleotide and protein sequences of the *BV2* subfamily members are illustrated in Figure 5.5. Maximal alignment of the nucleotide sequences requires a dinucleotide insertion near the 5' end of the *V* gene in the published BTB1 and BTB4 sequences, resulting in a marked difference in the amino acid sequence of this region to that of BTB10 and all the new sequences identified in this study. Again, this probably indicates an error in the published sequences, for reasons that will be discussed later. Taking this error into account, *V* genes (designated *BV2S1* and *BV2S3* respectively) corresponding to two of the published sequences (BTB4 and BTB10) were identified. In addition, the sequence designated *BV2S6* differed from the published sequence BTB1 by only 5 nucleotides, and therefore could represent an allelic variant. The remaining four sequences represent distinct new *BV2* subfamily members. Comparison of the nucleotide sequences of the *BV2* subfamily members with one another and with the published sequences revealed that they are much more closely related than the members of *BV1* (see Table 5.3). The percentage nucleotide identity between the different subfamily members is greater than 90% in all cases and ranges from 92.1% to 98.7%, while the amino acid identity between the different sequences ranges from 84.0 to 94.6%.

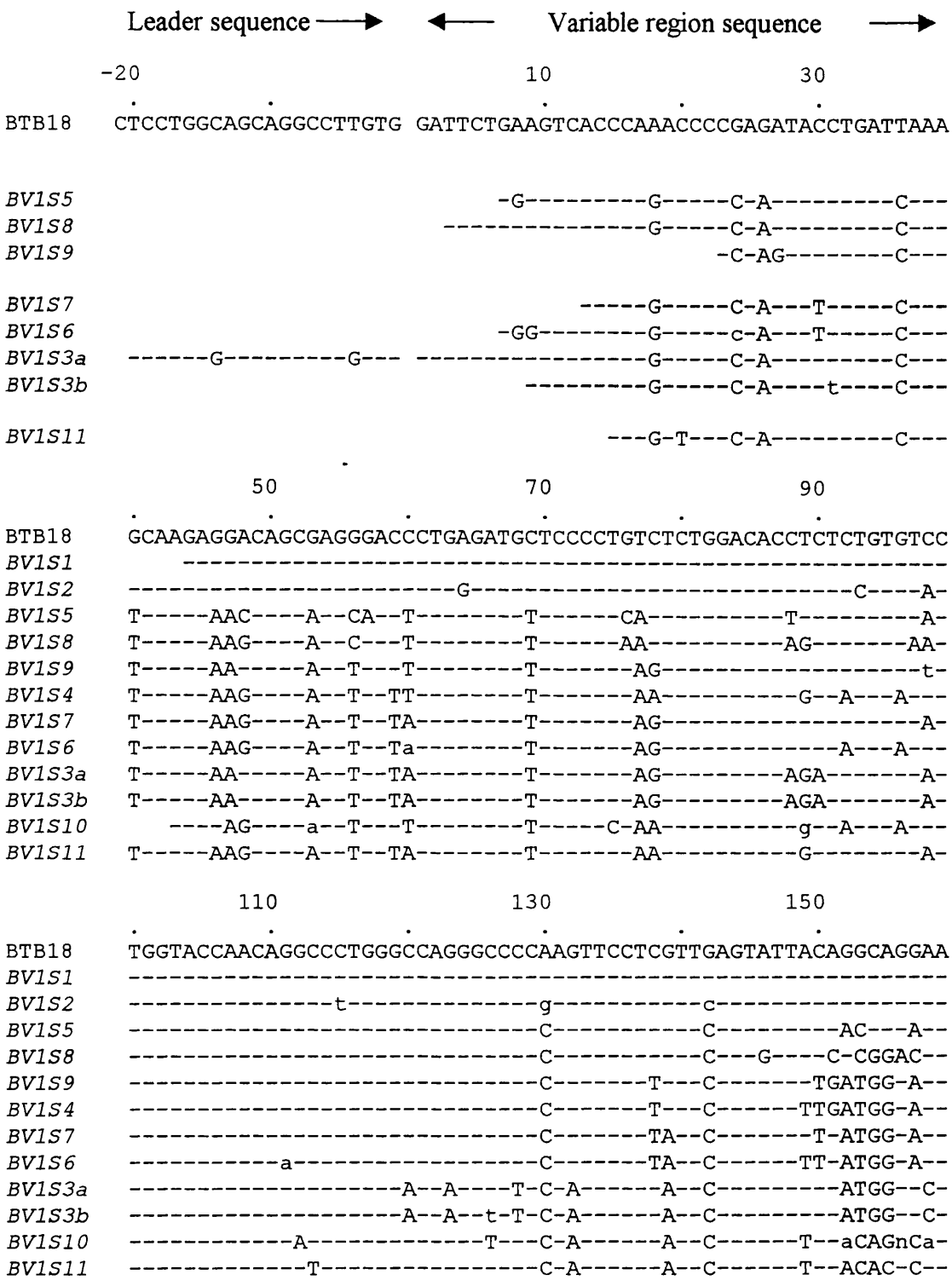

Figure 5.4. A. Alignment of nucleotide sequences of members of the bovine *TCRBV1* subfamily. Identical residues are shown as dashes. Letters in lower case indicate bases that require further sequencing for confirmation of identity. Gaps have been introduced at position 165 in *BV1S1*, *BV1S2*, *BV1S5* and *BV1S8*, at position 170 in *BV1S9*, *BV1S4*, *BV1S7*, *BV1S6*, *BV1S3a*, *BV1S3b*, *BV1S10* and *BV1S11*, and at position 191 in BTB18 to maximize the alignment (see over).

```
                170                 190                 210
        .           .           .           .           .           .
BTB18   GTGAGATGGAGAAGCACAGCTCCCGGATCGA.TCTCAGTAAAACAGTTTAGTGACTTTCG
BV1S1   -----.-------------------------T--------------------------
BV1S2   -----.G------------------------T------G--------------------A
BV1S5   -----.g------T-T--C----t-------T------G---------C-------C---
BV1S8   --T--.-A---G--A-A-CA-G--A------T------C------A--------------
BV1S9   ---TATCAA-.---G-A-CA-AT-A-----GG------G---------C-----TGC-GC
BV1S4   ---C-tAcA-.---G-A-CA-G--T------T------GTG-------C-------C---
BV1S7   -A--ATGA--.---G-a-CA-G--A------T------G--------------------A
BV1S6   -A--ATGA--.---G-A-CA-G--A------T---T--GTG-------C-------C-A-
BV1S3a  -A-TATGA--.---G-A-CA-AT-A------T------G---------C-------C-A-
BV1S3b  -A-TATGA--.---G-A-CA-AT-A------G------G---------C-------C-A-
BV1S10  CA--aTGa--.---G-a-CA-AT-A------T------G---------C-------C-A-
BV1S11  -A--ATGA--.---G-A-CA-AT-A------T------G---------C-------C-A-

                230                 250                 270
        .           .       .   .           .           .           .
BTB18   CTCCGAGCTGAACTTGAGCTCCTTGGAGCTGACAGACTCAGCCATGTATCTCTGTGCCAG
BV1S1   ------------------------------------------------------------
BV1S2   ---T---------------------------------------G----------------
BV1S5   ---T------------------------------------------------------
BV1S8   ---T--------T-------------------------------G----------------
BV1S9   ---T-------G-c---C-C-----------------------G----------------
BV1S4   ---TC--A-----C-----------------------------G----------------
BV1S7   ---T--------------------------------G---------g----------------
BV1S6   ---tC--A-----C-----------------------------------------------
BV1S3a  ---T-------------CT-------------AG---------G----------------
BV1S3b  ---T-------------CT--------------G---------G----------------
BV1S10  ---T-------------CT--------------G---------G----------------
BV1S11  ---T-------------CT--------------G---------G----------------


        .
BTB18   CAGC
BV1S1   ----
BV1S2   ----
BV1S5   ----
BV1S8   ----
BV1S9   ----
BV1S4   ----
BV1S7   ----
BV1S6   ----
BV1S3a  ----
BV1S3b  ----
BV1S10  ----
BV1S11  ----
```

Figure 5.4. A (cont.). Alignment of nucleotide sequences of members of the bovine *TCRBV1* subfamily.

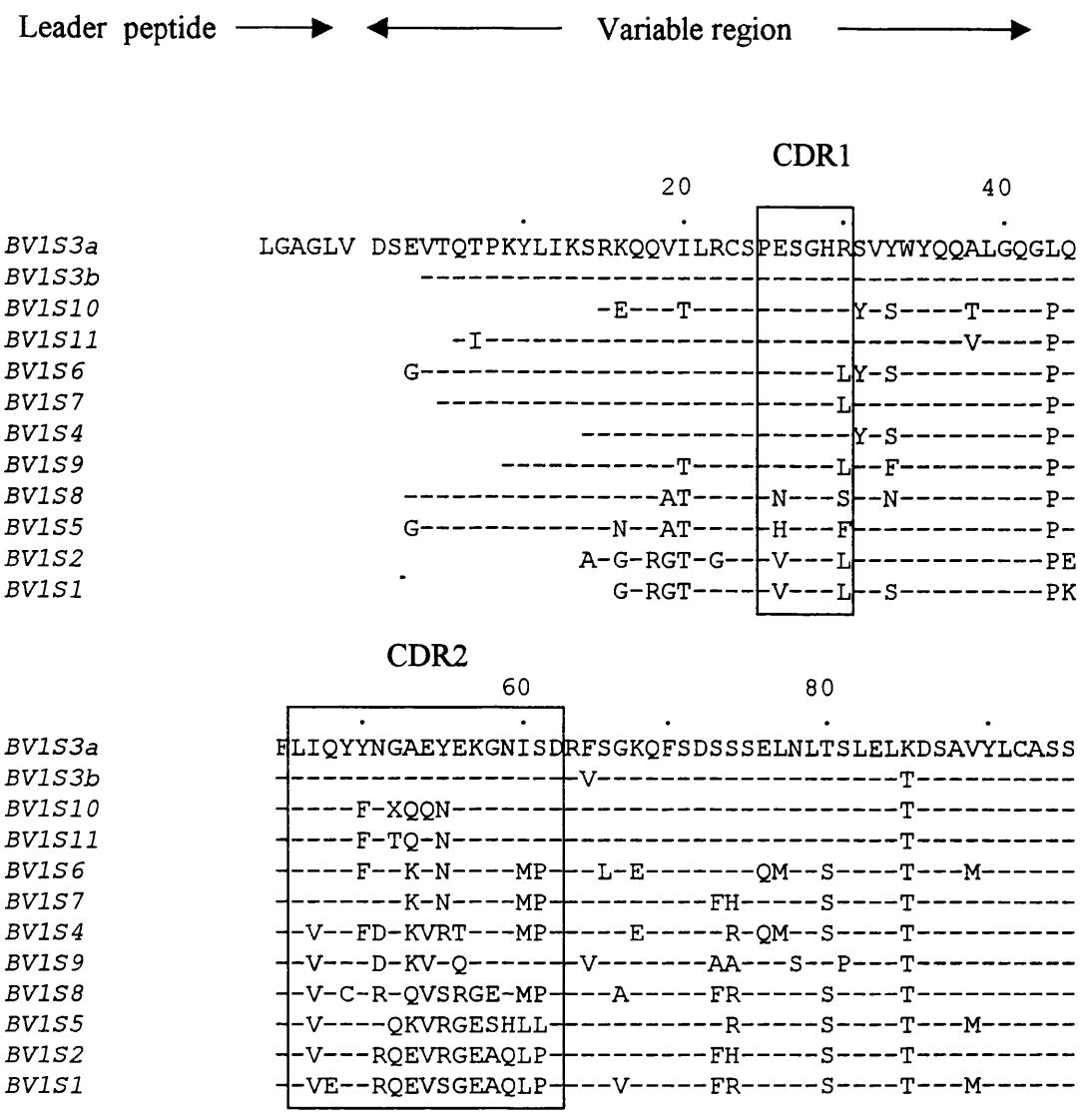

Figure 5.4. B. Alignment of the amino acid sequences of the members of the bovine *TCRBV1* subfamily. Identical residues are shown as dashes. The amino acid residues are numbered according to the system of Kabat *et al.* (1991). The complementarity regions CDR1 and CDR2, as defined by Chothia *et al.* (1988), are shown in boxes.

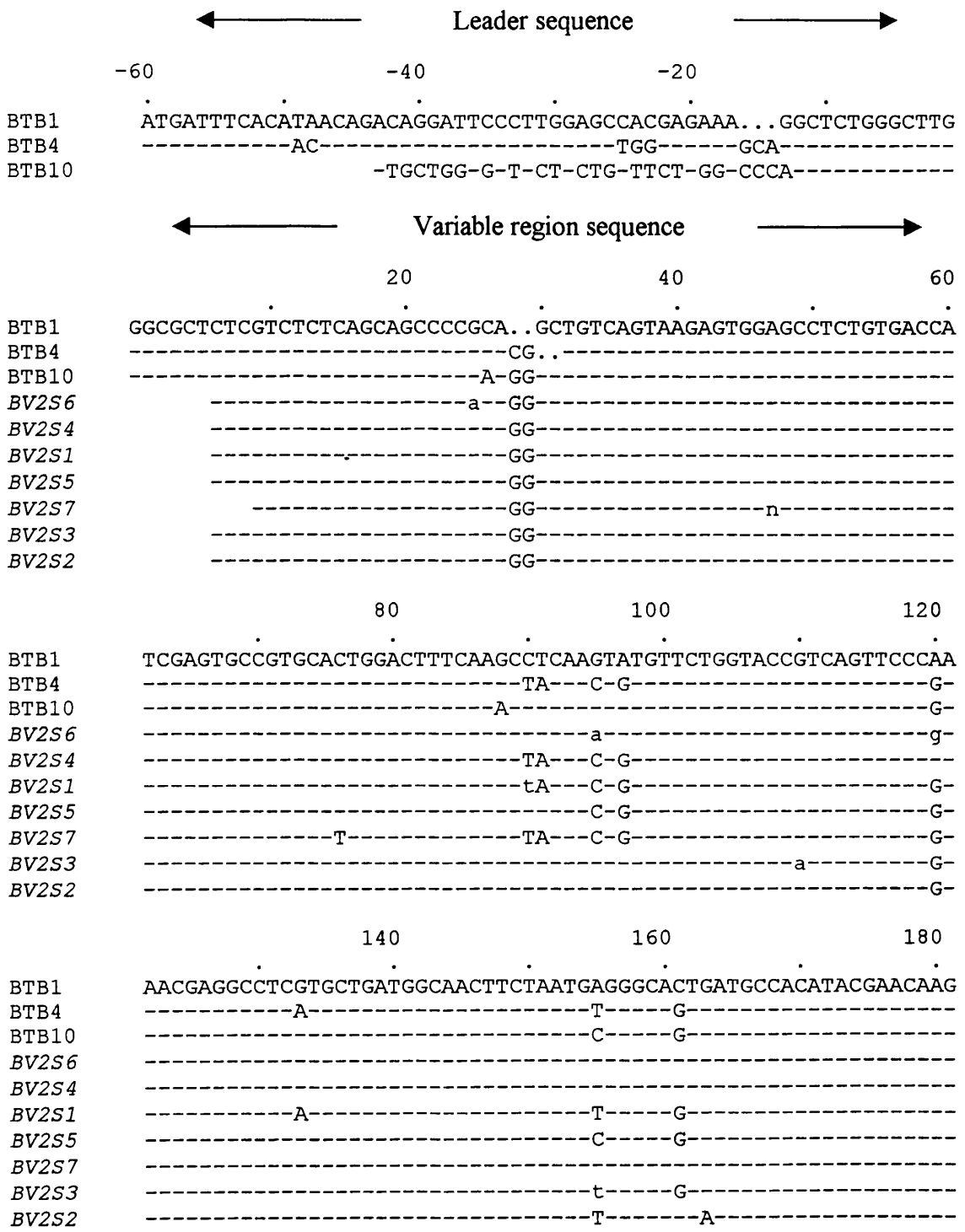

Figure 5.5. A. Alignment of the nucleotide sequences of members of the bovine *TCRBV2* subfamily. Identical residues are shown as dashes. To maximize the alignment, gaps have been introduced at positions 29 and 30 in the variable region sequence of BTB1, and at positions 31 and 32 in the variable region sequence of BTB4.

```
                        200                 220                 240
                .       .       .       .       .       .       .
BTB1        GTTATAACAAGGACAAGTTTCCCATCAGTCAGCCAGACCGAACATTTTCATCTCTGATGG
BTB4        ----C--T---------A-------------A-------T-----------------C--
BTB10       ----------------A--------------A-A---T-----------------C--
BV2S6       ------------------------------------------------------------
BV2S4       ----C-----------------T---------------------------------------
BV2S1       ----C--T---------A-------------A-------T-----------------C--
BV2S5       ------------------------------T-----------------------------
BV2S7       ------C-----------------------T-------T-----------------C--
BV2S3       ----------------A-----------------A---T-----------------C--
BV2S2       ------C-----------------------T-------T-----------------C--

                        260                 280
                .       .       .       .       .
BTB1        TGATAAGTGTGGATCCTACAGACAGCAGCCTCTACTTCTGCAGTGCTAGA
BTB4        ---C-C-----------G----------------------G---T-CAC
BTB10       ---C-C-----------G----------------------G----C---
BV2S6       ---C------------------------g---------------------.--
BV2S4       ---C---G---------G--------G-----------------c----g
BV2S1       ---C-C-----------G----------------------G--
BV2S5       ---C-C-----------G----------------------G---A---C
BV2S7       ---C-C-----------G----------------------TG---a--TG
BV2S3       ---C-C-----------G------------------------------t
BV2S2       ---C-C-----------G--------G----------------C--GG
```

Figure 5.5. A. (cont.) Alignment of nucleotide sequences of members of the bovine *TCRBV2* subfamily.

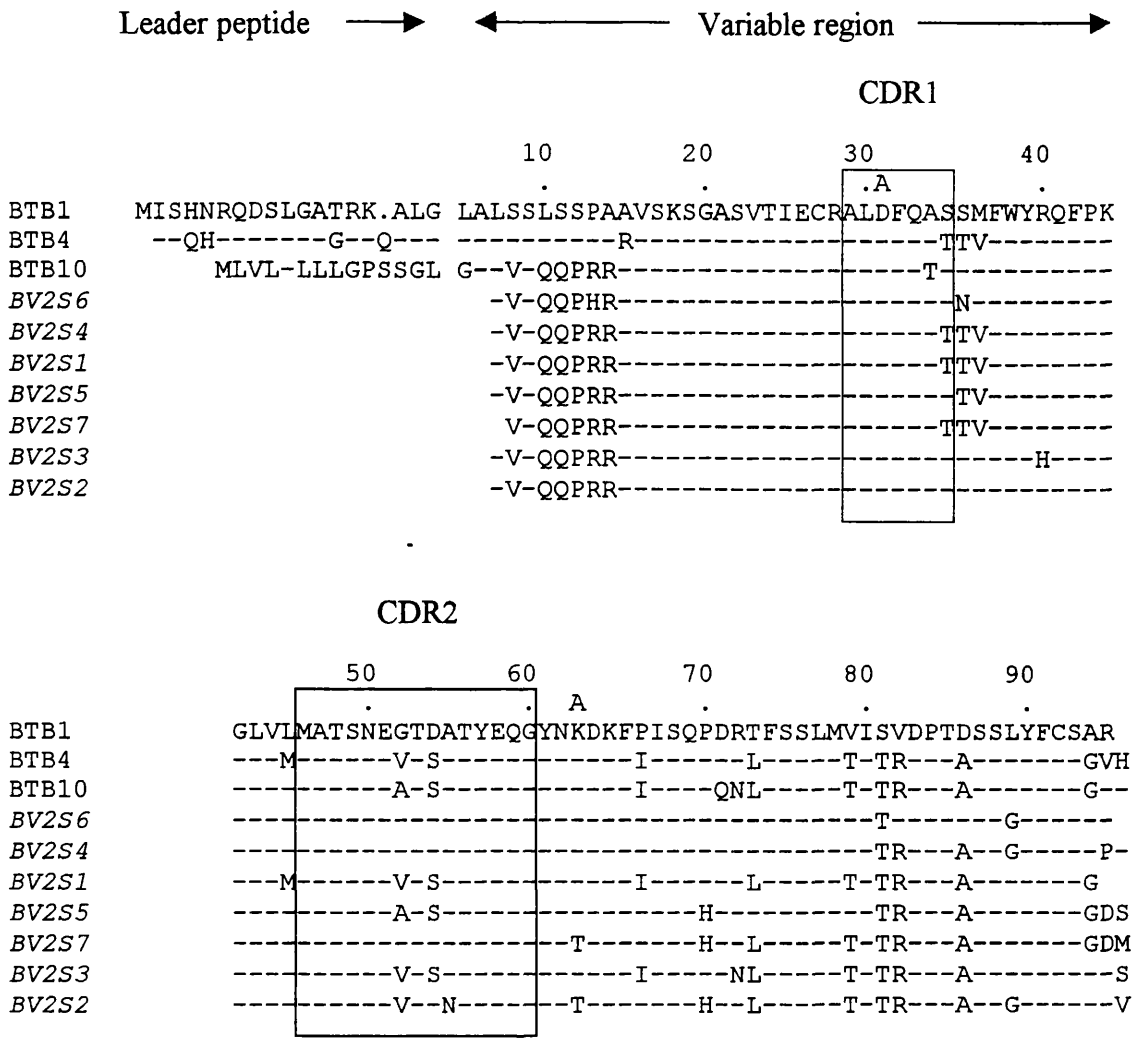

Figure 5.5. B. Alignment of the amino acid sequences of members of the *TCRBV2* subfamily. Identical residues are shown as dashes. The amino acid residues are numbered according to the system of Kabat *et al.*, 1991.

Single new members were identified for the subfamilies *BV4*, *BV6*, and *BV17*, represented respectively by clones BTB93, BTB50 and BTB90 of Tanaka *et al.* The new member of *BV4* was represented by a single clone (D16), and reliable sequence of the entire *V* gene was not obtained. Comparison of the partial sequence with BTB93 revealed 90.1% identity at the nucleotide level and 82.7% identity at the amino acid level; the differences between the sequences are illustrated in Figure 5.6.

The clones corresponding to BTB50 (*BV6S1*) contained the entire sequence of the *V* gene and maintained an open reading frame, in contrast to the published sequence which is truncated and has a stop codon (TGA) near the 5' end. Buitkamp *et al.* (1993), in an analysis of germline polymorphisms of artiodactyl *TCRBV6* elements, identified and partially sequenced another member of the bovine *BV6* subfamily, which they named Vb6a (*BV6S2*). The alignments of the sequence identified in this study (designated *BV6S3*) with the nucleotide and protein sequences of BTB50 and Vb6a are illustrated in Figure 5.7. There is much closer homology between the sequences of *BV6S1* and *BV6S3* (93.5% at the nucleotide level) than between either sequence and *BV6S2* (85.1% and 84.3% nucleotide identity, respectively).

The percentage similarity between the nucleotide sequences of BTB90 and IC46 was less than 75% (71.1%); however, when compared with human sequences, both showed maximum homology to *BV17S1*, with percentage nucleotide similarities of 77% and 73% respectively. The alignment of the nucleotide and protein sequences of IC46 with BTB90 is shown in Figure 5.8. The sequences are most divergent near the 5'end of the *V* gene. The subfamily member identified in this study is represented by only two clones (IC46 and IC85) which were sequenced on one strand (3'-5'). Thus the divergence has probably arisen through an error in sequencing in the 5' region, which could be resolved by sequencing on the other strand.

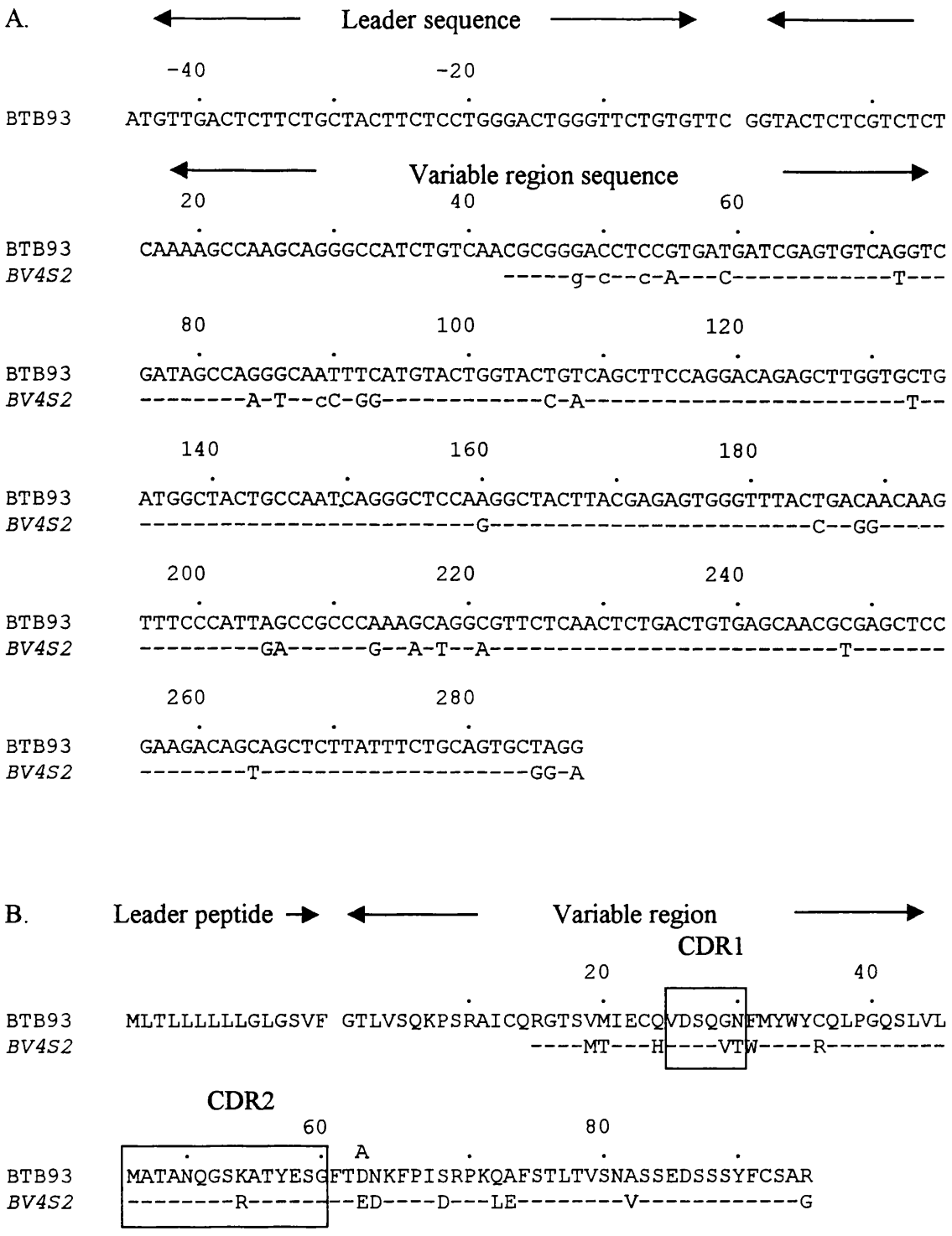

Figure 5.6. Alignment of the partial nucleotide (A) and amino acid (B) sequences of a new member of the bovine *TCRBV4* subfamily (*BV4S2*) with the original sequence published by Tanaka *et al.* (1990) (BTB93). Identical residues are shown as dashes. Amino acid residues are numbered according to the system of Kabat *et al.* (1991).

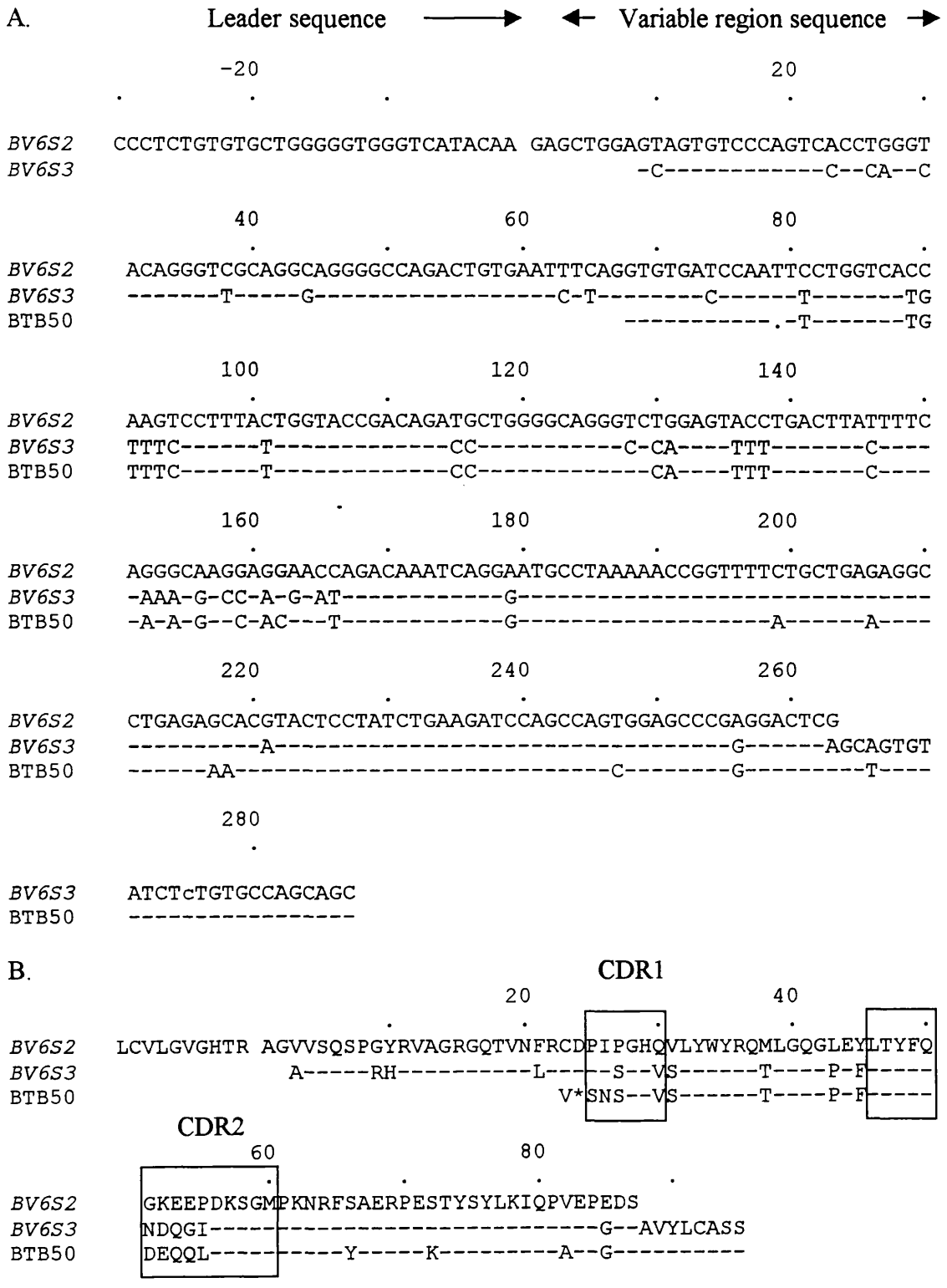

Figure 5.7. Alignment of the nucleotide (A) and amino acid (B) sequences of a new member of the bovine *TCRBV6* subfamily (*BV6S3*) with the sequences published by Tanaka *et al.* (1990) (BTB50) and Buitkamp *et al.* (1993) (*BV6S2*).

A.

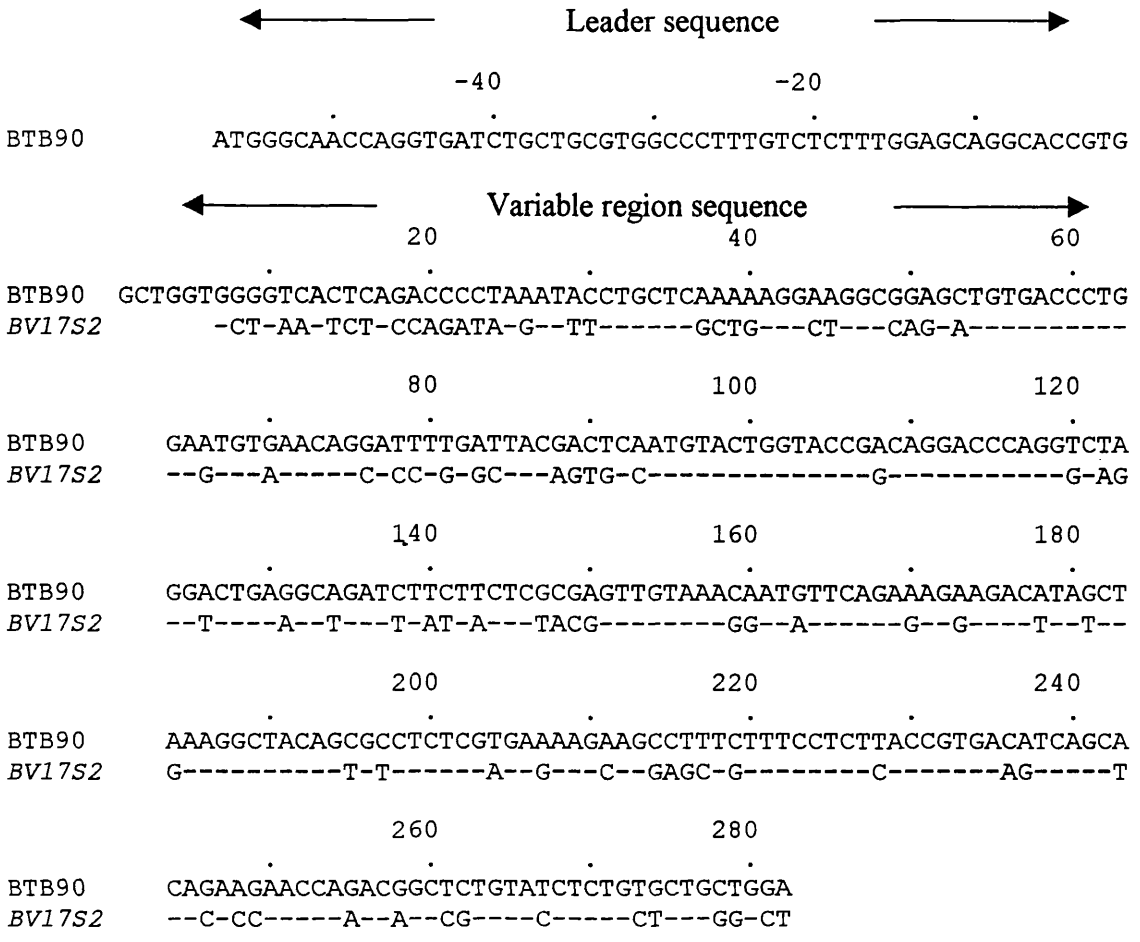

B.

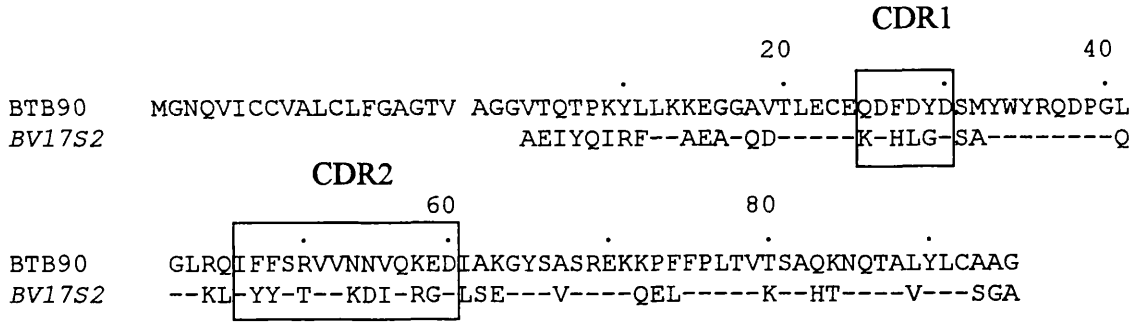

Figure 5.8. Alignment of nucleotide (A) and amino acid (B) sequences of a new member of the bovine *TCRBV17* subfamily (*BV17S2*) with the sequence published by Tanaka *et al.* (1990).

Table 5.1. Comparison of the sequences of new bovine *TCRBV* subfamily members with published bovine and human sequences.

Bovine subfamily designation	No. of clones	Represent -tative clone	Percentage identity with published bovine *TCRBV* sequences			Percentage identity with human *TCRBV* sequences		
			Clone	nt	aa	Segment	nt	aa
BV1S1	4	IC5	BTB18[a]	100	100	*BV1S1*[c]	78	63
BV1S2	4	IC93	BTB18	94.7	81.5	*BV1S1*	78	67
BV1S3	6	C20	BTB18	82.0	66.0	*BV1S1*	79	72
BV1S4	4	C12	BTB18	81.1	65.4	*BV1S1*	79	63
BV1S5	3	C50	BTB18	87.7	75.8	*BV1S1*	77	66
BV1S6	6	C55	BTB18	80.7	64.8	*BV1S1*	77	65
BV1S7	3	C125	BTB18	83.8	70.0	*BV1S1*	81	72
BV1S8	2	C54	BTB18	84.7	73.9	*BV1S1*	76	64
BV1S9	4	IC58	BTB18	80.9	66.3	*BV1S1*	77	63
BV1S10	1	C30	BTB18	80.7	62.5	*BV1S1*	77	67
BV1S11	1	C47	BTB18	81.6	61.8	*BV1S1*	76	66
BV2S1	4	IC47	BTB4[a]	98.9	92.5	*BV2S1*[c]	79	66
BV2S2	1	IC14	BTB10[a]	95.4	88.3	*BV2S1*	79	65
BV2S3	6	D28	BTB10	99.6	98.9	*BV2S1*	78	63
BV2S4	3	C23	BTB1[a]	95.4	85.3	*BV2S1*	78	63
BV2S5	2	C56	BTB1	95.4	83.9	*BV2S1*	78	63
BV2S6	4	C36	BTB1	97.5	90.4	*BV2S1*	77	64
BV2S7	1	IC44	BTB10	94.2	86.2	*BV2S1*	78	66
BV3S1	2	C10	BTB91[a]	100	100	*BV3S1*[c]	77	72
BV4S2	1	D16	BTB93[a]	90.1	82.7	*BV4S1*[d]	80	77
BV6S3	5	D22	BTB50[a] VB6a[b]	93.5 84.3	84.9 81.2	*BV6S1-S5*[d,e,f,g]	74-77	62-77
BV7S1	2	C25	BTB27[a]	99.0	97.1	*BV7S1-S3*[f,h]	69-77	52-68
BV12S1	2	IC61	BTB13[a]	99.6	98.7	*BV12S1*[g] *BV12S2*[f]	66 65	55 55
BV15S1	1	D23	BTB22[a]	98.9	97.8	*BV15S1*[g]	83	70
BV15S2	2	C49	BTB45[a]	100	98.9	*BV15S1*	82	69
BV17S2	2	IC46	BTB90[a]	71.1	55.8	*BV17S1*[e]	74	64

Notes: nt=nucleotide; aa=amino acid. The sequences used for comparison are contained in the following references; GenBank accession numbers are shown in square brackets: Tanaka *et al.* (1990)[a] [D90121-D90133]; Buitkamp *et al.* (1993)[b] [L18952];Concannon *et al.* (1986)[c] [M13836, M13842, M13843]; Kimura *et al.* (1986)[d] [X04934]; Kimura *et al.* (1987)[e] [M27383, M27388]; Ferradini *et al.* (1991)[f] [X58806, X58805, X58813, X58811, X58808]; Tillinghast *et al.* (1986)[g] [M14262, M14268, M14269]; Santamaria *et al.* (1993)[h] [L06887].

Table 5.2. Comparison of the nucleotide sequences of bovine *TCRBV1* subfamily members.

	S1	*S2*	*S3*	*S4*	*S5*	*S6*	*S7*	*S8*	*S9*	*S10*	*S11*
S1	-	**95.4**	79.9	82.5	90.2	81.6	85.5	85.9	80.8	82.5	80.3
S2		-	80.2	81.0	89.3	**79.3**	85.5	84.7	81.0	81.8	79.6
S3			-	84.4	84.4	88.3	91.5	86.5	87.7	93.7	89.6
S4				-	84.8	93.4	89.7	85.6	88.5	86.8	86.3
S5					-	84.4	87.4	88.4	84.6	86.2	82.5
S6						-	93.7	83.5	87.3	89.6	87.9
S7							-	88.1	89.6	92.2	88.3
S8				-				-	83.8	85.8	82.9
S9									-	87.3	85.0
S10										-	94.6
S11											-

Table 5.3. Comparison of the nucleotide sequences of bovine *TCRBV2* subfamily members.

	S1	*S2*	*S3*	*S4*	*S5*	*S6*	*S7*
S1	-	95.0	95.6	95.0	96.4	93.5	96.0
S2		-	96.0	94.6	96.1	95.8	**96.7**
S3			-	**93.0**	**96.7**	94.9	94.5
S4				-	95.1	96.1	94.0
S5					-	96.1	96.4
S6						-	93.9
S7							-

Notes: Pairwise comparisons of the nucleotide sequences of the different subfamily members in *BV1* and *BV2* were performed using the BESTFIT and FASTA programs in the GCG package (Devereux *et al.*,1984). The percentage nucleotide identities between the sequences are shown in the above tables. The percentage nucleotide identities of the most similar and the least similar members within each subfamily are shown in bold type in shaded boxes.

5.3.2.2. New *TCRBV* subfamilies.

A number of clones contained sequences which had less than 75% nucleotide coding region homology with published bovine *TCRBV* sequences. These were tentatively assigned to seven new *TCRBV* subfamilies and where possible, consensus sequences were derived. The sequences were screened against human *TCRBV* sequences, and the new subfamilies were assigned numbers corresponding to the human *BV* genes to which they showed the closest homology. Comparisons of the new subfamily sequences with human *TCRBV* sequences are shown in Table 5.4.

Two of the new subfamilies, *BV10* and *BV13*, consisted of at least 3 closely related but distinct sequences. The alignments of the nucleotide and protein sequences of the three members of *BV10* are shown in Figure 5.9. The nucleotide sequence similarity between different members of *BV10* ranged from 87.5 to 94.9% and the amino acid identity between protein sequences was 79.1-91.3%. Many of the amino acid differences between the protein sequences are found within the proposed hypervariable regions (CDRs). One sequence is shorter than the other two by one amino acid, due to deletion of a codon at position 114, as shown in the alignment. Since this subfamily member is represented by two clones from the same PCR reaction, it is possible that the deletion may have been introduced during amplification. However, the sequence contains additional differences that distinguish it from the other subfamily members, suggesting that it does represent a distinct gene segment.

The nucleotide and protein sequences of the three members of *BV13* are compared in Figure 5.10. The percentage nucleotide similarity between the different members is 88.7-95.6%, with 77.2-91.2% identity at the amino acid level. In this subfamily, the coding differences between the members are distributed throughout the length of the molecule, rather than being concentrated in the CDRs.

Three new subfamilies consisted of a single member, as all the clones assigned to *BV14*, *BV20* and *BV24* contained identical or almost identical sequences. Two of the new subfamilies, *BV9* and *BV16*, were represented by only one sequence each. These sequences and the deduced peptide sequences are shown in Figure 5.11.

A.

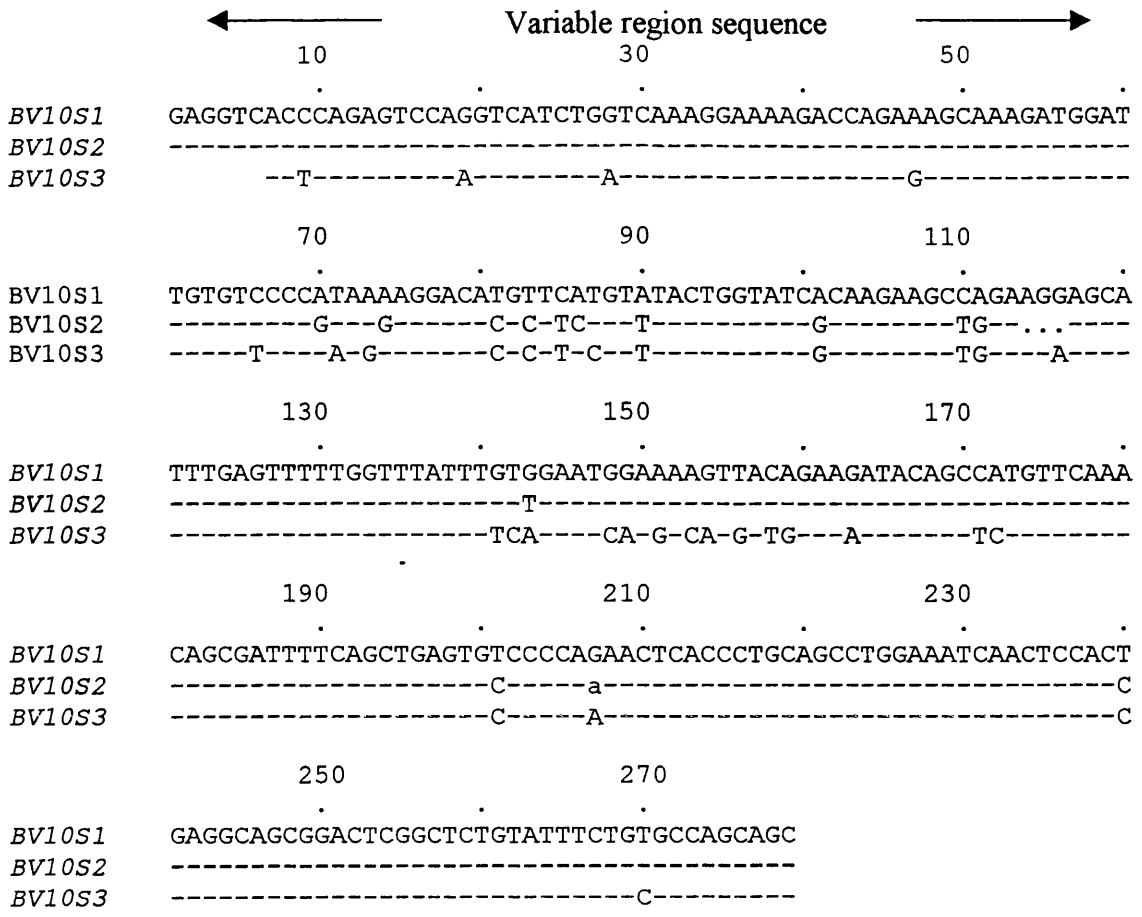

B.

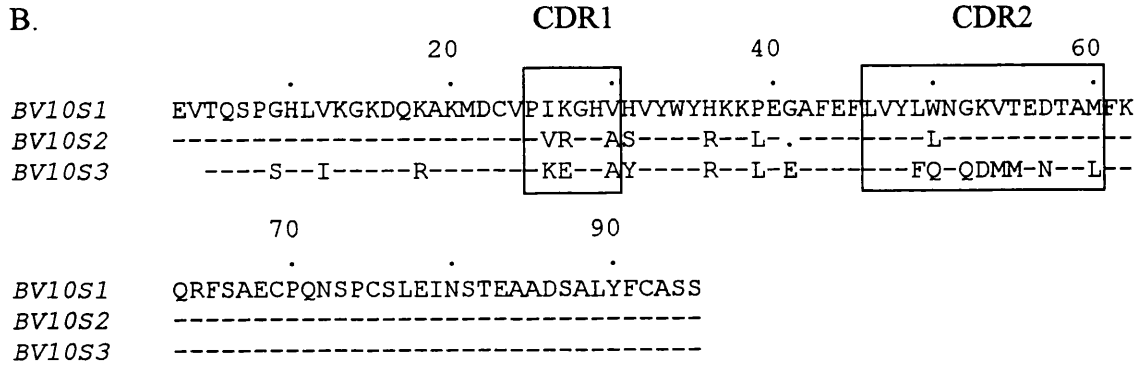

Figure 5.9. Alignment of the nucleotide (A) and amino acid (B) sequences of the members of the bovine *TCRBV10* subfamily. To maximize the alignment, gaps have been introduced at positions 114, 115 and 116 of the nucleotide sequence and the corresponding amino acid position 41 in the peptide sequence of *BV10S2*.

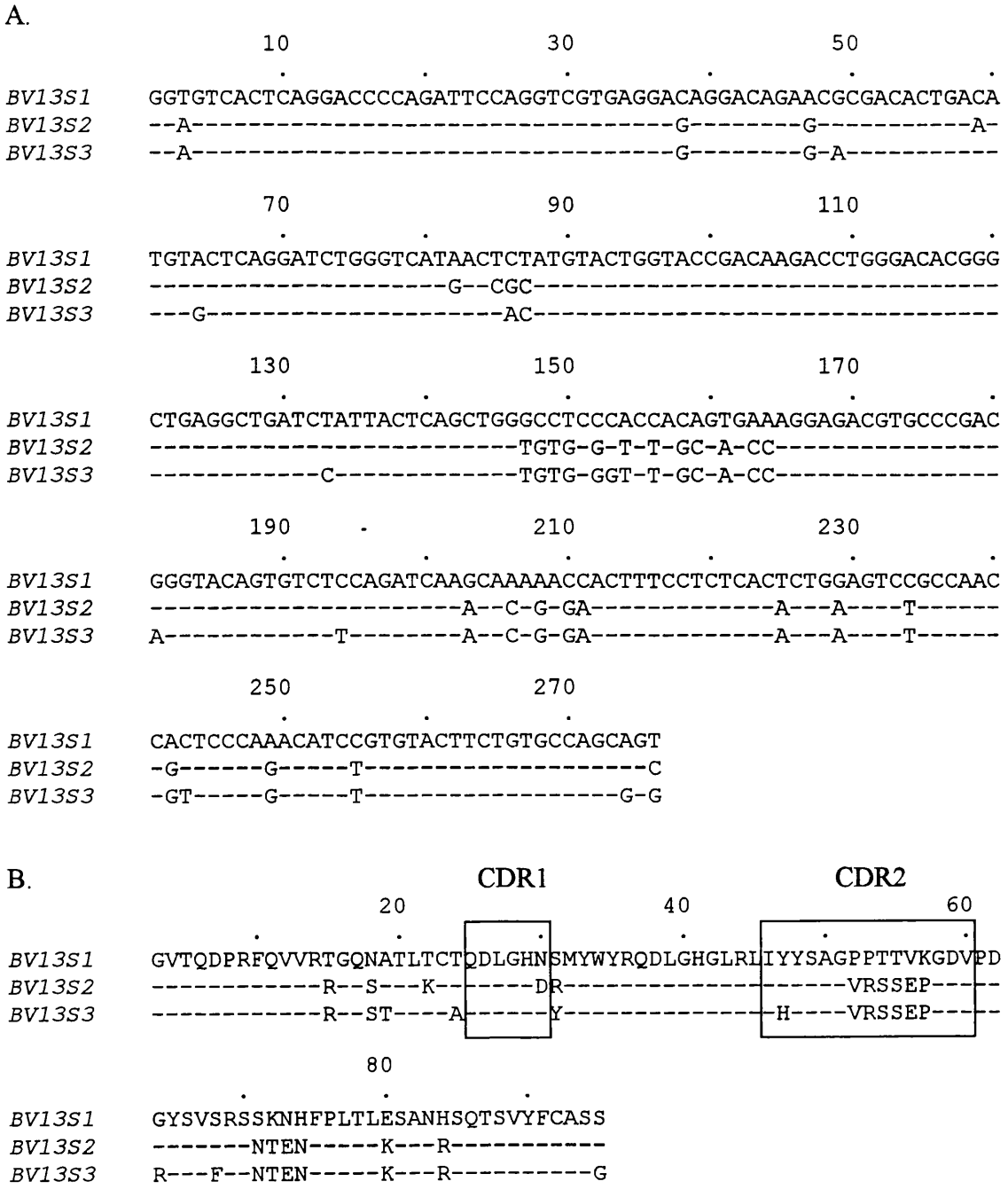

Figure 5.10. Alignment of the nucleotide (A) and amino acid (B) sequences of the members of the bovine *TCRBV13* subfamily.

A. *BV9S1*

```
TAGAACATCCTAGAATGTGAGCAAAAGcTGGAACATGATAGTATGTATTGGTATAAGCAG
* N I L E C E Q K L E H D S M Y W Y K Q

GACTCCAAGAAATTGCTGAAGGCTATGTTTAGCTACAATAATAAGCTACTCGTTGGAAAT
D S K K L L K A M F S Y N N K L L V G N

GAAACGGTGCCAAGTCGTTTCTCACCGGAGTCTCCTGACAAAGCTCATTTAAACCTTCAC
E T V P S R F S P E S P D K A H L N L H

ATCGACTCCCTGGAGCCAGGCGACTCTGCCATGTATTTCTGTGCCAGCAGC
I D S L E P G D S A M Y F C A S S
```

B. *BV14S1*

```
GAGCCCAAGACACCGCATCACAGAGACCAGAAAGAGGGTGACATTGACTTGTTCTCAGAA
 S P R H R I T E T R K R V T L T C S Q N

TATGAACCATGATGCGATGTACTGGTATCGACAaGACCCAGGGCTGGGTCCAAAGCTGAT
 M N H D A M Y W Y R Q D P G L G P K L I

CTACTTTTCAAGGAATGTTGGGTTTATTGAAAATGGAGATATCCCTGATGGATACAcTGC
 Y F S R N V G F I E N G D I P D G Y T A

CTCTCGAGAAGAGAAACCAAACTTCCCCCTGACCTTGGAGTTGGCCAGCACCaACCAGAC
 S R E E K P N F P L T L E L A S T N Q T

CTCCTTGTACCTCTGTGCCAGCagt
 S L Y L C A S S
```

Figure 5.11. Nucleotide and amino acid sequences of new bovine single-member *TCRBV* subfamilies. A – *BV9S1*. B – *BV14S1*.

C. *BV16S1*

```
GAAGTCGCCCAGTCCCCCAGCCACAGGGTCATAGAGAAGAAACAGGCTGTGAATCTGAGT
E  V  A  Q  S  P  S  H  R  V  I  E  K  K  Q  A  V  N  L  S

TGTGACCaTATTTCTGGACATGAATcTCTTTTTTGGTACTACCATGCTGTGGGGAAAGAA
C  D  H  I  S  G  H  E  S  L  F  W  Y  Y  H  A  V  G  K  E

ATGAAACTTCTGATTTACTTCCTAAGAGAGTCTAtGCAGGATGACTCGGGGATGCCCAAA
M  K  L  L  I  Y  F  L  R  E  S  M  Q  D  D  S  G  M  P  K

GGCCGATTCACAGCAGAAAGGATGGAAGGGACATCtTCtACGCTGAGGGTCCACTCTGCA
G  R  F  T  A  E  R  M  E  G  T  S  S  T  L  R  V  H  S  A

GAGcTGGGTGACTCAGGAGTGTATcTCtGTGCCAGCAGT
E  L  G  D  S  G  V  Y  L  C  A  S  S
```

D. *BV20S1*

```
ACCATCCATCAGTGGCCATCCACGAGGGTGCAGCCTGCAGGCAGCCCGCTCTCTcTGGAG
T  I  H  Q  W  P  S  T  R  V  Q  P  A  G  S  P  L  S  L  E

TGCaCCGTGAAGGGGACATCAAACCCCACCCTGTACTGGTACCGGCAGGAGGCAGGGGGG
C  T  V  K  G  T  S  N  P  T  L  Y  W  Y  R  Q  E  A  G  G

AGCCTCCAGCAGCTCTTCTACTCTGTTAGTGCTGGCCAGATAGAACCTAGGGAGTTCCAG
S  L  Q  Q  L  F  Y  S  V  S  A  G  Q  I  E  P  R  E  F  Q

AACTTCAAAGCTTCCAGGCCCCAGGACGGCCAGTTTACCCTGAGTTCTAAGAAGCTGCAG
N  F  K  A  S  R  P  Q  D  G  Q  F  T  L  S  S  K  K  L  Q

CTCAACAACTCTGGCTTcTACTTCTGTGCCTGGAg.
L  N  N  S  G  F  Y  F  C  A  W  X
```

Figure 5.11. (cont.) Nucleotide and amino acid sequences of new bovine single-member *TCRBV* subfamilies. C – *BV16S1*. D – *BV20S1*.

E. *BV24S1*

```
ATGgTcGTTCAGAACCCAAGATACCTGGTtACCGGGCTGGGAAAACCAGTGACCCTGAGC
M  V  V  Q  N  P  R  Y  L  V  T  G  L  G  K  P  V  T  L  S

TGTTCTCAGAATATGAAGCATGATGCCATGTACTGGTACCAACAGAAGCCAAGCCAAGCA
C  S  Q  N  M  K  H  D  A  M  Y  W  Y  Q  Q  K  P  S  Q  A

CCAAAACTGCTGTTGTACTACTATGATACACAAATCACCAAGGAAAAAAACACCTCTGAA
P  K  L  L  L  Y  Y  Y  D  T  Q  I  T  K  E  K  N  T  S  E

AACTTCCAGTCCAGCCGGCcTAACaCCTCTTTCTGTTCTCTTGACATCCGCTCGGCAGGC
N  F  Q  S  S  R  P  N  T  S  F  C  S  L  D  I  R  S  A  G

CTGGGGGACTCAGCCGTATATcTCTGTGCCAGCAgC
L  G  D  S  A  V  Y  L  C  A  S  S
```

Figure 5.11. (cont.) Nucleotide and amino acid sequences of new bovine single-member *TCRBV* subfamilies. E – *BV24S1*.

Table 5.4. Comparison of the sequences of new bovine *TCRBV* subfamilies with human *TCRBV* sequences.

Bovine subfamily designation	No. of clones	Represent-ative clone	Percentage identity with human *TCRBV* sequences		
			Segment	**nt**	**aa**
BV9S1	1	C68	*BV9S1*[a]	84	78
BV10S1	4	C63	*BV10S1*[b]	76	56
BV10S2	2	C21	*BV10S1*	76	55
BV10S3	3	D13	*BV10S1*	77	59
BV13S1	3	IC20	*BV13S1-S6*[a,b,c]	72-76	62-70
BV13S2	2	C48	*BV13S1-S6*	72-77	62-65
BV13S3	1	IC100	*BV13S1-S6*	71-76	62-65
BV14S1	3	C43	*BV14S1*[d]	81	63
BV16S1	1	D23	*BV16S1*[e]	76	62
BV20S1	4	C74	*BV20S1*[f]	80	74
BV24S1	5	C53	*BV24S1*[g]	80	69

Notes: nt=nucleotide; aa=amino acid. The sequences used in the comparisons are contained in the following references; GenBank accession numbers are given in square brackets: Ferradini *et al.* (1991)[a] [X58814, X58809, X58810, X58815]; Concannon *et al.* (1986)[b] [M13860, M13863]; Li *et al.* (1991)[c] [X61445, X61447]; Tillinghast *et al.* (1986)[d] [M14267]; Plaza *et al.* (1991)[e] [X57723]; Charmley *et al* (1993)[f] [Z13967]; Robinson (1991)[g] [M62376].

5.3.3. Analysis of the protein sequence of bovine Vβ regions.

An alignment of the deduced amino acid sequences of representative members of each bovine *TCRBV* subfamily is shown in Figure 5.12. The sequences for *BV9* and *BV16* have been omitted as these gene segments were represented by only a single clone each, and the complete sequence of the *V* genes was not obtained. The sequences are aligned according to the Kabat numbering system, which has been commonly adopted in similar studies (Kabat *et al.*,1991). The hypervariable regions (CDR1 and CDR2) defined by Chothia *et al.* (1988) are indicated by boxes. Seven amino acids that are present in >90% of TCR Vβ sequences of other species are conserved in almost all of the bovine sequences; these are Cys-23, Trp-34, Tyr-35, Gln-37, Leu-77, Tyr-90 and Cys-92. The only exception occurs in Vβ10, where a lysine is found at position 37 instead of glutamine; however a lysine is also present at this position in the predicted human Vβ10 protein sequence and in three functional mouse *TCRBV* genes (*BV9S1*, *BV19S1A1* and *BV20S1*). Chothia *et al.* modelled the three-dimensional structure of the TCR by comparison with the immunoglobulin structures available from crystallographic analysis, and identified other framework residues that are highly conserved in both molecules, indicating that they are probably important in maintaining the overall protein structure. These residues are indicated with asterisks in Figure 5.12. Recent crystallographic analysis of the protein structure of the α/β TCR has confirmed the importance of some of these residues in interactions between the Vβ domain and the Cβ and Vα domains, and in determining the conformation of the CDR loops (Garcia *et al.*, 1996).

The sequences could be further classified by comparison with defined subgroups of TCR Vβ sequences. Schiffer *et al.* (1986) divided TCR Vβ sequences into two subgroups based on the presence of paired residues that can form a salt bridge, a structural feature of immunoglobulin domains revealed by crystallographic studies. Sequences in subgroup I have an aspartic acid residue at position 86, which can form a salt bridge with an arginine, lysine or histidine at position 64, while subgroup II sequences do not contain these residues. In addition, subgroup I sequences have a phenylalanine at position 65 and a serine at position 87, whereas subgroup II sequences have tyrosine at position 65, a glutamine at 86 and a threonine at 87. Chothia *et al.* (1988) grouped protein sequences

that are >50% identical within a species or >40% identical between species to form five Vβ subgroups. The majority of human Vβ proteins are in subgroups I and IV. Subgroups I-III correspond to Schiffer's subgroup I, while subgroup IV corresponds to Schiffer's subgroup II. Subgroup V contains only two sequences, one human (Vβ20) and one murine (Vβ14, the homologue of human Vβ20), which have a leucine at position 65. As new subfamilies were discovered the classification was extended; Robinson (1991) proposed that the human Vβ23 sequence, along with a mouse Vβ sequence homologous to Vβ23, should form a new subgroup related to, but distinct from, subgroup I. These sequences contain a glutamine at position 64 rather than arginine, but have other residues that could potentially form a reverse salt bridge.

In general, the bovine TCR Vβ protein sequences can be assigned to the same subgroups as their human counterparts, but there are some exceptions. One member of *BV1* has valine at position 65 instead of phenylalanine, and three members of *BV2* have isoleucine at this position (see Figures 5.4 and 5.5). These are conservative substitutions which would not be expected to alter the structural features of the protein; however, both could arise as a result of a single base change in the nucleotide sequence. That this may be due to PCR or sequencing errors is unlikely in view of the fact the sequences for all these subfamily members except one were derived from at least three clones from two different PCR reactions. The bovine Vβ20 sequence has an asparagine at position 64 and phenylalanine at position 65, but does not fit into the previous classification because it contains an asparagine at position 86 (see Figure 5.12). This difference is almost certainly genuine, as the consensus sequence for the bovine *BV20* gene was derived from four clones from three different PCR reactions.

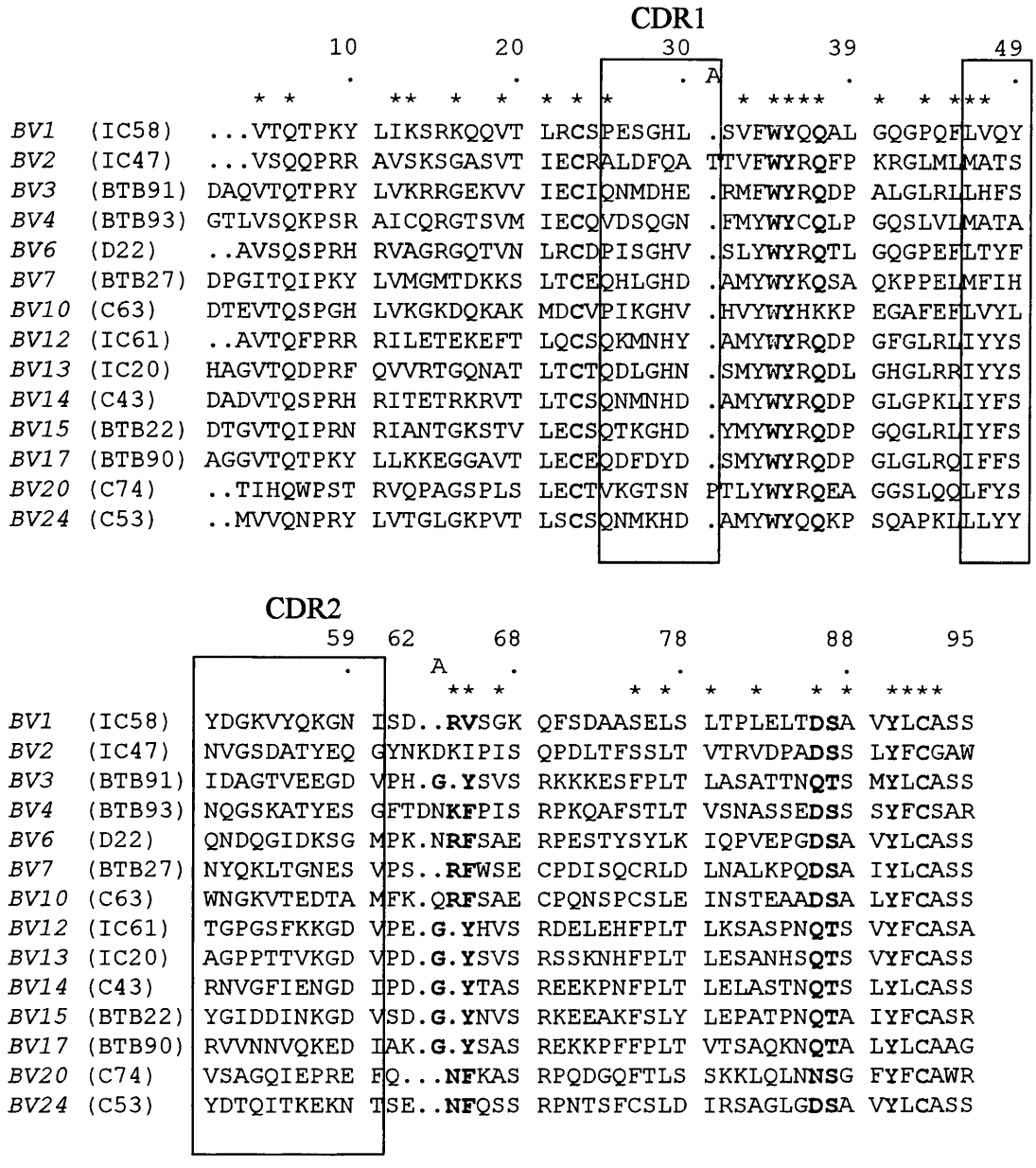

Figure 5.12. Alignment of the protein sequences of members of the different bovine *TCRBV* subfamilies. The clones representing each subfamily are shown in parentheses. The sequences are numbered according to the system of Kabat *et al.* (1991), and the boxes show the CDR1 and CDR2 regions, as defined by Chothia *et al.* (1988). The asterisks indicate important structural residues conserved between immunoglobulin and T cell receptors (Chothia *et al.*, 1988). Invariant (or almost invariant) residues are shown in red. Residues used for defining bovine *TCRBV* subgroups are shown in green (see text for explanation of subgroups).

5.3.4. Analysis of *TCRBD*, *BJ* and *BC* sequences.

The third hypervariable region (CDR3) of the TCR β-chain spans the region encoded by the 3' end of the *BV* gene segment and the *BD* and *BJ* minigenes; the region is further diversified by N region addition of nucleotides at the junctions between the gene segments. Comparison of the sequences encoded by *TCRB* mRNA transcripts with those of germline gene segments is necessary to determine with certainty the contribution of different *BD* and *BJ* gene segments to the generation of junctional diversity. As yet, the germline sequences of bovine *TCRB* gene segments have not been determined, so that precise identification and classification of the *BD* and *BJ* genes in the transcripts sequenced in this study was not possible. Tanaka *et al.* (1990) classified the *BJ* gene segments in their cDNA clones, which they defined as the 13 codons before the *TCRBC* region, into twelve different members. This region contains the highly conserved Phe-Gly-X-Gly motif, which is characteristic of all TCR J segments (Kabat *et al.*, 1991).

Based on this approach, the amino acid sequences of the Jβ segments of 100 clones containing unique in-frame transcripts were examined, and 21 different sequences were identified at the protein level. The sequences formed 13 groups containing members that differed by only one or two amino acids. These groups may represent different *BJ* gene segments; there are 13 functional *BJ* genes in humans and 12 in mice. The variant sequences may have arisen from germline polymorphisms but, since they are all represented in only one clone, it is possible that they are the result of PCR or sequencing errors. Three sequences differed from another by only one amino acid at the 5' end, which may be accounted for by variation introduced by N nucleotide addition. The protein sequences of the different *BJ* gene segments are shown in Table 5, along with the frequency with which they were identified in the clones examined. All the segments identified by Tanaka *et al.* (1990) were included in these clones except for one, and are indicated by asterisks in Table 5. Although Tanaka *et al.* stated that they found 12 different *BJ* sequences, sequence data for only seven were presented in the paper. In the present study, two *BJ* genes were represented at particularly high frequencies in both the individuals studied. Interestingly, one of these genes was also found in 5 out of 13 clones sequenced by Tanaka *et al.* (1990). Studies in humans have also demonstrated a bias in

BJ gene usage, with three *BJ* gene segments being preferentially rearranged in most individuals (Rosenberg *et al.*, 1992; Jores and Meo, 1993).

The remainder of the junctional region, encoded by the *BD* gene segment and N region nucleotides, varied in length from 2-13 amino acids. The *TCRBD* genes are highly conserved among different species (Schrenzel *et al.*, 1994) and encode at least one glycine in all three reading frames of the gene. Of the 102 clones analyzed, 70 coded for at least one glycine within the estimated diversity gene region.

In common with the other species examined to date, cattle possess two distinct *TCRBC* genes (*BC1* and *BC2*), which were sequenced and identified as the products of separate loci by Tanaka *et al.* (1990). The location of the *TCRBC*-specific antisense oligonucleotide used in the anchor PCR resulted in the inclusion of 41 bases of the 5'end of the *BC* gene segment in the cloned transcripts. Although the *BC* gene segments show close sequence homology within the coding region, the 5' region can be used to distinguish which of the two genes is being used. The two nucleotides at positions 14 and 15 differ between *BC1* and *BC2*, resulting in a glutamine (CAG) or an arginine (CGC) at the corresponding position in the respective peptide sequences (see Figure 5.13). Examination of the *BC* sequences of 101 clones containing unique transcripts revealed that 60 clones had the codon CGG at this position, which represents a single nucleotide difference from the sequence of either *BC1* or *BC2*, and codes for an arginine. All three sequences were found in clones from animal 5158 (D), whereas only the *BC2* sequence and the variant sequence were isolated from animal 3327 (C). The most likely explanation for these results is that the variant sequence represents an allele of the bovine *BC1* gene segment because, in other species, both *BC* genes are usually expressed. Again, this question can only be resolved by examination of the *BC* sequences at the genomic level.

Table 5.5. Repertoire of *BJ* gene segments expressed in bovine TCR β-chain messenger RNA.

BJ gene segment Amino acid sequence	Number of clones containing *BJ* gene segment (%)			
	C	IC	D	Total
PLHFGIGTRLIVT	3(6.8)	-	1(5.9)	4
DYHFGPGTKLTVV	9(20.4)	9(23.1)	4(23.5)	22
--R----------	1(2.3)	-	-	1
GYHFGPGTKLSVV	1(2.3)	-	-	1
EVFFGKGTRLTVV	1(2.3)	2(5.1)	-	3
-------I-----	1(2.3)	-	-	1
RLYFGNGTKLSVL	2(4.5)	2(5.1)	2(11.8)	6
TQYFGAGTRLSVL	5(11.4)	1(2.6)	-	6
P---------T--*	1(2.3)	-	-	1
EQYFGPGTKLTVL*	4(9.1)	8(20.5)	2(11.8)	14
R----------	1(2.3)	-	-	1
EQHFGPGTRLIVL*	1(2.3)	3(7.7)	-	4
-L----------	-	1(2.6)	-	1
IQYFGPGTRLLVL	1(2.3)	2(5.1)	-	3
QLYFGAGSKLTVL	2(4.5)	-	-	2
P----------*	-	2(5.1)	-	2
PLYFGGGTRLLVL*	9(20.5)	7(17.9)	5(29.4)	21
ELYFGPGTRLQVL	1(2.3)	-	-	1
T----------	-	1(2.6)	3(17.6)	4
ALTFGAGSWLTVV*	1(2.3)	-	-	1
--------R---L	-	1(2.6)	-	1
	44	39	17	100

Notes: The predicted amino acid sequences of the 13 codons preceding the *TCRBC* gene segment in 100 clones are shown in the left-hand column. Sequences differing by only one or two amino acids have been grouped; identical residues are shown as dashes. Single amino acid substitutions at the 5' end of the sequence may be encoded by N region nucleotides. Other differences may be due to the presence of allelic variants or may have arisen through sequencing errors. The sequences identified previously by Tanaka *et al.* (1990) are indicated by asterisks.

A.

```
                    10        20        30        40
                     .         .         .         .
TCRBC1              GATGATCTGAGCCAGGTCCACCCGCCCAAGGTGACTGTGTTCGAA
TCRBC2              ------------GC------------------------------
Variant             ------------G-------------------------------
```

B.

```
                    10
                     .
TCRBC1              DDLSQVHPPKVTVFE
TCRBC2              ----R----------
Variant             ----R----------
```

Figure 5.13. Nucleotide (A) and amino acid (B) sequences of the 5' end of the *TCRBC1* and *TCRBC2* genes identified by Tanaka *et al.* (1990), and the variant sequence identified in the present study.

5.4. Discussion.

The results presented in this chapter have expanded the available data on the extent of the bovine *TCRBV* repertoire. Previous data published by Tanaka *et al.* (1990) identified members of nine bovine *TCRBV* subfamilies, but the small numbers of sequences did not permit a detailed classification. In the present study, sequencing of more than 100 clones resulted in the discovery of 29 new *TCRBV* gene segments, and allowed a classification system for bovine *TCRBV* genes to be established. Seven new subfamilies were identified, on the basis that their sequences showed less than 75% nucleotide similarity to the published bovine *TCRBV* sequences, and closer homology to the corresponding human *TCRBV* subfamilies. Two of the new subfamilies, *BV10* and *BV13*, were multi-membered, each containing 3 distinct sequences; the other five new subfamilies, *BV9*, *BV14*, *BV16*, *BV20* and *BV24*, contained a single member each. In addition, a large number of new members were identified in subfamilies *BV1* and *BV2*, and new single members were assigned to the *BV4*, *BV6*, and *BV17* subfamilies. This brings the total number of bovine *TCRBV* gene segments so far identified to forty-one.

One drawback of examining the TCR repertoire at the level of mRNA expression is the difficulty in distinguishing between allelic variants and closely related subfamily members at distinct loci. This can only be resolved definitively by sequencing and mapping of germline *TCRBV* gene segments. Arden *et al.* (1995a,b), found that *TCRBV* alleles in mice and humans rarely differ by more than 5 nucleotides, while different subfamily members usually differ by at least 10 nucleotides. There are exceptions to this rule, however; for example, the closely related human *BV8S1* and *BV8S2* gene segments differ by only 5 nucleotides (Siu *et al.*,1986) and alleles of the *BV10* gene in mice show 9 base substitutions (Smith *et al.*,1990). In the present study, identical sequences and those that differed by only a few nucleotides were grouped together to provide a consensus sequence and clones identical to the consensus were designated representative of that particular gene segment and used in sequence comparisons. The sequences that differed from the consensus by 1-4 bases may represent allelic variants, or alternatively could have arisen from misincorporation of nucleotides by the DNA polymerase enzyme during the amplification or sequencing reactions. In a few instances, a consensus sequence could also be established for the variant; however in many cases they were represented by only

one or two clones. Sequencing of a larger number of clones from different PCR reactions would be required to verify the variant sequences and eliminate errors.

Sequence errors arising from misincorporation of nucleotides by enzymes could have been introduced at four different stages of the isolation, cloning and sequencing of the bovine *TCRBV* genes. First, errors may have occurred during the synthesis of cDNA by the reverse transcriptase enzyme. Errors may also have arisen during the anchored PCR reaction and the PCR reaction used to amplify cloned inserts for preparation of single-stranded sequencing template. Finally, errors could have occurred during the sequencing reactions performed either with *Taq* DNA polymerase or modified T7 DNA polymerase (Sequenase®).

The majority of errors found in cloned sequences are most likely to have occurred during the amplification of cDNA in the anchored PCR. Ennis *et al.* (1990), in an analysis of errors introduced by *Taq* DNA polymerase during amplification of HLA-A and B alleles, found point mutations, deletions, insertions and recombinant sequences, with point mutations being the most frequent types of error. *In vitro* recombination can arise during the amplification of closely related sequences as a result of incompletely elongated DNA strands annealing to heterologous target sequences, followed by extension and completion in a subsequent cycle. The estimated error rate (mutations per nucleotide per cycle) of *Taq* DNA polymerase varies from 2×10^{-4} during PCR (Saiki *et al.*, 1988) to 2×10^{-5} for point mutations produced during a single round of DNA synthesis of the *lacZα* gene (Eckert and Kunkel, 1990). The fidelity of the enzyme is influenced by a number of variables in the reaction conditions, including the relative concentrations of Mg^{2+} and deoxynucleotide triphosphates (dNTPs), pH and temperature (Eckert and Kunkel, 1993). Recombination between similar sequences is promoted by high initial target DNA concentration, short extension times and a large number of amplification cycles (Meyerhans *et al.*, 1990). In order to anneal to heterologous target sequences, incomplete extension products must compete with the normal oligonucleotide primers for target sequences. The probability of this occurring increases as the ratio of normal PCR primers to target DNA progressively decreases with successive rounds of amplification. The frequency of errors of all types also increases as the number of

amplification cycles increases and so it is desirable to keep the number of cycles to the minimum possible.

Optimal conditions for high fidelity PCR have to be balanced against requirements for efficient amplification. Unfortunately, because of the relatively low efficiency of the anchored PCR, a large number of amplification cycles are required to obtain sufficient DNA for cloning (thirty-five in the present study). A number of modifications to the PCR protocol were introduced when amplifying the *TCRBV* sequences of $CD2^{-}CD8^{+}$ T cells isolated from animal 5158, to try to reduce the number of errors. More *Taq* DNA polymerase was included in the reactions to avoid exhaustion of the enzyme, and it was supplemented with *Taq* Extender, which contains 3'-5' exonuclease (proof-reading) activity, and therefore reduces the rate of nucleotide misincorporation. The extension time at 72°C was increased from one to two minutes to reduce the likelihood of prematurely terminated strands resulting in recombinants. The success of these modifications in reducing the frequency of errors was difficult to assess, however, because the number of clones from this reaction that were sequenced was relatively small. Also, since the sequences were derived from a different animal than the one used with the original protocol, it was difficult to distinguish differences due to expression of another allele in the second animal from those due to PCR error. Nevertheless, some sequences derived from animal 5158 were identical to those found in animal 3327.

In an attempt to minimize errors during the amplification of cloned inserts, the reactions were performed using Vent® DNA polymerase (derived from *Thermococcus litoralis*), an enzyme with 3'-5' exonuclease activity which results in increased fidelity of DNA replication in comparison to *Taq* DNA polymerase (Cariello *et al.*,1991). In a number of clones, sequence from the antisense strand was derived from cycle sequencing of amplified inserts, while sequence from the complementary strand was obtained by directly sequencing plasmid DNA using Sequenase®. In the region in which these sequences overlapped, there were no mismatches found between the bases. Although this comparison was possible only in a relatively small number of clones, it suggests that few errors occurred during PCR amplification of cloned inserts using Vent®. During sequencing reactions, more errors would be expected using cycle sequencing than with

Sequenase, as T7 DNA polymerases have been reported to show higher fidelity than *Taq* DNA polymerase (Cariello *et al.*,1990). However, Koop *et al.* (1993) found almost identical error rates when comparing manual Sequenase™ and automated *Taq* cycle sequencing methods in a large-scale genome sequencing project.

Comparison of the sequences in subfamilies *BV1* and *BV2* with published sequences revealed some anomalies in the published sequences. Alignment of nucleotide sequences of *BV1* subfamily members with BTB18 required a frameshift in all the sequences in order to maximize the alignment, leading to a complete change in 9 amino acids of the deduced protein sequence in this region. The resultant protein sequence of BTB18 eliminated the subgroup-specific residues Arg-64 and Phe-65 found in nearly all other members of the subfamily and in homologous human sequences. This suggests that the anomaly is due to an error in the published sequence of BTB18.

In the *BV2* subfamily, maximal alignment of the sequences most closely related to BTB1 and BTB4 with the published sequences required the introduction of a gap of two base pairs near the 5'end of the published sequences. This resulted in a change in the deduced protein sequence over the first 10-12 residues of the variable region, so that in this region the new sequences were identical to BTB10 at the amino acid level. The protein sequences for BTB4 and BTB1 do not contain a valine or isoleucine at position 4, glutamine at position 6 or proline at position 8, residues that are conserved in almost every TCR Vβ gene segment. However, these residues are found in BTB10 and in the deduced protein sequences of every subfamily member identified in the present study. These findings suggest that the deletion of two nucleotides near the 5' ends of BTB1 and BTB4 may arise from defective mRNA transcripts or are the result of errors in sequencing of these clones.

Comparison of the bovine and human *TCRBV* gene segments confirms the observation made when comparing mouse and human sequences, that members of one subfamily were closer to a human *BV* gene than to members of other bovine subfamilies. Thus, 14 of the 20 mouse *TCRBV* subfamilies share more than 60% identity to their human homologues at the protein level, while a comparison between subfamily members within

a species shows identities below 40% at the amino acid level (Clark *et al.*, 1995; Arden *et al.*, 1995b). The bovine *TCRBV* subfamily members also show greater than 60% identity to their human counterparts at the protein level, except for members of *BV10* (57%) and *BV12* (55%). However, the average amino acid similarity between the genes in different bovine *BV* subfamilies is 50%. In physical maps of the *TCRB* locus in mice and humans, the relative order of the *TCRBV* homologues is highly conserved, although internal duplications have occurred in the human locus (Lai *et al.*, 1988; Rowen *et al.*, 1996). These observations have been cited in support of the hypothesis of trans-species evolution i.e. the retention of ancestral *V* gene segments through speciation. Different species have subsequently used different diversification strategies, including gene duplication and deletion. In contrast to mice, in which the majority of *TCRBV* subfamilies contain a single member, many human *TCRBV* subfamilies are multi-membered, the largest being *BV5* (7 members), *BV6* (9 members), *BV8* (5 members) and *BV13* (8 members) (Arden *et al.*,1995a,b).

The present study shows that many bovine *TCRBV* subfamilies are also multi-membered, but the largest subfamilies are *BV1* and *BV2*, both of which contain a single functional member in humans. Three members of the bovine *BV13* subfamily were identified, while the sequence for bovine *BV6* found here differs from two previously published partial sequences, indicating that this subfamily may also contain at least three members. Bovine homologues of human *BV5* and *BV8* were not identified in this study. These findings suggest that, in comparison to humans and mice, the basic germline *TCRBV* repertoire in the bovine has been diversified by different duplication and/or deletion events following divergence of the species. Interestingly, Schrenzel *et al.* (1994) identified four unique members in the horse *TCRBV2* subfamily, suggesting that duplications involving this gene segment may also be found in species more closely related to cattle.

Previously, Tanaka *et al.* (1990) attempted to estimate the number of members within each bovine *TCRBV* subfamily and to assess polymorphism of the *TCRB* genes by genomic Southern blot analysis using DNA from four different breeds of cattle. No restriction fragment length polymorphisms (RFLP) were identified with two different *BC*-specific probes and eight *BV*-specific probes (*BV2*, *BV3*, *BV4*, *BV6*, *BV7*, *BV12*, *BV15* and *BV17*), after digestion of genomic DNA with two different enzymes (*Pst* I and

Eco RI). However, in another study, four different RFLP alleles were detected in *Taq* I-digested genomic DNA with a single bovine *TCRBV* probe, but the *BV* gene segment to which they corresponded was not determined (Lundén *et al*, 1991). Based on the number of bands observed in Southern blots of genomic DNA hybridized with bovine *BV*-specific probes, Tanaka *et al.* concluded that *TCRBV* subfamilies contain relatively few members. These findings are not in agreement with the present study, in which a total of seven potential members were identified in the *BV2* subfamily, which was one of those examined by Tanaka *et al.* There are a number of possible explanations for this discrepancy. First, the *BV2* subfamily members may be closely linked genes and therefore localized to only one or two restriction fragments. The major fragment of *Pst*I-digested genomic DNA which hybridized to the *BV2*-specific probe in Tanaka's study was 3.4kb long, and therefore could accommodate two, or possibly three, closely linked genes. However, a few additional faint bands were also detected with this probe. Second, the probe may not hybridize to all members of the subfamily with equal efficiency, so that some members would not be detected. This possibility is perhaps less likely, given the close homology between the sequences of the *BV2* subfamily members and the low stringency of the hybridization procedure used in Tanaka's study. Third, some of the unique *BV2* sequences may represent allelic variants encoded at the same locus, reducing the estimated number of separate gene segments. Unless the allelic polymorphisms were associated with specific RFLPs, these variants would localize to the same fragment in the Southern blot. However, the different *BV2* subfamily members differ by nine or more nucleotides, making it more probable that they are products of distinct loci.

Buitkamp *et al.* (1993) investigated germline polymorphisms of the *BV6* gene in a number of artiodactyl species by sequencing of clones following amplification with primers based on the human sequence. In cattle, they identified only one amino acid polymorphism in five individuals representing three different breeds (Simmental, N'Dama and Zebu), and the sequences reported here and by Tanaka *et al.* (1990) were not isolated. This may be because the PCR products selected for sequencing by Buitkamp *et al.* hybridized to a $(CA)_8$ probe designed to detect GT dinucleotide repeats within the intron sequence. Thus, *BV6* gene segments that lack these dinucleotide repeats in the intron, or hybridize inefficiently to the probe, could have been overlooked. Alternatively, since the primers used in the PCR were based on human *BV6* sequences, they may not

hybridize efficiently to all members of the bovine *BV6* subfamily. In support of this, both *BV6S1* (Tanaka *et al.*, 1990) and *BV6S3* (this study) show nucleotide sequence similarities of ~85% to *BV6S2* (Buitkamp *et al.*, 1993), but are much more closely related to one another (93.5% identity at the nucleotide level). This suggests that, following gene duplication, some gene segments diverge more rapidly than others, presumably as a result of selection pressure, but others show a high degree of conservation across species.

In summary, seven new bovine *TCRBV* subfamilies and about 20 new members of previously described subfamilies have been identified using the anchored PCR to amplify the V region of *TCRB* mRNA transcripts. Further sequencing on both strands of a number of clones from different PCR reactions is required to eliminate errors and confirm the sequence variants that differ by only a few nucleotides. The full extent of the bovine *TCRBV* repertoire and the precise definition of alleles and distinct *BV* gene segments awaits the more detailed examination of germline *BV* sequences and mapping of the bovine *TCRB* locus.

CHAPTER SIX

ANALYSIS OF *TCRBV* GENE USAGE IN THE PRIMARY IMMUNE RESPONSE TO *THEILERIA PARVA*.

6.1. Introduction.

As previously discussed, the diversity of the T cell receptor variable regions is generated by the somatic recombination of different *V*, *D* (β and δ chains) and *J* gene segments. Further diversity in the junctional regions is introduced by imprecise joining of gene segments and N region addition of non-germline encoded nucleotides. The pairing of different α and β (or γ and δ) TCR chains results in an estimated 10^{16} potential junctional combinations for the resulting heterodimers (Davis and Bjorkman, 1988). However, the TCR repertoire expressed by peripheral α/β T cells is much more limited than that which would be predicted by completely random association of different gene segments, and is shaped by a variety of influences. Certain *TCRBV* and *TCRBJ* gene segments are preferentially used in all individuals of a species, regardless of their genetic background, although the mechanisms controlling differential expression are unknown (Rosenberg *et al.*, 1992; Jores and Meo, 1993). Germline deletions within the *TCRB* locus, involving the loss of *TCRBV* gene segments, have been found in both laboratory and wild mouse strains and in the human population (Behlke *et al.*, 1986; Pullen *et al.*, 1990a; Zhao *et al.*, 1994). The human *TCRBV* repertoire is limited by various molecular defects that prevent the expression of functional transcripts for a number of *TCRBV* gene segments and alleles (Charmley *et al.*, 1993; Barron and Robinson, 1994; Posnett *et al.*, 1994; Currier *et al.*, 1996). The processes of positive and negative selection during T cell maturation in the thymus also have an important role in shaping the peripheral α/β TCR repertoire. Although it has been shown that the MHC genes have a major influence on the outcome of thymic selection, there is also evidence for the involvement of non-MHC genes (Bill *et al.*, 1988; Fry *et al.*, 1989; Akolkar *et al.*, 1993,1995). In mice, the most striking example of the effect of non-MHC genes on selection of the TCR repertoire is the deletion of subsets of T cells expressing specific Vβ elements by the self-superantigens encoded by endogenous retroviruses (reviewed by Simpson *et al.*, 1993).

Finally, the TCR repertoire may be modified by environmental factors such as exposure to antigens, superantigens or mitogens. In particular, the *TCRBV* repertoire of $CD8^+$ T cells in the PBMC of normal human subjects can be altered by the oligoclonal expansion of $CD8^+$ subsets, presumably in response to infections. These expanded subsets, which express the 'memory' cell marker CD45RO, often persist over long periods of time (Hingorani *et al.*, 1993).

During immune responses to pathogenic organisms, naive T cells are activated following recognition of foreign antigen, i.e. peptides in association with self-MHC molecules, by the TCR. These antigen-specific T cells are clonally expanded to form effector populations of $CD4^+$ Th cells and $CD8^+$ cytotoxic cells. The repertoire of different *V* and *J* gene segments used by the TCR of the responding cells may be restricted or diverse, depending on the specific epitope, the restricting MHC element and the individual TCR repertoire. For example, in mice, T cell clones and lines responding to epitopes from proteins such as cytochrome c, myelin basic protein (MBP) or HLA-Cw3 in the context of a defined MHC molecule express a very limited TCR repertoire (Hedrick *et al.*, 1988; Urban *et al.*, 1988; Casanova *et al.*, 1992). In contrast, highly diverse repertoires are selected in responses to epitopes derived from influenza virus haemagglutinin, *Plasmodium berghei* circumsporozoite protein and tetanus toxin (Taylor *et al.*, 1990; Casanova *et al.*, 1991; Boitel *et al.*, 1992). Similarly, the *in vivo* response to viral infection may be dominated by $CD8^+$ cytotoxic T cells directed against a single immunodominant epitope, i.e. oligoclonal, or polyclonal, depending on the MHC phenotype and the TCR repertoire of the individual (Pantaleo *et al.*, 1994; Burrows *et al.*, 1995; Daly *et al.*, 1995). Oligoclonal expansions in complex mixtures of lymphocytes can be revealed by analysis of CDR3 length and sequence (Pannetier *et al.*, 1995), as perturbations in the TCR repertoire of the whole population are not always evident based on the analysis of V region usage alone. The unique properties of superantigens result in polyclonal activation of T cells bearing a restricted subset of Vβ elements, irrespective of the paired Vα domain or the MHC molecule which presents the superantigen (Kappler *et al.*, 1989). *In vivo*, T cell activation is often followed by clonal deletion or anergy of the superantigen-reactive T cells (Webb *et al.* 1990; MacDonald *et al.*, 1991). A superantigen associated with an infectious agent would be expected to stimulate Vβ-

specific expansion of T cells without clonal restriction or use of conserved CDR3 motifs, in individuals of differing MHC phenotype. In mice infected with MMTV by subcutaneous inoculation or by the oral route, initial marked expansion of superantigen-reactive cells is found in the drainage lymph nodes and Peyer's patches, respectively (Held *et al.*, 1992; Karapetian *et al.*, 1994). In humans, expansions of $V\beta2^+$ T cells in the blood of patients with toxic shock syndrome and Kawasaki syndrome, and over-representation of $V\beta8^+$ T cells in the pleural fluid of individuals with tuberculous pleuritis have been taken as evidence of superantigenic stimulation (Choi *et al.*, 1990b; Abe *et al.*, 1993; Ohmen *et al.*, 1994).

In naive cattle infected with *Theileria parva*, there is a dramatic increase in uninfected T lymphoblasts in the lymph node draining the site of inoculation, coinciding with initial detection of very low numbers of schizonts (as discussed in Chapter 3). One possible explanation for this observation is that a parasite-derived superantigen may be driving the T cell expansion. The aim of this study was initially to determine the normal *TCRBV* repertoire expressed in a peripheral lymph node, and then to compare this with the *TCRBV* repertoire expressed by the responding T cells during *T. parva* infection in the same animal. If expansion of cells expressing a restricted repertoire of *TCRBV* genes were observed, the study could then be extended to individuals with differing MHC haplotypes. In addition, since an unusual subset of $CD2^-CD8^+$ α/β T cells form a significant component of the early T cell response (see Chapter 3), the *TCRBV* repertoire of a purified population of these cells was also examined.

In the absence of monoclonal antibodies to bovine TCR Vβ elements, *TCRBV* expression was examined at the RNA level using the anchored PCR. This technique allows amplification of all the *TCRBV* genes in the T cell population with a single pair of primers, so that even genes for which no sequence information is available are included. Since all sequences should theoretically be amplified with equal efficiency, the frequency with which different sequences are represented in the clones of the amplified product reflect their frequency in the starting mRNA population.

6.2. Materials and Methods.

The methods used for isolation of lymphocytes and responding T cells, and amplification, cloning and sequencing of *TCRBV* genes for repertoire analysis have been described in detail in Chapters 2 and 5.

6.3. Results.

In initial experiments, the *TCRBV* repertoire of the T cell population in a normal resting prefemoral lymph node was determined (animal 3327). This population will be referred to as C below. Subsequently the same animal was infected with *T. parva*, and the drainage lymph node (prescapular) was removed on day 9 of infection. To ensure that changes in the TCR repertoire were not masked by the presence of unactivated T cells, a purified population of T lymphoblasts were obtained from the lymph node cells by two colour indirect immuno-fluorescent staining with monoclonal antibodies to CD3 and MHC class II molecules, and FACS sorting of cells expressing both markers (population IC). As described in Chapter 3, the expansion of a subset of $CD2^-CD8^+$ α/β T cells is a distinctive feature of the lymph node response to primary infections with *T. parva*, and a large proportion of these cells appear to be blasting, based on their large size. This population was purified from the lymph node of a second calf (5158) on day 9 of infection with *T. parva* by two-colour indirect immunofluorescent staining and FACS sorting of $CD2^-CD8^+$ cells (population D). The gates used for sorting are illustrated inFigure 3.1. The purity of the sorted population was 99%.

The *TCRBV* transcripts from each population were amplified by anchor PCR and cloned into a plasmid vector; a random selection of clones were then sequenced to determine the frequency with which different *BV* gene segments were represented in each population. Table 6.1 shows the number of clones from each population that were sequenced and the number that contained functional rearranged *TCRBV-BD-BJ-BC* transcripts. The nature of the inserts in clones that did not contain functional *TCRB* transcripts has been discussed in Chapter 5. The classification of the *BV* genes of functional transcripts into different *TCRBV* subfamilies was also described in Chapter 5.

Table 6.1. Numbers of clones containing functional *TCRB* transcripts in each T cell population.

T cell population	Total no. of clones sequenced	No. of clones containing functional *TCRB* transcripts
C	51	42
IC	57	45
D	26	21
Total	134	108

Only *TCRBV* gene sequences from clones containing functional *TCRB* transcripts were included in the analysis of the frequency of *BV* usage by the different T cell populations. The distribution of the *BV* sequences from each population among the *TCRBV* subfamilies is illustrated in Figure 1. In this analysis, the members of different subfamilies have been grouped together. For multi-membered subfamilies, more detailed information on the frequency of representation of different members in the three cell populations is given in Table 2. A limited number of *BV* subfamilies constituted almost 80% of the repertoire of T cells from a resting peripheral lymph node (*BV1*, *BV2*, *BV10* and *BV24*), while others were rarely used. The presence of multiple members in *BV1* and *BV2* explains the dominant contribution of these subfamilies to the *TCRBV* repertoire. However, none of the gene segments within these populations were predominant, as no more than four copies of any particular gene were isolated.

Comparison of the *TCRBV* repertoire of the normal bovine lymph node T cell population with the repertoire of T lymphoblasts responding to *T. parva* (populations C and IC, respectively) revealed a remarkably similar pattern of *BV* usage in both populations (see Figure 6.1.A and Table 6.2.). The numbers of sequences were too small for meaningful statistical analysis. However, analysis of the *TCRBV* repertoire of T cell blasts purified from the infected lymph node rather than the whole T cell population should markedly

accentuate any differences due to expression of a restricted repertoire by the responding cells. In some instances, small increases in the proportion of certain gene segments (e.g. *BV2.2, BV2.5* or *BV13.3*) in the IC population were due to the repeated isolation of clones containing identical sequences throughout the *V-D-J* region. These probably have arisen from clonal expansion of antigen-specific T cells.

The observation that an unusual subset of $CD2^-CD8^+$ α/β T cells form a substantial component of the primary lymph node T cell response to *T. parva* suggests that these cells are selectively activated as a result of the parasite infection. To rule out the possibility that bystander activation of other T cells was masking the expression of a restricted number of *TCRBV* genes by the $CD2^-CD8^+$ subset, the *BV* repertoire of a purified population of these cells was examined (population D). Although the *TCRBV* repertoire of this population was more restricted than that expressed by T cells in the resting lymph node (C), a broad range of *TCRBV* genes were represented (see Figure 6.1.B and Table 6.2). The most commonly represented subfamilies were *BV1*, *BV2*, *BV6* and *BV10*; however members of *BV3*, *BV7*, *BV9*, *BV12*, *BV13*, *BV17* and *BV24* detected in animal 3327 were not found. Only one member of the *TCRBV2* subfamily (*BV2S3*) was detected in clones derived from $CD2^-CD8^+$ T cells. It is possible that the explanation for the more restricted repertoire of the $CD2^-CD8^+$ T cells is that sequence analysis was carried out on a smaller number of clones derived from this population, than from C or IC. Despite the variation in the expression of individual *BV* genes between populations C and D, the differences may reflect the differing genetic background (particularly the MHC phenotype) of the calves rather than changes brought about by the response to infection. Thus, there was no evidence of restricted *TCRBV* gene usage in the $CD2^-CD8^+$ α/β T cell population involved in the *in vivo* response to *T. parva*.

Table 6.2. Comparison of the distribution of *TCRBV* genes among different subfamilies in T cell populations C, IC and D.

T cell population	C		IC		D	
TCRBV gene segment	No. of clones	%	No. of clones	%	No. of clones	%
BV1S1	2	4.8	2	4.4	-	-
BV1S2	1	2.4	1	2.2	2	9.5
BV1S3	3	7.1	2	4.4	1	4.7
BV1S4	3	7.1	1	2.2	-	-
BV1S5	3	7.1	-	-	-	-
BV1S6	1	2.4	3	6.7	2	9.5
BV1S7	-	-	2	4.4	1	4.7
BV1S8	1	2.4	-	-	1	4.7
BV1S9	-	-	3	6.7	1	4.7
BV1S10	1	2.4	-	-	-	-
BV1S11	1	2.4	-	-	-	-
BV2S1	2	4.8	2	4.4	-	-
BV2S2	-	-	3	6.7	-	-
BV2S3	1	2.4	2	4.4	3	14.3
BV2S4	1	2.4	2	4.4	-	-
BV2S5	2	4.8	-	-	-	-
BV2S6	4	9.5	-	-	-	-
BV2S7	-	-	1	2.2	-	-
BV3S1	1	2.4	1	2.2	-	-
BV4S2	-	-	-	-	1	4.7
BV6S3	-	-	1	2.2	3	14.3
BV7S1	1	2.4	1	2.2	-	-
BV9S1	1	2.4	-	-	-	-
BV10S1	2	4.8	2	4.4	-	-
BV10S2	2	4.8	-	-	-	-
BV10S3	-	-	-	-	2	9.5
BV12S1	-	-	2	4.4	-	-

Table 6.2. Comparison of the distribution of *TCRBV* genes among different subfamilies in T cell populations C, IC and D (continued).

T cell population	C		IC		D	
TCRBV gene segment	No. of clones	%	No. of clones	%	No. of clones	%
BV13S1	1	2.4	2	4.4	-	-
BV13S2	1	2.4	1	2.2	-	-
BV13S3	-	-	2	4.4	-	-
BV14S1	1	2.4	1	2.2	1	4.7
BV15S1	-	-	-	-	1	4.7
BV15S2	1	2.4	1	2.2	-	-
BV16S1	-	-	-	-	1	4.7
BV17S2	-	-	2	4.4	-	-
BV20S1	2	4.8	1	2.2	1	4.7
BV24S1	3	7.1	2	4.4	-	-

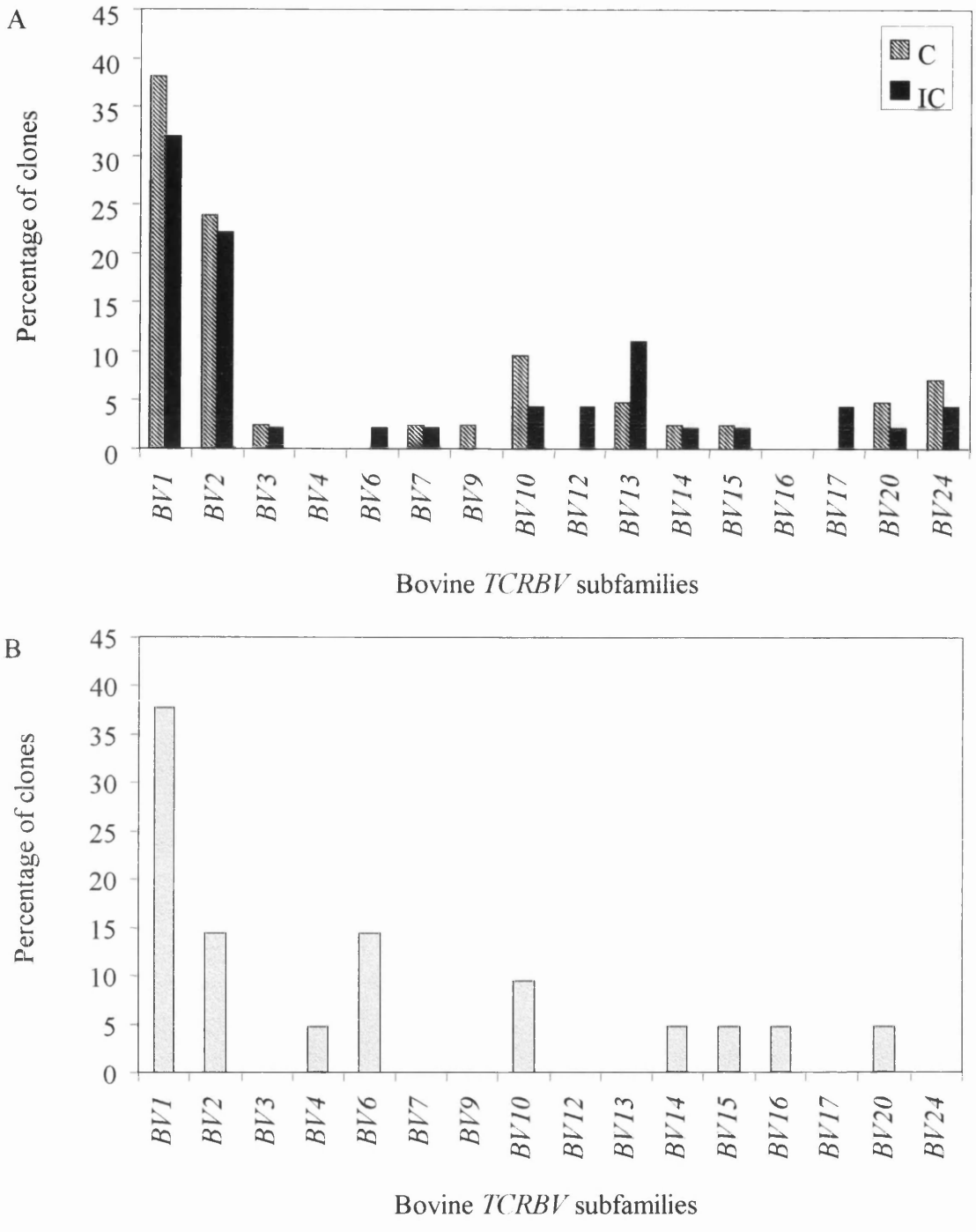

Figure 6.1. Comparison of *TCRBV* genes used in the primary immune response to *T. parva* with the *TCRBV* repertoire expressed in a normal lymph node. A: *TCRBV* sequences expressed by T cells from a normal peripheral lymph node of animal 3327 were amplified in the anchored PCR, cloned and sequenced. The frequencies with which different *TCRBV* subfamilies were represented among the clones are shown (C). A similar analysis was performed on T cell blasts isolated from the drainage lymph node of the same animal during infection with *T. parva* (IC). B: the $CD2^{-}CD8^{+}$ subset of T cells was purified from the drainage lymph node of another calf undergoing infection with *T. parva*, and the *TCRBV* repertoire expressed by these cells was analysed as above.

6.4. Discussion.

This study has established the normal *TCRBV* repertoire expressed by bovine T cells in the resting peripheral lymph node of one individual, providing a basis for comparison with the repertoire of *TCRBV* genes used by T cells participating in the primary lymph node response to *T. parva*. Expression of eleven *TCRBV* subfamilies was detected in the resting lymph node T cell population; however only four subfamilies (*BV1*, *BV2*, *BV10* and *BV24*) constituted almost 80% of the repertoire. This is consistent with studies in mice and humans, where a limited number of *TCRBV* subfamilies dominate the normal repertoire (Okada and Weissman, 1989; Rosenberg *et al.*, 1992; Malhotra *et al.*, 1992). The dominance of the *BV1* and *BV2* subfamilies in the bovine *TCRBV* repertoire is explained by the existence of multiple members of these subfamilies, as discussed in Chapter 5. Examination of the T cell population activated in the drainage lymph node during primary infection with *T. parva* revealed that these cells express an unrestricted repertoire of *TCRBV* genes. The overall pattern of expression was very similar to that found in the uninfected lymph node. In three cases, identical *TCRBV-BD-BJ-BC* transcripts were isolated from more than one clone, suggesting antigen-specific clonal expansion of certain T cells; however these expansions were insufficient to cause significant perturbation of the *TCRBV* repertoire. Surprisingly, the $CD2^-CD8^+$ T cell subpopulation that appears to be activated specifically in reponse to infection with *T. parva* also expresses a diverse repertoire of *TCRBV* gene segments. Although these cells were isolated from a different individual, the overall pattern of *TCRBV* gene usage was similar to that found in the resting lymph node T cell population. The differences that occur can probably be accounted for by inter-individual variation in the expression of different subfamilies, and differences in the *TCRBV* repertoire expressed by $CD4^+$ and $CD8^+$ T lymphocytes, which have previously been reported in man (Hawes *et al.*, 1993).

Various methods have been employed in the analysis of the TCR repertoire of mice and humans, including flow cytometry using Vβ-specific monoclonal antibodies (Akolkar *et al.*, 1993; Braun *et al.*, 1995), semi-quantitative PCR with Vβ subfamily-specific primers (Choi *et al.*, 1989; Genevée *et al.*, 1992), RNase protection assays (Okada and Weissman, 1989; Singer *et al.*, 1990), and anchored PCR (Rosenberg *et al.*, 1992;

Sarukhan *et al.*, 1994). The latter technique was the method of choice for the present study because no bovine Vβ-specific monoclonal antibodies are available and there was insufficient sequence information to generate a panel of Vβ-specific primers that would cover the entire bovine *TCRBV* repertoire. The disadvantages of using this technique are the possibility of introducing biases during PCR amplification, and the possibility that levels of mRNA expression may not correlate with surface expression of protein. While the occurrence of biases in the present study cannot be definitely ruled out without an independent method of verification of the *TCRBV* repertoire, the fact that a large number of different *BV* and *BJ* gene segments were represented in the amplified sequences suggests that this is not the case. The failure to identify members of certain subfamilies may merely reflect a low level of expression in the individuals studied, which would be revealed by sequencing larger numbers of clones. Two previous studies involving the use of anchored PCR to analyse the human TCR repertoire have demonstrated good correlation between the results obtained by this method and analysis using monoclonal antibodies (Loh *et al.*, 1989; Rosenberg *et al.*, 1992); however, due to limited availability of monoclonals, this verification was possible only for one or two Vβ regions. More recently, the use of anchored PCR to examine the *BV* repertoire of non-obese diabetic mice was validated by comparison with the results obtained by flow cytometry using a panel of eleven Vβ-specific monoclonal antibodies. There was close correlation between the estimates of the level of expression of different *BV* genes obtained using these methods, confirming that anchored PCR was a reliable tool for examination of the *TCRBV* repertoire (Sarukhan *et al.*, 1994).

The anchored PCR has a number of advantages over other techniques for analysis of the TCR repertoire. The amount of starting material required is small, which was important in this study, as the yield of cells obtained from sorting could be limiting. Sequence analysis allowed identification of individual subfamily members, whereas in most semi-quantitative PCR techniques, Vβ-specific primers amplify all subfamily members (Genevée *et al.*, 1992; Hall and Finn, 1992), and many monoclonal antibodies recognise more than one subfamily member. This is potentially significant in the investigation of superantigen responses, as there are examples of superantigens that selectively interact with only one subfamily member (Kappler *et al.*, 1988). It is particularly relevant in the

present study because of the large number of members identified in subfamilies *BV1* and *BV2*. In addition, this technique allows analysis of CDR3 sequences and *BJ* gene usage which can be useful in distinguishing superantigen-reactive T cells from oligoclonal expansions of antigen-specific T cells. Transcripts resulting from non-functional rearrangements can also be identified and excluded from the analysis.

The pattern of *TCRBV* gene usage by T cells activated in the drainage lymph node during primary infection with *T. parva* is inconsistent with a response to a superantigen or to a highly immunodominant peptide antigen. Responses to superantigens *in vivo* have been most extensively studied in mice. Initial experiments involving intravenous administration of staphylococcal enterotoxin B (SEB) or cells expressing endogenous mouse mammary tumour virus (MMTV) superantigens demonstrated a marked expansion of specific Vβ T cell subsets in the spleen and lymph nodes followed by deletion and anergy of these cells (Webb *et al.*, 1990; MacDonald *et al.*, 1991). However, neither of these models can be applied to the role of superantigens during a natural infection. Mice inoculated subcutaneously with exogenous MMTV also show marked expansion of superantigen-reactive $CD4^+$ T cells (approximately five-fold increase in absolute numbers) in the drainage lymph node (Held *et al.*, 1992). Similarly, in neonatal mice infected with MMTV by the natural route (orally), expansion of Vβ-specific T cells can be demonstrated in the intestinal Peyer's patches as early as 5 days after birth (Karapetian *et al.*, 1994). It should be noted that in all the studies mentioned above, expansions of superantigen-reactive cells were detected in the whole lymph node population by two-colour flow cytometric analysis using mAbs against CD4 and/or CD8 and specific Vβ elements, without prior enrichment of blasting cells. In humans, superantigen-mediated T cell activation and deletion associated with infectious disease has been more difficult to investigate. However, expansions of Vβ2-bearing T cells have been found in the peripheral blood of a number of patients with toxic shock syndrome, corresponding to the phenotype of T cells responding to the staphylococcal toxin TSST-1 *in vitro* (Choi *et al.*, 1989,1990b). Expansions of $V\beta2^+$ and $V\beta8.1^+$ T cells exhibiting extensive junctional region diversity have also been found in the circulation during the acute phase of Kawasaki disease, a disease of unknown aetiology with many clinical features similar to toxic shock syndrome (Abe *et al.*, 1993). Once again, these perturbations in the TCR

repertoire were evident from examination of whole PBMC rather than a selected responding population, although they were more variable and not as striking as those observed during MMTV infection.

Dramatic expansion of T cells expressing a restricted *TCRBV* repertoire can also be found in infections where there is no involvement of superantigens. For example, during the acute phase of infection with HIV, marked expansion of $CD8^+$ cytotoxic T cells bearing a restricted subset of Vβ subfamilies is sometimes found in the peripheral blood. In an extreme example, 40% of PBMC in one individual were found to express Vβ19 at the peak of the response to acute infection (Pantaleo *et al.*, 1994). However, in an outbred population, the TCR Vβ usage of the dominant clones in such a response will vary according to the MHC phenotype and TCR repertoire of the individual (Burrows *et al.* 1995; Daly *et al.*, 1995). The conservation of CDR3 length and sequence in the TCR of responding cells can also help to distinguish these responses from those driven by superantigens. In fact, such dramatic expansions of antigen-specific T cells are rarely found and oligoclonal expansions have been detected mostly at the level of the diseased tissue, for example, in autoimmune diseases (Oksenberg *et al.*, 1990; Howell *et al.*, 1991) and chronic infections such as leprosy (Wang *et al.*, 1993b). Even when cytotoxic T cells can be detected at a high frequency in peripheral blood and are dominated by clones expressing a highly restricted TCR repertoire, e.g. during infections with HIV or EBV, there may be no obvious expansion of the relevant Vβ families relative to the overall repertoire (Silins *et al.*, 1996).

The diverse repertoire of *TCRBV* genes expressed by T cell blasts isolated from the drainage lymph node during infection with *T. parva* suggest that the parasite induces polyclonal T cell activation. Since protozoa are much more complex organisms than viruses, multiple T cell immunostimulatory peptides may be generated from different proteins, leading to stimulation of a large number of naive T cells with a highly diverse *TCRBV* repertoire. Another possibility is that the close similarity between the *TCRBV* repertoire expressed by the responding cells and that of the normal lymph node T cell population may be due to mitogenic activity associated with one or more parasite molecules, causing antigen-independent activation of the majority of T cells.

Interestingly, human T cells within the $CD45RO^+$ ('memory') population proliferate strongly in response to *Plasmodium falciparum* antigens despite lack of previous exposure to the parasite (Jones *et al.*, 1990). Parasite-specific T cell clones generated from non-immune individuals have been shown to cross-react with common environmental micro-organisms (Currier *et al.*, 1995) and express a diverse repertoire of *TCRBV* segments (Fell *et al.*, 1996). Similarly, the strong proliferative response of human PBMC from naive individuals to *in vitro* stimulation with *Trypanosoma cruzi* is also dominated by T cells expressing a diverse TCR repertoire (Piuvezam *et al.*, 1993). This suggests that polyclonal activation of T cells expressing an unrestricted repertoire of *TCRBV* genes may be a common feature of infections with a number of different protozoan parasites. However, recently evidence has been put forward for the existence of a superantigen associated with *Toxoplasma gondii* (Denkers *et al.*, 1994,1996). *In vitro* stimulation of non-immune splenocytes with intact tachyzoites or soluble antigen induced strong proliferative responses and selective expansion of $CD8^+$ T cells expressing Vβ5. The response was not MHC restricted and did not depend on antigen processing. Although dramatic increases in T cell numbers were not observed in mice during the acute phase of infection with *T. gondii*, moderate increases in the proportion of $V\beta5^+$ cells were found, and in chronic infections this subset exhibited specific non-responsiveness

In summary, the present study of the *TCRBV* repertoire expressed by cells involved in the blast response observed in the drainage lymph nodes of cattle undergoing primary infections with *T. parva* provides no evidence for stimulation by a superantigen. Analysis of purified populations of responding cells, both T cell blasts and the $CD2^-CD8^+$ α/β T cell subset, revealed expression of a diverse *TCRBV* repertoire that was very similar to that of the normal T cell population of a resting lymph node. This suggests that the response is directed against a number of different epitopes derived from one or more parasite antigens, resulting in polyclonal stimulation of T cells, or alternatively, that the parasite may possess a mechanism for antigen-independent T cell activation.

CHAPTER SEVEN

GENERAL DISCUSSION.

Infection of susceptible cattle with the protozoan parasite *Theileria parva* results in an acute lymphoproliferative disease characterized by lymphadenopathy and fever, the outcome of which is invariably fatal. Previous studies of experimentally infected cattle revealed a massive increase in the cellularity of the lymph node draining the site of the inoculation in the early stages of the infection, at a time when the proportion of schizont-infected cells in the node was very low (Morrison *et al.*, 1981). The increased cellularity was associated with a widespread increase in the numbers of lymphoblasts within the node. These results suggested that an immune response to the parasite occurs in the regional lymph nodes of naïve animals, but is ineffective in controlling the rapid multiplication of parasitized cells. However, the precise phenotype of the blast cells involved in the response, and possible mechanisms for widespread lymphocyte activation associated with parasite infection, have not been investigated. The objective of this study was to characterize the primary immune response in the drainage lymph nodes of cattle infected with *T. parva*, with a particular emphasis on determining whether or not a parasite superantigen is involved. The experiments carried out during the study led to four significant findings:

1) An unusual $CD2^-CD8^+$ subset of α/β T cells forms a major component of the lymph node response to *T. parva* in susceptible animals. The phenotype of the responding cells in the drainage lymph nodes of infected cattle was investigated using a combination of flow cytometry and immunocytochemical staining of lymph node sections. In most animals, $CD8^+$ T lymphocytes formed a large proportion of the responding cells. Most notably, a subset of $CD8^+$ T cells that lacked expression of CD2 was found in all the animals studied. These cells were assumed to express the α/β TCR because they all expressed CD3, and most of them were negative for the γ/δ TCR. The appearance of this subset coincided with the initial detection of parasites in the node at about day 7 post-infection, and they reached a peak of up to 30% of the lymph node mononuclear cell population. However, their numbers declined rapidly as the proportion of parasitized cells increased. In contrast to the response *in vivo*, the response of PBMC

from naïve animals to *in vitro* stimulation with autologous parasitized cells was dominated by γ/δ T cells, and cells with the phenotype $CD2^-CD8^+\alpha/\beta$ TCR^+ were not detected. An *in vitro* model for studying the stimulatory requirements of these cells was therefore not available.

2) The lymph node response to *T. parva* also involves a large influx of macrophages. Another interesting feature of the response to *T. parva* within the regional lymph node was the accumulation of large numbers of macrophages in the cortical region from day 7 to day 9 post-infection. These cells were characterized by expression of CD14, CD11b, and a molecule (MyD-1) found on bovine monocytes/macrophages and dendritic cells, and had an active lysosomal system, revealed by staining for the enzyme acid phosphatase. Macrophages play an important role in host resistance to a number of protozoan parasites, particularly during primary infections. However, in the case of *T. parva*, this population of macrophages is clearly ineffective in inhibiting parasite replication and preventing the progression of the infection.

3) New data on the bovine *TCRBV* repertoire was obtained. The *TCRBV* repertoire expressed at the mRNA level in normal lymph node T cells was established by anchored PCR and sequencing. Nine bovine *TCRBV* subfamilies (*BV1*, *BV2*, *BV3*, *BV4*, *BV6*, *BV7*, *BV12*, *BV15* and *BV17*) were previously defined by Tanaka *et al.* (1990). In the present study, expression of 37 different *TCRBV* gene segments was detected, 29 of which were identified for the first time. Using this data and the previously published sequences, a classification system for bovine *TCRBV* gene segments was devised, in which subfamilies were named according to the human *BV* genes to which they showed closest homology. A further seven *TCRBV* subfamilies were defined, with a total of 11 members (*BV9*, *BV10*, *BV13*, *BV14*, *BV16*, *BV20* and *BV24*); the remaining 18 new sequences were assigned to the existing *BV1*, *BV2*, *BV4*, *BV6* and *BV17* subfamilies. A large number of the new gene segments were classified as members of the *BV1* and *BV2* subfamilies, indicating that considerable diversification of the bovine *TCRBV* repertoire has occurred by duplication of these genes, whereas the homologous genes in humans and mice form single-member subfamilies. It is probable that, although further *TCRBV* gene segments remain to be discovered, that the genes identified in this study and by Tanaka *et al.*

(1990) form the major proportion of the expressed repertoire. This information and the reagents that have been generated will be useful in future studies of bovine immune responses. It should be possible to develop a panel of *BV*-specific primers, similar to those used in many studies of the human TCR repertoire, for use in a semi-quantitiative PCR to examine *TCRBV* usage by T cells involved in the immune responses to infectious agents. The sequence information can also be used to develop *BV*-specific probes and primers for mapping and sequencing of the germline *TCRBV* loci.

4) The lymph node T cell response is polyclonal and does not involve a superantigen. The possibility that a superantigen might be triggering T cell activation in the drainage lymph node of *T. parva*-infected animals was investigated by examining the *TCRBV* repertoire expressed by the responding cells. Analysis of the *TCRBV* repertoire expressed by purified populations of activated $CD3^+$ cells and $CD2^-CD8^+$ T cells showed no evidence for the restricted usage of a subset of *TCRBV* gene segments. The T cell response to *T. parva* in the drainage lymph node is therefore unlikely to be stimulated by a parasite-derived superantigen.

Although this study has provided some interesting observations relating to the lymph node responses of cattle undergoing primary infection with *T. parva*, it was not possible to determine the mechanisms governing these processes. There is no suitable model for the disease in a laboratory animal species, which restricts the scope of *in vivo* investigations because of the relative lack of immunological reagents for cattle, and the constraints placed on the number of animals that may be used by economic and welfare considerations. In addition, immune responses in an outbred population are more variable so that, in combination with the small numbers of animals sampled, it may be difficult to attach statistical significance to the observations made. Under these circumstances, it is desirable to attempt to reproduce the response *in vitro*, so that an understanding of the underlying mechanisms can be gained from studies in a controlled environment, and tested in future *in vivo* experiments.

In the current study, it was a consistent observation in all infected animals that a subset of α/β T lymphocytes with the phenotype $CD2^-CD8^+$ were involved in the primary lymph node response to *T. parva*, although their numbers varied considerably in different individuals. The appearance of the $CD2^-CD8^+\alpha/\beta$ T cell subset is intriguing because cells with a similar phenotype have not been reported to participate in immune responses in other species, and

there is therefore no previous information from which their function may be inferred. Using a sensitive limiting dilution assay, both the $CD2^-CD8^+$ and the $CD2^+CD8^+$ fractions of efferent lymph lymphocytes from *T. parva*-infected animals were shown to contain very low frequencies (less than 1:20000) of cytotoxic precursors, capable of killing both autologous and allogeneic infected target cells (Taracha, 1991). Therefore, despite the $CD8^+$ blast cell response between days 7 and 10 post-infection, a normal cytotoxic T cell response is not induced in primary infections with *T. parva*. However, it is possible that the $CD2^-CD8^+$ T cell subset may exert an effector function through the secretion of cytokines. Studies of the small numbers of $CD2^-CD8^+$ T cells purified from the lymph nodes of infected animals revealed that they expressed mRNA for IFNγ and, to a lesser extent, IL-10, and a diverse repertoire of *TCRBV* genes. The latter observation suggested that these cells were not responding to a parasite superantigen.

In contrast to $CD2^+CD8^+$ T cells, the $CD2^-CD8^+\alpha/\beta$ T cells isolated from infected animals were refractory to stimulation *in vitro*, and cells with this phenotype were not generated by *in vitro* stimulation of PBMC with autologous parasitized cell lines. The failure to generate cell lines prevented the functional characterization of these cells using *in vitro* assays, so that important questions relating to their possible role in pathogenesis could not be addressed. The explanation for the non-responsiveness of $CD2^-CD8^+$ cells *in vitro* may be that these cells are anergic or committed to programmed cell death in the activated state, or that appropriate conditions for stimulation of the cells were not reproduced *in vitro*. While the possibility that this subset arises as the result of downregulation of CD2 expression on activated $CD8^+$ T lymphocytes cannot be excluded, it seems more likely that a small pre-existing population of cells is expanded during infection with *T. parva*, as discussed previously. Since $CD2^-CD8^+$ T cells were not detected in peripheral blood, the precursors of this subset may be localized within the lymph nodes. Further work is needed to establish whether suitable conditions can be found for *in vitro* expansion of these cells from lymph node preparations, using parasitized stimulator cells.

The failure to demonstrate that T lymphoblasts were responding to a superantigen does not rule out the possibility that *T. parva* has an alternative mechanism for inducing non-specific T cell activation, with similar effects on pathogenesis in terms of the potential for cytokines to promote the proliferation of parasitized cells. As discussed previously, other protozoan

parasites such as *Plasmodium falciparum* and *Trypanosoma cruzi* are capable of inducing strong proliferative responses in T lymphocytes from naïve individuals independently of a superantigen. In the case of *P. falciparum*, the high frequency of T cells responding to the parasite is due to activation of cross-reactive memory $CD4^+$ cells. Other possible mechanisms by which the parasite might induce potent T cell responses are through expression of a molecule with mitogenic properties or presentation of multiple immunostimulatory epitopes.

In the present study, investigation of the role of cytokines in the pathogenesis of the infection was hampered by lack of reagents. The "background" expression of cytokines in the lymph nodes of apparently healthy cattle made it difficult to assess exactly which cytokines were produced in the response to infection. In addition, the lack of a quantitative technique to determine the relative levels of expression of various cytokines prevented predictions about their potential influence on the outcome of infection. The observation that efferent lymph plasma from an infected animal produced enhanced proliferation of a parasitized cell line suggests that soluble factors (presumably cytokines) which have a positive effect on parasite growth were released by responding cells in the lymph node. However, in the absence of ELISA assays for different bovine cytokines, and monoclonal antibodies capable of neutralizing their activity, it was not possible to identify which cytokines were responsible for this effect. In mouse models of disease, it is also possible to assess the influence of different cytokines on the outcome of infection *in vivo* by injecting neutralizing antibodies to individual cytokines or their receptors, or using transgenic mice with targeted disruption of specific cytokine genes ("knockout" mice). Such studies are much more difficult in cattle because, even when suitable reagents are available, large quantities may be required to produce the desired effect.

The failure to generate an effective immune response during primary infections with *T. parva* may also be due to inappropriate antigen presentation. Normally, T cell responses are initiated by "professional" antigen presenting cells that originate in the infected tissue and take up antigen by macropinocytosis. These cells then migrate to the regional lymph nodes and upregulate expression of costimulatory molecules, to become the mature interdigitating dendritic cells of the paracortical T cell areas. They are capable of inducing the activation of naïve $CD4^+$ and $CD8^+$ T lymphocytes circulating through these areas, leading to their differentiation into effector cells. In the case of *T. parva*, however, it is most likely that

infected lymphocytes act as antigen presenting cells in the drainage lymph node. It is not known whether costimulatory molecules are expressed on parasitized lymphoblasts but, by analogy with activated B and T cells of other species, they would be expected to upregulate expression of B7 molecules. They would therefore theoretically be capable of inducing activation of naïve T cells. However, differences in the level of expression of costimulatory molecules or the range of cytokines produced by the parasitized lymphocytes might influence the type of response that is generated. One possible explanation for the predominance of $CD2^{-}CD8^{+}$ T cells in the primary response to *T. parva* could be that these cells are able to respond to parasite antigens presented by lymphocytes, while conventional naïve $CD4^{+}$ and $CD8^{+}$ T cells have a strict requirement for antigen presentation on dendritic cells. The different anatomical location of the antigen-presenting cells may also have an influence on the type of cells that respond. The distribution of schizont-infected cells and lymphoblasts in the regional lymph nodes at different time points after infection suggests that the response is initiated in the medullary region, and later involves the paracortical and cortical regions as the infection progresses.

The presence of large numbers of macrophages in the cortical regions of the drainage lymph nodes of *T. parva*-infected cattle may result from migration of macrophages from an inflammatory focus at the site of stabilate inoculation in the skin, or recruitment and activation of monocytes from the peripheral blood. The observation of an increased proportion of monocytes in PBMC, coinciding with the increased numbers in the lymph node, suggests that the latter is the more likely explanation. Extravasation of monocytes into sites of inflammation occurs by a process of chemotaxis in response to a range of chemoattractant molecules, such as the chemokines MCP-1 and RANTES (Strieter *et al.*, 1996). Chemokines are synthesized by macrophages themselves, but also by endothelial cells, keratinocytes, and fibroblasts, and in some instances by activated T cells. It is possible only to speculate on the role of macrophages in *T. parva* infections. Macrophage activation can be induced by IFNγ and is characterized by increased expression of MHC molecules and costimulatory molecules, production of cytokines, and increased microbicidal activity mediated, for example, by reactive oxygen intermediates. The results of RT-PCR have demonstrated that mRNA for IFNγ and TNFα (which synergizes with IFN□ in macrophage activation) are found in the drainage lymph nodes of cattle infected with *T. parva*. Therefore, the conditions necessary for macrophage activation do potentially exist within the infected nodes. However, the presence

of macrophages is not sufficient to prevent the progress of the infection, suggesting that the microbicidal mechanisms of the macrophages may be ineffective against *T. parva*. Alternatively, the macrophages could be contributing to the pathogenesis of the infection in a number of ways. The oxygen metabolite NO is an important mediator of parasiticidal mechanisms by murine macrophages; however, NO also suppresses normal antigen-specific T cell responses, particularly in the Th1 $CD4^+$ subset (Liew, 1995). Spontaneous synthesis of NO by PBMC has been demonstrated during infections of naïve cattle with *T. parva* (Visser *et al.*, 1995), suggesting that large quantities of NO are being produced by monocytes. Activated macrophages also produce a range of cytokines including IL-1, IL-6, IL-12, TNFα and IFNα some of which may be able to potentiate the proliferation of parasitized cells.

It is clear that the primary immune response to *T. parva* in the regional lymph nodes of cattle involves complex cellular interactions, and further studies are essential to gain an understanding of the mechanisms governing the response and its effects on the outcome of infection. The complexity of the response and the practical difficulties associated with *in vivo* experiments in cattle mean that the most fruitful approaches will be through the development of appropriate *in vitro* models.

The $CD2^-CD8^+$ T cells could be relevant to the pathogenesis of the infection in a number of different ways. They may produce cytokines capable of promoting the proliferation of parasitized cells, or they may be able to suppress the generation of normal T cell responses. Alternatively, they could represent a component of the innate immune system, analogous to NK cells, which are rapidly activated on their first encounter with a pathogen, and mediate the recruitment and activation of macrophages. Although this would be an effective means of controlling the initial replication of many bacterial or parasitic pathogens in non-immune individuals, it may not be an appropriate response against *T. parva*. The intracellular location of the parasite within healthy, actively dividing lymphocytes would effectively allow it to evade phagocytosis by macrophages. In addition, as discussed above, the presence of large numbers of activated macrophages in the lymph nodes could actually have a detrimental effect on the generation of normal immune responses.

Development of methods to culture $CD2^-CD8^+$ cells *in vitro* would allow several important questions relating to these hypotheses to be addressed. For example: What are the

requirements for antigen recognition and activation of these cells? Which cytokines do they produce (including chemokines capable of recruiting macrophages)? What are the effects of co-culture of $CD2^-CD8^+$ T cells with macrophages? The role of macrophages could be further investigated by isolating these cells from the lymph nodes of infected animals, and examining their state of activation, the cytokines they secrete, and their production of NO. In addition, the influence of both $CD2^-CD8^+$ T cells and macrophages on the growth of parasitized cells and the induction of immune responses could be studied using *in vitro* co-culture techniques. Experiments to investigate the expression of costimulatory molecules by infected lymphocytes, and to examine the responses they induce in purified $CD4^+$ and $CD8^+$ T cell subsets *in vitro*, might shed light on their potential for effective antigen presentation *in vivo*.

In summary, the results presented in this study support the view that cattle undergoing primary infections with *T. parva* mount an abnormal immune response that is not capable of controlling the infection. It has been established, by analysis of the *TCRBV* repertoire of the responding T cells, that the response is not provoked by the action of a superantigen. The observation of large numbers of $CD2^-CD8^+$ α/β T cells and macrophages in the regional lymph nodes of infected cattle has raised intriguing questions for future investigation.

Appendix A. Solutions used for Leucocyte Isolation and Culture.

A.1. Phosphate buffered saline (PBS)

NaCl	0.17M
KCl	3.4mM
Na_2HPO_4	9.2mM
KH_2PO_4	1.8mM
pH 6.8	

A.2. Alsever's solution

Citric acid	2.9mM
D-glucose	113.8mM
NaCl	71.9mM
Trisodium citrate	27.2mM

A.3. Standard culture medium

RPMI 1640 medium with Glutamax (Gibco BRL)
25mM HEPES
10% foetal bovine serum
100U/ml penicillin
100µg/ml streptomycin

A.4. Medium for proliferation assays

RPMI 1640 medium with Glutamax (Gibco BRL)
25mM HEPES
10% foetal bovine serum
5×10^{-5}M 2-mercaptoethanol (Sigma)
100U/ml penicillin
100µg/ml streptomycin

A.5. Sheath fluid for FACScan analysis.

PBS filtered through a 0.2µm filter

B. Solutions used for Preparation and Examination of Lymph Node Sections.

B.1. Fixatives.

B.1.1. Neutral buffered formalin

NaH_2PO_4	375mM
Na_2HPO_4	387mM
NaCl	1.45M

- dissolved in formaldehyde (40% w/v)

B.1.2. Mercuric formalin

- 9 parts saturated mercuric chloride solution and 1 part formaldehyde (40% w/v)

B.2. Solutions used for *in situ* hybridization.

All solutions were made using water treated with diethyl pyrocarbonate (DEPC) and glassware baked at 180°C for 4h to avoid contamination with ribonucleases (RNases).

B.2.1. Preparation of DEPC-treated water

- sterile double distilled water (DDW) was treated with 0.02% v/v DEPC (Sigma) at room temperature overnight, then autoclaved at 15lb/in^2 for 15min to inactivate DEPC

B.2.2. 20X SSC

NaCl	3M
Sodium citrate	300mM
pH 7.0	

B.2.3. Buffer 1

Tris-HCl, pH 7.5	100mM
NaCl	150mM

B.2.4. Buffer 2

Maleic acid	100mM
NaCl	150mM
pH 7.5	

B.2.5. Buffer 3

Tris-HCl, pH9.5	100mM
NaCl	100mM
$MgCl_2$	50mM

B.2.6. Preparation of salmon sperm DNA.

- the salmon sperm DNA (Sigma) was dissolved in water to a concentration of 10mg/ml. DNA was sheared by passing it several times through an 18 gauge hypodermic needle, then boiled for 10min, and stored in aliquots at -20°C. Immediately prior to inclusion on the hybridization solution, the DNA was denatured by heating at 95°C for 5min.

B.2.7. Hybridization mixture.

Formamide (Gibco BRL)	5ml
50% w/v dextran sulphate (Sigma)	1ml
20X SSC	1ml

NB. High molecular weight (i.e. >500 000) dextran sulphate was used.

B.2.8. Blocking buffer.

Bovine serum albumin (BSA)	3% w/v
Triton X-100	0.05% v/v

- dissolved in buffer 1

B.2.9. Gelatin mountant (Kaiser jelly).

Gelatin	10g
Sodium azide	0.17g
Solid phenol	0.25g
Glycerol	70ml
DDW	60ml

C. Reagents for Molecular Biology.

C.1. Reaction buffers.

C.1.1. 10X reverse transcriptase buffer (Promega)

Tris-HCl, pH8.3	500mM
KCl	500mM
$MgCl_2$	100mM
Spermidine	5mM
Dithiothreitol (DTT)	100mM

C.1.2. 10X PCR buffer (Gibco BRL)

Tris-HCl, pH 8.4	200mM
KCl	500mM

C.1.3. 10X *Taq* Extender buffer (Stratagene)

Tris-HCl, pH8.8	200mM
KCl	100mM
$(NH_4)_2SO_4$	100mM
$MgSO_4$	20mM
Triton X-100	1% v/v
BSA	1mg/ml

C.1.4. 10X ThermoPol PCR buffer (for use with Vent® DNA polymerase; NEB)

Tris-HCl, pH 8.8	200mM
$(NH_4)_2SO_4$	100mM
KCl	100mM
$MgSO_4$	20mM
Triton X-100	0.1% v/v

C.1.5. 10X ligation buffer (Invitrogen)

Tris-HCl, pH 7.5	60mM
$MgCl_2$	60mM
NaCl	50mM
BSA	1mg/ml
β-mercaptoethanol	70mM
ATP	1mM
DTT	2mM
Spermidine	10mM

C.1.6. 10X restriction enzyme buffer (NEBuffer 2, New England Biolabs)

Tris-HCl, pH 7.9	100mM
$MgCl_2$	100mM
NaCl	500mM
DTT	10mM

C.1.7. dNTP mixture

-10mM each of dATP, dCTP, dGTP, and dTTP, diluted in DEPC-treated water from 100mM stocks (Promega)

C.2. Other buffers.

C.2.1. TE buffer

Tris-HCl, pH 7.5 or 8.0	10mM
EDTA (disodium salt)	1mM

C.2.2. Binding and Washing (BW) buffer for Dynabeads®.

Tris-HCl, pH 7.5	10mM
EDTA (disodium salt)	1mM
NaCl	2M

C.3. Buffers for agarose gel electrophoresis.

C.3.1. 10X Tris-borate electrophoresis buffer (TBE)

Tris base	890mM
Orthoboric acid	890mM
EDTA (disodium salt)	20mM
pH 8.0	

C.3.2. 6X gel loading buffer

Bromophenol blue	0.25% v/v
Xylene cyanol FF	0.25% v/v
Glycerol	30% v/v

C.4. Bacteria and media used for cloning.

C.4.1. Genotype of One Shot® *E. Coli* (INVαF') competent cells (Invitrogen).

F' *end*A1 *rec*A1 *hsd*R17($r_k^- m_k^+$) *sup*E44 *thi*-1 *gyr*A96 *rel*A1 ϕ80*lac*Z$\alpha\Delta$M15Δ(*lac*ZYA-*arg*F) U169 λ^-

C.4.2. Luria-Bertani (LB) medium

Bacto-tryptone	10g
Bacto-yeast extract	5g
NaCl	10g

pH adjusted to 7.0 with 5N NaOH
Made up to a total volume of 1 litre in distilled water.

C.4.3. LB agar plates with ampicillin

- LB agar has the same composition as LB medium but contains 15g/l bacto-agar. The agar was heated until molten and a solution containing 1mg/ml ampicillin (sodium salt; Gibco BRL) was added to give a final concentration of 100μg/ml ampicillin. The agar was poured in approximately 20ml amounts into sterile Petri dishes (Sterilin, Stone, Staffs., UK).

C.4.4. SOC medium.

Bacto-tryptone	20g
Bacto-yeast extract	5g
NaCl	0.5g
KCl	0.186g
Glucose	20mM

pH adjusted to 7.0 with 5N NaOH
Made up to a total volume of 1 litre with distilled water.

C.5. Reagents for small-scale preparation of plasmid DNA (minipreps).

C.5.1. Resuspension buffer P1 (Qiagen)

Tris-HCl, pH 8.0	50mM
EDTA (disodium salt)	10mM
RNase A	100μg/ml

C.5.2. GTE resuspension buffer (ABI)

Tris-HCl, pH 8.0	25mM
EDTA (disodium salt)	10mM
Glucose	50mM

C.5.3. Lysis buffer P2 (Qiagen and ABI)

NaOH	200mM
Sodium dodecyl sulphate	1% w/v

C.5.4. Neutralization buffer P3 (Qiagen)

K acetate, pH 5.5	3M

C.5.5 Neutralization buffer (ABI)

K acetate, pH 4.8	3M

C.5.6. Equilibration buffer QBT (Qiagen)

NaCl	750mM
3-[N-Morpholino]propane-sulphonic acid (MOPS)	50mM
Ethanol	15% v/v
Triton X-100	0.15% v/v
pH 7.0	

C.5.7. Wash buffer QC (Qiagen)

NaCl	1M
MOPS	50mM
Ethanol	15%
pH7.0	

C.5.8. Elution buffer QF (Qiagen)

NaCl	1.25M
Tris-HCl, pH8.5	50mM
Ethanol	15%

C.6. Reagents for sequencing reactions.

C.6.1. Terminator premix for the cycle sequencing kit (Perkin Elmer).

Dye-labelled ddATP	1.58μM
Dye-labelled ddTTP	94.74μM
Dye-labelled ddGTP	0.42μM
Dye-labelled ddCTP	47.37μM
dITP	78.95μM
dATP	15.79μM
dCTP	15.79μM
dTTP	15.79μM
Tris-HCl, pH 9.0	168.42mM
$(NH_4)_2SO_4$	4.21mM
$MgCl_2$	42.1mM
AmpliTaq® DNA polymerase	0.42U/μl

The precise compostion of the terminator premix in the updated version of the kit containing AmpliTaq FS was not given, but the listed components were similar to those above, although $(NH_4)_2SO_4$ was omitted and thermal stable pyrophosphatase had been added.

C.6.2. Reagents for the Sequenase® version 2.0 DNA sequencing kit.

C.6.2.1. Sequenase® reaction buffer

Tris-HCl, pH 7.5	200mM
$MgCl_2$	100mM
NaCl	250mM

C.6.2.2. 5X labelling mix

dGTP	7.5μM
dCTP	7.5μM
dTTP	7.5μM

C.6.2.3. Termination mixes (4)

dGTP	80μM
dATP	80μM
dCTP	80μM
dTTP	80μM
ddGTP, ddATP, ddCTP or ddTTP	8μM
NaCl	50mM

C.6.2.4. Stop solution

Formamide	95% v/v
EDTA (disodium salt)	20mM
Bromophenol Blue	0.05% v/v
Xylene Cyanol FF	0.05% v/v

C.6.2.5. Glycerol enzyme dilution buffer

Tris-HCl, pH 7.5	20mM
DTT	2mM
EDTA (disodium salt)	0.1M
Glycerol	50% v/v

C.6.2.6. 20X glycerol tolerant electrophoresis buffer

Tris base	1.8M
Taurine	575mM
EDTA (disodium salt)	10mM

Appendix D. Changes in the phenotype of leucocytes in the prescapular lymph nodes of cattle infected with *T. parva*.

Phenotype	Calf number	Days post-infection						
		0	3	6	7	8	9	10
		Percentage positive cells						
CD3	4260	72	68	53	62	76	58	58
	4282	80	83	-	87	86	72	83
	4291	70	37	79	87	72	54	-
	5158	61	53	60	48	38	47	-
	5178	45	46	61	76	67	-	-
CD4	4260	35	33	20	23	30	21	24
	4282	34	35	28	39	25	20	21
	4291	32	17	32	37	21	24	-
	5158	18	25	29	26	18	22	-
	5178	18	25	36	37	30	-	-
CD8	4260	24	23	20	32	37	30	33
	4282	34	34	31	34	52	46	62
	4291	25	13	38	39	45	27	-
	5158	11	10	23	14	14	19	-
	5178	13	15	19	25	30	-	-
γ/δ TCR	4260	12	10	10	9	8	10	14
	4282	10	10	15	8	13	10	11
	4291	8	16	6	12	7	10	-
	5158	21	10	6	14	4	5	-
	5178	5	7	7	-	5	-	-
Surface Ig	4260	14	18	25	22	14	20	18
	4282	15	9	12	7	11	11	7
	4291	22	42	17	9	23	20	-
	5158	32	34	30	34	42	37	-
	5178	38	32	26	19	19	-	-
Monocytes	4260	4	2	4	5	3	11	18
	4282	4	2	7	2	5	11	11
	4291	4	2	2	4	6	4	-
	5158	3	6	2	2	3	8	-
	5178	-	10	9	1	6	-	-

Appendix E. Changes in the phenotype of peripheral blood mononuclear cells in cattle infected with *T. parva*.

Phenotype	Calf number	Days post-infection						
		0	3	6	7	8	9	10
		Percentage positive cells						
CD3	4260	48	51	53	57	51	33	30
	4282	55	56	52	58	53	47	45
	4291	58	58	56	66	50	-	-
CD4	4260	19	19	17	19	18	12	11
	4282	22	21	20	23	22	18	15
	4291	25	20	23	25	20	-	-
CD8	4260	9	9	10	10	9	6	7
	4282	18	17	13	14	10	14	20
	4291	17	13	14	20	11	-	-
γ/δ TCR	4260	19	23	29	33	25	16	14
	4282	14	16	20	22	20	13	10
	4291	27	27	29	29	21	-	-
Surface Ig	4260	21	13	15	19	16	18	14
	4282	21	13	17	16	13	16	13
	4291	20	22	27	20	18	-	-
Monocytes	4260	18	22	18	17	30	49	50
	4282	23	22	25	22	30	35	33
	4291	18	22	21	10	32	-	-

REFERENCES

Abe, J., Kotzin, B. L., Meissner, C., Melish, M. E., Takahashi, M., Fulton, D., Romagne, F., Malissen, B., and Leung, D. Y. (1993). Characterization of T cell repertoire changes in acute Kawasaki disease. *J. Exp. Med.* **177**, 791-796.

Abergel, C., and Claverie, J. M. (1991). A strong propensity toward loop formation characterizes the expressed reading frames of the D segments at the Ig H and T cell receptor loci. *Eur. J. Immunol.* **21**, 3021-3025.

Acha-Orbea, H., Shakhov, A. N., Scarpellino, L., Kolb, E., Muller, V., Vessaz Shaw, A., Fuchs, R., Blochlinger, K., Rollini, P., Billotte, J., Sarafidon, M., MacDonald, H. R., and Diggelmann, H. (1991). Clonal deletion of Vβ14-bearing T cells in mice transgenic for mammary tumour virus. *Nature* **350**, 207-211.

Acha-Orbea, H., and MacDonald, H. R. (1995). Superantigens of mouse mammary tumor virus. *Annu. Rev. Immunol.* **13**, 459-486.

Ahmed, J. S., Wiegers, P., Steuber, S., Schein, E., Williams, R. O., and Dobbelaere, D. (1993). Production of interferon by *Theileria annulata*- and *T. parva*-infected bovine lymphoid cell lines. *Parasitol. Res.* **79**, 178-182.

Akolkar, P. N., Gulwani-Akolkar, B., Pergolizzi, R., Bigler, R. D., and Silver, J. (1993). Influence of HLA genes on T cell receptor V segment frequencies and expression levels in peripheral blood lymphocytes. *J. Immunol.* **150**, 2761-2773.

Akolkar, P. N., Gulwani-Akolkar, B., Robinson, M. A., and Silver, J. (1995). The influence of non-HLA genes on the human T-cell receptor repertoire. *Scand. J. Immunol.* **42**, 248-256.

Allsopp, B. A., and Allsopp, M. T. E. P. (1988). *Theileria parva*: genomic DNA studies reveal intra-specific sequence diversity. *Mol. Biochem. Parasitol.* **28**, 77-84.

Amadori, M., Archetti, I. L., Verardi, R., and Berneri, C. (1992). Target recognition by bovine mononuclear, MHC-unrestricted cytotoxic cells. *Vet. Microbiol.* **33**, 383-392.

Arden, B., Clark, S. P., Kabelitz, D., and Mak, T. W. (1995a). Human T-cell receptor variable gene segment families. *Immunogenetics* **42**, 455-500.

Arden, B., Clark, S. P., Kabelitz, D., and Mak, T. W. (1995b). Mouse T-cell receptor variable gene segment families. *Immunogenetics* **42**, 501-530.

Azuma, M., Phillips, J. H., and Lanier, L. L. (1993). $CD28^-$ T lymphocytes. Antigenic and functional properties. *J. Immunol.* **150**, 1147-1159.

Azuma, M., Yssel, H., Phillips, J. H., Spits, H., and Lanier, L. L. (1993). Functional expression of B7/BB1 on activated T lymphocytes. *J. Exp. Med.* **177**, 845-850.

Baccala, R., Kono, D. H., Walker, S., Balderas, R. S., and Theofilopoulos, A. N. (1991). Genomically imposed and somatically modified human thymocyte Vβ gene repertoires. *Proc. Natl. Acad. Sci. USA*. **88**, 2908-2912.

Baldwin, C. L., Goddeeris, B. M., and Morrison, W. I. (1987). Bovine helper T cell clones specific for lymphocytes infected with *Theileria parva* (Muguga). *Parasite Immunol.* **9**, 499-513.

Baldwin, C. L., Black, S. J., Brown, W. C., Conrad, P. A., Goddeeris, B. M., Kinuthia, S. W., Lalor, P. A., MacHugh, N. D., Morrison, W. I., Morzaria, S. P., Naessens, J., and Newson, J. (1988). Bovine T cells, B cells and null cells are transformed by the protozoan parasite *Theileria parva*. *Infect. Immun.* **56**, 462-467.

Baldwin, C. L., Iams, K. P., Brown, W. C., and Grab, D. J. (1992). *Theileria parva*: $CD4^+$ helper and cytotoxic T-cell clones react with a schizont-derived antigen associated with the surface of *Theileria parva*-infected lymphocytes. *Exp. Parasitol.* **75**, 19-30.

Bancroft, J. D. (1982). Enzyme histochemistry. In *Theory and Practice of Histological Techniques.*, J. D. Bancroft and A. Stevens, eds. (New York: Churchill Livingstone), pp. 387.

Bandeira, A., Mengel, J., Burlen-Defranoux, O., and Coutinho, A. (1991). Proliferative T cell anergy to Mls-1^a does not correlate with *in vivo* tolerance. *Int. Immunol.* **3**, 923-931.

Barron, K. S., and Robinson, M. A. (1994). The human T-cell receptor variable gene segment *TCRBV6S1* has two null alleles. *Hum. Immunol.* **40**, 17-19.

Barth, R. K., Kim, B. S., Lan, N. C., Hunkapiller, T., Sobieck, N., Winoto, A., Gerschenfield, H., Okada, C., Hansburg, D., Weissman, I. L., and Hood, L. (1985). The murine T cell receptor uses a limited repertoire of expressed Vβ gene segments. *Nature* **316**, 517-523.

Behlke, M. A., Chou, H. S., Huppi, K., and Loh, D. Y. (1986). Murine T-cell receptor mutants with deletions of β-chain variable region genes. *Proc. Natl. Acad. Sci. USA* **83**, 767-771.

Behr, C. and Dubois, P. (1992). Preferential expansion of Vγ9Vδ2 T cells following stimulation of peripheral blood lymphocytes with extracts of *Plasmodium falciparum*. *Int. Immunol.* **4**, 361-366.

Bellio, M., Lone, Y. C., de la Calle-Martin, O., Malissen, B., Abastado, J. P., and Kourilsky, P. (1994). The Vβ complementarity determining region 1 of a major histocompatibility complex (MHC) class I-restricted T cell receptor is involved in the recognition of peptide/MHC I and superantigen/MHC II complex. *J. Exp. Med.* **179**, 1087-1097.

Bensaid, A., and Hadam, M. (1991). Individual antigens of cattle. Bovine CD4 (BoCD4). *Vet. Immunol. Immunopathol.* **27**, 51-54.

Bette, M., Schafer, M. K., van Rooijen, N., Weihe, E., and Fleischer, B. (1993). Distribution and kinetics of superantigen-induced cytokine gene expression in mouse spleen. *J. Exp. Med.* **178**, 1531-1539.

Bevan, D. J., and Chisholm, P. M. (1986). Co-expression of CD4 and CD8 molecules and *de novo* expression of MHC class II antigens on activated rat T cells. *Immunology* **59**, 621-625.

Bill, J., Appel, V. B., and Palmer, E. (1988). An analysis of T-cell receptor variable region gene expression in major histocompatability complex disparate mice. *Proc. Natl. Acad. Sci. USA* **85**, 9184-9188.

Bjorkman, P. J., Saper, M. A., Samraoui, B., Bennett, W. S., Strominger, J. L., and Wiley, D. C. (1987). Structure of the human class I histocompatibility antigen, HLA-A2. *Nature* **329**, 506-512.

Blue, M.-L., Daley, J. F., Levine, H., and Schlossman, S. F. (1985). Coexpression of T4 and T8 on peripheral blood T cells demonstrated by two-color fluorescence flow cytometry. *J. Immunol.* **134**, 2281-2286.

Boitel, B., Ermonval, M., Panina-Bordignon, P., Mariuzza, R. A., Lanzavecchia, A., and Acuto, O. (1992). Preferential Vβ gene usage and lack of junctional sequence conservation among human T cell receptors specific for a tetanus toxin-derived peptide: Evidence for a dominant role of a germline-encoded V region in antigen/major histocompatibility complex recognition. *J. Exp. Med.* **175**, 765-777.

Borrero, H., Donson, D., Cervera, C., Rexer, C., and Macphail, S. (1995). T cell receptor Vα4 is expressed by a subpopulation of Vβ6 T cells that respond to the bacterial superantigen staphylococcal enterotoxin B. *J. Immunol.* **154**, 4247-4260.

Bowness, P., Moss, P. A., Rowland-Jones, S., Bell, J. I., and McMichael, A. J. (1993). Conservation of T cell receptor usage by HLA B27-restricted influenza-specific cytotoxic T lymphocytes suggests a general pattern for antigen-specific major histocompatibility complex class I-restricted responses. *Eur. J. Immunol.* **23**, 1417-1421.

Braun, M. Y., Jouvin-Marche, E., Marche, P. N., MacDonald, H. R., and Acha-Orbea, H. (1995). T cell receptor Vβ repertoire in mice lacking endogenous mouse mammary tumor provirus. *Eur. J. Immunol.* **25**, 857-862.

Brenner, M. B., McLean, J., Dialynas, D. P., Strominger, J. L., Smith, J. A., Owen, F. L., Seidman, J. G., Ip, S., Rosen, F., and Krangel, M. S. (1986). Identification of a putative second T-cell receptor. *Nature* **322**, 145-149.

Brocklesby, D. W., Barnett, S. F., and Scott, G. R. (1961). Morbidity and mortality rates in East Coast fever (*Theileria parva* infection) and their application to drug screening procedures. *Brit. Vet. J.* **117**, 529-531.

Brooke, G. P., and Howard, C. J. (1996). Characterization, cloning and sequencing of a novel molecule, MyD-1, expressed on cattle and human antigen presenting cells. *Immunology* **89** , 41.

Brown, C. G. D., Stagg, D. A., Purnell, R. E., Kanhai, G. K., and Payne, R. C. (1973). Infection and transformation of bovine lymphoid cells *in vitro* by infective particles of *Theileria parva. Nature* **245**, 101-103.

Brown, C. G. D. (1983). *Theileria.* In In Vitro *Cultivation of Protozoan Parasites.*, J. B. Jensen, ed. (London: CRC Press), pp. 243-284.

Brown, W. C., and Logan, K. S. (1986). Bovine T cell clones infected with *Theileria parva* produce a factor with IL-2-like activity. *Parasite Immunol.* **8**, 189-192.

Brown, W. C., Sugimoto, C., and Grab, D. J. (1989). *Theileria parva*: Bovine helper T cell clones specific for both infected lymphocytes and schizont membrane antigens. *Exp. Parasitol.* **69**, 234-248.

Brown, W. C., Woods, V. M., Chitko-McKown, C. G., Hash, S. M., and Rice-Ficht, A. C. (1994). Interleukin-10 is expressed by bovine type 1 helper, type 2 helper, and unrestricted parasite-specific T-cell clones and inhibits proliferation of all three subsets in an accessory-cell-dependent manner. *Infect. Immun.* **62**, 4697-4708.

Buitkamp, J., Schwaiger, F. W., and Epplen, J. T. (1993). *Vb6* T-cell receptor elements in artiodactyls: conservation and germline polymorphisms. *Mamm. Genome* **4**, 504-510.

Burrows, S. R., Silins, S. L., Moss, D. J., Khanna, R., Misko, I. S., and Argaet, V. P. (1995). T cell receptor repertoire for a viral epitope in humans is diversified by tolerance to a background major histocompatibility complex antigen. *J. Exp. Med.* **182**, 1703-1715.

Büscher, G., Morrison, W. I., and Nelson, R. T. (1984). Titration in cattle of infectivity and immunogenicity of autologous cell lines infected with *Theileria parva. Vet. Parasitol.* **15**, 29-38.

Campbell, J. D., Howie, S. E., Odling, K. A., and Glass, E. J. (1995). *Theileria annulata* induces abberrant T cell activation *in vitro* and *in vivo. Clin. Exp. Immunol.* **99**, 203-210.

Campos, M., Rossi, C. R., Bielefeldt Ohmann, H., Beskorwayne, T., Rapin, N., and Babiuk, L. A. (1992). Characterization and activation requirements of bovine lymphocytes acquiring cytotoxic activity after interleukin-2 treatment. *Vet. Immunol. Immunopathol.* **32**, 205-223.

Cariello, N. F., Swenberg, J. A., and Skopek, T. R. (1991). Fidelity of *Thermococcus litoralis* DNA polymerase (Vent) in PCR determined by denaturing gradient gel electrophoresis. *Nucleic Acids Res.* **19**, 4193-4198.

Casanova, J. L., Romero, P., Widmann, C., Kourilsky, P., and Maryanski, J. L. (1991). T cell receptor genes in a series of class I major histocompatibility complex-restricted cytotoxic T lymphocyte clones specific for a *Plasmodium berghei* nonapeptide: implications for T cell allelic exclusion and antigen-specific repertoire. *J. Exp. Med.* **174**, 1371-1383.

Casanova, J. L., Cerottini, J. C., Matthes, M., Necker, A., Gournier, H., Barra, C., Widmann, C., MacDonald, H. R., Lemonnier, F., Malissen, B., and Maryanski, J. L. (1992). H-2-restricted cytolytic T lymphocytes specific for HLA display T cell receptors of limited diversity. *J. Exp. Med.* **176**, 439-447.

Charmley, P., Chao, A., Concannon, P., Hood, L., and Gatti, R. A. (1990). Haplotyping the human T-cell receptor β-chain gene complex by use of restriction fragment length polymorphisms. *Proc. Natl. Acad. Sci. USA* **87**, 4823-4827.

Charmley, P., Wang, K., Hood, L., and Nickerson, D. A. (1993). Identification and physical mapping of a polymorphic human T cell receptor Vβ gene with a frequent null allele. *J. Exp. Med.* **177**, 135-143.

Choi, Y., Kotzin, B., Herron, L., Callahan, J., Marrack, P., and Kappler, J. (1989). Interaction of *Staphylococcus aureus* toxin "superantigens" with human T cells. *Proc. Natl. Acad. Sci. USA* **86**, 8941-8945.

Choi, Y., Herman, A., DiGiusto, D., Wade, T., Marrack, P., and Kappler, J. (1990a). Residues of the variable region of the T-cell receptor β-chain that interact with *S. aureus* toxin superantigens. *Nature* **346**, 471-473.

Choi, Y., Lafferty, J. A., Clements, J. R., Todd, J. K., Gelfand, E. W., Kappler, J., Marrack, P., and Kotzin, B. L. (1990b). Selective expansion of T cells expressing Vβ2 in toxic shock syndrome. *J. Exp. Med.* **172**, 981-984.

Choi, Y., Kappler, J. W., and Marrack, P. (1991). A superantigen encoded in the open reading frame of the 3' long terminal repeat of mouse mammary tumour virus. *Nature* **350**, 203-207.

Choi, Y., Marrack, P., and Kappler, J. W. (1992). Structural analysis of a mouse mammary tumor virus superantigen. *J. Exp. Med.* **175**, 847-852.

Chomczynski, P., and Sacchi, N. (1987). Single-step method of RNA isolation by acid guanidium thiocyanate-phenol-chloroform extraction. *Anal. Biochem.* **162** , 156-159.

Chothia, C., Boswell, D. R., and Lesk, A. M. (1988). The outline structure of the T-cell αβ receptor. *EMBO J.* **7**, 3745-3755.

Clark, S. P., Arden, B., Kabelitz, D., and Mak, T. W. (1995). Comparison of human and mouse T-cell receptor variable gene segment subfamilies. *Immunogenetics* **42**, 531-540.

Clement, L. T., Grossi, C. E., and Gartland, G. L. (1984). Morphologic and phenotypic features of the subpopulation of Leu-2^+ cells that suppresses B cell differentiation. *J. Immunol.* **133**, 2461-2468.

Cole, B. C., and Atkin, C. L. (1991). The *Mycoplasma arthritidis* T-cell mitogen, MAM: a model superantigen. *Immunol. Today* **12**, 271-276.

Collins, R. A., Sopp, P., Gelder, K. I., Morrison, W. I., and Howard, C. J. (1996). Bovine γ/δ TcR^+ T lymphocytes are stimulated to proliferate by autologous *Theileria annulata* -infected cells in the presence of interleukin-2. *Scand. J. Immunol.* **44** , 444-452.

Concannon, P., Pickering, L. A., Kung, P., and Hood, L. (1986). Diversity and structure of human T-cell receptor β-chain variable region genes. *Proc. Natl. Acad. Sci. USA* **83**, 6598-6602.

Conrad, P. A., Iams, K., Brown, W. C., Sohanpal, B., and ole-MoiYoi, O. K. (1987a). DNA probes detect genomic diversity in *Theileria parva* stocks. *Mol. Biochem. Parasitol.* **25**, 213-226.

Conrad, P. A., Stagg, D. A., Grootenhuis, J. G., Irvin, A. D., Newson, J., Njamunggeh, R. E. G., Rossiter, P. B., and Young, A. S. (1987b). Isolation of *Theileria* parasites from African buffalo (*Syncerus caffer*) and characterization with anti-schizont monoclonal antibodies. *Parasitology* **94**, 413-423.

Conrad, P. A., Ole-MoiYoi, O. K., Baldwin, C. L., Dolan, T. T., O'Callaghan, C. J., Njamunggeh, R. E. G., Grootenhuis, J. G., Stagg, D. A., Leitch, B. L., and Young, A. S. (1989a). Characterization of buffalo-derived theilerial parasites with monoclonal antibodies and DNA probes. *Parasitology* **98**, 179-188.

Conrad. P. A., Baldwin, C. L., Brown, W. C., Sohanpal, B., Dolan, T. T., Goddeeris, B. M., DeMartini, J. C., and ole-MoiYoi, O. K. (1989b). Infection of bovine T cell clones with genotypically distinct *Theileria parva* parasites and analysis of their cell surface phenotype. *Parasitology* **99**, 205-213.

Cook, J. K. A., Jones, B. V., Ellis, M. M., Jing, L., and Cavanagh, D. (1993). Antigenic differentiation of strains of turkey rhinotracheitis virus using monoclonal antibodies. *Avian Pathology* **22**, 257-273.

Coquerelle, T. M., Eichhorn, M., Magnuson, N. S., Reeves, R., Williams, R. O., and Dobbelaere, D. A. E. (1989). Expression and characterization of the interleukin 2 receptor in *Theileria parva*-infected bovine lymphocytes. *Eur. J. Immunol.* **19**, 655-659.

Cornélis, F., Pile, K., Loveridge, J., Moss, P., Harding, R., Julier, C., and Bell, J. (1993). Systematic study of human αβ T cell receptor V segments shows allelic variations resulting in a large number of distinct T cell receptor haplotypes. *Eur. J. Immunol.* **23**, 1277-1283.

Cunningham, M. P., Brown, C. G. D., Burridge, M. J., and Purnell, R. E. (1973). Cryopreservation of infective particles of *Theileria parva*. *Int. J. Parasitol.* **3**, 583-587.

Cunningham, M. P., Brown, C. G. D., Burridge, M. J., Musoke, A. J., Purnell, R. E., Radley, D. E., and Sempebwa, C. (1974). East Coast fever: titration in cattle of suspensions of *Theileria parva* derived from ticks. *Brit. Vet. J.* **130**, 336-345.

Currier, J., Sattabongkot, J., and Good, M. F. (1992). 'Natural' T cells responsive to malaria: evidence implicating immunological cross-reactivity in the maintenance of TCR $\alpha\beta^+$ malaria-specific responses from non-exposed donors. *Int. Immunol.* **4**, 985-994.

Currier, J., Beck, H. P., Currie, B., and Good, M. F. (1995). Antigens released at schizont burst stimulate *Plasmodium falciparum*-specific $CD4^+$ T cells from non-exposed donors: potential for cross-reactive memory T cells to cause disease. *Int. Immunol.* **7**, 821-833.

Currier, J. R., Yassai, M., Robinson, M. A., and Gorski, J. (1996). Molecular defects in *TCRBV* genes preclude thymic selection and limit the expressed TCR repertoire. *J. Immunol.* **157**, 170-175.

Dadaglio, G., Garcia, S., Montagnier, L., and Gougeon, M. L. (1994). Selective anergy of $V\beta8^+$ T cells in human immunodeficiency virus-infected individuals. *J. Exp. Med.* **179**, 413-424.

Daly, K., Nguyen, P., Woodland, D. L., and Blackman, M. A. (1995). Immunodominance of major histocompatibility complex class I-restricted influenza virus epitopes can be influenced by the T-cell receptor repertoire. *J. Virol.* **69**, 7416-7422.

Davis, M. M., and Bjorkman, P. J. (1988). T-cell antigen receptor genes and T-cell recognition. *Nature* **334**, 395-402.

Davis, W. C., and Splitter, G. S. (1991). Individual antigens of cattle. Bovine CD2 (BoCD2). *Vet. Immunol. Immunopathol.* **27** , 43-50.

Davis, W. C., MacHugh, N. D., Park, Y. H., Hamilton, M. J., and Wyatt, C. R. (1993). Identification of a monoclonal antibody reactive with the bovine orthologue of CD3 (BoCD3). *Vet. Immunol. Immunopathol.* **39** , 85-91.

Davis, W. C., Brown, W. C., Hamilton, M. J., Wyatt, C. R., Orden, J. A., Khalid, A. M., and Naessens, J. (1996). Analysis of monoclonal antibodies specific for the $\gamma\delta$ TcR. *Vet. Immunol. Immunopathol.* **52** , 275-283.

Day, C. E., Schmitt, K., and Robinson, M. A. (1994). Frequent recombination in the human T-cell receptor beta gene complex. *Immunogenetics* **39**, 335-342.

Dellabona, P., Peccoud, J., Kappler, J., Marrack, P., Benoist, C., and Mathis, D. (1990). Superantigens interact with MHC class II molecules outside of the antigen groove. *Cell* **62**, 1115-1121.

Del Prete, G., De Carli, M., Almerigogna, F., Giudizi, M. G., Biagiotti, R., and Romagnani, S. (1993). Human IL-10 is produced by both type 1 helper (Th1) and type 2 helper (Th2) T cell clones and inhibits their antigen-specific proliferation and cytokine production. *J. Immunol.* **150**, 353-360.

DeMartini, J. C., and Moulton, J. E. (1973a). Responses of the bovine lymphatic system to infection by *Theileria parva.* I. Histology and ultrastructure of lymph nodes in experimentally-infected calves. *J. Comp. Path.* **83**, 281-298.

DeMartini, J. C., and Moulton, J. E. (1973b). Responses of the bovine lymphatic system to infection by *Theileria parva.* II. Changes in the central lymph in experimentally infected calves. *J. Comp. Path.* **83**, 299-306.

DeMartini, J. C., and Baldwin, C. L. (1991). Effects of gamma interferon, tumor necrosis factor alpha, and interleukin-2 on infection and proliferation of *Theileria parva*-infected bovine lymphoblasts and production of interferon by parasitized cells. *Infect. Immun.* **59**, 4540-4546.

DeMartini, J. C., MacHugh, N. D., Naessens, J., and Teale, A. J. (1993). Differential *in vitro* and *in vivo* expression of MHC class II antigens in bovine lymphocytes infected by *Theileria parva. Vet. Immunol. Immunopathol.* **35**, 253-273.

Dembic, Z., Haas, W., Weiss, S., McCubrey, J., Kiefer, H., von Boehmer, H., and Steinmetz, M. (1986). Transfer of specificity by murine α and β T–cell receptor genes. *Nature* **320**, 232-238.

Denkers, E. Y., Caspar, P., and Sher, A. (1994). *Toxoplasma gondii* possesses a superantigen activity that selectively expands murine T cell receptor Vβ5-bearing $CD8^+$ lymphocytes. *J. Exp. Med.* **180**, 985-994.

Denkers, E. Y., Caspar, P., Hieny, S., and Sher, A. (1996). *Toxoplasma gondii* infection induces specific nonresponsiveness in lymphocytes bearing the Vβ5 chain of the mouse T cell receptor. *J. Immunol.* **156**, 1089-1094

de Waal Malefyt, R., Abrams, J., Bennett, B., Figdor, C. G., and de Vries, J. E. (1991). Interleukin 10 (IL-10) inhibits cytokine synthesis by human monocytes: an autoregulatory role of IL-10 produced by monocytes. *J. Exp. Med.* **174**, 1209-1220.

de Waal Malefyt, R., Verma, S., Bejarano, M. T., Ranes-Goldberg, M., Hill, M., and Spits, H. (1993). CD2/LFA-3 or LFA-1/ICAM-1 but not CD28/B7 interactions can augment cytotoxicity by virus-specific $CD8^+$ cytotoxic T lymphocytes. *Eur. J. Immunol.* **23**, 418-424.

Devereux , J., Haeberli, P., and Smithies, O. (1984). A comprehensive set of sequence analysis programs for the VAX. *Nucleic Acids Res.* **12**, 387-395

Ding, L., and Shevach, E. M. (1992). IL-10 inhibits mitogen-induced T cell proliferation by selectively inhibiting macrophage costimulatory function. *J. Immunol.* **148**, 3133-3139.

Dobbelaere, D. A. E., Spooner, P. R., Barry, W. C., and Irvin, A. D. (1984). Monoclonal antibody neutralizes the sporozoite stage of different *Theileria parva* stocks. *Parasite Immunol.* **6**, 361-370.

Dobbelaere, D. A. E., Coquerelle, T. M., Roditi, I. J., Eichhorn, M., and Williams, R. O. (1988). *Theileria parva* infection induces autocrine growth of bovine lymphocytes. *Proc. Natl. Acad. Sci. USA* **85**, 4730-4734.

Dobbelaere, D. A. E., Prospero, T. D., Roditi, I. J., Kelke, C., Baumann, I., Eichhorn, M., Williams, R. O., Ahmed, J. S., Baldwin, C. L., Clevers, H., and Morrison, W. I. (1990). Expression of Tac antigen component of bovine interleukin-2 receptor in different leukocyte populations infected with *Theileria parva* or *Theileria annulata*. *Infect. Immun.* **58**, 3847-3855.

Dobbelaere, D. A., Roditi, I. J., Coquerelle, T. M., Kelke, C., Eichhorn, M., and Williams, R. O. (1991). Lymphocytes infected with *Theileria parva* require both cell-cell contact and growth factor to proliferate. *Eur. J. Immunol.* **21**, 89-95.

Dolan, T. T., Young, A. S., Losos, G. J., McMilian, I., Minders, C. E., and Soulsby, K. (1984a). Dose dependent responses of cattle to *Theileria parva* stabilate. *Int. J. Parasitol.* **14**, 89-95.

Dolan, T. T., Linyonyi, A., Mbogo, S. K., and Young, A. S. (1984b). Comparison of long acting oxytetracycline and parvaquone in immunisation against East Coast fever by infection and treatment. *Res. Vet. Sci.* **37**, 175-178.

Dolan, T. T., Teale, A. J., Stagg, D. A., Kemp, S. J., Cowan, K. M., Young, A. S., Groocock, C. M., Leitch, B. L., Spooner, R. L., and Brown, C. G. D. (1984c). A histocompatability barrier to immunization against East Coast fever using *Theileria parva*-infected lymphoblastoid cell lines. *Parasite Immunol.* **6**, 243-250.

Duffus, W. P. H., Wagner, G. G., and Preston, J. M. (1978). Initial studies on the properties of a bovine lymphoid cell culture line infected with *Theileria parva*. *Clin. Exp. Immunol.* **34**, 347-353.

Dyson, P. J., Knight, A. M., Fairchild, S., Simpson, E., and Tomonari, K. (1991). Genes encoding ligands for deletion of Vβ11 T cells cosegregate with mammary tumour virus genomes. *Nature* **349**, 531-532.

Eckert, K. A., and Kunkel, T. A. (1990). High fidelity DNA synthesis by the *Thermus aquaticus* DNA polymerase. *Nucleic Acids Res.* **18**, 3739-3744.

Eckert , K. A., and Kunkel, T. A. (1993). The fidelity of DNA polymerases used in the polymerase chain reactions. In *PCR: A Practical Approach*. M. J. McPherson, P. Quirke, and G. R. Taylor, eds. (Oxford; IRL Press), pp

Ehrich, E. W., Devaux, B., Rock, E. P., Jorgensen, J. L., Davis, M. M., and Chien, Y. H. (1993). T cell receptor interaction with peptide/major histocompatibility complex (MHC) and superantigen/MHC ligands is dominated by antigen. *J. Exp. Med.* **178**, 713-722.

Eichhorn, M., and Dobbelaere, D. A. E. (1994). Induction of signal transduction pathways in lymphocytes infected by *Theileria parva*. *Parasitol. Today* **10**, 469-472.

Elloso, M. M., van der Heyde, H. C., Troutt, A., Manning, D.D., and Weidanz, W. P. (1996). Human γδ T cell subset-proliferative response to malarial antigen *in vitro* depends on $CD4^+$ T cells or cytokines that signal through components of the IL-2R. *J. Immunol.* **157**, 2096-2102.

Emery, D. L. (1981a). Kinetics of infection with *Theileria parva* (East Coast fever) in the central lymph of cattle. *Vet. Parasitol.* **9**, 1-16.

Emery, D. L. (1981b). Adoptive transfer of immunity to infection with *Theileria parva* (East Coast fever) between cattle twins. *Res. Vet. Sci.* **30**, 364-367.

Emery, D. L., and Morrison, W. I. (1980). Generation of autologous mixed leucocyte reactions during the course of infection with *Theileria parva* (East Coast fever) in cattle. *Immunology* **40**, 229-237.

Emery, D. L., Morrison, W. I., Nelson, R. T., and Murray, M. (1981a). The induction of cell-mediated immunity in cattle inoculated with cell lines parasitized with *Theileria parva.* In *Advances in the Control of Theileriosis.*, A. D. Irvin, M. P. Cunningham and A. S. Young, eds. (The Hague: Martinus Nijhoff), pp. 295-310.

Emery, D. L., Eugui, E. M., Nelson, R. T., and Tenywa, T. (1981b). Cell-mediated immune responses to *Theileria parva* (East Coast fever) during immunization and lethal infections in cattle. *Immunology* **43**, 323-336.

Emery, D. L., Morrison, W. I., Buscher, G., and Nelson, R. T. (1982). Generation of cell-mediated cytotoxicity to *Theileria parva* (East Coast fever) after inoculation of cattle with parasitized lymphoblasts. *J. Immunol.* **128**, 195-200.

Emery, D. L., MacHugh, N. D., and Morrison, W. I. (1988). *Theileria parva* (Muguga) infects bovine T lymphocytes *in vivo* and induces co-expression of BoT4 and BoT8. *Parasite Immunol. 1988*, 379-391.

Engel, I., and Hedrick, S. M. (1988). Site-directed mutations in the VDJ junctional region of a T cell receptor β chain cause changes in antigenic peptide recognition. *Cell* **54**, 473-484.

Ennis, P. D., Zemmour, J., Salter, R. D., and Parham, P. (1990). Rapid cloning of HLA-A,B cDNA by using the polymerase chain reaction: frequency and nature of errors produced in amplification. *Proc. Natl. Acad. Sci. USA* **87**, 2833-2837.

Entrican, G., McInnes, C. J., Logan, M., Preston, P. M., Martinod, S., and Brown, C. G. (1991). Production of interferons by bovine and ovine cell lines infected with *Theileria annulata* or *Theileria parva*. *Parasite Immunol.* **13**, 339-343.

Estes, D. M., Turaga, P. S., Sievers, K. M., and Teale, J. M. (1993). Characterization of an unusual cell type ($CD4^+$ $CD3^-$) expanded by helminth infection and related to the parasite stress response. *J. Immunol.* **150**, 1846-1856.

Eugui, E. M., and Emery, D. L. (1981). Genetically restricted cell-mediated cytotoxicity in cattle immune to *Theileria parva. Nature* **290**, 251-254.

Fawcett, D. W., Buscher, G., and Doxsey, S. (1982a). Salivary gland of the tick vector of East Coast fever. III. The ultrastructure of the sporogony in *Theileria parva. Tissue Cell* **14**, 183-206.

Fawcett, D. W., Buscher, G., and Doxsey, S. (1982b). Salivary gland of the tick vector of East Coast fever. IV. Cell type selectivity and host cell responses to *Theileria parva. Tissue Cell* **14**, 397-414.

Fawcett, D. W., Doxsey, S., Stagg, D. A., and Young, A. S. (1982c). The entry of sporozoites of *Theileria parva* into bovine lymphocytes *in vitro*. Electron microscopic observations. *Eur. J. Cell Biol.* **27**, 10-21.

Fawcett, D. W. and Stagg, D. A. (1986). Passive endocytosis of sporozoites of *Theileria parva* in macrophages at 1-2°C. *J. Submicrosc. Cytol.* **18**, 11-19.

Fell, A. H., Silins, S. L., Baumgarth, N., and Good, M. F. (1996). *Plasmodium falciparum*-specific T cell clones from non-exposed and exposed donors are highly diverse in TCR β chain V segment usage. *Int. Immunol.* **8**, 1877-1887.

Ferradini, L., Roman-Roman, S., Azocar, J., Michalaki, H., Triebel, F., and Hercend, T. (1991). Studies on the human T cell receptor α/β variable region genes. II. Identification of four additional Vβ subfamilies. *Eur. J. Immunol.* **21**, 935-942.

Festenstein, H. (1973). Immunogenetic and biological aspects of *in vitro* lymphocyte allotransformation (MLR) in the mouse. *Transplant. Rev.* **15**, 62-88.

Fields, B. A., Malchiodi, E. L., Li, H., Ysern, X., Stauffacher, C. V., Schlievert, P. M., Karjalainen, K., and Mariuzza, R. A. (1996). Crystal structure of a T-cell receptor β-chain complexed with a superantigen. *Nature* **384**, 188-192.

Fiorentino, D. F., Bond, M. W., and Mosmann, T. R. (1989). Two types of mouse T helper cell. IV. Th2 clones secrete a factor that inhibits cytokine production by Th1 clones. *J. Exp. Med.* **170**, 2081-2095.

Fischer, H., Dohlsten, M., Andersson, U., Hedlund, G., Ericsson, P., Hansson, J., and Sjögren, H. O. (1990). Production of TNFα and TNFβ by staphylococcal enterotoxin A activated human T cells. *J. Immunol.* **144**, 4663-4669.

Fleischer, B., Schrezenmeier, H., and Conradt, P. (1989). T lymphocyte activation by staphylococcal enterotoxins: role of class II molecules and T cell surface structures. *Cell. Immunol.* **120**, 92-101.

Frankel, W. N., Rudy, C., Coffin, J. M., and Huber, B. T. (1991). Linkage of *Mls* genes to endogenous mammary tumour viruses of inbred mice. *Nature* **349**, 526-528.

Fry, A. M., Cotterman, M. M., and Matis, L. A. (1989). The influence of self-MHC and non-MHC on the selection of an antigen-specific T cell receptor repertoire. *J. Immunol.* **143**, 2723-2729.

Fuchs, E. J. and Matzinger, P. (1992). B cells turn off virgin but not memory T cells. *Science* **258**, 1156-1159.

Gahm, S. J., Fowlkes, B. J., Jameson, S. C., Gascoigne, N. R., Cotterman, M. M., Kanagawa, O., Schwartz, R. H., and Matis, L. A. (1991). Profound alteration in an αβ T-cell antigen receptor repertoire due to polymorphism in the first complementarity-determining region of the β chain. *Proc. Natl. Acad. Sci. USA* **88**, 10267-10271.

Garcia, K. C., Degano, M., Stanfield, R. L., Brunmark, A., Jackson, M. R., Peterson, P. A., Teyton, L., and Wilson, I. A. (1996). An αβ T cell receptor structure at 2.5 Å and its orientation in the TCR-MHC complex. *Science* **274**, 209-219.

Gaus, H., Miethke, T., Wagner, H., and Heeg, K. (1994). Superantigen-induced anergy of $V\beta8^+$ $CD4^+$ T cells induces functional but non-proliferative T cells *in vivo*. *Immunology* **83**, 333-340.

Gazzinelli, R. T., Oswald, I. P., James, S. L., and Sher, A. (1992a). IL-10 inhibits parasite killing and nitrogen oxide production by IFN-gamma-activated macrophages. *J. Immunol.* **148**, 1792-1796.

Gazzinelli, R. T., Oswald, I. P., Hieny, S., James, S. L., and Sher, A. (1992b). The microbicidal activity of interferon-gamma-treated macrophages against *Trypanosoma cruzi* involves an L-arginine-dependent, nitrogen oxide-mediated mechanism inhibitable by interleukin-10 and transforming growth factor-beta. *Eur. J. Immunol.* **22**, 2501-2506.

Genevée, C., Diu, A., Nierat, J., Caignard, A., Dietrich, P. Y., Ferradini, L., Roman-Roman, S., Triebel, F., and Hercend, T. (1992). An experimentally validated panel of subfamily-specific oligonucleotide primers (Vα1-w29/Vβ1-w24) for the study of human T cell receptor variable V gene segment usage by polymerase chain reaction. *Eur. J. Immunol.* **22**, 1261-1269.

Gerdes, J., Lemke, H., Baisch, H., Wacker, H., Schwab, U., and Stein, H. (1984). Cell cycle analysis of a cell proliferation-associated human nuclear antigen defined by the monoclonal antibody Ki67. *J. Immunol.* **133**, 1710-1715.

Goddeeris, B. M., Morrison, W. I., and Teale, A. J. (1986a). Generation of bovine cytotoxic cell lines, specific for cells infected with the protozoan parasite *Theileria parva* and restricted by products of the major histocompatibility complex. *Eur. J. Immunol.* **16**, 1243-1249.

Goddeeris, B. M., Morrison, W. I., Teale, A. J., Bensaid, A., and Baldwin, C. L. (1986b). Bovine cytotoxic T-cell clones specific for cells infected with the protozoan parasite *Theileria parva*: Parasite strain specificity and class I major histocompatibility complex restriction. *Proc. Natl. Acad. Sci. USA* **83**, 5238-5242.

Goddeeris, B. M., and Morrison, W. I. (1987). The bovine autologous *Theileria* mixed leucocyte reaction: influence of monocytes and phenotype of the parasitized stimulator cell on proliferation and parasite specificity. *Immunology* **60**, 63-69.

Goddeeris, B. M., and Morrison, W. I. (1988). Techniques for the generation, cloning and characterization of bovine cytotoxic T cells specific for the protozoan *Theileria parva*. *Journal of Tissue Culture Methods* **11**, 101-110.

Goddeeris, B. M., Morrison, W. I., Toye, P. G., and Bishop, R. (1990). Strain specificity of bovine *Theileria parva*-specific cytotoxic T cells is determined by the phenotype of the restricting class I MHC. *Immunology* **69**, 38-44.

Goddeeris, B. M., Dunlap, S., Bensaid, A., MacHugh, N. D., and Morrison, W. I. (1991). Cell surface phenotype of two cloned populations of bovine lymphocytes displaying non-specific cytotoxic activity. *Vet. Immunol. Immunopathol.* **27**, 195-199.

Goldbach-Mansky, R., King, P. D., Taylor, A. P., and Dupont, B. (1992). A co-stimulatory role for CD28 in the activation of $CD4^+$ T lymphocytes by staphylococcal enterotoxin B. *Int. Immunol.* **4**, 1351-1360.

Gollob, J. A., Li, J., Kawasaki, H., Daley, J. F., Groves, C., Reinherz, E. L., and Ritz, J. (1996). Molecular interaction between CD58 and CD2 counter-receptors mediates the ability of monocytes to augment T cell activation by IL-12. *J. Immunol.* **157**, 1886-1893.

Gollob, J. A., Li, J., Reinherz, E. L., and Ritz, J. (1995). CD2 regulates responsiveness of activated T cells to interleukin 12. *J. Exp. Med.* **182**, 721-731.

Golovkina, T. V., Chervonsky, A., Dudley, J. P., and Ross, S. R. (1992). Transgenic mouse mammary tumor virus superantigen expression prevents viral infection. *Cell* **69**, 637-645.

Gonzalo, J. A., Martinez, C., Springer, T. A., and Gutierrez-Ramos, J. C. (1995). ICAM-1 is required for T cell proliferation but not for anergy or apoptosis induced by *Staphylococcus aureus* enterotoxin B *in vivo*. *Int. Immunol.* 7, 1691-1698.

Good, M. F., Quakyi, I. A., Saul, A., Berzofsky, J. A., Carter, R., and Miller, L. H. (1987). Human T cell clones reactive to the sexual stages of *Plasmodium falciparum* malaria. High frequency of gamete-reactive T cells in peripheral blood from nonexposed donors. *J. Immunol.* **138**, 306-311.

Goodier, M., Fey, P., Eichmann, K., and Langhorne, J. (1992). Human peripheral blood γδ T cells respond to antigens of *Plasmodium falciparum*. *Int. Immunol.* 4, 33-41.

Groettrup, M., and von Boehmer, H. (1993). A role for a pre-T-cell receptor in T-cell development. *Immunol. Today* **14**, 610-614.

Gückel, B., Berek, C., Lutz, M., Altevogt, P., Schirrmacher, V., and Kyewski, B. A. (1991). Anti-CD2 antibodies induce T cell unresponsiveness *in vivo*. *J. Exp. Med.* **174**, 957-967.

Hall, B. L., and Finn, O. J. (1992). PCR-based analysis of the T-cell receptor Vβ multigene family: experimental parameters affecting its validity. *Biotechniques* **13**, 248-257.

Hall, G. A., Sopp, P., and Howard, C. J. (1993). An investigation of temporary workshop clusters reacting with cells of the mononuclear phagocytic system. *Vet. Immunol. Immunopathol.* **39**, 225-236.

Hawes, G. E., Struyk, L. and van den Elsen, P. J. (1993). Differential usage of T cell receptor V gene segments in $CD4^+$ and $CD8^+$ subsets of T lymphocytes in monozygotic twins. *J. Immunol.* **150**, 2033-2045.

Hedrick, S. M., Cohen, D. I., Nielsen, E. A., and Davis, M. M. (1984). Isolation of cDNA clones encoding T cell-specific membrane-associated proteins. *Nature* **308**, 149-153.

Hedrick, S. M., Engel, I., McElligott, D. L., Fink, P. J., Hsu, M.-L., Hansburg, D., and Matis, L. A. (1988). Selection of amino acid sequences in the beta chain of the T cell antigen receptor. *Science* **239**, 1541-1544.

Heeg, K., Gaus, H., Griese, D., Bendigs, S., Miethke, T., and Wagner, H. (1995). Superantigen-reactive T cells that display an anergic phenotype *in vitro* appear functional *in vivo*. *Int. Immunol.* **7**, 105-114.

Heinzel, F. P., Sadick, M. D., Mutha, S. S., and Locksley, R. M. (1991). Production of interferon γ, interleukin 2, interleukin 4, and interleukin 10 by $CD4^+$ lymphocytes *in vivo* during healing and progressive murine leishmaniasis. *Proc. Natl. Acad. Sci. USA* **88**, 7011-7015.

Held, W., Shakhov, A. N., Waanders, G., Scarpellino, L., Luethy, R., Kraehenbuhl, J. P., MacDonald, H. R., and Acha-Orbea, H. (1992). An exogenous mouse mammary tumor virus with properties of Mls-1^a (*Mtv-7*). *J. Exp. Med.* **175**, 1623-1633.

Held, W., Shakhov, A. N., Izui, S., Waanders, G. A., Scarpellino, L., MacDonald, H. R., and Acha-Orbea, H. (1993a). Superantigen-reactive $CD4^+$ T cells are required to stimulate B cells after infection with mouse mammary tumor virus. *J. Exp. Med.* **177**, 359-366.

Held, W., Waanders, G. A., Shakhov, A. N., Scarpellino, L., Acha-Orbea, H., and MacDonald, H. R. (1993b). Superantigen-induced immune stimulation amplifies mouse mammary tumor virus infection and allows virus transmission. *Cell* **74**, 529-540.

Held, W., Waanders, G. A., Acha-Orbea, H., and MacDonald, H. R. (1994a). Reverse transcriptase-dependent and –independent phases of infection with mouse mammary tumour virus: Implications for superantigen function. *J. Exp. Med.* **180**, 2347-2351.

Held, W., Waanders, G. A., MacDonald, H. R., and Acha Orbea, H. (1994b). MHC class II hierarchy of superantigen presentation predicts efficiency of infection with mouse mammary tumor virus. *Int. Immunol.* **6**, 1403-1407.

Herrmann, T., Acolla, R. S., and R., M. H. (1989). Different staphylococcal enterotoxins bind preferentially to distinct major histocompatibility complex class II isotypes. *Eur. J. Immunol.* **19**, 2171-2174.

Herrmann, T., Maryanski, J. L., Romero, P., Fleischer, B., and MacDonald, H. R. (1990). Activation of MHC class I-restricted $CD8^+$ CTL by microbial T cell mitogens. Dependence upon MHC class II expression of the target cells and Vβ usage of the responder T cells. *J. Immunol.* **144**, 1181-1186.

Herrmann, T., Baschieri, S., Lees, R. K., and MacDonald, H. R. (1992). *In vivo* responses of $CD4^+$ and $CD8^+$ cells to bacterial superantigens. *Eur. J. Immunol.* **22**, 1935-1938.

Heussler, V. T., Eichhorn, M., Reeves, R., Magnuson, N. S., Williams, R. O., and Dobbelaere, D. A. (1992). Constitutive IL-2 mRNA expression in lymphocytes, infected with the intracellular parasite *Theileria parva*. *J. Immunol.* **149**, 562-567.

Hingorani, R., Choi, I. H., Akolkar, P., Gulwani-Akolkar, B., Pergolizzi, R., Silver, J., and Gregersen, P. K. (1993). Clonal predominance of T cell receptors within the $CD8^+$ $CD45RO^+$ subset in normal human subjects. *J. Immunol.* **151**, 5762-5769.

Howard, C. J., Morrison, W. I., Bensaid, A., Davis, W., Eskra, L., Gerdes, J., Hadam, M., Hurley, D., Leibold, W., Letesson, J. J., MacHugh, N., Naessens, J., O'Reilly, K., Parsons, K. R., Schlote, D., Sopp, P., Splitter, G., and Wilson, R. (1991). Summary of workshop findings for leukocyte antigens of cattle. *Vet. Immunol. Immunopathol.* **27**, 21-27.

Howell, M. D., Diveley, J. P., Lundeen, K. A., Esty, A., Winters, S. T., Carlo, D. J., and Brostoff, S. W. (1991). Limited T-cell receptor β-chain heterogeneity among interleukin 2 receptor-positive synovial T cells suggests a role for superantigen in rheumatoid arthritis. *Proc. Natl. Acad. Sci. USA* **88**, 10921-10925.

Hsieh, C. S., Heimberger, A. B., Gold, J. S., O'Garra, A., and Murphy, K. M. (1992). Differential regulation of T helper phenotype development by interleukins 4 and 10 in an αβ T-cell-receptor transgenic system. *Proc. Natl. Acad. Sci. USA* **89**, 6065-6069.

Hudson, K. R., Tiedemann, R. E., Urban, R. G., Lowe, S. C., Strominger, J. L., and Fraser, J. D. (1995). Staphylococcal enterotoxin A has two cooperative binding sites on major histocompatibility complex class II. *J. Exp. Med.* **182**, 711-720.

Hulliger, L., Wilde, J. K. H., Brown, C. G. D., and Turner, L. (1964). Mode of multiplication of *Theileria* in cultures of bovine lymphocytic cells. *Nature* **203**, 728-730.

Ignatowicz, L., Kappler, J., and Marrack, P. (1992). The effects of chronic infection with a superantigen-producing virus. *J. Exp. Med.* **175**, 917-923.

Inaba, K., Metlay, J. P., Crowley, M. T., and Steinman, R. M. (1990). Dendritic cells pulsed with protein antigens *in vitro* can prime antigen-specific, MHC-restricted T cells *in situ*. *J. Exp. Med.* **172**, 631-640

Irvin, A. D., Brown, C. G. D., Kanhai, G. K., and Stagg, D. A. (1975). Comparative growth of bovine lymphosarcoma cells and lymphoid cells infected with *Theileria parva* in athymic (nude) mice. *Nature* **255**, 713-714.

Irvin, A. D., Ocama, J. G. R., and Spooner, P. R. (1982). Cycle of bovine lymphoblastoid cells parasitised by *Theileria parva*. *Res. Vet. Sci.* **33**, 298-304.

Irvin, A. D., Dobbelaere, D. A. E., Mwamachi, D. M., Minami, T., Spooner, P. R., and Ocama, J. G. R. (1983). Immunisation against East Coast fever: correlation between monoclonal antibody profiles of *Theileria parva* stocks and cross immunity *in vivo*. *Res. Vet. Sci.* **35**, 341-346.

Irvin, A. D., and Morrison, W. I. (1987). Immunopathology, Immunology and Immunoprophylaxis of *Theileria* infections. In *Immune Responses in Parasitic Infections: Immunology, Immunopathology and Immunoprophylaxis. Vol. III.*, E. J. L. Soulsby, ed. (London: CRC Press), pp. 223-274.

Ishiguro, N., Tanaka, A., and Shinagawa, M. (1990). Sequence analysis of bovine T-cell receptor α-chain. *Immunogenetics* **31**, 57-60.

Isono, T., Isegawa, Y., and Seto, A. (1994). Sequence and diversity of variable gene segments coding for rabbit T-cell receptor beta chains. *Immunogenetics* **39**, 243-248.

Ivanov, V., Stein, B., Baumann, I., Dobbelaere, D. A. E., Herrlich, P., and Williams, R. O. (1989). Infection with the intracellular protozoan parasite *Theileria parva* induces constitutively high levels of NF-κB in bovine T lymphocytes. *Mol. Cell. Biol.* **9**, 4677-4686.

Jardetzky, T. S., Brown, J. H., Gorga, J. C., Stern, L. J., Urban, R. G., Chi, Y. I., Stauffacher, C., Strominger, J. L., and Wiley, D. C. (1994). Three-dimensional structure of a human class II histocompatibility molecule complexed with superantigen. *Nature* **368**, 711-718.

Jarrett, W. F. H., Crighton, G. W., and Pirie, H. M. (1969). *Theileria parva*: Kinetics of replication. *Exp. Parasitol.* **24**, 9-25.

Jones, K. R., Hickling, J. K., Targett, G. A. T., and Playfair, J. H. L. (1990). Polyclonal *in vitro* proliferative responses from nonimmune donors to *Plasmodium falciparum* malaria antigens require UCHL1$^+$ (memory) T cells. *Eur. J. Immunol.* **20**, 307-315.

Jores, R., Alzari, P. M., and Meo, T. (1990). Resolution of hypervariable regions in T-cell receptor β chains by a modified Wu-Kabat index of amino acid diversity. *Proc. Natl. Acad. Sci. USA* **87**, 9138-9142.

Jores, R., and Meo, T. (1993). Few V gene segments dominate the T cell receptor β-chain repertoire of the human thymus. *J. Immunol.* **151**, 6110-6122.

Kabat, E. A., Wu, T. T., Perry, H. M., Gottesman, K. S., and Foeller, C. (1991). Sequences of Proteins of Immunological Interest. 5th edn. NIH Publ. No. 91-3242. US Dep. Health Hum. Serv. NIH, Washington D.C.

Kabelitz, D., Conradt, P., Schondelmaier, S., Wagner, H., and Haars, R. (1989). A novel subset of $CD2^-$, CD3/T cell receptor α/β^+ human peripheral blood T cells. Phenotypic and functional characterization of interleukin 2-dependent $CD2^-$ $CD3^+$ T cell clones. *J. Exp. Med.* **170**, 559-569.

Kappler, J., Kubo, R., Haskins, K., Hannum, C., Marrack, P., Pigeon, M., McIntyre, B., Allison, J., and Trowbridge, I. (1983). The major histocompatibility complex-restricted antigen receptor on T cells in mouse and man: identification of constant and variable peptides. *Cell* **35**, 295-302.

Kappler, J. W., Staerz, U., White, J., and Marrack, P. C. (1988). Self-tolerance eliminates T cells specific for *Mls*-modified products of the major histocompatability complex. *Nature* **332**, 35-40.

Kappler, J., Kotzin, B., Herron, L., Gelfand, E. W., Bigler, R. D., Boylston, A., Carrel, S., Posnett, D. N., Choi, Y., and Marrack, P. (1989). Vβ-specific stimulation of human T cells by staphylococcal toxins. *Science* **244**, 811-813.

Kappler, J. W., Herman, A., Clements, J., and Marrack, P. (1992). Mutations defining functional regions of the superantigen staphylococcal enterotoxin B. *J. Exp. Med.* **175**, 387-396.

Karapetian, O., Shakhov, A. N., Kraehenbuhl, J. P., and Acha-Orbea, H. (1994). Retroviral infection of neonatal Peyer's patch lymphocytes: the mouse mammary tumor virus model. *J. Exp. Med.* **180**, 1511-1516.

Kariuki, D. P., Young, A. S., Morzaria, S. P., Lesan, A. C., Mining, S. K., Omwoyo, P., Wafula, J. L., and Molyneux, D. H. (1995). *Theileria parva* carrier state in naturally infected and artificially immunised cattle. *Trop. Anim. Hlth. Prod.* **27**, 15-25.

Karp, D. R., Teletski, C. L., Scholl, P., Geha, R., and Long, E. O. (1990). The α1 domain of the HLA-DR molecule is essential for high-affinity binding of the toxic shock syndrome toxin-1. *Nature* **346**, 474-476.

Kawabe, Y., and Ochi, A. (1990). Selective anergy of $V\beta8^+$, $CD4^+$ T cells in staphylococcus enterotoxin B-primed mice. J. *Exp. Med.* **172**, 1065-1070.

Kawabe, Y., and Ochi, A. (1991). Programmed cell death and extrathymic reduction of $V\beta8^+$ $CD4^+$ T cells in mice tolerant to *Staphylococcus aureus* enterotoxin B. *Nature* **349**, 245-248.

Khan, I. A., Matsuura, T., and Kasper, L. H. (1995). IL-10 mediates immunosuppression following primary infection with *Toxoplasma gondii* in mice. *Parasite Immunol.* **17**, 185-195.

Kimura, N., Toyonaga, B., Yoshikai, Y., Du, R.-P., and Mak, T. W. (1987). Sequences and repertoire of the human T cell receptor α and β chain variable region genes in thymocytes. *Eur. J. Immunol.* **17**, 375-383.

Klotz, J. L., Barth, R. K., Kiser, G. L., Hood, L. E., and Kronenberg, M. (1989). Restriction fragment length polymorphisms of the mouse T-cell receptor gene families. *Immunogenetics* **29**, 191-201.

Kondo, S., Shimizu, A., Maeda, M., Tagaya, Y., Yodoi, J., and Honjo, T. (1986). Expression of functional human interleukin-2 receptor in mouse T cells by cDNA transfection. *Nature* **320**, 75-77.

Koop, B. F., Rowan, L., Chen, W. Q., Deshpande, P., Lee, H., and Hood, L. (1993). Sequence length and error analysis of Sequenase and automated Taq cycle sequencing methods. *Biotechniques* **14**, 442-447.

Korman, A. J., Bourgarel, P., Meo, T., and Rieckhof, G. E. (1992). The mouse mammary tumour virus long terminal repeat encodes a type II transmembrane glycoprotein. *EMBO J.* **11**, 1901-1905.

Kotzin, B. L., Barr, V. L., and Palmer, E. (1985). A large deletion within the T-cell receptor beta-chain gene complex in New Zealand White mice. *Science* **229**, 167-171.

Kronenberg, M. (1994). Antigens recognized by γδ T cells. *Curr. Opin. Immunol.* **6**, 64-71.

Kumar, V., and Sercarz, E. (1994). Holes in the T cell repertoire to myelin basic protein owing to the absence of the Dβ2-Jβ2 gene cluster: implications for T cell receptor recognition and autoimmunity. *J. Exp. Med.* **179**, 1637-1643.

Lafon, M., Lafage, M., Martinez-Arends, A., Ramirez, R., Vuillier, F., Charron, D., Lotteau, V., and Scott-Algara, D. (1992). Evidence for a viral superantigen in humans. *Nature* **358**, 507-510.

Lai, E., Concannon, P., and Hood, L. (1988). Conserved organization of the human and murine T-cell receptor β-gene families. *Nature* **331**, 543-546.

Lalor, P. A., Morrison, W. I., and Black, S. J. (1986). Monoclonal antibodies to bovine leucocytes define heterogeneity of target cells for *in vitro* parasitosis by *Theileria parva.* In *The Ruminant Immune System in Health and Disease.*, W. I. Morrison, ed. (Cambridge: Cambridge University Press), pp. 72-87.

Lanzavecchia, A., Roosnek, E., Gregory, T., Berman, P., and Abrignani, S. (1988). T cells can present antigens such as HIV gp120 targeted to their own surface molecules. *Nature* **334**, 530-532.

Lehner, P. J., Wang, E. C., Moss, P. A., Williams, S., Platt, K., Friedman, S. M., Bell, J. I., and Borysiewicz, L. K. (1995). Human HLA-A0201-restricted cytotoxic T lymphocyte recognition of influenza A is dominated by T cells bearing the Vβ17 gene segment. *J. Exp. Med.* **181**, 79-91.

Lewis, D. E., Puck, J. M., Babcock, G. F., and Rich, R. R. (1985). Disproportionate expansion of a minor T cell subset in patients with lymphadenopathy syndrome and acquired immunodeficiency syndrome. *J. Infect. Dis.* **151**, 555-559.

Lewis, D. E., Ng Tang, D. S., Adu Oppong, A., Schober, W., and Rodgers, J. R. (1994). Anergy and apoptosis in $CD8^+$ T cells from HIV-infected persons. *J. Immunol.* **153**, 412-420.

Li, Y., Szabo, P., Robinson, M. A., Dong, B., and Posnett, D. N. (1990). Allelic variations in the human T cell receptor Vβ6.7 gene products. *J. Exp. Med.* **171**, 221-230.

Li, Y., Szabo, P., and Posnett, D. N. (1991). The genomic structure of human Vβ6 T cell antigen receptor genes. *J. Exp. Med.* **174**, 1537-1547.

Liew, F. Y., Millott, S., Parkinson, C., Palmer, R. M., and Moncada, S. (1990). Macrophage killing of *Leishmania* parasites *in vivo* is mediated by nitric oxide from L-arginine. *J. Immunol.* **144**, 4794-4797.

Lipkowitz, S., Greene, W. C., Rubin, A. L., Novogrodsky, A., and Stenzel, K. H. (1984). Expression of receptors for interleukin 2: role in the commitment of T lymphocytes to proliferate. *J. Immunol.* **132**, 31-37.

Liu, H., Lampe, M. A., Iregui, M. V., and Cantor, H. (1991). Conventional antigen and superantigen may be coupled to distinct and cooperative T-cell activation pathways. *Proc. Natl. Acad. Sci. USA* **88**, 8705-8709.

Loh, E. Y., Elliot, J. F., Cwirla, S., Lanier, L. L., and Davis, M. M. (1989). Polymerase chain reaction with single-sided specificity: Analysis of T cell receptor δ chain. *Science* **243**, 217-220.

Louie, M. C., Nelson, C. A., and Loh, D. Y. (1989). Identification and characterization of new murine T cell receptor β chain variable region (Vβ) genes. *J. Exp. Med.* **170**, 1987-1998.

Lundén, A., Sigurdardóttir, S., and Andersson, L. (1991). Restriction fragment length polymorphism of a bovine T-cell receptor β gene. *Anim. Genet.* **22**, 497-501.

Luyrink, L., Gabriel, C. A., Thompson, S. D., Grom, A. A., Maksymowych, W. P., Choi, E., and Glass, D. N. (1993). Reduced expression of a human Vβ6.1 T-cell receptor allele. *Proc. Natl. Acad. Sci. USA* **90**, 4369-4373.

Macdonald, H. R., Schneider, R., Lees, R. K., Howe, R. C., Acha-Orbea, H., Festenstein, H., Zinkernagel, R. M., and Hengartner, H. (1988). T-cell receptor Vβ use predicts reactivity and tolerance to Mls^a-encoded antigens. *Nature* **332**, 40-45.

MacDonald, H. R., Glasebrook, A. L., Schneider, R., Lees, R. K., Pircher, H., Pedrazzani, T., Kanagawa, O., Nicolas, J.-F., Howe, R. C., Zinkernagel, R. M., and Hengartner, H. (1989). T-cell reactivity and tolerance to Mls^a-encoded antigens. *Immunol. Rev.* **107**, 89-108.

MacDonald, H. R., Baschieri, S., and Lees, R. K. (1991). Clonal expansion precedes anergy and death of $V\beta8^+$ peripheral T cells responding to staphylococcal enterotoxin B *in vivo*. *Eur. J. Immunol.* **21**, 1963-1966.

MacHugh, N. D., Bensaid, A., Howard, C. J., Davis, W. C., and Morrison, W. I. (1991). Analysis of the reactivity of anti-bovine CD8 monoclonal antibodies with cloned T cell lines and mouse L-cells transfected with bovine CD8. *Vet. Immunol. Immunopathol.* **27**, 169-172.

MacHugh, N. D., and Sopp, P. (1991). Individual antigens of cattle. Bovine CD8 (BoCD8). *Vet. Immunol. Immunopathol.* **27** , 65-69.

MacHugh, N. D., Taracha, E. L., and Toye, P. G. (1993). Reactivity of workshop antibodies on L cell and COS cell transfectants expressing bovine CD antigens. *Vet. Immunol. Immunopathol.* **39** , 61-67.

MacPhail, S., Ishizaka, S. T., Bykowsky, M. J., Lattime, E. C., and Stutman, O. (1985). Specific neonatally induced tolerance to *Mls* locus determinants. *J. Immunol.* **135**, 2967-2974.

Makni, H., Malter, J. S., Reed, J. C., Nobuhiko, S., Lang, G., Kioussis, D., Trinchieri, G., and Kamoun, M. (1991). Reconstitution of an active surface CD2 by DNA transfer in $CD2^-CD3^+$ Jurkat cells facilitates CD3 T cell receptor-mediated IL-2 production.
J. Immunol. **146**, 2522-2529.

Malhotra, U., Spielman, R., and Concannon, P. (1992). Variability in T cell receptor Vβ gene usage in human peripheral blood lymphocytes. Studies of identical twins, siblings, and insulin-dependent diabetes mellitus patients. *J. Immunol.* **149**, 1802-1808.

Marrack, P., and Kappler, J. (1990). The staphylococcal enterotoxins and their relatives. *Science* **248**, 705-711.

Mattner, F., Magram, J., Ferrante, J., Launois, P., Di Padova, K., Behin, R., Gately, M. K., Louis, J. A., and Alber, G. (1996). Genetically resistant mice lacking interleukin-12 are susceptible to infection with *Leishmania major* and mount a polarized Th2 cell response. *Eur. J. Immunol.* **26**, 1553-1559.

McCormack, J. E., Callahan, J. E., Kappler, J., and Marrack, P. C. (1993). Profound deletion of mature T cells *in vivo* by chronic exposure to exogenous superantigen.
J. Immunol. **150**, 3785-3792.

McKeever, D. J., Taracha, E. L., Innes, E. L., MacHugh, N. D., Awino, E., Goddeeris, B. M., and Morrison, W. I. (1994). Adoptive transfer of immunity to *Theileria parva* in the $CD8^+$ fraction of responding efferent lymph. *Proc. Natl. Acad. Sci. USA* **91**, 1959-1963.

McKeever, D. J., Nyanjui, J. K., and Ballingall, K. T. (1997). *In vitro* infection with *Theileria parva* is associated with IL-10 expression in all bovine lymphocyte lineages. *Parasite Immunol.* **19**, 319-324.

Mehlhorn, H., and Schein, E. (1984). The Piroplasms: Life cycle and sexual stages. *Adv. Parasitol.* **23**, 38-103.

Merkenschlager, M., Terry, L., Edwards, R. and Beverley, P. C. L. (1988). Limiting dilution analysis of proliferative responses in human lymphocyte populations defined by the monoclonal antibody UCHL1: implications for differential CD45 expression in T cell memory formation. *Eur. J. Immunol.* **18**, 1653-1661.

Meyerhans, A., Vartanian, J. P., and Wain-Hobson, S. (1990). DNA recombination during PCR. *Nucleic Acids Res.* **18**, 1687-1691.

Miethke, T., Duschek, K., Wahl, C., Heeg, K., and Wagner, H. (1993). Pathogenesis of the toxic shock syndrome: T cell mediated lethal shock caused by the superantigen TSST-1. *Eur. J. Immunol.* **23**, 1494-1500.

Minami, T., Spooner, P. R., Irvin, A. D., Ocama, J. G. R., Dobbelaere, D. A. E., and Fujinaga, T. (1983). Characterization of stocks of *Theileria parva* by monoclonal antibody profiles. *Res. Vet. Sci.* **35**, 334-340.

Mollick, J. A., Cook, R. G., and Rich, R. R. (1989). Class II MHC molecules are specific receptors for staphylococcus enterotoxin A. *Science* **244**, 817-820.

Mombaerts, P., Clarke, A. R., Rudnicki, M. A., Iacomini, J., Itohara, S., Lafaille, J. J., Wang, L., Ichikawa, Y., Jaenisch, R., Hooper, M. L., and Tonegawa, S. (1992). Mutations in T-cell antigen receptor genes α and β block thymocyte development at different stages. *Nature* **360**, 225-231.

Morris, L., Troutt, A. B., Handman, E., and Kelso, A. (1992). Changes in the precursor frequencies of IL-4 and IFN-gamma secreting $CD4^+$ cells correlate with resolution of lesions in murine cutaneous leishmaniasis. *J. Immunol.* **149**, 2715-2721.

Morrison, W. I., Büscher, G., Murray, M., Emery, D. L., Masake, R. A., Cook, R. H., and Wells, P. W. (1981). *Theileria parva*: kinetics of infection in the lymphoid system of cattle. *Exp. Parasitol.* **52**, 248-260.

Morrison, W. I., Lalor, P. A., Goddeeris, B. M., and Teale, A. J. (1986). Theilerosis: Antigens and host-parasite interactions. In *Parasite Antigens: Towards New Strategies for Vaccines.*, T. W. Pearson, ed. (New York and Basel: Marcel Dekker, Inc.), pp. 167-214.

Morrison, W. I., Goddeeris, B. M., Teale, A. J., Groocock, C. M., Kemp, S. J., and Stagg, D. A. (1987). Cytotoxic T-cells elicited in cattle challenged with *Theileria parva* (Muguga): evidence for restriction by class I MHC determinants and parasite strain specificity. *Parasite Immunol.* **9**, 563-578.

Morrison, W. I., Baldwin, C. L., MacHugh, N. D., Teale, A. J., Goddeeris, B. M., and Ellis, J. (1988). Phenotypic and functional characterisation of bovine lymphocytes. In *Progress in Veterinary Microbiology and Immunology. Vol. 4.* R. Pandey, ed. (Basel: Karger), pp134-164.

Morrison, W. I., and Davis, W. C. (1991). Individual antigens of cattle. Differentiation antigens expressed predominantly on $CD4^-$ $CD8^-$ T lymphocytes (WC1, WC2). *Vet. Immunol. Immunopathol.* **27**, 71-76.

Morrison, W. I., MacHugh, N. D., and Lalor, P. A. (1996). Pathogenicity of *Theileria parva* is influenced by the host cell type infected by the parasite. *Infect. Immun.* **64**, 557-562.

Mosmann, T. R., and Coffman, R. L. (1989). Th1 and Th2 cells: Different patterns of lymphokine secretion lead to different functional properties. *Annu. Rev. Immunol.* **7**, 145-173.

Moss, P. A., Moots, R. J., Rosenberg, W. M., Rowland-Jones, S. J., Bodmer, H. C., McMichael, A. J., and Bell, J. I. (1991). Extensive conservation of α and β chains of the human T-cell antigen receptor recognizing HLA-A2 and influenza A matrix peptide. *Proc. Natl. Acad. Sci. USA* **88**, 8987-8990.

Muhammed, S. I., Lauerman, L. H., and Johnson, L. W. (1975). Effect of humoral antibodies on the course of *Theileria parva* infection (East Coast fever) of cattle. *Am. J. Vet. Res.* **36**, 399-402.

Muraille, E., De Becker, G., Bakkus, M., Thielemans, K., Urbain, J., Moser, M., and Oberdan, L. (1995). Co-stimulation lowers the threshold for activation of naive T cells by bacterial superantigens. *Int. Immunol.* **7**, 295-304.

Musoke, A. J., Nantulya, V. M., Büscher, G., Masake, R. A., and Otim, B. (1982). Bovine immune response to *Theileria parva*: neutralizing antibodies to sporozoites. *Immunology* **45**, 663-668.

Musoke, A. J., Nantulya, V. M., Rurangirwa, F. R., and Büscher, G. (1984). Evidence for a common protective antigenic determinant on sporozoites of several *Theileria parva* strains. *Immunology* **54**, 231-238.

Musoke, A., Morzaria, S., Nkonge, C., Jones, E., and Nene, V. (1992). A recombinant sporozoite surface antigen of *Theileria parva* induces protection in cattle. *Proc. Natl. Acad. Sci. USA* **89**, 514-518.

Naessens, J., Newson, J., Bensaid, A., Teale, A. J., Magondu, J. G., and Black, S. J. (1985). *De novo* expression of T cell markers on *Theileria parva*-transformed lymphoblasts in cattle. *J. Immunol.* **135**, 4183-4188.

Naessens, J., Newson, J., Williams, D. J. L., and Lutje, V. (1988). Identification of isotypes and allotypes of bovine immunoglobulin M with monoclonal antibodies. *Immunology* **63** , 569-574.

Naessens, J., Grab, D. J. and Fritsch, G. (1996). Characterisation of bovine transferrin receptor on normal activated and *Theileria parva*-transformed lymphocytes by a new monoclonal antibody. *Vet. Immunol. Immunopathol.* **52**, 65-76.

Nalefski, E. A., Kasibhatla, S., and Rao, A. (1992). Functional analysis of the antigen binding site on the T cell receptor α chain. *J. Exp. Med.* **175**, 1553-1563.

Nanda, N. K., Apple, R., and Sercarz, E. (1991). Limitations in plasticity of the T-cell receptor repertoire. **Proc. Natl. Acad. Sci. USA 88**, 9503-9507.

Nelson, R. T., and Hirumi, H. (1981). *In vitro* cloning of *Theileria*-infected bovine lymphoblastoid cells: Standardization and characterization. In *Advances in the Control of Theileriosis.*, A. D. Irvin, M. P. Cunningham and A. S. Young, eds. (The Hague: Martinus Nijhoff), pp. 120-121.

Nene, V., Iams, K. P., Gobright, E., and Musoke, A. J. (1992). Characterisation of the gene encoding a candidate vaccine antigen of *Theileria parva* sporozoites. *Mol. Biochem. Parasitol.* **51**, 17-27.

Nene, V., Musoke, A., Gobright, E., and Morzaria, S. (1996). Conservation of the sporozoite p67 vaccine antigen in cattle-derived *Theileria parva* stocks with different cross-immunity profiles. *Infect. Immun.* **64**, 2056-2061.

Nickoloff, B. J., Mitra, R. S., Green, J., Zheng, X. G., Shimizu, Y., Thompson, C., and Turka, L. A. (1993). Accessory cell function of keratinocytes for superantigens. Dependence on lymphocyte function-associated antigen-1/intercellular adhesion molecule-1 interaction. *J. Immunol.* **150**, 2148-2159.

Nossal, G. J. (1994). Negative selection of lymphocytes. *Cell* **76**, 229-239.
Ohmen, J. D., Barnes, P. F., Grisso, C. L., Bloom, B. R., and Modlin, R. L. (1994). Evidence for a superantigen in human tuberculosis. *Immunity* **1**, 35-43.

Okada, C. Y., and Weissman, I. L. (1989). Relative Vβ transcript levels in thymus and peripheral lymphoid tissues from various mouse strains. Inverse correlation of I-E and *Mls* expression with relative abundance of several Vβ transcripts in peripheral lymphoid tissues. *J. Exp. Med.* **169**, 1703-1719.

Oksenberg, J. R., Stuart, S., Begovich, A. B., Bell, R. B., Erlich, H. A., Steinman, L., and Bernard, C. C. A. (1990). Limited heterogeneity of rearranged T-cell receptor Vα transcripts in brains of multiple sclerosis patients. *Nature* **345**, 344-347.

Oyaizu, N., Chirmule, N., Yagura, H., Pahwa, R., Good, R. A., and Pahwa, S. (1992). Superantigen staphylococcal enterotoxin B-induced T-helper cell activation is independent of CD4 molecules and phosphatidylinositol hydrolysis. *Proc. Natl. Acad. Sci. USA* **89**, 8035-8039.

Paliard, X., de Waal-Malefyt, R., de Vries, J. E., and Spits, H. (1988). Interleukin-4 mediates CD8 induction on human $CD4^+$ T-cell clones. *Nature* **335**, 642-644.

Paliard, X., West, S. G., Lafferty, J. A., Clements, J. R., Kappler, J. W., Marrack, P., and Kotzin, B. L. (1991). Evidence for the effects of a superantigen in rheumatoid arthritis. *Science* **253**, 325-329.

Palmer, L. D., Saha, B., Hodes, R. J., and Abe, R. (1996). The role of CD28 costimulation in immune-mediated responses against mouse mammary tumor viruses. *J. Immunol.* **156**, 2112-2118.

Pannetier, C., Even, J., and Kourilsky, P. (1995). T-cell repertoire diversity and clonal expansions in normal and clinical samples. *Immunol. Today* **16**, 176-181.

Pantaleo, G., Demarest, J. F., Soudeyns, H., Graziosi, C., Denis, F., Adelsberger, J. W., Borrow, P., Saag, M. S., Shaw, G. M., Sekaly, R. P., and Fauci, A. S. (1994). Major expansion of $CD8^+$ T cells with a predominant Vβ usage during the primary immune response to HIV. *Nature* **370**, 463-467.

Park, C. G., Jung, M. Y., Choi, Y., and Winslow, G. M. (1995). Proteolytic processing is required for viral superantigen activity. *J. Exp. Med.* **181**, 1899-1904.

Patten, P., Yokota, T., Rothbard, J., Chien, Y., Arai, K., and Davis, M. M. (1984). Structure, expression and divergence of T cell receptor β-chain variable regions. *Nature* **312**, 40-46.

Patten, P. A., Rock, E. P., Sonoda, T., Fazekas de St. Groth, B., Jorgensen, J. L., and Davis, M. M. (1993). Transfer of putative complementarity-determining region loops of T cell receptor V domains confers toxin reactivity but not peptide/MHC specificity. *J. Immunol.* **150**, 2281-2294.

Pearson, T. W., Lundin, L. B., Dolan, T. T., and Stagg, D. A. (1979). Cell-mediated immunity to *Theileria*-transformed cell lines. *Nature* **281**, 678-680.

Pearson, T. W., Hewett, R. S., Roelants, G. E., Stagg, D. A., and Dolan, T. T. (1982). Studies on the induction and specificity of cytotoxicity to *Theileria*-transformed cell lines. *J. Immunol.* **128**, 2509-2513.

Pinder, M., Kar, S., Withey, K. S., Lundin, L. B., and Roelants, G. E. (1981). Proliferation and lymphocyte stimulatory capacity of *Theileria*-infected lymphoblastoid cells before and after the elimination of intracellular parasites. *Immunology* **44**, 51-60.

Pipano, E. (1981). Schizonts and tick stages in immunization against *Theileria annulata* infection. In *Advances in the Control of Theileriosis.*, A. D. Irvin, M. P. Cunningham and A. S. Young, eds. (The Hague: Matinus Nijhoff), pp. 242-252.

Pirie, H. M., Jarrett, W. F. H., and Crighton, G. W. (1970). Studies on vaccination against East Coast fever using macroschizonts. *Exp. Parasitol.* 27, 343-349.

Piuvezam, M. R., Russo, D. M., Burns, J. M., Jr., Skeiky, Y. A., Grabstein, K. H., and Reed, S. G. (1993). Characterization of responses of normal human T cells to *Trypanosoma cruzi* antigens. *J. Immunol.* **150**, 916-924.

Plaza, A., Kono, D. H., and Theofilopoulos, A. N. (1991). New human Vβ genes and polymorphic variants. *J. Immunol.* **147**, 4360-4365.

Pohl, T., Pechhold, K., Oberg, H. H., Wilbert, O. M., and Kabelitz, D. (1995). Antigen-induced death of alloreactive human T-lymphocytes occurs in the absence of low molecular weight DNA fragmentation. *Cell. Immunol.* **166**, 187-195.

Porcelli, S. A., Morita, C. T. and Modlin, R. L. (1996). T-cell recognition of non-peptide antigens. *Curr. Opin. Immunol.* **8**, 510-516.

Posnett, D. N. (1990). Allelic variations of human TCR V gene products. *Immunol. Today* **11**, 368-373.

Posnett, D. N., Vissinga, C. S., Pambuccian, C., Wei, S., Robinson, M. A., Kostyu, D., and Concannon, P. (1994). Level of human *TCRBV3S1* (Vβ3) expression correlates with allelic polymorphism in the spacer region of the recombination signal sequence. *J. Exp. Med.* **179**, 1707-1711.

Prasad, G. S., Earhart, C. A., Murray, D. L., Novick, R. P., Schlievert, P. M., and Ohlendorf, D. H. (1993). Structure of toxic shock syndrome toxin 1. *Biochemistry* **32**, 13761-13766.

Preston, P. M., Brown, C. G., and Richardson, W. (1992). Cytokines inhibit the development of trophozoite-infected cells of *Theileria annulata* and *Theileria parva* but enhance the proliferation of macroschizont-infected cell lines. *Parasite Immunol.* **14**, 125-141.

Pullen, A. M., Potts, W., Wakeland, E. K., Kappler, J., and Marrack, P. (1990a). Surprisingly uneven distribution of the T cell receptor Vβ repertoire in wild mice. *J. Exp. Med.* **171**, 49-62.

Pullen, A. M., Wade, T., Marrack, P., and Kappler, J. W. (1990b). Identification of the region of T cell receptor β chain that interacts with the self-superantigen Mls-1^a. *Cell* **61**, 1365-1374.

Radley, D. E., Brown, C. G. D., Burridge, M. J., Cunningham, M. P., Pierce, M. A., and Purnell, R. E. (1974). East Coast fever: Quantitative studies of *Theileria parva* in cattle. *Exp. Parasitol.* **36**, 278-287.

Radley, D. E., Young, A. S., Brown, C. G. D., Burridge, M. J., Cunningham, M. P., Musisi, F. L., and Purnell, R. E. (1975). East Coast fever: 2. Cross-immunity trials with a Kenya strain of *Theileria lawrencei*. *Vet. Parasitol.* **1**, 43-50.

Radley, D. E. (1981). Infection and treatment method of immunization against theileriosis. In *Advances in the Control of Theileriosis.*, A. D. Irvin, M. P. Cunningham and A. S. Young, eds. (The Hague: Martinus Nijhoff), pp. 227-237.

Rammensee, H.-G., Kroschewski, R., and Frangoulis, B. (1989). Clonal anergy induced in mature $V\beta6^+$ T lymphocytes on immunizing *Mls-1^b* mice with Mls-1^a expressing cells. *Nature* **339**, 541-544.

Reiner, S. L., Zheng, S., Wang, Z. E., Stowring, L., and Locksley, R. M. (1994). *Leishmania* promastigotes evade interleukin 12 (IL-12) induction by macrophages and stimulate a broad range of cytokines from $CD4^+$ T cells during initiation of infection. *J. Exp. Med.* **179**, 447-456.

Renno, T., Hahne, M., and MacDonald, H. R. (1995). Proliferation is a prerequisite for bacterial superantigen-induced T cell apoptosis *in vivo*. *J. Exp. Med.* **181**, 2283-2287.

Renno, T., and Acha-Orbea, H. (1996). Superantigens in autoimmune diseases: still more shades of gray. *Immunol. Rev.* **154**, 175-191.

Reyburn, H., Cornélis, F., Russell, V., Harding, R., Moss, P., and Bell, J. (1993). Allelic polymorphism of human T-cell receptor V alpha gene segments. *Immunogenetics* **38**, 287-291.

Robinson, M. A. (1989). Allelic sequence variations in the hypervariable region of a T-cell receptor β-chain: correlation with restriction fragment length polymorphism in human families and populations. *Proc. Natl. Acad. Sci. USA* **86**, 9422-9426.

Robinson, M. A. (1991). The human T cell receptor β-chain gene complex contains at least 57 variable gene segments. Identification of six Vβ genes in four new gene families. *J. Immunol.* **146**, 4392-4397.

Robinson, M. A., Mitchell, M. P., Wei, S., Day, C. E., Zhao, T. M., and Concannon, P. (1993). Organization of human T-cell receptor β-chain genes: clusters of Vβ genes are present on chromosomes 7 and 9. *Proc. Natl. Acad. Sci. USA* **90**, 2433-2437.

Roessner, K., Fikrig, E., Russell, J. Q., Cooper, S. M., Flavell, R. A. and Budd, R. C. (1994). Prominent T cell lymphocyte response to *Borrelia burgdorferi* from peripheral blood of unexposed donors. *Eur. J. Immunol.* **24**, 320-324.

Rosenberg, W. M., Moss, P. A., and Bell, J. I. (1992). Variation in human T cell receptor Vβ and Jβ repertoire: analysis using anchor polymerase chain reaction. *Eur. J. Immunol.* **22**, 541-549.

Rowen, L., Koop, B. F., and Hood, L. (1996). The complete 685-kilobase DNA sequence of the human β T cell receptor locus. *Science* **272**, 1755-1762.

Rüthlein, J., James, S. P., and Strober, W. (1988). Role of CD2 in activation and cytotoxic function of CD8/Leu-7-positive T cells. *J. Immunol.* **141**, 3791-3797.

Saiki, R. K., Gelfand, D. H., Stoffel, S., Scharf, S. J., Higuchi, R., Horn, G. T., Mullis, K. B., and Erlich, H. A. (1988). Primer-directed enzymatic amplification of DNA with a thermostable DNA polymerase. *Science* **239**, 487-491.

Sambrook, J., Fritsch, E. F., and Maniatis, T. (1989). In *Molecular Cloning: A Laboratory Manual.* Cold Spring Harbour Laboratory Press, USA.

Sanger, N., Nicklen, S., and Coulson, A. R. (1977). DNA sequencing with chain-terminating inhibitors. *Proc. Natl. Acad. Sci. USA* **74**, 5463-5467.

Santamaria, P., Lewis, C., and Barbosa, J. J. (1993). Amino acid sequences of seven Vβ, eight Vα, and thirteen Jα novel human TCR genes. *Immunogenetics* **38**, 163.

Sarukhan, A., Gombert, J. M., Olivi, M., Bach, J. F., Carnaud, C., and Garchon, H. J. (1994). Anchored polymerase chain reaction based analysis of the Vβ repertoire in the non-obese diabetic (NOD) mouse. *Eur. J. Immunol.* **24**, 1750-1756.

Schatz, D. G., Oettinger, M. A., and Baltimore, D. (1989). The V(D)J recombination activating gene, RAG-1. *Cell* **59**, 1035-1048.

Schein, E., Warnecke, M., and Kirmse, P. (1977). Development of *Theileria parva* (Theiler, 1904) in the gut of *Rhipicephalus appendiculatus* (Neumann, 1901). *Parasitology* **75**, 309-316.

Schiffer, M., Wu, T. T., and Kabat, E. A. (1986). Subgroups of variable region genes of β-chains of T cell receptors for antigen. *Proc. Nat. Acad. Sci. USA* **83**, 4461-4463.

Schofield, L., Ferreira, A., Altszuler, R., Nussenzweig, V., and Nussenzweig, R. S. (1987). Interferon-γ inhibits the intrahepatocytic development of malaria parasites *in vitro*. *J. Immunol.* **139**, 2020-2025.

Scholl, P., Diez, A., Mourad, W., Parsonnet, J., Geha, R. S., and Chatila, T. (1989). Toxic shock syndrome toxin 1 binds to major histocompatibility complex class II molecules. *Proc. Natl. Acad. Sci. USA* ***86***, 4210-4214.

Schrenzel, M. D., Watson, J. L., and Ferrick, D. A. (1994). Characterization of horse (*Equus caballus*) T-cell receptor beta chain genes. *Immunogenetics* **40**, 135-144.

Schrenzel, M. D., and Ferrick, D. A. (1995). Horse (*Equus caballus*) T-cell receptor alpha, gamma, and delta chain genes: nucleotide sequences and tissue-specific gene expression. *Immunogenetics* **42**, 112-122.

Seboun, E., Robinson, M. A., Kindt, T. J., and Hauser, S. L. (1989). Insertion/deletion-related polymorphisms in the human T cell receptor β gene complex. *J. Exp. Med.* **170**, 1263-1270.

Seder, R. A., Gazzinelli, R., Sher, A., and Paul, W. E. (1993). Interleukin 12 acts directly on $CD4^+$ T cells to enhance priming for interferon gamma production and diminishes interleukin 4 inhibition of such priming. *Proc. Natl. Acad. Sci. USA* **90**, 10188-10192.

Seth, A., Stern, L. J., Ottenhoff, T. H., Engel, I., Owen, M. J., Lamb, J. R., Klausner, R. D., and Wiley, D. C. (1994). Binary and ternary complexes between T-cell receptor, class II MHC and superantigen *in vitro*. *Nature* **369**, 324-327.

Shatry, A. M., Wilson, A. J., Varma, S., and Dolan, T. T. (1981). Sequential study of lymph node and splenic aspirates during *Theileria parva* infection in calves. *Res. Vet. Sci.* **30**, 181-184.

Shaw, M. K., Tilney, L. G., and Musoke, A. J. (1991). The entry of *Theileria parva* sporozoites into bovine lymphocytes: evidence for MHC class I involvement. *J. Cell. Biol.* **113**, 87-101.

Shaw, M. K., Tilney, L. G., and McKeever, D. J. (1993). Tick salivary gland extract and interleukin-2 stimulation enhance susceptibility of lymphocytes to infection by *Theileria parva* sporozoites. *Infect. Immun.* **61**, 1486-1495.

Shaw, M. K., Tilney, L. G., Musoke, A. J., and Teale, A. J. (1995). MHC class I molecules are an essential cell surface component involved in *Theileria parva* sporozoite binding to bovine lymphocytes. *J. Cell. Sci.* **108**, 1587-1596.

Shinkai, Y., Rathbun, G., Lam, K. P., Oltz, E. M., Stewart, V., Mendelsohn, M., Charron, J., Datta, M., Young, F., Stall, A. M., and Alt, F. W. (1992). RAG-2-deficient mice lack mature lymphocytes owing to inability to initiate V(D)J rearrangement. *Cell* **68**, 855-867.

Shortman, K. (1992). Cellular aspects of early T-cell development. *Curr. Opin. Immunol.* **4**, 140-146.

Silins, S. L., Cross, S. M., Elliott, S. L., Pye, S. J., Burrows, S. R., Burrows, J. M., Moss, D. J., Argaet, V. P., and Misko, I. S. (1996). Development of Epstein-Barr virus-specific memory T cell receptor clonotypes in acute infectious mononucleosis. *J. Exp. Med.* **184**, 1815-1824.

Sim, G. K., Yague, J., Nelson, J., Marrack, P., Palmer, E., Augustin, A., and Kappler, J. (1984). Primary structure of the human T-cell receptor α-chain. *Nature* **312**, 771-775.

Simpson, E., Dyson, P. J., Knight, A. M., Robinson, P. J., Elliott, J. I., and Altmann, D. M. (1993). T-cell receptor repertoire selection by mouse mammary tumor viruses and MHC molecules. *Immunol. Rev.* **131**, 93-115.

Singer, P. A., Balderas, R. S., and Theofilopoulos, A. N. (1990). Thymic selection defines multiple T cell receptor Vβ 'repertoire phenotypes' at the CD4/CD8 subset level. *EMBO J.* **9**, 3641-3648.

Siu, G., Strauss, E. C., Lai, E., and Hood, L. E. (1986). Analysis of a human Vβ gene subfamily. *J. Exp. Med.* **164**, 1600-1614.

Smith, L. R., Plaza, A., Singer, P. A., and Theofilopoulos, A. N. (1990). Coding sequence polymorphisms among Vβ T cell receptor genes. *J. Immunol.* **144**, 3234-3237.

Sopp, P. (1996). Ruminant cluster CD21. *Vet. Immunol. Immunopathol.* **52**, 249.

Sopp, P., Kwong, L. S., and Howard, C. J. (1996). Identification of bovine CD14. *Vet. Immunol. Immunopathol.* **52** , 323-328.

Spooner, R. L., and Brown, C. G. D. (1980). Bovine lymphocyte antigens (BoLA) of bovine lymphocytes and derived lymphoblastoid lines transformed by *Theileria parva* and *Theileria annulata*. *Parasite Immunol.* **2**, 163-174.

Spooner, R. L., Innes, E. A., Glass, E. J., Millar, P., and Brown, C. G. D. (1988). Bovine mononuclear cell lines transformed by *Theileria parva* or *Theileria annulata* express different subpopulation markers. *Parasite Immunol.* **10**, 619-629.

Spooner, R. L., Innes, E. A., Glass, E. J., and Brown, C. G. D. (1989). *Theileria annulata* and *T. parva* infect and transform different bovine mononuclear cells. *Immunology* **66**, 284-288.

Stagg, D. A., Dolan, T. T., Leitch, B. L., and Young, A. S. (1981). The initial stages of infection of cattle cells with *Theileria parva* sporozoites *in vitro*. *Parasitology* **83**, 191-197.

Stevens, A. (1982). The haematoxylins. In *Theory and Practice of Histological Techniques.*, J. D. Bancroft and A. Stevens, eds. (New York: Churchill Livingstone), pp. 109-121.

Subramanyam, M., McLellan, B., Labrecque, N., Sekaly, R. P., and Huber, B. T. (1993). Presentation of the Mls-1 superantigen by human HLA class II molecules to murine T cells. *J. Immunol.* **151**, 2538-2545.

Sundstedt, A., Dohlsten, M., Hedlund, G., Höidén, I., Björklund, M., and Kalland, T. (1994). Superantigens anergize cytokine production but not cytotoxicity *in vivo*. Immunology **82**, 117-125.

Sutkowski, N., Palkama, T., Ciurli, C., Sekaly, R. P., Thorley-Lawson, D. A., and Huber, B. T. (1996). An Epstein-Barr virus-associated superantigen. *J. Exp. Med.* **184**, 971-980.

Suzuki, Y., Orellana, M. A., Schreiber, R. D., and Remington, J. S. (1988). Interferon-γ: the major mediator of resistance against *Toxoplasma gondii*. *Science* **240**, 516-518.

Swaminathan, S., Furey, W., Pletcher, J., and Sax, M. (1992). Crystal structure of staphylococcal enterotoxin B, a superantigen. *Nature* **359**, 801-806.

Takamatsu, H. H., Kirkham, P. A., and Parkhouse, R. M. E. (1997). A γδ T cell specific surface receptor (WC1) signaling G0/G1 cell cycle arrest. *Eur. J. Immunol.* **27**, 105-110

Takeuchi, N., Ishiguro, N., and Shinagawa, M. (1992). Molecular cloning and sequence analysis of bovine T-cell receptor γ and δ chain genes. *Immunogenetics* **35**, 89-96.

Tanaka, A., Ishiguro, N., and Shinagawa, M. (1990). Sequence and diversity of bovine T-cell receptor β-chain genes. *Immunogenetics* **32**, 263-271.

Taracha, E. L. N. (1991). Investigation of cytotoxic T-lymphocyte responses of cattle to *Theileria parva* by limiting dilution analyses. Ph.D. thesis. Brunel University, UK.

Taracha, E. L. N., Goddeeris, B. M., Scott, J. R., and Morrison, W. I. (1992). Standardization of a technique for analysing the frequency of parasite-specific cytotoxic T lymphocyte precursors in cattle immunized with *Theileria parva*. *Parasite Immunol.* **14**, 143-154.

Taracha, E. L., Goddeeris, B. M., Morzaria, S. P., and Morrison, W. I. (1995a). Parasite strain specificity of precursor cytotoxic T cells in individual animals correlates with cross-protection in cattle challenged with *Theileria parva*. *Infect. Immun.* **63**, 1258-1262.

Taracha, E. L., Goddeeris, B. M., Teale, A. J., Kemp, S. J., and Morrison, W. I. (1995b). Parasite strain specificity of bovine cytotoxic T cell responses to *Theileria parva* is determined primarily by immunodominance. *J. Immunol.* **155**, 4854-4860.

Taylor, A. H., Haberman, A. M., Gerhard, W., and Caton, A. J. (1990). Structure-function relationships among highly diverse T cells that recognize a determinant from influenza virus hemagglutinin. *J. Exp. Med.* **172**, 1643-1651.

Thein, S. L., and Wallace, R. B. (1986). The use of synthetic oligonucleotides as specific hybridization probes in the diagnosis of genetic disorders. In *Human Genetic Diseases: A Practical Approach.*, K. E. Davis, ed. (Virginia: IRL Press), pp. 33.

Thibodeau, J., Labrecque, N., Denis, F., Huber, B. T., and Sekaly, R. P. (1994). Binding sites for bacterial and endogenous retroviral superantigens can be dissociated on major histocompatibility complex class II molecules. *J. Exp. Med.* **179**, 1029-1034.

Thiesen, H-J., Casorati, G., Lauster, R., and Wiles, M. V. (1990). Application of polymerase chain reaction in molecular immunology. In *Immunological Methods. Vol. IV.*, I. Lefkovits, ed. (Academic Press) pp35-60

Tillinghast, J. P., Behlke, M. A., and Loh, D. Y. (1986). Structure and diversity of the human T-cell receptor β-chain variable region genes. *Science* **233**, 879-883.

Tomai, M., Kotb, M., Majumdar, G., and Beachey, E. H. (1990). Superantigenicity of streptococcal M protein. *J. Exp. Med.* **172**, 359-362.

Toye, P. G., Goddeeris, B. M., Iams, K., Musoke, A. J., and Morrison, W. I. (1991). Characterization of a polymorphic immunodominant molecule in sporozoites and schizonts of *Theileria parva*. *Parasite Immunol.* **13**, 49-62.

Toyonaga, B., Yoshikai, Y., Vadasz, V., Chin, B., and Mak, T. W. (1985). Organization and sequences of the diversity, joining and constant region genes of the human T cell receptor β-chain. *Proc. Nat. Acad. Sci. USA* **82**, 8624-8628.

Trowbridge, I. S., and Omary, M. B. (1981). Human cell surface glycoprotein related to cell proliferation is the receptor for transferrin. *Proc. Natl. Acad. Sci. USA* **78**, 3039-3043.

Uematsu, Y., Ryser, S., Dembic, Z., Borgulya, P., Krimpenfort, P., Berns, A., von Boehmer, H., and Steinmetz, M. (1988). In transgenic mice the introduced functional T cell receptor β gene prevents expression of endogenous β genes. *Cell* **52**, 831-841.

Uilenberg, G. (1981). Theilerial species of domestic livestock. In *Advances in the Control of Theileriosis.*, A. D. Irvin, M. P. Cunningham and A. S. Young, eds. (The Hague: Martinus Nijhoff), pp. 4-37.

Urban, J. L., Kumar, V., Kono, D. H., Gomez, C., Horvath, S. J., Clayton, J., Ando, D. G., Sercarz, E. E., and Hood, L. (1988). Restricted use of T cell receptor V genes in murine autoimmune encephalomyelitis raises possibilities for antibody therapy. *Cell* **54**, 577-592.

Vacchio, M. S., and Hodes, R. J. (1989). Selective decreases in T cell receptor Vβ expression. Decreased expression of specific Vβ families is associated with expression of multiple MHC and non-MHC gene products. *J. Exp. Med.* **170**, 1335-1346.

Van Houten, N., Mixter, P. F., Wolfe, J., and Budd, R. C. (1993). CD2 expression on murine intestinal intraepithelial lymphocytes is bimodal and defines proliferative capacity. *Int. Immunol.* **5**, 665-672.

Visser, A. E., Abraham, A., Sakyi, L. J., Brown, C. G., and Preston, P. M. (1995). Nitric oxide inhibits establishment of macroschizont-infected cell lines and is produced by macrophages of calves undergoing bovine tropical theileriosis or East Coast fever. *Parasite Immunol.* **17**, 91-102.

von Boehmer, H. (1994). Positive selection of lymphocytes. *Cell* **76**, 219-228.

Vukusic, B., Poplonski, L., Phillips, L., Pawling, J., Delovitch, T., Hozumi, N., and Wither, J. (1995). Both MHC and background gene heterozygosity alter T cell receptor repertoire selection in an antigen-specific response. *Mol. Immunol.* **32**, 1355-1367.

Waanders, G. A., Lussow, A. R., and MacDonald, H. R. (1993). Skewed T cell receptor Vα repertoire among superantigen reactive murine T cells. *Int. Immunol.* **5**, 55-61.

Wade, T., Bill, J., Marrack, P. C., Palmer, E., and Kappler, J. W. (1988). Molecular basis for the nonexpression of Vβ17 in some strains of mice. *J. Immunol.* **141**, 2165-2167.

Wagner, G. G., Duffus, W. P. H., and Burridge, M. J. (1974). The specific immunoglobulin response in cattle immunized with isolated *Theileria parva* antigens. *Parasitology* **69**, 43-53.

Wagner, G. G., Duffus, W. P. H., Akwabi, C., Burridge, M. J., and Lule, M. (1975). The specific immunoglobulin response in cattle to *Theileria parva* (Muguga) infection. *Parasitology* **70**, 95-102.

Wang, E. C., Taylor-Wiedeman, J., Perera, P., Fisher, J., and Borysiewicz, L. K. (1993a). Subsets of $CD8^+$, $CD57^+$ cells in normal, healthy individuals: correlations with human cytomegalovirus (HCMV) carrier status, phenotypic and functional analyses. *Clin. Exp. Immunol.* **94**, 297-305.

Wang, X., Golkar, L., Uyemura, K., Ohmen, J. D., Villahermosa, L. G., Fajardo, T. T., Jr., Cellona, R. V., Walsh, G. P., and Modlin, R. L. (1993b). T cells bearing Vβ6 T cell receptors in the cell-mediated immune response to *Mycobacterium leprae*. *J. Immunol.* **151**, 7105-7116.

Wang, E. C., Lehner, P. J., Graham, S., and Borysiewicz, L. K. (1994). $CD8^{high}$ ($CD57^+$) T cells in normal, healthy individuals specifically suppress the generation of cytotoxic T lymphocytes to Epstein-Barr virus-transformed B cell lines. *Eur. J. Immunol.* **24**, 2903-2909.

Webb, S., Morris, C., and Sprent, J. (1990). Extrathymic tolerance of mature T cells: clonal elimination as a consequence of immunity. *Cell* **63**, 1249-1256.

Webb, S. R., and Gascoigne, N. R. (1994). T-cell activation by superantigens. *Curr. Opin. Immunol.* **6**, 467-475.

Webb, S. R., Hutchinson, J., Hayden, K., and Sprent, J. (1994). Expansion/deletion of mature T cells exposed to endogenous superantigens *in vivo*. *J. Immunol.* **152**, 586-597.

Wen, R., Cole, G. A., Surman, S., Blackman, M. A., and Woodland, D. L. (1996). Major histocompatibility complex class II-associated peptides control the presentation of bacterial superantigens to T cells. *J. Exp. Med.* **183**, 1083-1092.

Wesselborg, S., Janssen, O., and Kabelitz, D. (1993). Induction of activation-driven death (apoptosis) in activated but not resting peripheral blood T cells. *J. Immunol.* **150**, 4338-4345.

Westby, M., Manca, F., and Dalgleish, A. G. (1996). The role of host immune responses in determining the outcome of HIV infection. *Immunol. Today* **17**, 120-126.

Wilde, J. K. H. (1966). Changes in bovine bone marrow during the course of East Coast fever. *Res. Vet. Sci.* **7**, 213-224.

Wijngaard, P. L. J., Metzelaar, M. J., MacHugh, N. D., Morrison, W. I. And Clevers, H. C. (1992). Molecular characterisation of the WC1 antigen expressed specifically on bovine $CD4^-CD8^-$ γδ T lymphocytes. *J. Immunol.* **149**, 3273-3277.

Wijngaard, P. L. J., MacHugh, N. D., Metzelaar, M. J., Romberg, S., Bensaid, A., Pepin, L., Davis, W. C., and Clevers, H. C. (1994). Members of the novel WC1 gene family are differentially expressed on subsets of bovine $CD4^-CD8^-$ γδ T lymphocytes. *J. Immunol.* **152**, 3476-3482.

Williams, A. F., Strominger, J. L., Bell, J., Mak, T. W., Kappler, J., Marrack, P., Arden, B., Lefranc, M. P., Hood, L., Tonegawa, S., and Davis, M. (1993). Nomenclature for T-cell receptor (TCR) gene segments of the immune system. *Bull. WHO* **71**, 113-115.

Williams, D. J. L., Newson, J., and Naessens, J. (1990). Quantitation of bovine immunoglobulin isotypes and allotypes using monclonal antibodies. *Vet. Immunol. Immunopathol.* **24**, 267-283.

Winslow, G. M., Scherer, M. T., Kappler, J. W., and Marrack, P. (1992). Detection and biochemical characterization of the mouse mammary tumor virus 7 superantigen ($Mls\text{-}1^a$). *Cell* **71**, 719-730.

Winslow, G. M., Marrack, P., and Kappler, J. W. (1994). Processing and major histocompatibility complex binding of the MTV-7 superantigen. *Immunity* **1**, 23-33.

Woodland, D. L., and Blackman, M. A. (1993). How do T-cell receptors, MHC molecules and superantigens get together? *Immunol. Today* **14**, 208-212.

Woodland, D. L., Smith, H. P., Surman, S., Le, P., Wen, R., and Blackman, M. A. (1993). Major histocompatibility complex-specific recognition of Mls-1 is mediated by multiple elements of the T cell receptor. *J. Exp. Med.* **177**, 433-442.

Yagi, J., Baron, J., Buxser, S., and Janeway, C. A. (1990). Bacterial proteins that mediate the association of a defined subset of T cell receptor:CD4 complexes with class II MHC. *J. Immunol.* **144**, 892-901.

Yazdanbakhsh, K., Park, C. G., Winslow, G. M., and Choi, Y. (1993). Direct evidence for the role of COOH terminus of mouse mammary tumor virus superantigen in determining T cell receptor Vβ specificity. *J. Exp. Med.* **178**, 737-741.

Yoshikai, Y., Clark, S. P., Taylor, S., Sohn, U., Wilson, B. I., Minden, M. D., and Mak, T. W. (1985). Organization and sequences of the variable, joining and constant region genes of the human T-cell receptor α-chain. *Nature* **316**, 837-839.

Zhao, T. M., Whitaker, S. E., and Robinson, M. A. (1994). A genetically determined insertion/deletion related polymorphism in human T cell receptor β chain (TCRB) includes functional variable gene segments. *J. Exp. Med.* **180**, 1405-1414.

Zheng, B., Xue, W., and Kelsoe, G. (1994). Locus-specific somatic hypermutation in germinal centre T cells. *Nature* **372**, 556-559.